ITUM
INSTITUTE OF TECHNOLOGY
UNIVERSITY OF MORATUWA

INSTITUTE OF TECHNOLOGY UNIVERSITY OF MORATUWA

CONFERENCE PROCEEDINGS



ITUM-IRC 2026

5TH INTERNATIONAL RESEARCH CONFERENCE

"Engineering & Technology in Times of Uncertainty: Preserving Human Values and Cultural Heritage During Global Conflicts"

5th International Research Conference - 2026

05 NOVEMBER 2026 | ITUM, HOMAGAMA, SRI LANKA

VOLUME: 12 **ISSN: 2773-7055**

Foreword

We are pleased to present the proceedings of the 5th International Research Conference of the Institute of Technology, University of Moratuwa (ITUM-IRC 2026). This year's theme is,

"Engineering & Technology in Times of Uncertainty: Preserving Human Values and Cultural Heritage During Global Conflicts".

This volume brings together extended abstracts from a wide range of disciplines, offering a platform for academics, professionals, and industrialists engaged in research to exchange knowledge and showcase their work. The proceedings document the outcomes of the conference held on 5th November, 2026 at the Institute of Technology, University of Moratuwa (ITUM), Diyagama, and serve as a record of the valuable contributions made by our researchers.

ISSN: 2773-7055

Research Unit

Head	Dr. (Ms.) PND Tissera Senior Lecturer (II) Division of Textile and Clothing Technology
Members	Dr. (Mrs.) GK Jayathunga Senior Lecturer (I) Division of Polymer and Chemical Engineering Technology
	Dr. PDC Kumara Senior Lecturer (II) Division of Mechanical Engineering Technology
	Dr. RN Wijesena Senior Lecturer (II) Division of Textile and Clothing Technology
	Dr. (Mrs.) PBTK Premarathne Senior Lecturer (II) Division of Interdisciplinary Studies
	Dr. AUVB Bulathsinhala Senior Lecturer (II) Division of Civil Engineering Technology
	Mrs. AWCK Atugoda Lecturer Division of Electrical, Electronics and Telecommunication Engineering Technology
	Dr. NDI Kumarage Lecturer (Probationary) Division of Polymer and Chemical Engineering Technology
	Mrs. DAS Ruwanmini Lecturer (Probationary) Division of Information Technology
	Mr. KKTS Bandara Lecturer (Probationary) Division of Interdisciplinary Studies
	Mr. K Jinadasa Training Engineer Industrial Training, Career Guidance and Post Diploma Unit

Editorial Committee Acknowledgements

The Editorial Committee is pleased to present the proceedings of the 5th International Research Conference of ITUM (ITUM-IRC 2026), which brings together a wide range of scholarly contributions under the theme “Engineering & Technology in Times of Uncertainty: Preserving Human Values and Cultural Heritage During Global Conflicts”.

This volume reflects the commitment of authors who shared their research, as well as the reviewers whose careful evaluations helped to strengthen the quality of the submissions. We believe that the proceedings of ITUM-IRC 2026 will provide a meaningful resource for researchers, academics, and professionals, and contribute to advancing dialogue on sustainable and resilient solutions.

We sincerely thank all who contributed to making this publication possible.

Sincerely,

Editorial Committee

ITUM International Research Conference 2026

Dr. (Ms.) PND Tissera
Division of Textile and Clothing Technology

Dr. (Mrs.) PBTK Premarathne
Division of Interdisciplinary Studies

Dr. (Mrs.) GK Jayathunga
Division of Polymer and Chemical Engineering Technology

Dr. RN Wijesena
Division of Textile and Clothing Technology

Dr. AUVB Bulathsinhala
Division of Civil Engineering Technology

Dr. NDI Kumarage
Division of Polymer and Chemical Engineering Technology

Mrs. DAS Ruwanmini
Division of Information Technology

Mr. KKTS Bandara
Division of Interdisciplinary Studies

Advisory Panel

Director Institute of Technology University of Moratuwa	Major General (RETD) SK Thirunavukarasu RSP VSV USP
Deputy Registrar Institute of Technology University of Moratuwa	Mr. ND Kuruppuarachchi
Deputy Bursar Institute of Technology University of Moratuwa	Mrs. SPD Peiris

Conference Organizing Committee

Research Unit Head	Dr. (Ms.) PND Tissera Division of Textile and Clothing Technology
Conference Chair	Dr. (Mrs.) PBTK Premarathne Division of Interdisciplinary Studies
Conference Co-Chair	Dr. (Mrs.) GK Jayathunga Division of Polymer and Chemical Engineering Technology
	Dr. RN Wijesena Division of Textile and Clothing Technology
Conference Secretary	Mr. KKTS Bandara Division of Interdisciplinary Studies
Committee Members	Dr. PDC Kumara Division of Mechanical Engineering Technology
	Dr. AUVB Bulathsinhala Division of Civil Engineering Technology
	Mrs. AWCK Atugoda Division of Electrical, Electronics and Telecommunication Engineering Technology
	Dr. NDI Kumarage Division of Polymer and Chemical Engineering Technology
	Mr. K Jinadasa Industrial Training, Career Guidance and Post Diploma Unit
Compiled by	Mrs. DAS Ruwanmini Division of Information Technology
Graphic Design and Network Management	Mr. JMP Gunasekera Head , Systems Management Unit
	Mr. R Suriyage Systems Management Unit
Finance Management	Mrs. WNJ Alwis Assistant Bursar-Payments, Finance Division
General Administration	Mrs. LP Perera Senior Assistant Registrar, General Administration Division

List of Reviewers

Prof. (Dr.) A. M. Muzathik	Department of Mechanical Engineering, Faculty of Engineering, South Eastern University of Sri Lanka
Prof. A. A. G. K. Siriwardana	Department of Material and Mechanical Technology, Faculty of Technology, University of Sri Jayewardenepura, Sri Lanka
Prof. A. Jayakody	Department of Computer Systems Engineering , Faculty of Computing, Sri Lanka Institute of Information Technology (SLIIT), Sri Lanka
Prof. V.G.T.N. Vidanagama	Department of Computing & Information Systems, Faculty of Applied Sciences,Wayamba University of Sri Lanka
Prof. R. Widyalankara	Department of Education and Languages, CINEC Campus, Sri Lanka
Dr. C.L. Jayasinghe	Department of Statistics, Faculty of Applied Sciences, University of Sri Jayewardenepura, Sri Lanka
Dr. M. Perera	Department of Statistics, Faculty of Applied Sciences, University of Sri Jayewardenepura, Sri Lanka
Dr. D. Dahanayake	Department of Biomedical Science, Faculty of Science, NSBM Green University, Sri Lanka
Dr. S. Jayalath	ABR Center for Bioplastic and Bio composites, University of Queensland, Brisbane, Queensland, Australia
Dr. H. Chathuranga	Department of Chemical and Process Engineering, Faculty of Engineering, University of Moratuwa, Sri Lanka
Dr. D. D. D. Suraweera	Department of Electrical and Electronics Technology, Faculty of Engineering Technology, University of Vocational Technology, Sri Lanka
Dr. H. Abeyasena	Faculty of Foundation Skills,Salisbury Campus, TAFE SA, Australia
Dr. U. S. P. R. Arachchige	Department of Mechatronic and Industrial Engineering, NSBM Green University, Sri Lanka
Dr. K. D. R. N. Kalubowila	Department of Instrumentation and Automation Technology, Faculty of Technology, University of Colombo, Sri Lanka
Dr. K.M. Musthafa	Malaysia-Japan International Institute of Technology (MJIIT), Universiti Teknologi Malaysia, Malaysia
Dr. K.R. S. D. Gunawardhana	Primary Department School of Electronic Engineering, Dublin City University, Ireland
Dr. M. Amjath	Postdoctoral researcher, Atlantic Technological University, Letterkenny, Co.Donegal,Ireland
Dr. M. I. Bin Muhamad	Department of Electrical & Electronic Engineering, Faculty of Engineering Universiti Putra Malaysia, Malaysia

Dr. (Mrs). G.D.M.N. Samaradiwakara	Division of Acquisition University of Sri Jayewardenepura, Sri Lanka
Dr.(Ms) R.P.T.P. Keerthisinghe	Department of Chemical and Process Engineering, Faculty of Engineering University of Moratuwa, Sri Lanka
Dr.(Ms) R. Samarasinghe	Department of Electrical Engineering, Faculty of Engineering University of Moratuwa, Sri Lanka
Dr. (Ms.) S. Weerasinghe	Department of Sports Science, University of Sri Jayewardenepura, Sri Lanka
Dr. T. Lakshika	University of Colombo School of Computing, Sri Lanka
Dr. T. Wijethilake	University of Colombo School of Computing, Sri Lanka
Dr. (Mrs.) K.M.W. Abeykoon	Division of Textile and Clothing Technology, Institute of Technology, University of Moratuwa, Sri Lanka
Dr. R.N. Wijesena	Division of Textile and Clothing Technology, Institute of Technology, University of Moratuwa, Sri Lanka
Dr. (Eng.) P. D. C. Kumara	Division of Mechanical Engineering Technology, Institute of Technology, University of Moratuwa, Sri Lanka
Dr. (Mrs.) M.C.W. Somarathne	Division of Polymer and Chemical Engineering Technology, Institute of Technology, University of Moratuwa, Sri Lanka
Dr.(Mrs.) S.C. Mathugama	Division of Interdisciplinary Studies, Institute of Technology, University of Moratuwa, Sri Lanka
Dr. (Mrs.) D.D.G.A.D.S. Saparamadu	Division of Interdisciplinary Studies, Institute of Technology, University of Moratuwa, Sri Lanka
Dr. (Mrs.) G. K. Jayatunga	Division of Polymer and Chemical Engineering Technology, Institute of Technology, University of Moratuwa, Sri Lanka
Dr. (Mrs.) I. R. Samarathunga	Division of Polymer and Chemical Engineering Technology, Institute of Technology, University of Moratuwa, Sri Lanka
Dr. (Mrs.) K. Galappaththi	Division of Information Technology Institute of Technology, University of Moratuwa, Sri Lanka
Dr. (Mrs.) P. B. T. K. Premarathne	Division of Interdisciplinary Studies, Institute of Technology, University of Moratuwa, Sri Lanka
Dr. A.U.V.B. Bulathsinhala	Division of Civil Engineering Technology, Institute of Technology, University of Moratuwa, Sri Lanka
Dr. K.A.B. Weerasinghe	Division of Civil Engineering Technology, Institute of Technology, University of Moratuwa, Sri Lanka
Dr. (Mrs.) N. P. K. Semananda	Division of Civil Engineering Technology, Institute of Technology, University of Moratuwa, Sri Lanka
Dr. (Ms) N. D. Tissera	Division of Textile and Clothing Technology, Institute of Technology, University of Moratuwa, Sri Lanka

Dr. S.G.J Perera	Division of Polymer and Chemical Engineering Technology, Institute of Technology, University of Moratuwa, Sri Lanka
Dr. S. Siriwardena	Division of Polymer and Chemical Engineering Technology, Institute of Technology, University of Moratuwa, Sri Lanka
Dr. (Ms.) W. V. W. H. Wickramaarachchi	Division of Polymer and Chemical Engineering Technology, Institute of Technology, University of Moratuwa, Sri Lanka
Ms. A. A. Gunawardana	Department of Language Studies, University of Vocational Technology, Sri Lanka
Mrs. A. Liyanage	Department of Food Science and Technology, Faculty of Applied Sciences, University of Moratuwa, Sri Lanka
Ms. J.A.M. B. Karunarathna	Department of Language Studies, University of Vocational Technology, Sri Lanka
Mr.(Eng.) M. N. C. Samarawickrama	Department of Civil Engineering, Faculty of Engineering Technology, The Open University of Sri Lanka
Mrs. M. Sirisuriya	Department of Computer Science, Faculty of Computing, General Sir John Kotelawala Defence University, Sri Lanka
Mrs. D.R.T. Jayasundara	Department of Mathematics, Faculty of Engineering, University of Moratuwa, Sri Lanka
Mr. M. A. H. Sasono	Intelligent System and Robotics Laboratory, Department of Electrical Engineering, Faculty of Engineering, University of Jember, Indonesia
Mrs. M. M. P. D. Samarasekara	Division of Civil Engineering, Institute of Technology, University of Moratuwa, Sri Lanka
Mr. W. L. S. Maduranga	Division of Civil Engineering Technology, Institute of Technology, University of Moratuwa, Sri Lanka
Mr.(Eng.) M. M. Mafroos	Division of Electrical, Electronics and Telecommunication Engineering Technology,Institute of Technology, University of Moratuwa, Sri Lanka
Mrs. (Eng.) D. Y. T. Bambaravanage	Division of Electrical, Electronics and Telecommunication Engineering Technology, Institute of Technology, University of Moratuwa, Sri Lanka
Mrs. S.M. Kannangara	Division of Electrical, Electronics and Telecommunication Engineering Technology, Institute of Technology, University of Moratuwa, Sri Lanka
Mr. (Eng.) J.M.P. Gunasekera	Division of Mechanical Engineering Technology, Institute of Technology, University of Moratuwa, Sri Lanka
Mr. (Eng.) L.G. Chamath	Division of Mechanical Engineering Technology, Institute of Technology, University of Moratuwa, Sri Lanka
Mr. (Eng.) H. M. S. Bandara	Division of Mechanical Engineering Technology, Institute of Technology, University of Moratuwa, Sri Lanka

Message from the Director, Institute of Technology, University of Moratuwa

It gives me great pleasure to send this message to the proceedings of the 5th International Research Conference of the Institute of Technology, University of Moratuwa (ITUM-IRC 2026).

Since its inception, ITUM has been committed to producing skilled engineering technologists who contribute directly to the nation's development. Alongside this mission, research has grown into a vital pillar of our institute, strengthening the quality of our teaching, connecting us with industry, and enabling our staff and students to engage with challenges that matter to society. The steady growth of this conference over the past five years is a clear reflection of that commitment.

The theme of this year's conference, "Engineering & Technology in Times of Uncertainty: Preserving Human Values and Cultural Heritage During Global Conflicts," is both timely and thought-provoking. In a world facing conflict, economic pressures and rapid change, it reminds us that technological progress must remain grounded in human values and respect for the heritage that defines us. I am pleased to see researchers from diverse disciplines responding to this call with work that is innovative, practical and socially responsible.

I take this opportunity to congratulate all authors whose research is published in these proceedings, and to thank the keynote speakers, reviewers and session chairs for sharing their expertise. I also commend the Head of the Research Unit, Dr. (Ms.) Nadeeka D. Tissera, the Conference Chair, Co-chairs, Conference Secretary and the organizing committee, together with the academic and non-academic staff, for their dedication in organizing this event. My sincere thanks also go to our sponsors and partners for their valued support.

I am confident that ITUM-IRC 2026 will foster meaningful dialogue, new collaborations and research that serves both industry and society. I wish the conference every success.

Major General (RETD) S.K. Thirunavukarasu RSP VSV USP

Director
Institute of Technology, University of Moratuwa

Message from the Head of the Research Unit

It is with great pleasure that I welcome you to the 5th International Research Conference of the Institute of Technology, University of Moratuwa (ITUM-IRC 2026), held on 5th November 2026 at ITUM, Diyagama, Homagama.

This year's theme, "Engineering & Technology in Times of Uncertainty: Preserving Human Values and Cultural Heritage During Global Conflicts," addresses an increasingly urgent question. As conflict, instability and rapid technological change reshape societies, engineering and technology must not only drive innovation but also protect the values and heritage that give communities their strength. This conference offers a platform to reflect on that responsibility.

The research in these proceedings spans six interdisciplinary tracks, from sustainable infrastructure, energy and intelligent systems, and mechanical and marine engineering, to advanced materials, digital technologies and AI, and education in times of uncertainty. Together, they reflect a shared commitment to resilient, sustainable and human-centred solutions. All accepted extended abstracts have been published under ISSN 2773-7055, ensuring wider visibility of this work.

The Research Unit remains dedicated to fostering a vibrant research culture at ITUM and strengthening collaboration with national and international partners.

I extend my sincere gratitude to the Director of ITUM for continuous guidance and support, and to the Conference Chair, Co-chairs and Conference Secretary for their tireless leadership. My thanks also go to the keynote speakers, reviewers, session chairs, organizing committee, staff and sponsors, and above all to the authors and participants whose research forms the heart of this event.

I wish all participants a rewarding and memorable conference.

Dr. (Ms.) Nadeeka D. Tissera
Head, Research Unit
Institute of Technology, University of Moratuwa

Message from the Conference Chair

It is my great honour and privilege to welcome you to this year's International Conference (ITUMIRC 2026) under the timely and thought-provoking theme:

"Engineering and Technology in Times of Uncertainty: Preserving Human Values and Cultural Heritage during Global Conflicts."

We come together at a time of profound global uncertainty. Ongoing conflicts and rising geopolitical tensions remind us of how fragile peace is and of the devastating consequences when it is compromised. Climate change continues to intensify natural disasters, threatening not only human lives and livelihoods but also the cultural heritage and historical landmarks that embody our collective identity. At the same time, misinformation weakens social cohesion, while the misuse of technologies, including cyberattacks and unethical applications of artificial intelligence, demonstrates that innovation without ethical responsibility can undermine stability rather than advance progress.

Against this backdrop, our conference highlights an essential truth: technological advancement must be accompanied by ethical responsibility, human-centred values, and a commitment to preserving our cultural heritage for future generations.

As Conference Chair, I extend my heartfelt gratitude to the Advisory panel and the Organising Committee for their tireless dedication and commitment to making this event a success. I am also deeply appreciative of our sponsors and well-wishers for their generous support.

My sincere thanks go to all the authors and researchers who submitted their valuable research contributions for consideration. I wish to acknowledge the exceptional efforts of our reviewers, meta-reviewers, session chairs, and co-chairs, whose expertise and commitment to maintaining the highest academic standards have been instrumental in ensuring the quality and integrity of this conference.

I would also like to express my deepest appreciation to our distinguished Chief Guest and Keynote Speaker, Dr. Gina Maswabi, Commonwealth National Climate Finance Advisor for Sri Lanka, and to our esteemed guest speaker, Mr. Venkatesh, Managing Director of SRP Synthetic and Rubber Products Group of Industries, India, for generously sharing their expertise and insights. Special thanks also go to the special speaker, Mrs. M.M.P.D. Samarasekara, Senior Lecturer (Grade I) in Civil Engineering, Institute of Technology, University of Moratuwa.

This conference is more than a gathering of scholars, researchers, and professionals. It is a platform for meaningful dialogue, knowledge exchange, innovation, and the formation of partnerships that transcend disciplines and borders. Throughout this event, we will explore emerging research, engage in thought-provoking discussions and foster collaborations that will help shape a more resilient and sustainable future.

I encourage all participants to engage actively throughout the conference. Share your insights, challenge existing perspectives, learn from one another, and embrace the collaborative spirit that drives innovation and progress. Together, let us contribute to building a more resilient, sustainable, and peaceful future.

I wish you a productive, rewarding, and inspiring conference experience, and I look forward to the meaningful contributions, innovative ideas, and lasting partnerships that will emerge from our time together.

Dr. PBTK Premarathne
Conference Chair
ITUMIRC 2026

Table of Contents

KEYNOTE SPEECH

Harnessing Engineering, Technology and Climate Finance to Safeguard Humanity, Sustainability and Cultural Heritage in Times of Uncertainty

Dr. Gina Maswabi xix

PLENARY SPEECH

Business Leadership and Entrepreneurship

Mr. K.S. Venkatesh xx

SPECIAL SPEECH

From Credit Accumulation to Outcome-Based Engineering Technology Education

Mrs. M.M.P.D. Samarasekara xxi

Track 1 – Sustainable Infrastructure, Built Environment & Resilient Systems in Uncertain Contexts 1

EXTRACTION AND CHARACTERIZATION OF NATURAL PIGMENTS FROM MARIGOLD (TAGETES ERECTA L.) FOR PLANT-BASED DYE APPLICATIONS

G K Jayatunga[1*], E M U M Ekanayaka[1], P A I Eranda[1], O D S Fonseka[1], N V E Harshani[1], W M Y B Wanninayake[1] 1

DRYING KINETICS AND EXTRACTION OF OLEORESIN FROM MORINGA OLEIFERA LEAVES USING CONVECTION TRAY DRYER

G K Jayatunga[1*], L K C A Hasarangi[1], K P S S Jayawickrama[1], W A M Geethma[1] . 6

DEVELOPMENT OF NON-CONVENTIONAL CREAM CHEESE ANALOGUE USING SOYA MILK AND PEANUT PASTE: EFFECT OF FORMULATION ON PHYSICOCHEMICAL AND TEXTURAL PROPERTIES

W V W H Wickramaarachchi[1*], C D A Samarasekara[1], S O M T H Samarasekara[1], L A Sanchila[1], S D S Sankalpana[1], W M Y B Wanninayake[1] 12

DRYING KINETICS AND MATHEMATICAL MODELLING OF ASH PLANTAIN IN A CONVECTION TRAY DRYER

G K Jayatunga[1*], R M T N Rathnayake[1] 19

PREDICTION OF ROCK SOCKET SHEAR STRENGTH IN HARD CRYSTALLINE ROCKS USING PILE LOAD TEST DATA AND ROCK MASS QUALITY PARAMETERS

Jepanesan Jinthusan[1], Ayodya Bulathsinhala[2*], Anurudda Puswewala[3] 25

RESILIENT RECONSTRUCTION OF CRITICAL INFRASTRUCTURE IN POST-CONFLICT AND DISASTER CONTEXTS: A SUSTAINABLE QUANTITY SURVEYING FRAMEWORK FOR RECOVERY AND LONG-TERM RESILIENCE

N Z Nafrin[1*], Y A Adikari[1] 32

HYDROLYSIS ROUTE AS A KEY DETERMINANT OF FISH-WASTE LIQUID FERTILIZER QUALITY: A METHOD-CENTRED REVIEW

K A D Thathsarani[1*], W V W H Wickramaarachchi[1], N M L Fernando[1] 41

INFLUENCE OF BENTONITE INFILL ON THE SHEAR BEHAVIOUR OF BIOTITE GNEISS–CONCRETE INTERFACES UNDER CONSTANT NORMAL LOADING

Ayodya Bulathsinhala[1*], Anurudda Puswewala[2] 47

Tracks 2 & 3 – Energy, Electrical, Electronic & Intelligent Systems; Mechanical, Marine & Industrial Systems Engineering 53

META-CALIBRATED PROTOTYPE OPEN-SET ADAPTATION FOR CABLE-TERMINATION PARTIAL DISCHARGE DIAGNOSIS UNDER LABORATORY-TO-FIELD DOMAIN SHIFT

H P D S Madhuranga[1*], Wong Jee Keen Raymond[1], W L S Madhuranga[2] 53

THERMAL-ACOUSTIC PERFORMANCE ANALYSIS OF A DOUBLE-ACTING THERMOACOUSTIC GENERATOR IN WASTE HEAT RECOVERY APPLICATIONS

R K A Rathnayake[1*], Malin Gunasekara[1] 60

SOCIO-ENVIRONMENTAL SUSTAINABILITY IN CROSS-BORDER ELECTRICITY TRADE OF NEPAL

Rajendra Singh[1*], Vinesh Agrawal[1], Shree Raj Shakya[2] 67

REVIEW: PYROLYSIS OF BIOMASS AS A SUSTAINABLE ALTERNATIVE TO FOSSIL FUEL IN SRI LANKA

K A N I Kaluarachchi[1], O G D D M Jayawardhana[1], T G W M Kavinda[1], N K M S Karunarathna[1], G K Jayatunga[1*] 71

AN ETHICAL EVALUATION OF HYDROPOWER DEVELOPMENT USING AN ENERGY JUSTICE FRAMEWORK: BALANCING ECONOMIC, ENVIRONMENTAL AND SOCIAL IMPACTS

D H K Perera[1*], S S Morapitiya[1] 78

DESIGN AND DEVELOPMENT OF AN AUTOMATED BULK FILLING SYSTEM USING A CARTESIAN ROBOT FOR COCONUT OIL PACKAGING

H M N C Herath[1*], D H K Perera[1], P T K Sachintha[1], S S Morapitiya[1] 85

EFFECT OF AGITATION STRATEGY ON BIODIESEL PRODUCTION FROM WASTE COCONUT OIL

W V W H Wickramaarachchi[1*], H C Dilshan[1], D M H M A Disanayaka[1], D M M D Dissanayaka[1], W M T M Dewdunu[1] 92

Track 4 – Advanced Materials, Polymers, Textiles & Culturally Inspired Sustainable Products 98

ADOPTABILITY OF DUAL-COLOUR SOCKS FOR SCHOOL UNIFORMS: A STATISTICAL APPROACH

Aruna Ratnayake[1,2*], Ravindi Jayasundara[1], Prathibani Manthriratne[3] 98

STUDY OF THE STRETCH AND RECOVERY PROPERTIES OF COTTON/SPANDEX SINGLE JERSEY FABRICS MADE WITH FULL PLATING TECHNIQUE

K D S Seneviratne[1*], C N Herath[2] 104

IMAGE-BASED TURBIDIMETRIC DETERMINATION OF AVAILABLE SOIL POTASSIUM USING A CAPILLARY-DRIVEN MICROFLUIDIC DEVICE

H M C S Wijerathne[1,2], N D Tissera[3], G Priyadarshana[2], R N Wijesena[3*] 110

FIRE PERFORMANCE OF GLYCEROL-BASED BIO-EPOXY SYSTEMS

G K B M Gannoruwa[1*], L H J Jeewantha[1], Allan Manalo[1], Omar Alajarmeh[2], Stephen Clarke[3], Sean Steed[3] 116

DEVELOPING A SUSTAINABLE BLACK PRINT PIGMENT FROM COCONUT-COIR EXTRACT

M W M D Somarathna[1], K D S Senevirathne[1*], H A I Udeshika[1], D K A H J B Welikala[1], W P M S S Wijesooriya[1], H A S Wijewardhana[1], R N Wijesena[1] 123

DEVELOPMENT OF CHEMICALLY MODIFIED WOOL-BASED SUSTAINABLE ADSORBENTS FOR REMOVAL OF SYNTHETIC DYES FROM AQUEOUS SYSTEMS

M M Suraweera[1,2], N D Tissera[3], R N Wijesena[3], K A A Dilhari[4], G Priyadarshana[1*] 130

FERMENTATION PERFORMANCE OF SELECTED SRI LANKAN HERITAGE GRAINS FOR SPIRIT PRODUCTION UNDER ENZYME-FREE PROCESSING CONDITIONS

R H R W Lakshana[1], W M Y B Wanninayake[1], M L L Madhushan[1], D G Mallawaarachchi[1], W D M P L Malshan[1], G K Jayatunga[1*] 136

Track 5 – Digital Technologies, AI & Information Systems for Smart and Resilient Societies 142

TERRABOT: ENHANCED MODULAR PLATFORM WITH ON-DEVICE AI FOR PRECISION AGRICULTURE

Chanuka Jayasooriya[1*], Pasandul Kasthuri[1], Ravishan Hapukotuwa[1], Thosantha Thirandi[1], Heshadi Gayasha[1], A W C K Atugoda[1] 142

IDENTIFICATION OF THE EFFECTIVENESS OF USING STRUCTURED REFLECTION AND FLIPPED LEARNING TO MITIGATE MISCONCEPTIONS IN UML MODELLING

Pathini Lankika[1*], Chalini Silva[1], Shashika Ruwanmini[1] 149

ADAPTIVE DEEP REINFORCEMENT LEARNING FOR MISINFORMATION MANAGEMENT: A CRISIS-RESPONSE SIMULATION FRAMEWORK

L A S S S Samadhi[1*], P N T Pathirana[1] 155

DEVELOPMENT AND EVALUATION OF PHARMAAI: A HUMAN-CENTRED RULE-BASED EXPERT SYSTEM FOR MEDICATION SAFETY IN COMMUNITY PHARMACY

W S Kodippili[1*], K A D P Lankika[1], M P C M Silva[1] 162

MULTI-PARAMETER IoT SYSTEM FOR DISTRIBUTION TRANSFORMER CONDITION MONITORING: DESIGN AND PRELIMINARY VALIDATION

W M P L Nanayakkara[1*], M M K Munasinghe[1], H D O Tharinda[1], S M S N Rathnayake[1], Ms. Dinushi Ganepola[1], K W D C I Koswaththa[1] 169

EVALUATION OF OPEN-ACCESS AI TRANSLATION SYSTEMS FOR PRESERVING CULTURAL HERITAGE EXPRESSIONS

P N T Pathirana* 176

PREDICTING UNIVERSITY DROPOUT RISK USING MACHINE LEARNING

Y R C Ariyathilaka* 182

Track 6 (6A & 6B) – Social, Environmental & Ethical Renewal; Education in Times of Uncertainty 189

IDENTIFYING DOMINANT FACTORS ASSOCIATED WITH TUBERCULOSIS TREATMENT OUTCOMES IN THE KALMUNAI REGION, SRI LANKA: A LOGISTIC REGRESSION APPROACH

S A I M Samaraweera[1*], Hemalika T K Abeysundara[1] 189

STRIKING THE RIGHT NOTE: ENHANCING FOUNDATIONAL CALCULUS LEARNING THROUGH ACTIVE LYRIC COMPOSITION AND PERFORMANCE

K K T S Bandara* 195

FACTORS ASSOCIATED WITH SPORTS INJURY OCCURRENCE AMONG UNIVERSITY ATHLETES: A CASE STUDY FROM UVA WELLASSA UNIVERSITY, SRI LANKA

R P G Amithani[1*], D D G A D S Saparamadu[1] 201

MACROECONOMIC DETERMINANTS OF THE INDIAN RUPEE TO SRI LANKAN RUPEE EXCHANGE RATE: EVIDENCE FROM AN ARDL ANALYSIS

Nadunika Peiris[1*], Samanthi Mathugama[2], Ravindi Jayasundara[1] 207

RELATIONSHIP BETWEEN PARTICIPATION IN UNIVERSITY SPORTS AND FITNESS PROGRAMMES AND RESILIENCE AMONG UNIVERSITY STUDENTS

R G S Kaushalya Weerasinghe[*] 213

A NECROPOLITICAL ANALYSIS OF TAMIL TIGRESS BY NIROMI DE SOYZA AND IN THE SHADOW OF A SWORD BY ZAMILINI JEYAKUMARAN

U E Liyanarathna[*] 219

SHADOW TRAINING FOR ENHANCING PUBLIC SPEAKING SKILLS: EVIDENCE FROM ENGINEERING TECHNOLOGY UNDERGRADUATES

H G P Maheshika[1*], P B T K Premarathne[1] 224

THE STUDENTS' PERCEPTION OF AUTONOMY, COMPETENCE AND RELATEDNESS: A STUDY OF STUDENT MOTIVATION IN LEARNING ENGLISH THROUGH SELF-DETERMINATION THEORY

Bhagya Pabasarani[*] 229

EFFECTIVENESS OF PEER TEACHING ON MATHEMATICS FOR ENGINEERING STUDENTS: A CASE STUDY OF A LEADING UNIVERSITY IN SRI LANKA

Prabathara Erandi[1*], Ravindi Jayasundara[1] 234

EFFECT OF AN 8-WEEK PROGRESSIVE RESISTANCE TRAINING PROGRAM ON FULL-BODY FRONT-TURN MOVEMENT SPEED DURING THE SEOI-NAGE TECHNIQUE IN NOVICE JUDO ATHLETES

R M D L Rajasingha[1*]; S Othalawa[2] 241

PEDAGOGY OF STEAM EDUCATION IN NEPAL: FOSTERING INNOVATION IN THE CLASSROOM

Chudamani Phayal[1*] and Pooja Gupta[1] 246

Keynote Speech

Dr. Gina Maswabi

Commonwealth National Climate Finance Adviser for Sri Lanka

Harnessing Engineering, Technology and Climate Finance to Safeguard Humanity, Sustainability and Cultural Heritage in Times of Uncertainty

Synopsis

Global conflicts, climate change and economic instability increasingly threaten human well-being, essential infrastructure, livelihoods and cultural heritage. Engineering and technology offer vital solutions, but their responsible application requires a commitment to human dignity, sustainability and the protection of what communities value. Drawing on Sri Lanka's climate resilience priorities and wider Commonwealth experience, this keynote explores how renewable energy, resilient infrastructure and climate technologies can strengthen societies against interconnected risks. It examines the role of climate finance, institutional collaboration and investment planning in translating technological innovation into accessible, scalable and lasting solutions. Particular attention is given to ensuring that resilience investments protect vulnerable communities, sustain livelihoods and safeguard cultural heritage. The keynote argues that technological progress must be guided by human values and supported by financing that enables innovation to serve society, preserve heritage and advance sustainable development, even in times of profound uncertainty.

Plenary Speech

Mr. K.S. Venkatesh

Managing Director, SRP Synthetic Rubber Products Group of Industries, India

Business Leadership and Entrepreneurship

Synopsis

Entrepreneurial leaders do not simply run a business. They create long-term value, build products and systems that remain valuable for years, and demonstrate the importance of quality, engineering, innovation, and customer trust.

They think beyond existing procedures and systems and continuously seek new ideas, better methods and opportunities to solve problems. They contribute to economic growth by introducing innovative products, services, and technologies. They are problem-solvers and risk-takers who use creativity, knowledge, and persistence to achieve their goals.

Entrepreneurial leaders also share their knowledge and experience to develop future leaders. They believe that success is about more than making profits; it also means helping others and developing future generations. Entrepreneurial leaders believe that sharing knowledge helps people grow and improves the industry as a whole.

Special Speech

Mrs. M.M.P.D. Samarasekara

Senior Lecturer (Grade I), Division of Civil Engineering Technology, ITUM

From Credit Accumulation to Outcome-Based Engineering Technology Education

Synopsis

Engineering technology education should focus on developing graduates who can demonstrate the knowledge, skills and professional attributes required to address real-world engineering problems. However, curriculum development can become credit-driven, with subjects and contact hours converted into credits without adequately establishing the learning outcomes they are intended to achieve.

This presentation examines the shift towards outcome-based curriculum design, using the National Diploma in Technology (NDT) Civil Engineering Technology programme at the Institute of Technology, University of Moratuwa, as a case study. With reference to the Sri Lanka Qualifications Framework (SLQF) and Sydney Accord graduate attributes, it examines credit allocation, student workload, assessment evidence and the role of industrial training in developing professional competencies.

The presentation advocates designing curricula around graduate attributes, programme learning outcomes, appropriate learning experiences and assessment methods before determining realistic student workload and allocating credits. It concludes that credits should represent the learning effort required to achieve intended outcomes, rather than determine the structure and content of the curriculum.

ISSN: 2773-7055
Proceedings of the 5th International Research Conference
Institute of Technology, University of Moratuwa
November 5, 2026

Paper ID: 7

EXTRACTION AND CHARACTERIZATION OF NATURAL PIGMENTS FROM MARIGOLD (TAGETES ERECTA L.) FOR PLANT-BASED DYE APPLICATIONS

G K Jayatunga[1*], E M U M Ekanayaka[1], P A I Eranda[1], O D S Fonseka[1], N V E Harshani[1], W M Y B Wanninayake[1]

[1]Division of Polymer and Chemical Engineering Technology, Institute of Technology, University of Moratuwa, Homagama, Sri Lanka

*Corresponding author: gayanij@itum.mrt.ac.lk

ABSTRACT: Natural pigments derived from plant sources have attracted increasing attention as sustainable alternatives to synthetic colorants due to their biodegradability, non-toxicity, and potential environmental benefits. Marigold (*Tagetes erecta* L.) flowers are rich in carotenoid pigments and represent a promising source of natural dyes for industrial applications. This study investigated the extraction and characterization of pigments from locally cultivated marigold flowers in Sri Lanka. Fresh marigold petals were subjected to Soxhlet extraction using hexane as the solvent, and the effect of extraction time (30min , 1h , 2 h and 3 h) on pigment yield was evaluated. The moisture content of the petals was determined by the oven-drying method and was found to be 91.3%(for 2h and 3h samples) and 86.18%(for 30min and 1h samples) on a wet basis. The pigment yield increased from 6.729% to 30.64% on a dry basis when the extraction time was increased from 30min to 3 h, indicating improved extraction efficiency with longer solvent contact time. The extracted pigment appeared as a dark orange concentrate characteristic of carotenoid-rich compounds. Fourier-Transform Infrared (FTIR) spectroscopy revealed the presence of O–H, C–H, C=O, C=C, and C–O functional groups, confirming the presence of carotenoid-based pigments and related lipid compounds. The results demonstrate that a 3 h Soxhlet extraction period is more effective for pigment recovery than other extraction time periods. This study highlights the potential of locally cultivated marigold flowers as a sustainable source of natural pigments for applications in textile, cosmetic, and pharmaceutical industries.

Keywords: marigold flower, Soxhlet extraction, FTIR, color pigment, sustainability

1 INTRODUCTION

Natural pigments derived from botanical sources have gained considerable attention in recent years due to their biodegradability, non-toxicity, and health-promoting antioxidant properties. Their utilization aligns with the principles of sustainability and the circular economy by promoting the use of renewable biological resources, reducing dependence on synthetic chemicals, and minimizing environmental pollution. Consequently, natural pigments are increasingly being adopted in the food, pharmaceutical, and textile industries as eco-friendly alternatives to synthetic colorants. The valorization of plant-based materials for pigment extraction further contributes to resource efficiency and waste reduction, supporting the transition towards more sustainable production and consumption systems(Dey et al., 2025).

Marigold (*Tagetes erecta L.*) is one of the most widely cultivated ornamental flowering plants in tropical and subtropical regions worldwide. Although native to Mexico and Central America, it is extensively grown in many Asian countries, including Sri Lanka, where it is cultivated for ornamental, religious, and commercial purposes. (Kumari et al., 2025). Its abundant availability and high carotenoid content make it a promising source of natural pigments for sustainable dye applications. The extracted pigments of Marigold flowers have potential applications in textile

dyeing, food coloring, cosmetics, pharmaceuticals, and biodegradable materials (Qiu et al., 2024).

Flower pigments are typically extracted using solvent extraction methods at large scale, which are carried out in mechanically agitated stirred tank reactors or counter-current solvent extraction systems. As a more environmentally friendly alternative, supercritical CO_2 extraction can also be employed for pigment recovery. In laboratory-scale studies, Soxhlet extraction is commonly used for preliminary extraction and method evaluation (Chauhan et al., 2022).

Hexane, being a non-polar solvent, selectively extracts carotenoid pigments from marigold flowers, resulting in relatively pure pigment fractions, whereas polar solvents such as ethanol and methanol extract a broader range of bioactive compounds including carotenoids, chlorophylls, and phenolics, though with lower selectivity. The efficiency of extraction is highly dependent on the operational parameters like the type of solvents, sample-to-solvent ratio, and contact time. Too little extraction will reduce solvent penetration and/or solute mass transfer, while too much heat exposure will weaken the structure of the heat-sensitive carotenoids. This extraction behavior must be understood to evaluate the effect of extraction time on pigment recovery. Qualitative analysis using Fourier-Transform Infrared (FTIR) spectroscopy is necessary to ensure that these target compounds were successfully recovered without damage, as it would reveal the important chemical bonds and functional backbones.

Although extensive research has been conducted on pigment extraction from *Tagetes erecta* L., most studies are based on non-local cultivars and controlled conditions, with limited focus on Sri Lankan-grown marigold varieties (Kumari et al., 2025). In addition, there is insufficient information on the effect of extraction time on pigment yield for locally cultivated flowers, and limited integration of yield extraction time evaluation with FTIR-based characterization in natural dye studies. Therefore, further investigation is required to evaluate extraction efficiency and characterize pigments from Sri Lankan marigold varieties for sustainable dye applications.

The objective of this study is to evaluate the effect of extraction time (30 min, 1 h, 2 h, and 3 h) on the yield recovery of natural pigments from marigold flowers of a locally cultivated variety in Sri Lanka, and to use FTIR to characterize the functional groups of the isolated natural pigment. This enables the effect of extraction time on pigment yield to be compared under the experimental conditions used in this study.

2 METHODOLOGY

Fresh marigold flowers were collected from Horana, Sri Lanka and thoroughly washed with distilled water to remove dust and adhering contaminants. The petals were separated from the flower heads and subsequently shade-dried for about 30 minutes to eliminate surface moisture prior to further processing.

The moisture content of fresh marigold flower petals after shade drying was determined using the oven-drying method. Approximately 5g of sample was accurately weighed using an analytical balance and placed in an oven. The sample was dried at 102 $^{\circ}$C until a constant weight was achieved. The moisture content was calculated based on the difference in mass of the sample before and after drying to constant weight.

Twenty grams of marigold petals were weighed and placed in a cellulose thimble, which was then inserted into a Soxhlet apparatus. Two hundred milliliters of hexane were added to a round-bottom flask as the extraction solvent. The system was heated using a heating mantle, and the temperature was maintained between 65–70 $^{\circ}$C to ensure steady solvent reflux near the boiling point of hexane. The extraction was carried out for different time periods (30cmin, 1h , 2 h and 3 h) to evaluate the effect of extraction time on pigment yield.

After completion of extraction, the solvent containing dissolved pigments was collected and concentrated by evaporation at low temperature (60 $^{\circ}$C) in an oven. The yield of the extracted pigment was determined from the weight difference between the empty round-bottom flask and the flask containing the dried pigment extract. The analytical balance (Kern ABJ 200-4CM) and a hot air oven (Memmert UF110) were used for the experiments.

The resulting concentrated extract yielded a dark orange pigment, which was recovered for further Fourier Transform Infrared (FTIR) analysis. Figures 1(a) and 1(b) illustrate the fresh Marigold flowers used in the experiment and the extracted pigment obtained after processing.



(a) (b)

Figure 1. (a) Fresh Marigold flowers (b) Extracted Marigold flower pigment

FTIR spectroscopy was performed on the extracted pigment sample to identify the functional groups and major compounds present. The FTIR spectrum was analyzed based on characteristic absorption peaks corresponding to different chemical bonds and functional groups.

3 RESULTS AND DISCUSSION

The oven-drying method was used to determine the moisture content of fresh marigold petals. The average moisture content on a wet basis was found to be 91.3 %(for 2 h and 3 h samples) and 86.18 % (for 30 min and 1 h samples), indicating that fresh marigold petals contain a high proportion of water.

Pigment extraction was carried out using Soxhlet extraction for four extraction periods: 30 min, 1 h ,2 h and 3 h. The yield of the extracted pigment was determined gravimetrically from the weight difference between the empty round-bottom flask and the flask containing the dried pigment extract. Table 1 presents the pigment yield obtained at different extraction times.

Table 1. Effect of yield of color pigment with extraction time

Sample	Extraction time	Yield percentage % (dry basis)	Yield percentage % (wet basis)
1	30min	6.73	0.93

Sample	Extraction time	Yield percentage % (dry basis)	Yield percentage % (wet basis)
2	1h	12.07	1.66
3	2h	15.09	1.31
4	3h	30.64	2.67

The extraction time had a significant effect on pigment recovery. Increasing the extraction time from 2 h to 3 h increased the pigment yield from 15.09 % to 30.64 % on a dry basis and from 1.31% to 2.67% on a wet basis. This improvement can be attributed to the longer contact time between the solvent and the plant material, which enhances solvent penetration into the plant matrix and promotes the diffusion of carotenoid pigments into the extraction solvent. The results indicate that 3 h extraction period was more effective for recovering pigments from marigold petals under the experimental conditions employed in this study. Figure 2 shows the FTIR spectrum of the pigment extracted from marigold petals after 3 h of Soxhlet extraction, while Table 2 presents the corresponding absorption bands and their assignments.

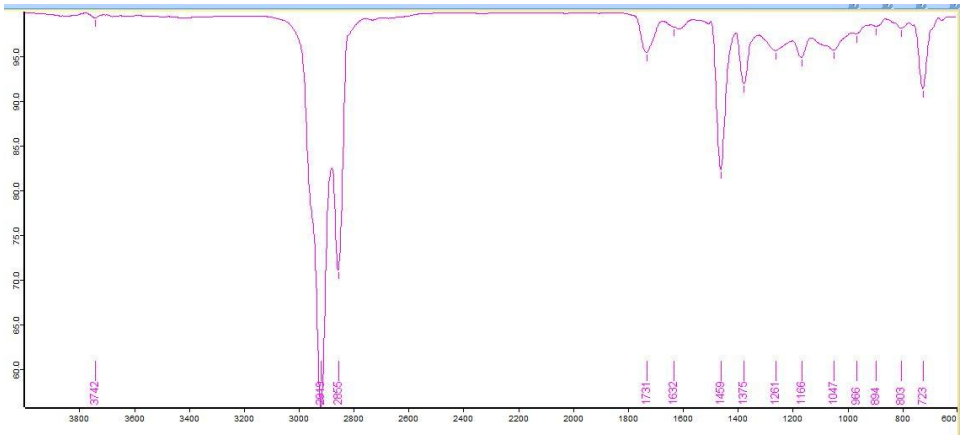


Figure 2. FTIR Spectrum of the pigment extracted from marigold petals

Table 2. FTIR absorption bands of the extracted marigold pigment and their possible compounds

Peak (cm^{-1})	**Functional Group**	**Possible Compound/Meaning**
3742	O–H stretching	Alcohols or phenolic compounds (small amount of moisture or hydroxyl compounds)
2920 and 2855	C–H stretching	Alkanes and long hydrocarbon chains commonly found in carotenoids, lipids, and essential oils
1731	C=O stretching	Ester or carbonyl groups, indicating carotenoids, fatty acids, or pigments
1632	C=C stretching	Unsaturated compounds and conjugated double bonds present in carotenoids
1459	CH_2 bending	Aliphatic compounds and hydrocarbons
1375	C–H bending	Methyl groups in organic compounds
1261 and 1168	C–O stretching	Esters and ether compounds
1047	C–O or C–C stretching	Alcohols and polysaccharide-related compounds
966, 894, 803, 723	=C–H bending	Unsaturated compounds and aromatic/aliphatic structures

As shown in Figure 2 and Table 2, the FTIR spectrum confirms that the extracted marigold pigment is primarily composed of carotenoids (the natural compounds giving marigolds their characteristic color) alongside plant lipids and fatty acid esters. The prominent peaks at 2920 and

2855 cm^{-1} represent the strong C–H stretching of long hydrocarbon chains, while key absorption bands at 1731 cm^{-1} (C=O stretching) and 1632 cm^{-1} (C=C stretching) highlight the ester groups and conjugated double bonds essential to carotenoid structures.

The FTIR analysis confirms that the hexane extract of marigold flowers contains carotenoid-based pigments along with lipid and ester compounds. The presence of characteristic bands corresponding to C–H, C=O, C=C, and C–O functional groups is consistent with previous studies reporting FTIR identification of carotenoids such as lutein in *Tagetes erecta L.* extracts (Saisugun & Sasidhar, 2019).

4 CONCLUSION

Natural pigments were successfully extracted from locally cultivated marigold (*Tagetes* erecta L.) petals using Soxhlet extraction with hexane as the solvent. Increasing the extraction time from 30min to 3 h increased the pigment yield from 6.729 % to 30.64 % on a dry basis, demonstrating improved extraction efficiency. FTIR analysis confirmed the presence of characteristic functional groups associated with carotenoid-based pigments, including O–H, C–H, C=O, and C=C bonds. The results indicate that a 3 h extraction period is more effective for pigment recovery than other time periods and that marigold flowers cultivated in Sri Lanka have potential as a sustainable source of natural colorants.

5 ACKNOWLEDGEMENTS

Authors acknowledge the Division of Polymer and Chemical Engineering Technology, ITUM for providing the laboratory facilities for the experimentation. Also, authors wish to acknowledge assistance given by laboratory assistants; Mrs. H. H. Galagedara and Mr. S.H.C.P. Senarathna.

6 REFERENCES

Chauhan, A. S., Chen, C.-W., Singhania, R. R., Tiwari, M., Sartale, R. G., Dong, C.-D., & Patel, A. K. (2022). Valorizations of marigold waste for high-value products and their industrial importance: A comprehensive review. *Resources*, *11*(10), 91.

Dey, P., Dey, P., Hoque, M. B., Baria, B., Rahman, M. M., Shovon, S., & Das, D. (2025). Sustainable and eco-friendly natural dyes: A holistic review on sources, extraction, and application prospects. *Textile Research Journal*, *95*(19–20), 2472–2499.

Kumari, S. S., Attanayake, A. M. A. S., & Eeswara, J. P. (2025). Evaluation of yield performance of local and imported marigold (Tagetes erecta L.) varieties. *Ceylon Journal of Science*, *54*(4), 1011–1021. https://doi.org/10.4038/cjs.v54i4.8499

Qiu, Y., Wang, R., Zhang, E., Shang, Y., Feng, G., Wang, W., Ma, Y., Bai, W., Zhang, W., Xu, Z., Shi, W., & Niu, X. (2024). Carotenoid biosynthesis profiling unveils the variance of flower coloration in *Tagetes erecta* and enhances fruit pigmentation in tomato. *Plant Science*, *347*, 112207. https://doi.org/10.1016/j.plantsci.2024.112207

Saisugun, J., & Sasidhar, R. L. C. (2019). Extraction and biological evaluation of esterified lutein from marigold flower petals. *J Pharmacogn Phytochem*, *8*(4), 3403–3410

ISSN: 2773-7055
Proceedings of the 5th International Research Conference
Institute of Technology, University of Moratuwa
November 5, 2026

Paper ID: 16

DRYING KINETICS AND EXTRACTION OF OLEORESIN FROM MORINGA OLEIFERA LEAVES USING CONVECTION TRAY DRYER

G K Jayatunga[1*], L K C A Hasarangi[1], K P S S Jayawickrama[1], W A M Geethma[1]

[1]Division of Polymer and Chemical Engineering Technology, Institute of Technology, University of Moratuwa, Homagama, Sri Lanka

*Corresponding author: gayanij@itum.mrt.ac.lk

ABSTRACT: *Moringa oleifera* leaves are an important source of nutrients and bioactive phytochemicals with potential applications in the food, pharmaceutical, and cosmetic industries. Drying is a critical pre-treatment that improves storage stability and extraction efficiency while preserving product quality. This study investigated the drying kinetics of *Moringa oleifera* leaves using a laboratory-scale convection tray dryer operated at 48 °C and an air velocity of 2.1 m/s. Moisture ratio, drying rate, and effective moisture diffusivity were determined to characterize the drying process. Subsequently, oleoresin and essential oil were extracted from the dried leaves using Soxhlet extraction with hexane and hydro-distillation using a Clevenger apparatus, respectively. The extracted oleoresin was further characterized by Fourier Transform Infrared (FTIR) spectroscopy. Fresh leaves contained approximately 75% moisture (wet basis). The drying process occurred entirely in the falling-rate period, indicating that internal moisture diffusion governed moisture transport. The effective moisture diffusivity was estimated as 1.14×10^{-10} m^2 /s. Soxhlet extraction produced an oleoresin yield of 2.55 % (w/w), while hydro-distillation yielded 2.00% (v/w) of essential oil. FTIR analysis confirmed the presence of lipid-rich phytochemicals, including aliphatic hydrocarbons, carbonyl-containing compounds, and phenolic constituents. The results demonstrate that convective tray drying is an effective pre-treatment for the recovery of value-added bioactive products from *Moringa oleifera* leaves and provide useful engineering data for the design and optimization of drying and extraction processes.

Keywords: Moringa oleifera, convective tray drying, moisture diffusivity, oleoresin extraction, FTIR

1 INTRODUCTION

Moringa oleifera Lam., commonly known as the drumstick tree, is widely cultivated in Sri Lanka and consumed as both a vegetable and a traditional medicinal plant. Its leaves possess exceptional nutritional value, being rich in proteins, dietary fiber, vitamins (A, C, and E), essential minerals, and bioactive phytochemicals such as polyphenols, flavonoids, carotenoids, and chlorophyll derivatives (Gopalakrishnan et al., 2016). Owing to their nutritional and phytochemical richness, *Moringa* leaves have attracted considerable interest as a source of value-added products, particularly oleoresins and essential oils. Oleoresins are obtained through solvent extraction and contain both volatile and non-volatile bioactive compounds, whereas essential oils are recovered by hydro-distillation and consist mainly of volatile aromatic compounds. These extracts exhibit antioxidant, preservative, flavoring, and therapeutic properties, making them valuable ingredients in food, pharmaceutical, and cosmetic applications (Leone et al., 2015).

Freshly harvested *Moringa oleifera* leaves have a high moisture content, making them susceptible to microbial spoilage and enzymatic deterioration during storage. Drying is therefore an essential pre-treatment that extends shelf life and improves extraction efficiency. Although traditional methods such as sun and shade drying are simple and economical, they are weather-dependent

and may result in non-uniform drying, contamination, and degradation of heat-sensitive bioactive compounds (Jayatunga and Amarasinghe, 2015).Artificial drying techniques, including packed-bed, fluidized-bed, and convection tray drying, provide better control over processing conditions and product quality. Among these, convection tray drying is widely employed because of its operational simplicity, low cost, and ability to achieve uniform drying under controlled conditions (Dissanayake et al., 2025) and (Jayatunga et al., 2025). Understanding the drying kinetics of Moringa leaves is therefore essential for optimizing moisture removal and enhancing the quality and yield of subsequent extracts.

Although the nutritional properties, drying behavior, and bioactive compound extraction of *Moringa oleifera* leaves have been widely studied, limited engineering data are available on convective tray-drying kinetics, effective moisture diffusivity, and their relationship to oleoresin recovery. Therefore, this study aimed to investigate the drying kinetics and effective moisture diffusivity of *Moringa oleifera* leaves during convective tray drying, determine the yields of oleoresin and essential oil extracted from the dried leaves, and characterize the oleoresin using Fourier Transform Infrared (FTIR) spectroscopy.

2 METHODOLOGY

Fresh *Moringa oleifera* leaves were collected from a residential ecosystem in Piliyandala, Sri Lanka. Healthy green leaves were separated from the stems, washed thoroughly to remove adhering impurities, and surface-dried before the experiments. Drying was carried out in a laboratory-scale convection tray dryer (GUNT CE 130) at an air temperature of 48 °C and an air velocity of 2.1 m/s for around 2 h. The leaves were uniformly spread on vertically stacked trays to ensure uniform airflow. Sample weight was recorded at regular intervals using the integrated weighing system to monitor moisture loss. Ambient temperature and relative humidity were measured using an EXTECH EasyView™ Digital Hygro-Thermometer (Model EA20), while air velocity was monitored using an EXTECH Vane Thermo-Anemometer (Model SDL300). The initial moisture content was determined by the oven-drying method (Memmert UF110). Moisture ratio, drying rate, and effective moisture diffusivity were subsequently determined to evaluate the drying characteristics of the leaves. All samples were weighed using an analytical balance (Kern ABJ 200-4CM).

For oleoresin extraction, 10 g of dried *Moringa* leaves was extracted with 150 ml of hexane in a Soxhlet apparatus for 3 h. The solvent was then evaporated to obtain the oleoresin, and the extraction yield was calculated based on the dry mass of the leaves. Essential oil extraction was performed by hydro-distillation using a Clevenger-type apparatus. A 100 g sample of dried leaves was mixed with 1500 ml of distilled water and distilled for 3 h. The essential oil collected in the graduated receiver was measured directly, and the extraction yield was determined.

The oleoresin obtained by Soxhlet extraction was characterized using Fourier Transform Infrared (FTIR) spectroscopy to identify its principal functional groups based on the characteristic absorption bands in the recorded spectra.

3 RESULTS AND DISCUSSION

The initial moisture content of fresh *Moringa oleifera* leaves, determined by the oven-drying method, was approximately 75 % (wet basis), indicating the need for drying prior to storage and extraction. Figure 1 illustrates the moisture content variation with time for *Moringa oleifera* leaves during convective tray drying at 48 °C. Moisture removal was rapid during the initial stage of drying due to the evaporation of unbound moisture from the leaf surface. As drying progressed, the moisture content decreased gradually, resulting in a continuous reduction in the drying rate. This behavior indicates that moisture migration was predominantly controlled by internal diffusion, consistent with Fick's second law of diffusion.

The drying rate continuously decreased with both drying time and moisture content, confirming that the drying process occurred entirely in the falling-rate period. No constant-rate period was observed, suggesting that surface moisture was removed rapidly and that subsequent moisture transport was governed by diffusion from the interior of the leaf tissue to the surface. This drying behavior is characteristic of many leafy agricultural materials, including spinach, basil, tea, curry leaves, and Moringa oleifera, where moisture movement is predominantly diffusion-controlled after a short initial period (Doymaz, 2006; Thuy et al., 2025).

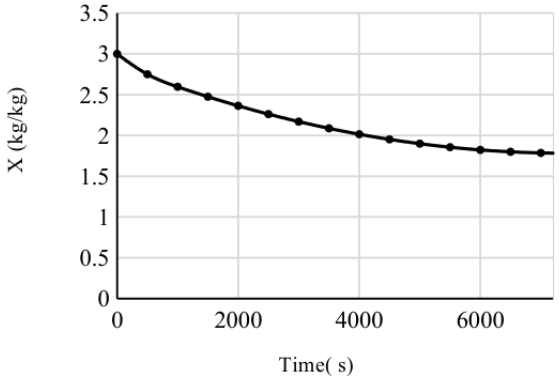


Figure 1. Moisture content versus drying time of Moringa oleifera leaves.

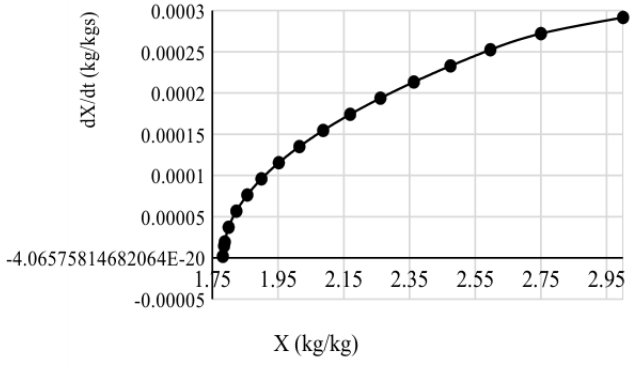


Figure 2. Rate of change of moisture removal vs drying time for *Moringa oleifera* leaves

The effective moisture diffusivity (D_{eff}) was estimated from the linear relationship between Ln(Moisture ratio) and drying time using the analytical solution of Fick's second law for an infinite slab. Since the leaf thickness was not measured experimentally, a literature value of 0.40

mm was assumed for fresh *Moringa oleifera* leaves, corresponding to a half-thickness of 0.20 mm**.** Based on the regression analysis, the effective moisture diffusivity at 48 °C was determined as 1.14 × 10^{-10} m^2 /s**.** The estimated diffusivity falls within the range commonly reported for leafy biological materials and is comparable with values reported for spinach, basil, tea, and curry leaves, indicating that internal moisture diffusion is the dominant mechanism governing moisture transport during convective drying (López-Ortiz et al., 2023) & (Anuththara et al., 2019).

The process parameters and extraction yields are summarized in Table 1. Soxhlet extraction using hexane produced an oleoresin yield of 2.55% (w/w), while hydro-distillation using a Clevenger apparatus yielded 2.00 % (v/w) of essential oil. The higher recovery obtained by solvent extraction can be attributed to the ability of hexane to dissolve a broad range of lipophilic constituents, including fatty acids, pigments, waxes, and other non-polar phytochemicals. In contrast, hydro-distillation primarily recovers volatile aromatic compounds, resulting in a comparatively lower yield.

Table 1. Process Parameters and Extraction Yields for Moringa oleifera Leaves

Extraction Method	Mass of Leaves (g)	Liquid Volume (ml)	Process Time (h)	Final Yield
Hexane Solvent Extraction	10 g	150 ml	3 hours	0.2551 g (2.55% w/w)
Clevenger Hydro-Distillation	100 g	1500 ml	3 hours	2.0000 ml (2.00% v/w)

The FTIR spectrum of the hexane-extracted *Moringa oleifera* oleoresin shown in Figure 3 revealed characteristic bands associated with non-polar bioactive compounds. Strong absorption peaks at 2920 and 2850 cm^{-1} correspond to aliphatic C–H stretching vibrations of lipids and fatty acids, while the bands at 1728 and 1704 cm^{-1} indicate carbonyl (C=O) groups of esters and fatty acid derivatives. The peak at 1505 cm^{-1} suggests the presence of phenolic compounds, which are known for their antioxidant properties. Absorption bands in the region of 1164–1057 cm^{-1} are attributed to C–O stretching vibrations of oxygenated organic compounds.

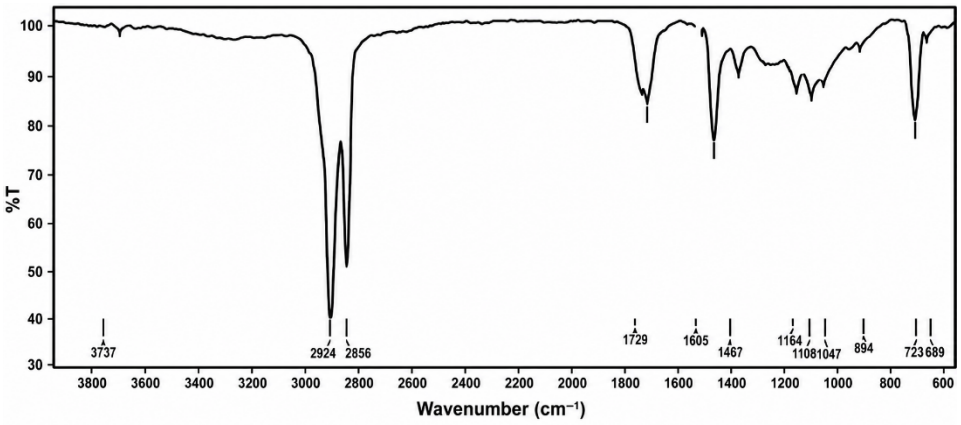


Figure 3. FTIR Spectrum of Moringa oleoresin

As hexane is a non-polar solvent, the oleoresin predominantly contains lipophilic constituents such as fatty acids, pigments, and phenolic compounds, whereas polar compounds including

vitamin C and proteins are not expected to be extracted efficiently. Overall, the FTIR analysis confirmed that the oleoresin obtained from tray-dried *Moringa oleifera* leaves contains lipid-rich phytochemicals together with antioxidant-associated functional groups, demonstrating the suitability of convective tray drying as a pretreatment for the recovery of valuable bioactive compounds.

4 CONCLUSION

Convective tray drying at 48 $^{\circ}$C effectively reduced the moisture content of *Moringa oleifera* leaves from approximately 75 % (wet basis) to a level suitable for extraction. The drying process occurred entirely within the falling-rate period, indicating that internal moisture diffusion was the dominant mechanism governing moisture transport. The effective moisture diffusivity was determined to be 1.14×10^{-10} m^2 /s, which is consistent with values reported for similar leafy materials.

The dried leaves yielded 2.55 % (w/w) oleoresin through Soxhlet extraction with hexane and 2.00 % (v/w) essential oil through hydro-distillation. FTIR analysis confirmed that the oleoresin contained characteristic functional groups associated with lipophilic phytochemicals, including fatty acids, esters, and phenolic compounds with antioxidant potential. These findings demonstrate that convective tray drying is an appropriate pre-treatment for preserving the quality of *Moringa oleifera* leaves and enhancing the recovery of value-added bioactive products. The engineering data generated in this study can contribute to the optimization of drying and extraction operations for the commercial utilization of Moringa leaves.

5 ACKNOWLEDGEMENTS

Authors acknowledge the Division of Polymer and Chemical Engineering Technology, ITUM for providing the laboratory facilities for the experimentation. Also, authors wish to acknowledge assistance given by Mrs. Kasuni Samarasinghe.

6 REFERENCES

Dissanayake, D., Abesekara, M. S., Amarasinghe, B., & Jayatunga, G. K. (2025). Investigation of drying characteristics and estimation of mass transfer parameters of Sri Lankan black pepper dried in a batch fluidized bed dryer. *Sri Lankan Journal of Applied Sciences*, *3*(2). https://sljoas.sljol.info/articles/1

Gopalakrishnan, L., Doriya, K., & Kumar, D. S. (2016). *Moringa oleifera*: A review on nutritive importance and its medicinal application. *Food Science and Human Wellness*, *5*(2), 49–56. https://doi.org/10.1016/j.fshw.2016.04.001

Jayatunga, G. K., & Amarasinghe, B. (2015). Mathematical modeling of drying kinetics of black pepper in a spouted bed dryer with and without non porous draft tubes. *2nd International Conference on Trends in Multidisciplinary Business and Economic Research (TMBER)*, 118–134.

Jayatunga, G. K., Rathnayake, R., & Thilakarathne, N. (2025). *DETERMINATION OF MOISTURE DIFFUSIVITY OF KOHILA DRYING IN A CONVECTION TRAY DRYER*. 44. https://irc.itum.mrt.ac.lk/conference_proceedings.pdf#page=62

Leone, A., Spada, A., Battezzati, A., Schiraldi, A., Aristil, J., & Bertoli, S. (2015). Cultivation, Genetic, Ethnopharmacology, Phytochemistry and Pharmacology of Moringa oleifera Leaves: An Overview. *International Journal of Molecular Sciences*, *16*(6), 12791–12835. https://doi.org/10.3390/ijms160612791

ISSN: 2773-7055
Proceedings of the 5th International Research Conference
Institute of Technology, University of Moratuwa
November 5, 2026

Paper ID: 24

DEVELOPMENT OF NON-CONVENTIONAL CREAM CHEESE ANALOGUE USING SOYA MILK AND PEANUT PASTE: EFFECT OF FORMULATION ON PHYSICOCHEMICAL AND TEXTURAL PROPERTIES

W V W H Wickramaarachchi[1*], C D A Samarasekara[1], S O M T H Samarasekara[1], L A Sanchila[1], S D S Sankalpana[1], W M Y B Wanninayake[1]

[1]Division of Polymer and Chemical Engineering Technology, Institute of Technology, University of Moratuwa, Homagama, Sri Lanka

*Corresponding author: wathsalav@itum.mrt.ac.lk

ABSTRACT: The increasing demand for plant-based dairy alternatives has encouraged the development of non-conventional cream cheese analogues using sustainable protein sources. This study investigated the effect of different soya milk and peanut paste formulations on the physicochemical and textural properties of cream cheese analogues. Five formulations containing varying proportions of soya milk and peanut paste (100:0, 75:25, 66.7:33.3, 50:50, and 0:100, wt%) were prepared by acid coagulation using vinegar. The products were evaluated for yield, moisture content, pH, whey drainage, and texture profile characteristics. The results showed that formulation significantly influenced the quality attributes of the cream cheese analogue. Product yield increased with peanut paste incorporation up to 33.3 wt% before decreasing markedly at the 50:50 formulation, while the peanut-only formulation exhibited the highest yield (32.1%). Moisture content followed a similar trend and remained within the acceptable range for fresh cream cheese analogues. Cream cheese pH ranged from 5.13 to 5.80, indicating successful acidification of all formulations. Texture profile analysis revealed that partial substitution of soya milk with peanut paste reduced hardness, whereas formulations containing 50 wt% and 100 wt% peanut paste exhibited hardness values comparable to the control, suggesting the formation of a denser protein–lipid matrix. The findings demonstrate that the proportion of soya milk and peanut paste plays a critical role in determining the physicochemical and textural properties of plant-based cream cheese analogues and provide useful information for developing affordable, non-dairy cream cheese products.

Keywords: cream cheese analogue, soya milk, peanut paste, textural analysis, physicochemical properties

1 INTRODUCTION

Cream cheese is a soft, fresh, unripened cheese characterized by its mild flavor, smooth spreadable texture, and high moisture content. It is widely used in culinary applications from bakery products to savory spreads. Conventionally, cream cheese is manufactured from full-fat dairy milk or cream through acidification and heat treatment, yielding a product with approximately 33% fat and moisture not exceeding 55% (Fox et al., 2017). However, dependence on animal-derived dairy inputs, escalating production costs, the global prevalence of lactose intolerance, and the growing consumer preference for vegetarian and vegan diets have collectively driven demand for plant-based dairy alternatives (Foegeding & Drake, 2007).

Vegetarian or plant-based cream cheeses are commonly produced using cashew nuts, almonds, soybeans, coconut oil, and oats owing to their favorable protein and lipid compositions, which contribute to desirable textural and sensory characteristics (Fox et al., 2017). Among plant-based raw materials, soya milk is considered one of the most suitable bases for cream cheese analogues because its major storage proteins, glycinin and β-conglycinin, undergo acid-induced gelation,

forming a stable protein network similar to that of dairy cheese. In addition, soya milk possesses good water-holding, emulsifying, and gel-forming properties, enabling the production of soft, spreadable cheese-like products (Kanauchi et al., 2015). Despite this, soya-based cream cheese analogues remain underexplored in systematic formulation studies, particularly regarding the incorporation of complementary legume-based ingredients (Liu, 1997). The dietary alternatives of plant-based products are developed to reproduce the nutritional, functional, and sensory properties of conventional dairy products (McClements & Grossmann, 2021).

Peanuts (Arachis hypogaea) are an affordable and protein-dense legume, widely cultivated in tropical regions, including Sri Lanka. Peanut paste, produced by grinding roasted peanuts, contributes both lipid (~50% fat) and protein fractions that can influence the texture, body, and flavour profile of a cheese-type product. The lipid component may serve as a functional ingredient, improving creaminess and mouthfeel in the analogue (Huang et al., 2011). To date, limited research has investigated the combined use of soya milk and peanut paste as co-bases for cream cheese analogue production. This trend is driven by concerns over animal welfare, environmental sustainability, lactose intolerance, and the growing popularity of vegan and flexitarian diets (Short et al., 2021).

This study, therefore, aimed to evaluate five soya–peanut cream cheese analogue formulations, examining the effect of varying soya and peanut proportions on yield, pH, moisture content, whey drainage, and textural hardness. The outcomes are intended to inform the development of an affordable, plant-based cream cheese product suitable for small-scale production in Sri Lanka.

2 METHODOLOGY

2.1 Raw Material Preparation

Soya milk was prepared from commercially available dried soyabeans soaked overnight (1:3 w/v, soyabean: water), drained, ground with fresh water (1:10 w/v), filtered through a double-layered muslin cloth to remove okara, and boiled for 10 minutes. Peanut paste was prepared by dry-roasting raw peanuts at 160 C for 20 minutes, removing skins, and grinding to a smooth paste in a food processor. Commercially available distilled white vinegar (5% acidity, v/v) was used as the acidulant.

2.2 Formulation Design and Processing

Five experimental formulations (Table 1) were prepared by varying soya milk and peanut paste proportions with fixed water addition (300 g) and vinegar (6 g). Each mixture was heated to 80 $^{\circ}$C with continuous stirring. Vinegar was added dropwise until complete curd formation was observed. The curd was then drained through cheesecloth, placed in a mould, and pressed at 4 $^{\circ}$C for 24 hours. All products were aged at 4°C for a total of 6 days before analysis.

Table 1. Formulation details of soya–peanut cream cheese analogues

Sample notation	Soya Milk (wt %)	Peanut Paste (wt %)	Water (g)	Vinegar (g)
S100:P0	100	0	300	6
S75:P25	75	25	300	6
S66.7:P33.3	66.7	33.3	300	6
S50:P50	50	50	300	6
S0:P100	0	100	300	6

2.3 Physicochemical Analysis

The yield of the cream cheese analogue was calculated using the weight of the final product after pressing according to Equation (1). The final product weight was measured using a digital balance with an accuracy of ±0.1 g.

$$Yield\ (\%) = \frac{Final\ cream\ cheese\ weight\ (g)}{Soya\ milk\ weight\ (g) + Peanut\ milk\ weight(g)} \times 100 \quad (1)$$

Cream cheese pH and whey pH were measured using a calibrated digital pH meter (HANNA Instruments, accuracy ±0.01).
Moisture content (%) was determined gravimetrically by drying 5 g samples at 105°C to constant weight and calculating weight loss.
Whey volume (ml) was collected and measured during the draining and pressing stage.

2.4 Texture Profile Analysis

Texture profile parameters were evaluated by penetration test using a cylindrical probe (diameter 10 mm) penetrating each sample to a depth of 10 mm at a constant speed of 1 mm/s. The maximum force at penetration (g) was recorded. Three replicates per formulation were analysed, and mean values are reported.

3 RESULTS AND DISCUSSION

3.1 Product Yield and Moisture Content

Figure 1 illustrates the variation in yield and moisture content of cream cheese produced at different ratios of soya milk to peanut paste. Yield improves up to 33.33 % peanut paste, and it drastically drops at 50 %. The lowest yield was seen with the 50:50 soya milk–peanut paste formulation. This can be attributed to the differences in behaviour of soya and peanut protein when mixed together in a 1:1 ratio. Perhaps their combination yielded a softer curd, which led to more protein and solids loss into the whey during separation. Thereby, less curd was left to recover, resulting in a low yield. This reduction may be attributed to poor protein coagulation and increased loss of solids into the whey due to the interaction between soya proteins and peanut components at equal proportions (Zhang et al., 2022). Peanut paste-only formulation produced the highest yield (32.1%). This indicates that peanut protein and lipids stayed in the curd more efficiently during coagulation. Another reason might be the high fat content of peanut paste.

The fat in peanut paste might have helped in making a compact curd that did not lose much during whey drainage, and hence a greater amount of cream cheese was recovered (Zhang et al., 2022).

The moisture content of the prepared cream cheese shows the same trend as the yield. Moisture content increases up to 25 % peanut paste, and adding more peanut paste to soya milk increases the moisture content. This indicates that incorporation of moderate peanut paste enhances the water-retaining capacity of the protein network. At 100% peanut paste, the moisture content increased again to 55.2 %, reflecting the ability of peanut proteins and lipids to retain moisture within the cheese matrix (Wei et al., 2026). All moisture values fall within the broad moisture range reported for fresh acid-coagulated cheese analogues (40–60 %), suggesting all formulations are physicochemically acceptable (Walstra et al., 2006).

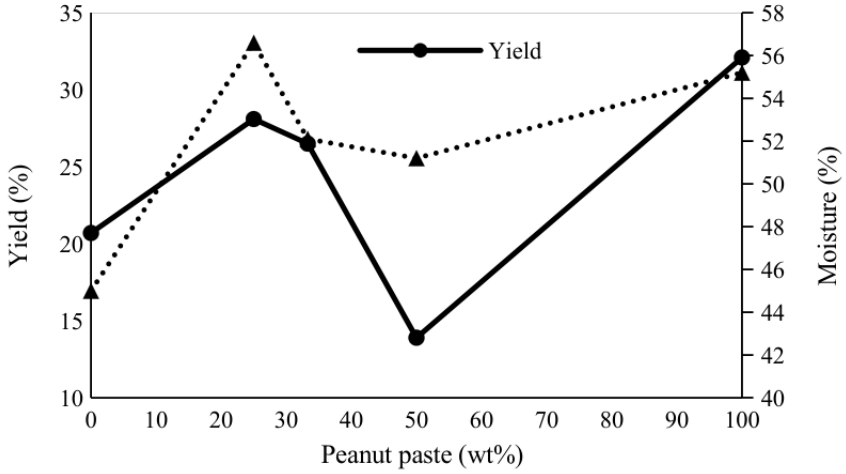


Figure 1. The variation of yield and moisture content of cream cheese in different formulas

3.2 pH of Cream Cheese and Whey

Cream cheese pH values ranged from 5.13 to 5.80 (Figure 2), indicating that acidification occurred across all formulations. Most formulations were within or close to the typical pH range reported for fresh cream cheese-type products (4.9–5.4) (Fox et al., 2017). peanut-only sample exhibits the highest curd pH (5.80), suggesting that peanut proteins possess a higher buffering capacity against acidification with vinegar compared to soya proteins. This partial resistance to acidification may also contribute to the elevated product yield, as incomplete protein denaturation would result in less tight gel formation and greater water retention. In all formulations, whey pH was slightly lower than cream cheese pH, which is expected as expelled acid migrates preferentially into the whey fraction during syneresis.

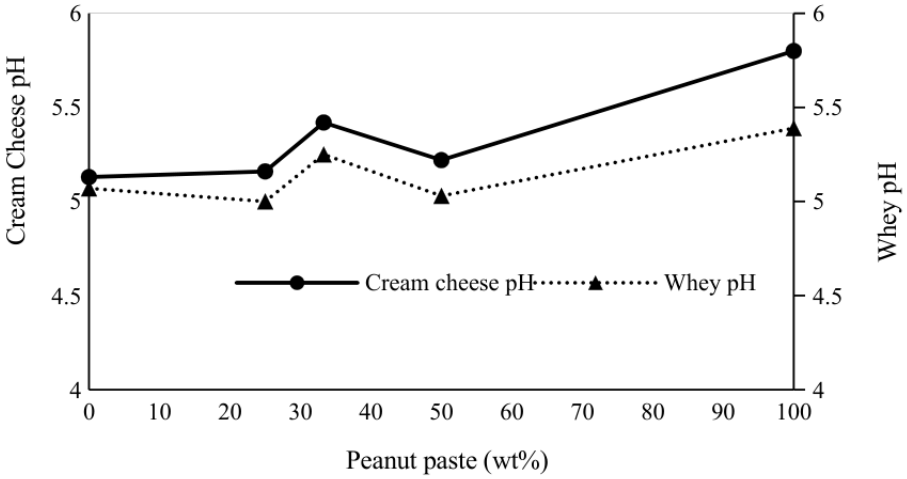


Figure 2. The pH variation of cream cheese and whey in different formulas

3.3 Textural Properties

Table 2 illustrates the parameters obtained from the texture profile analysis, which demonstrate the influence of the incorporation of peanut paste on the textural characteristics of cream cheese. The sample having 100% soya milk (S100:P0) exhibited the highest hardness (315 g), indicating the formation of a strong protein network by soya proteins (Renkema, 2002). Substituting 25% soya milk with peanut paste markedly reduced the hardness to 65 g, suggesting disruption of the continuous soya protein matrix and the formation of a softer, more spreadable product. Increasing the peanut paste content to 33.3% increased the hardness to 100 g, indicating partial reinforcement of the gel structure through additional solids and protein contributed by the peanut paste.

Table 2. The texture profile analysis

Sample	Hardness (g)	Adhesiveness	Adhesive force (g)	Resilience	Fracturability (g)	Total Work (mJ)
S100:P0	315.00	1.60	50.00	0.49	150.00	5.40
S75:P25	65.00	0.20	10.00	0.26	5.00	0.80
S66.7:P33.3	100.00	0.10	5.00	0.08	5.00	0.20
S50:P50	315.00	0.20	25.00	0.34	315.00	4.80
S0:P100	310.00	0.30	30.00	0.30	310.00	5.70

Further increasing the peanut paste proportion to 50% restored the hardness to 315 g, while the sample prepared solely from peanut paste (S0:P100) exhibited a comparable hardness of 310 g. These findings suggest that higher peanut paste concentrations produced a denser matrix capable of resisting compression (Arya et al., 2016).

A similar trend was observed for total work, which decreased from 5.40 mJ in the control to 0.20 mJ at 33.3% peanut paste before increasing to 4.80 and 5.70 mJ in the 50% and 100% peanut formulations, respectively. Adhesiveness and adhesive force also decreased with partial substitution of soya milk, indicating reduced stickiness, whereas resilience declined from 0.49 in the control to 0.08–0.34 in the blended formulations, suggesting reduced elastic recovery following compression. Overall, the results indicate that partial replacement of soya milk with

peanut paste weakened the protein gel network, whereas higher peanut paste concentrations contributed to the development of a firmer and more cohesive cream cheese structure.

4 CONCLUSION

The present study demonstrated that the formulation of soya milk and peanut paste significantly affected the physicochemical and textural properties of cream cheese analogues. The incorporation of peanut paste influenced product yield, moisture content, pH, and texture, indicating that the interaction between soya and peanut proteins plays an important role in curd formation and structural development. The peanut-only formulation produced the highest yield, while the 50:50 formulation exhibited the lowest yield, suggesting greater losses of solids during whey separation. Texture profile analysis showed that partial replacement of soya milk reduced hardness, whereas formulations containing 50 wt% and 100 wt% peanut paste produced firmer products comparable to the soya-based control. Overall, the results indicate that suitable proportions of soya milk and peanut paste can be used to develop plant-based cream cheese analogues with acceptable physicochemical and textural properties. Further studies should evaluate sensory characteristics, microstructure, and storage stability to optimize the formulation for commercial application.

5 ACKNOWLEDGEMENTS

The authors acknowledge the support of the Division of Polymer and cHemical Engineering Technology , Institute of Technology, University of Moratuwa, and Department of Food Science and Technology, University of Sri Jayewardenepura, for providing the facilities and technical assistance for this study.

6 REFERENCES

Arya, S. S., Salve, A. R., & Chauhan, S. (2016). Peanuts as functional food: A review. *Journal of Food Science and Technology*, *53*(1), 31–41. https://doi.org/10.1007/s13197-015-2007-9

Foegeding, E. A., & Drake, M. A. (2007). Invited review: Sensory and mechanical properties of cheese texture. *Journal of Dairy Science*, *90*(4), 1611–1624.

Fox, P. F., Guinee, T. P., Cogan, T. M., & McSweeney, P. L. H. (2017). *Fundamentals of cheese science* (2nd ed.). Springer.

Huang, A., Eibel, H., Klemann, L. P., Ferri, D. C., & Oxford, P. J. (2011). *Lipid compositions for increased fatty and creamy mouthfeel and uses thereof* (WO Patent No. 2011126891A2). WIPO (PCT). https://patents.google.com/patent/WO2011126891A2/en

Kanauchi, M., Hatanaka, S., & Shimoyamada, M. (2015). New cheese-like food production from soy milk—Utility of soy milk curdling yeast. In A. H. Eissa (Ed.), *Food production and industry* (pp. 79–104). IntechOpen. https://doi.org/10.5772/60848

Liu, K. (1997). *Soybeans: Chemistry, technology, and utilization*. Chapman & Hall.

McClements, D. J., & Grossmann, L. (2021). The science of plant-based foods: Constructing next-generation meat, fish, milk, and egg analogs. *Comprehensive Reviews in Food Science and Food Safety*, *20*(4), 4049–4100. https://doi.org/10.1111/1541-4337.12771

Renkema, J. M. (2002). Heat-induced gel formation by soy proteins at neutral pH. *Journal of Agricultural and Food Chemistry*, *50*(6), 1569–1573.

Short, E. C., Kinchla, A. J., & Nolden, A. A. (2021). Plant-based cheeses: A systematic review of sensory evaluation studies and strategies to increase consumer acceptance. *Foods*, *10*(4), Article 725. https://doi.org/10.3390/foods10040725

Walstra, P., Wouters, J. T. M., & Geurts, T. J. (2006). *Dairy science and technology* (2nd ed.). CRC Press.

Wei, L., Li, P., Liu, Y., & Xie, Y. (2026). Effects of drying methods, temperature, and initial moisture content on drying characteristics, nutritional quality, texture, and oxidative stability of peanuts. *Foods*, *15*(7), 1248. https://doi.org/10.3390/foods15071248

Zhang, S., Jiang, Y., Zhang, S., & Chen, L. (2022). Physical properties of peanut and soy protein-based emulsion gels induced by various coagulants. *Gels*, *8*(2), 79. https://doi.org/10.3390/gels8020079

ISSN: 2773-7055
Proceedings of the 5th International Research Conference
Institute of Technology, University of Moratuwa
November 5, 2026

Paper ID: 43

DRYING KINETICS AND MATHEMATICAL MODELLING OF ASH PLANTAIN IN A CONVECTION TRAY DRYER

G K Jayatunga[1*], R M T N Rathnayake[1]

[1]Division of Polymer and Chemical Engineering Technology, Institute of Technology, University of Moratuwa, Homagama, Sri Lanka

*Corresponding author: gayanij@itum.mrt.ac.lk

ABSTRACT: Ash plantain (*Musa paradisiaca* L), is an important cooking banana cultivar in Sri Lanka with high nutritional value but limited shelf life due to its high moisture content. This study investigated the drying kinetics and thin-layer mathematical modelling of ash plantain slices dried in a laboratory-scale convection tray dryer. Drying experiments were conducted at air temperatures of 58 °C, 63 °C, and 68 °C with bed weights of 550 g at a constant air velocity of 2.2 m s^{-1}. Moisture ratio, drying rate, effective moisture diffusivity, activation energy, and thin-layer drying models were evaluated. The drying process occurred entirely in the falling-rate period, indicating that moisture transport was governed primarily by internal diffusion. The effective moisture diffusivity increased from 5.06×10^{-10} to 1.01×10^{-9} m^2/s with increasing drying temperature. The temperature dependence of moisture diffusivity followed the Arrhenius relationship, yielding an activation energy of 65.1 kJ/mol. Among the evaluated thin-layer drying models, the Page model provided the best overall fit to the experimental data, exhibiting the highest coefficient of determination and the lowest RMSE and χ^2 values, while the Two term model also showed excellent predictive capability with fewer model parameters.

Keywords: Ash plantains, convection tray drying, drying kinetics, mathematical modelling, effective moisture diffusivity

1 INTRODUCTION

Ash plantain (Musa paradisiaca L.), locally known as Alu Kesel, is one of the major cooking banana cultivars in Sri Lanka. Ash plantain is rich in starch, dietary fiber, resistant starch, potassium, vitamins, and other bioactive compounds, making it a nutritious food with significant health benefits. It is commonly consumed in boiled, steamed, fried, and processed forms at different stages of maturity. However, its high moisture content results in rapid postharvest deterioration, leading to considerable quantitative and qualitative losses (Ajala et al., 2018).
Drying is one of the most effective preservation methods for extending the shelf life of fruits and vegetables by reducing moisture content to levels that inhibit microbial growth, enzymatic activity, and other deteriorative reactions (Jayatunga & Amarasinghe, 2015). Drying also provides opportunities for value addition. Dried ash plantain can be processed into flour, snack foods, breakfast cereals, bakery ingredients, and composite flours for functional and gluten-free food products. Owing to its high resistant starch content and relatively low glycaemic index, ash plantain flour has gained increasing attention as a functional food ingredient with potential nutraceutical applications. Open sun or shade drying can be applied for whatever agricultural crops because these methods require little investment and energy. However, sun drying is highly weather-dependent, requires long drying times, and often results in inconsistent product quality due to contamination, uneven drying, enzymatic browning, and nutrient losses.

Consequently, several mechanical drying methods, including hot-air (convection), vacuum, microwave, infrared, freeze, fluidized-bed, spouted bed, heat pump, and hybrid drying, have been developed to achieve faster drying, improved process control, and better product quality (Anuththara et al., 2019; Dissanayake et al., 2025) and (Jayatunga & Amarasinghe, 2014). Among these methods, convection tray drying is widely used in both research and industry because of its simple operation, low capital cost, scalability, and ability to provide controlled drying conditions.

Understanding the drying behavior of agricultural products is essential for the design and optimization of industrial drying processes. Although the drying characteristics of several banana cultivars have been widely investigated, a review of the available literature indicates limited information on the drying behavior of Sri Lankan ash plantain under controlled convection tray drying conditions. In particular, effect of drying temperature on drying kinetics, effective moisture diffusivity, activation energy, and mathematical model selection have not been comprehensively investigated. Therefore, this study aims to investigate the drying kinetics of ash plantain in a convection tray dryer, evaluate the effects of drying temperature, determine the effective moisture diffusivity and activation energy, and identify the most suitable thin-layer drying model for predicting its drying behavior.

2 METHODOLOGY

Fresh mature ash plantains were purchased from a local vendor in Homagama, Sri Lanka. The fruits were thoroughly washed with clean water to remove adhering dirt and impurities. The green peel was manually removed, and the pulp was sliced into circular discs of approximately 5 mm thickness using a stainless-steel knife. The average diameter of the slices ranged from 3.0 to 3.5 cm.

Drying experiments were carried out using a laboratory-scale forced convection tray dryer (GUNT CE 130, GUNT Gerätebau GmbH, Germany). The drying air was heated using an electric heater integrated with a temperature control unit, which maintained the desired drying temperature within ±0.5 $^{\circ}$C throughout the experiments. Three drying air temperatures (58 $^{\circ}$C, 63 $^{\circ}$C, and 68 $^{\circ}$C) were selected based on the recommended temperature range (55–70 °C) for drying agricultural products while minimizing the degradation of heat-sensitive constituents (Jayatunga & Amarasinghe, 2019). The drying air velocity was maintained at 2.2 m s^{-1}, providing sufficient airflow for efficient convective heat and mass transfer without causing movement or fluidization of the plantain slices on the trays. For each experiment, the sliced ash plantains were uniformly distributed on the drying trays in a single layer to promote uniform airflow and moisture removal. During drying, the reduction in sample weight was recorded at predetermined time intervals using the weighing system integrated with the dryer for a two-hour period. Drying kinetics, moisture ratio, drying rate, effective moisture diffusivity, and activation energy were evaluated using the experimental data. The experimental moisture ratio data were fitted to selected thin-layer drying models to describe the drying behavior of ash plantain slices. The Page model and Two-term model were selected because of their widespread application in modelling the drying characteristics of fruits and vegetables. Model parameters and the goodness of the fit

were estimated using nonlinear regression in MATLAB.

3 RESULTS AND DISCUSSION

Figure 1 shows the variation of moisture ratio with drying time for ash plantain slices dried in a convective tray dryer at three drying temperatures under a constant air velocity. The moisture ratio decreased continuously with drying time, and higher drying temperatures resulted in faster moisture removal and shorter drying times. The drying behavior was further evaluated using the relationship between the drying rate (rate of change of moisture content) and moisture content, as shown in Figure 2. The drying rate continuously decreased with decreasing moisture content, indicating that the drying process occurred entirely in the falling-rate period. No distinct constant-rate period was observed, suggesting that moisture removal was governed primarily by internal moisture diffusion, which is typical for most biological materials (Aghbashlo et al., 2008).

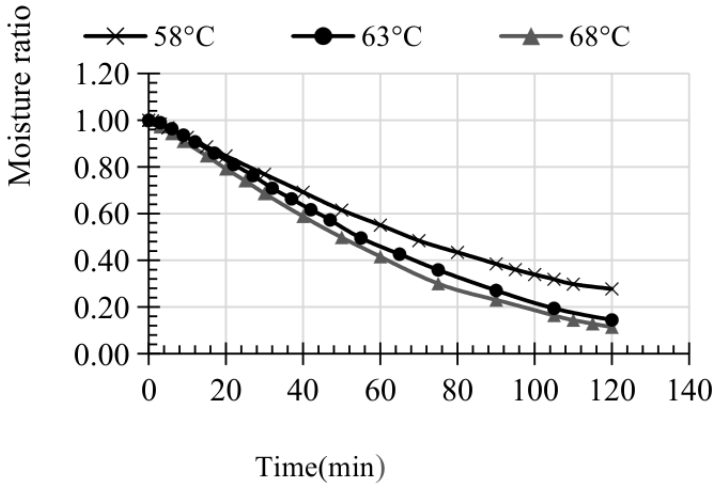


Figure 1. Moisture ratio vs time for drying of ash plantain slices in convection tray dryer

The effective moisture diffusivity (D_{eff}) of ash plantain increased with drying temperature, rising from 5.06×10^{-10} m^2/s at 58 °C to 7.59×10^{-10} m^2/s at 63 °C and reaching 1.01×10^{-9} m^2/s at 68 °C, indicating enhanced internal moisture migration at higher drying temperatures. The increase in D_{eff} indicates enhanced internal moisture migration at higher temperatures due to increased molecular mobility and reduced resistance to moisture diffusion. The obtained values are within the typical range (10^{-10} - 10^{-9} m^2/s) reported for hot-air drying of fruits and vegetables.

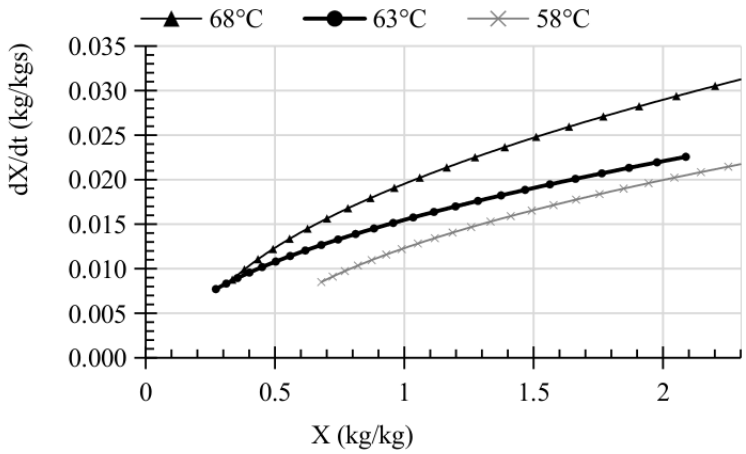


Figure 2. Rate of change of moisture content vs moisture content for the ash plantain slices drying in a convection tray dryer

The temperature dependence of D_{eff} followed the Arrhenius relationship, with an excellent linear fit (R^2 = 0.9921). Although the dryer energy consumption was not measured directly, the activation energy was calculated as 65.1 kJ/mol, indicating that moisture diffusion in ash plantain is strongly influenced by drying temperature. The relatively high activation energy may be attributed to the dense starchy structure of the plantain, which requires greater thermal energy for internal moisture transport. These findings demonstrate that increasing the drying temperature enhances moisture diffusion and improves drying efficiency under convection tray drying conditions (Aghbashlo et al., 2008).

Increasing the drying temperature from 58 °C to 68 °C increased the moisture diffusivity and reduced the drying time, indicating that the higher temperatures, within acceptable product quality limits, could improve the drying efficiency and potentially reduce energy consumption per unit of dried product. At industrial scale, factors such as greater bed depth, air recirculation, and non-uniform airflow and humidity influence drying behavior (Mujumdar, 2014). Nevertheless, the fundamental mass transfer parameters obtained in this study namely the effective moisture diffusivity and activation energy provide vital baseline data required for the mathematical modeling, design, and scale-up of ash plantain drying systems.

The Page and Two-term models were fitted to the experimental drying data of ash plantain to evaluate their ability to describe the drying kinetics. Figure 3 compares the experimental moisture ratio data with the predicted values obtained from both models. Overall, the Page model provided a more accurate representation of the drying behavior of ash plantain, particularly at 63 °C and 68 °C, where it produced higher coefficients of determination (R^2 = 0.9942 - 0.9971) and lower root mean square error (RMSE = 0.0170 - 0.0207) than the Two-term model. At 58 °C, however, the Two-term model showed a slightly better fit, yielding a higher R^2 (0.9939) and a lower RMSE (0.0208) than the Page model.

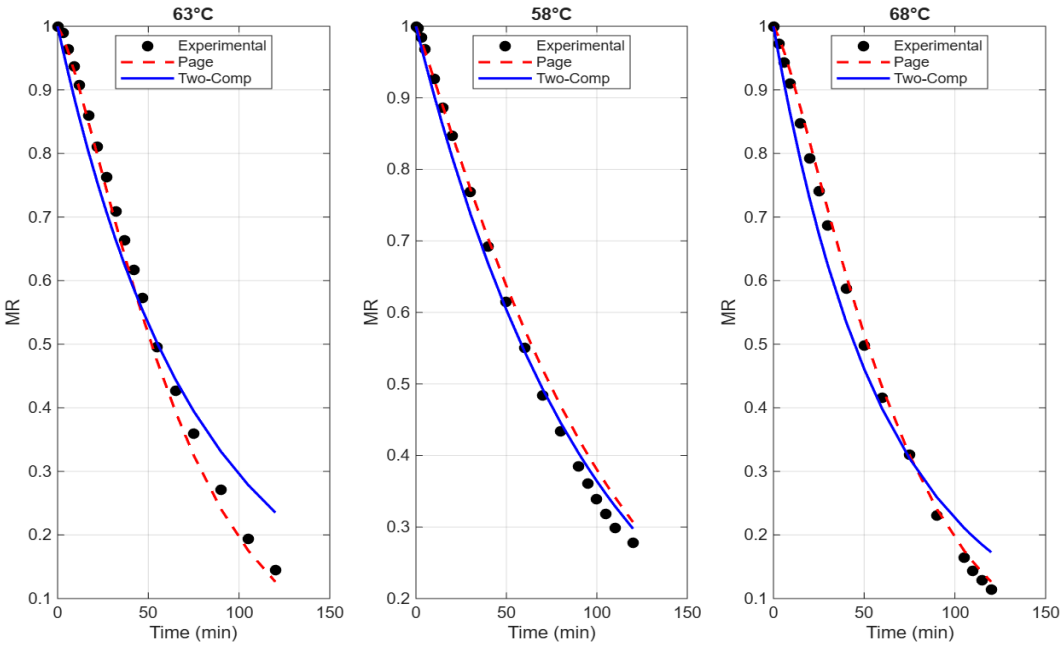


Figure 3. Comparison between the experimental moisture ratio and predicted moisture ratio using Page model and Two term model for three different drying temperatures

Despite this improvement at the lowest drying temperature, the Page model demonstrated superior overall performance across the investigated temperature range while using fewer model parameters. Therefore, the Page model was selected as the most appropriate model for describing the thin-layer drying characteristics of ash plantain. The estimated model coefficients and goodness-of-fit statistics for both models are presented in Table 1.

Table 1. Estimated model coefficients and goodness-of-fit statistics for the Page and Two-term drying models of ash plantain at different drying temperatures.

Temperatue	Model	Equation	RMSE	R^2
58 °C	Page	$MR = exp(-0.0061t^{1.1})$	0.026329	0.990235
	Two- term	$MR = 0.2\exp\exp(-0.0101t) + 0.8\ exp$ (-0.0.0101t)	0.020751	0.993934
63 °C	Page	$MR = exp(-0.0041t^{1.3})$	0.02072	0.994246
	Two- term	$MR = 0.7\exp\exp(-0.0101t)$ +0.3 exp(-0.0201t)	0.048363	0.968651
68 °C	Page	$MR = exp(-0.0041t^{1.3})$	0.017006	0.997145
	Two- term	$MR = 0.4\exp\exp(-0.101t) + 0.6\ exp$(-0.0201t)	0.046412	0.978739

4 CONCLUSION

This study investigated the drying characteristics of ash plantain slices in a laboratory-scale convection tray dryer under different drying temperatures and bed weights. Drying occurred entirely in the falling-rate period, indicating that internal moisture diffusion was the dominant mechanism governing moisture removal. Increasing the drying temperature accelerated the drying process and increased the effective moisture diffusivity from 5.06×10^{-10} to 1.01×10^{-9} m^2/s. The Arrhenius relationship adequately described the effect of temperature on moisture

diffusivity, with an activation energy of 65.1 kJ/mol. Thin-layer drying models successfully represented the drying behavior of ash plantain, and the Page model showed the best overall predictive performance, while the Two-term model also provided accurate predictions with a simpler mathematical form.

5 ACKNOWLEDGEMENTS

The authors acknowledge the Division of Polymer and Chemical Engineering Technology, Institute of Technology, University of Moratuwa, for the support provided during this study. Also, authors wish to acknowledge assistance given bylaboratory assistant Mr. S.H.C.P. Senarathna of Unit Operations Laboratory.

6 REFERENCES

Aghbashlo, M., kianmehr, M. H., & Samimi-Akhijahani, H. (2008). Influence of drying conditions on the effective moisture diffusivity, energy of activation and energy consumption during the thin-layer drying of berberis fruit (Berberidaceae). *Energy Conversion and Management*, *49*(10), 2865–2871. https://doi.org/10.1016/j.enconman.2008.03.009

Ajala, A. S., Ajagbe, O. A., Abioye, A. O., & Bolarinwa, I. F. (2018). Investigating the effect of drying factors on the quality assessment of plantain flour and wheat-plantain bread. *International Food Research Journal*, *25*(4), 1566–1573.

Anuththara, J. G. M., Edirisinghe, E., Amarasinghe, B., & Jayatunga, G. K. (2019). Kinetics and mathematical modeling of drying of parboiled paddy in a packed bed dryer. *2019 Moratuwa Engineering Research Conference (MERCon)*, 181–186. https://ieeexplore.ieee.org/abstract/document/8818766/

Dissanayake, D., Abesekara, M. S., Amarasinghe, B., & Jayatunga, G. K. (2025). Investigation of drying characteristics and estimation of mass transfer parameters of Sri Lankan black pepper dried in a batch fluidized bed dryer. *Sri Lankan Journal of Applied Sciences*, *3*(2). https://sljoas.sljol.info/articles/1

Jayatunga, G. K., & Amarasinghe, B. (2014). Drying kinetics of black pepper dried in a spouted bed dryer with or without draft tubes. *International Journal of Manufacturing Industrial Engineering–IJMIE*, *1*(2), 6–10.

Jayatunga, G. K., & Amarasinghe, B. (2015). Mathematical modeling of drying kinetics of black pepper in a spouted bed dryer with and without non porous draft tubes. *2nd International Conference on Trends in Multidisciplinary Business and Economic Research (TMBER)*, 118–134.

Mujumdar, A. S. (Ed.). (2014). *Handbook of Industrial Drying* (4th ed.). CRC Press. https://doi.org/10.1201/b17208

ISSN: 2773-7055
Proceedings of the 5th International Research Conference
Institute of Technology, University of Moratuwa
November 5, 2026

Paper ID: 48

PREDICTION OF ROCK SOCKET SHEAR STRENGTH IN HARD CRYSTALLINE ROCKS USING PILE LOAD TEST DATA AND ROCK MASS QUALITY PARAMETERS

Jepanesan Jinthusan[1], Ayodya Bulathsinhala[2*], Anurudda Puswewala[3]

[1,3]Department of Civil Engineering, Faculty of Engineering, Sri Lanka Institute of Information Technology, Sri Lanka

[2]Division of Civil Engineering Technology, Institute of Technology, University of Moratuwa, Sri Lanka

*Corresponding author: bulathsinhalau@itum.mrt.ac.lk

ABSTRACT: Rock-socketed bored cast-in-situ piles are widely used in building construction projects in Sri Lanka because the country's geology is dominated by hard crystalline metamorphic rocks such as biotite gneiss and granulite. Current design practice, however, relies mostly on empirical methods developed for softer sedimentary rocks, which tends to underestimate the actual load-carrying capacity of these piles. This paper presents an analysis of static maintained pile load test (MLT) data collected from construction projects in Sri Lanka, with the objective of establishing empirical relationship between mobilised rock socket shear strength and key rock mass quality parameters, namely Uniaxial Compressive Strength (UCS), Rock Quality Designation (RQD), and Core Recovery (CR). The Chin hyperbolic method was used to determine mobilised ultimate shaft resistance from load-settlement data, and the Chin-Kondner and Decourt extrapolation methods were applied to estimate ultimate pile capacity. Shaft and end-bearing resistance components were separated, and unit rock socket shear values were computed. These values were then plotted against UCS, RQD, and CR for a dataset of twelve piles, the resulting linear regression equations were developed and preliminary calibrated against a separate set of three additional piles. The results indicate that mobilised rock socket shear strength increases with all three parameters and that values observed in Sri Lankan hard crystalline rocks are 200% higher than those predicted by Williams and Pells (1981) method. The study proposes three locally calibrated regression equations (R^2=0.23 (CR); R^2=0.36 (UCS); R^2=0.40 (RQD)) as practical design tools for rough estimating socket friction in hard crystalline rock conditions, and further calibration using more test results will refine the equation contributing to more economical and reliable pile foundation design in Sri Lanka and will enable to estimate mobilised skin friction of rock sockets without MLTs.

Keywords: pile load test, skin friction, UCS, RQD, Core Recovery

1 INTRODUCTION

The use of pile foundations is very common in modern building construction in Sri Lanka, especially in urban areas where structures must be founded on hard crystalline metamorphic rocks found at relatively shallow depths. The most commonly used type is the bored cast-in-situ pile socketed into rock, which transfers heavy structural loads through both shaft resistances along the pile-rock interface and end bearing at the pile toe. A large share of the total load-carrying capacity of such piles comes from the shaft resistance mobilised within the rock socket. Despite this importance, current design practice in Sri Lanka relies heavily on empirical methods such as Williams and Pells (1981) method and Wyllie's (1991) method that were originally developed for sedimentary or weaker rock types. These methods consistently underestimate the mobilised shaft resistance in hard crystalline rocks, leading to overly conservative and costly pile designs in Sri Lankan rocks.

In rock-socketed piles, shaft resistance involves mechanical interlocking and friction at the pile-rock interface, governed by rock strength, joint conditions, and construction quality. Williams and Pells (1981) developed widely referenced correlations between ultimate unit shaft resistance and unconfined compressive strength (UCS) using sedimentary rocks (sandstone, mudstone, shale); however, their direct application to hard crystalline rocks is questionable given the fundamentally different rock types. UCS captures intact rock strength, while rock quality designation (RQD) and core recovery (CR) reflect jointing and continuity; using all three together gives a more complete picture of rock mass quality and reduces design uncertainty (Thilakasiri, 2018). Research by Thilakasiri (2018) based on instrumented load tests in Sri Lanka demonstrated that mobilised rock socket shaft resistance in biotite gneiss and granulite formations is consistently higher than values predicted by international guidelines, confirming that using foreign designs are highly conservative. Performing load tests to estimate the mobilised skin friction is always uneconomical and hence a lot of empirical equations are designed by many researches to estimate the mobilised skin friction several strength and rock mass parameters and are not relevant to the hard metamorphic bed rock conditions (Samarawickrama, 2026). Therefore, validated local correlations between mobilised shear strength and rock strength and rock mass parameters such as UCS, RQD, and CR remain unavailable for Sri Lankan conditions, a gap this study directly addresses. Several studies conducted in Sri Lanka have shown that mobilised rock socket shaft resistance in gneiss and granulite formations is considerably higher than what conservative international guidelines predict (Thilakasiri, 2018; Bulathsinhala and Puswewala, 2026). However, well-validated local empirical correlations between mobilised socket shear strength and easily measurable rock mass parameters such as UCS, RQD, and CR are not yet available for Sri Lankan geological conditions. This study addresses that gap by analyzing static maintained pile load test results from twelve piles socketed into hard crystalline rocks across multiple construction sites in Sri Lanka. The mobilised unit rock socket shear strength is derived from each test using the Chin hyperbolic interpretation method, and linear regression correlations are developed with UCS, RQD, and CR. The correlations are then validated using data from three additional piles. The findings provide a practical, locally calibrated framework for improving pile design practice in Sri Lanka.

2 METHODOLOGY

2.1 Data collection

Static maintained pile load test (MLT) data were collected from completed and ongoing piling projects in Sri Lanka where piles were socketed into hard crystalline metamorphic rock formations. A total of twelve test piles formed the primary dataset, with three additional piles used for validation. For each pile, the following information was recorded: pile diameter, socket length, rock type at founding level, applied load increments, measured pile head settlements, and the termination load of the test. Rock mass quality indices were obtained from corresponding borehole logs and laboratory reports, including CR, RQD, UCS, and where available, the Fracture Index (FI). Representative values of UCS, RQD, and CR for the rock socket zone were used in the correlation analysis. Table 1 presents a summary of the test pile and borehole details for the

reference case (TP-39).

Table 1. Summary of Test Pile and Borehole Details (TP-39) (Bulathsinhala and Puswewala, 2025)

Test Pile ID	Project Location	Pile Diameter (mm)	Socket Length (m)	Rock Type	Test Method
TP-39	Port Access Elevated Highway, Colombo	1200	2.5	Fresh biotite gneiss	Instrumented MLT (IMLT)

2.2 Use of Chin hyperbolic method to find mobilised skin friction

The Chin hyperbolic method was used as the primary method to determine mobilised shaft resistance from load-settlement data, assuming the load-settlement relationship follows a hyperbolic trend. A plot of settlement divided by applied load (S/P) versus settlement (S) is constructed, and a straight line is fitted to the linear portion: $S/P = C_1 + C_2S$; the mobilised ultimate load is the reciprocal of the slope, Q_{su}, Chin = 1/m. This method was selected because most pile load tests in Sri Lanka are terminated at 1.5 to 3.0 times the working load without reaching clear plunging failure, and it provides more consistent results than graphical methods such as Van Weele's approach, having been successfully applied in instrumented load tests on rock-socketed piles in Sri Lanka (Pile Test Consultants, 2020).

2.3 Ultimate pile capacity and component separation

Ultimate pile capacity was estimated by averaging the values obtained from the Chin (1970) extrapolation method and the ultimate end bearing capacity was calculated as the difference between the total ultimate capacity and the mobilised shaft resistance. For piles passing through soil and rock layers, soil shaft resistance was estimated separately using conventional methods and deducted from the total to isolate the rock socket contribution. Unit rock socket shear stress (τ) was then computed by dividing the rock socket shaft resistance by the socket surface area ($\pi \times D \times Ls$).

2.4 Correlation and validation

Unit rock socket shear values (τ, kPa) derived from the twelve primary test piles were plotted against UCS (MPa), RQD (%), and CR (%) individually, and linear regression lines were fitted to each scatter plot. The three additional validation piles were then plotted on the same axes to examine consistency with the established trends.

3 RESULTS AND DISCUSSION

3.1 Results of primary data of 12 piles

Figure 1(a) illustrates the relationship between the mobilised rock socket shear strength (τ) and Rock Quality Designation (RQD) for the twelve primary test piles. The data show an overall positive linear trend, represented by the Equation 1.

$$\tau = 11.926 \times RQD + 557.23 \; ; \; (R^2 = 0.3978) \tag{1}$$

The positive slope indicates that the mobilised rock socket shear strength generally increases with increasing RQD, suggesting that piles socketed into more intact and less fractured rock masses tend to develop higher shaft resistance. However, the relatively low coefficient of determination (R^2 = 0.3978) indicates that RQD alone explains only approximately 39.78% of the variation in the measured shear strength. This suggests that other factors, such as UCS, CR, joint characteristics, socket roughness, construction quality, and drilling conditions, also have a significant influence on the mobilization of rock socket shear resistance.

Figure 1(b) illustrates the relationship between the mobilised rock socket shear strength (τ) and Uniaxial Compressive Strength (UCS) for the twelve primary test piles. The data exhibit an overall positive linear trend as depicted in Equation 2:

$$\tau = 12.022 \times UCS + 630.95 \ (R^2 = 0.3562) \quad (2)$$

The positive slope of the regression line indicates that the mobilised rock socket shear strength generally increases with increasing UCS.

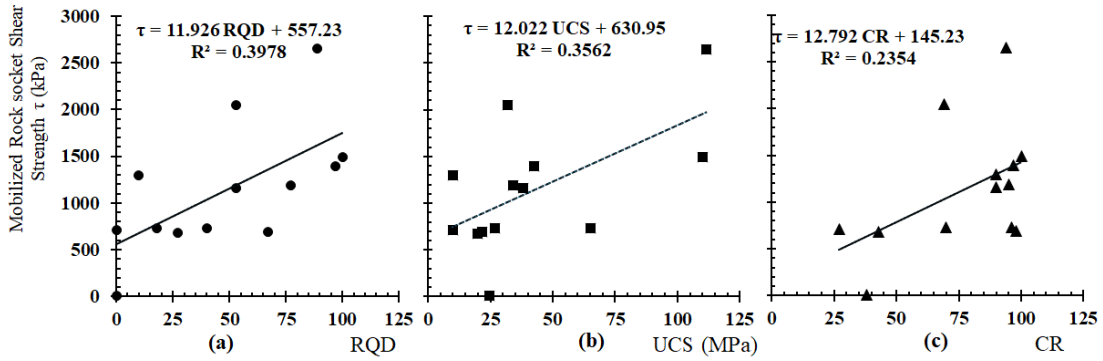


Figure 1. (a) Variation of mobilised rock socket shear strength Vs RQD; (b) Variation of mobilised rock socket shear strength Vs UCS; (c) Variation of mobilised rock socket shear strength Vs CR

However, the relatively low coefficient of determination (R^2 = 0.3562) indicates that UCS alone explains only approximately 35.6% of the variation in the measured shear strength. The regression slope of approximately 12 is considerably higher than the values generally predicted by the Williams and Pells (1981) empirical model developed for sedimentary rocks, further supporting the conclusion that hard crystalline rocks in Sri Lanka are capable of mobilizing substantially higher rock socket shear resistance. Figure 1(c) illustrates the relationship between the mobilised rock socket shear strength (τ) and CR for the twelve primary test piles. The data exhibit an overall positive linear trend, represented by Equation 3.

$$\tau = 12.792 \times CR + 145.23 \ (R^2 = 0.2354) \quad (3)$$

Among the three regression relationships developed in this study, the CR-based regression exhibits the least R^2 value of 0.23 which shows it has the least impact in estimating the mobilised skin friction value over other parameters tested in this study. Nevertheless, the relatively low coefficient of determination suggests that CR should be used together with other rock mass parameters, such as UCS and RQD, to achieve more reliable predictions of mobilised rock socket shear strength.

3.2 Validation Dataset — Three Additional Piles

To evaluate the reliability of the regression equations developed from the primary dataset, three additional pile load test results were used as an independent validation dataset against the established trends for RQD, UCS, and CR. Table 2 depicts the percentage deviation of mobilised skin friction values with values calculated by empirical equations.

Table 2. Deviation of mobilised skin friction with values calculated by empirical equations

Pile ID	Parameter	Value	Calculated Skin Friction using empirical equations (kPa)	Mobilised Skin friction Capacity (kPa)	Deviation %
1	RQD	30.82	924.82	800.57	-13.43
	UCS (MPa)	15.00	811.28		-1.32
	CR	84.96	1231.98		-35.02
2	RQD	36.74	995.38	1000.84	0.55
	UCS (MPa)	15.43	816.51		22.57
	CR	83.22	1209.75		-17.27
3	RQD	26.76	876.35	1400.97	59.86
	UCS (MPa)	83.22	1631.39		-14.12
	CR	96.00	1373.26		2.02

The three validation piles exhibit mobilised rock socket shear strengths ranging from approximately 800.5 to 1400.9 kPa, with UCS values between 14 and 37 MPa, RQD values between 15 and 31%, and CR values between 83 and 96%. Although the validation dataset consists of only three piles, R^2 values generally follow the same overall trends observed in the primary dataset as shown in Table 3 except case of RQD.

Table 3. Correlation strength of additional piles used for the validation

Parameter Method	Data Pairs (Calculated vs. Mobilised)	R^2 Value	Prediction Correlation Strength
RQD	(924.82, 800.57), (995.38, 1000.84), (876.35, 1400.97)	0.421	Moderate linear relationship
UCS (MPa)	(811.28, 800.57), (816.51, 1000.84), (1631.39, 1400.97)	0.957	Very Strong linear relationship
CR	(1231.98, 800.57), (1209.75, 1000.84), (1373.26, 1400.97)	0.902	Strong linear relationship

Notably, despite the relatively low R^2 of RQD values of the validation piles indicating moderately to highly fractured rock masses, mobilised shear strengths of 800.5–1400.9 kPa were still achieved with a strong linear relationship by UCS and CR, further supporting the conclusion that even moderately fractured hard crystalline rocks in Sri Lanka are capable of mobilizing significant shaft resistance. However, 3 piles are not sufficient to validate the results since at least 9-15 piles are required in the similar geological setup to calibrate the model equations.

3.3 Comparison with Existing Methods

The mobilised unit rock socket shear strength values observed in this study, ranging from approximately 670 to over 2600 kPa, are substantially higher than values typically predicted by international empirical methods developed for sedimentary rocks. The Williams and Pells

(1981) method predicts considerably lower shaft resistance for the UCS range observed here (10–110 MPa), derived from sandstone, mudstone, and shale; similarly, the Hong Kong Guidelines (Geotechnical Engineering Office, 2006) recommend conservative upper limits. Direct application of these international methods to hard crystalline rock formations in Sri Lanka may therefore result in overly conservative, unnecessarily larger pile dimensions, whereas the locally calibrated equations developed here offer a more representative alternative.

3.4 Practical Regression Equations

Table 4 depicts three regression equations (Equation 1, 2, and 3) proposed as locally applicable tools for estimating unit rock socket shear strength in hard crystalline rocks (gneiss, granulite) in the Sri Lankan basement, and should not be applied to sedimentary or heavily weathered rocks without further validation.

Table 4. Proposed Regression Equations for Rock Socket Shear Strength

Parameter	Regression Equation	Remarks
RQD (%)	τ = 11.926 × RQD + 557.23	Analyzed data range for RQD 0–100%, R^2 = 0.3978
UCS (MPa)	τ = 12.022 × UCS + 630.95	Analyzed data range for UCS 10–120 MPa, R^2 = 0.3562
CR (%)	τ = 12.792 × CR + 145.23	Analyzed data range for CR 25–100%, R^2 = 0.2354

4 CONCLUSION

The Chin (1970) hyperbolic method was used to derive mobilised unit shear stress values from load-settlement data, and these were correlated with UCS, RQD, and CR obtained from borehole investigations. Mobilised rock socket shear strength shows a clear positive relationship with UCS, RQD, and CR in hard crystalline rocks, with CR showing the steepest regression slope. Observed values (approximately 670–2650 kPa) are significantly higher than those predicted by international guidelines developed for sedimentary rocks, confirming that current design practice in Sri Lanka is overly conservative. Three locally calibrated linear regression equations were developed providing simple and practical tools for estimating socket friction in design. Validation against three additional piles showed that their shear values are fairly consistent with the regression trends, supporting the partial reliability of the proposed equations. However, the reliability and generalizability of these equations may be limited, as they were developed based on only 12 piles and validated using three additional piles, which may not provide a sufficiently large dataset to capture the inherent variability in rock-socket strength. Hence these findings must be used to refine the pile design with new pile load data set to increase the R^2 value of the trend lines to device more realistic mobilised skin friction capacities of rock sockets.

5 ACKNOWLEDGEMENTS

The author thanks Ms. Iromi Dyes (CINEC Campus) and all project teams who provided pile load test and borehole data used in this research.

6 REFERENCES

Bulathsinhala, A. U. V. B., & Puswewala, U. G. A. (2025). Performance-based optimization of pile socket design in Sri Lankan metamorphic bedrock. In Proceedings of the 4th International Research Conference, Institute of Technology, University of Moratuwa (pp. 1–5). Institute of Technology, University of Moratuwa. ISSN 2773-7055. DOI: 10.64752/GCNL4751

Bulathsinhala, A. U. V. B., & Puswewala, U. G. A. (2026). Optimization of Pile Socket Design in Sri Lankan Metamorphic Bedrock by Laboratory Experiments and Piles' Performance. PES Journal, Vol 8, No. 2. doi: 10.24874/PES08.02B.013

Chin, F. K. (1970). Estimation of the ultimate load of piles from tests not carried to failure. Proceedings of the 2nd Southeast Asian Conference on Soil Engineering, Singapore, 81–90.

Geotechnical Engineering Office. (2006). Foundation Design and Construction, Civil Engineering and Development, The Government of the Hong Kong Special Administrative Region (Vol. Geo Publication No.01).

PileTest Consultants (Pvt) Ltd. (2020). Instrumented static load test report: Port Access Elevated Highway Project, Colombo. Unpublished technical report.

Samarawickrama, M. N. C. (2026). Rock socket skin friction behavior of Cast in-situ bored piles in Hard crystalline rock- Emphasis on Sri Lankan Metamorphic rocks. PhD Dissertation. University of Moratuwa.

Thilakasiri, H. S. (2018). Investigation of rock quality parameters and development of skin friction for rock-socketed bored piles in Sri Lanka. Engineer: Journal of the Institution of Engineers, Sri Lanka, 51(3), 1–12.

Williams, A. F., & Pells, P. J. N. (1981). Side resistance rock sockets in sandstone, mudstone and shale. Canadian Geotechnical Journal, 18(4), 502–513. https://doi.org/10.1139/t81-060

Wyllie, D. C. (199). Foundations on Rock (1 ed.). E & FN Spon.

ISSN: 2773-7055
Proceedings of the 5th International Research Conference
Institute of Technology, University of Moratuwa
November 5, 2026

Paper ID: 58

RESILIENT RECONSTRUCTION OF CRITICAL INFRASTRUCTURE IN POST-CONFLICT AND DISASTER CONTEXTS: A SUSTAINABLE QUANTITY SURVEYING FRAMEWORK FOR RECOVERY AND LONG-TERM RESILIENCE

N Z Nafrin[1*], Y A Adikari[1]

[1]Faculty of Engineering, Horizon Campus, Malabe, Sri Lanka

*Corresponding author: nafrinzee03@gmail.com

ABSTRACT: Reconstruction of critical infrastructure after armed conflict and natural disaster requires built environment professionals to balance rapid recovery with long-term sustainability and resilience. Quantity Surveyors hold a central commercial management role in construction delivery, yet their contribution to resilient reconstruction remains fragmented across separate strands of literature on procurement, risk management, cost planning and disaster recovery, leaving no integrated framework for early-stage recovery decisions. This study addresses that gap by developing a conceptual Sustainable Quantity Surveying Framework for Resilient Reconstruction, structured around three layers (recovery planning, delivery and outcomes) and twelve integrated components, with stakeholder collaboration and continuous monitoring and improvement positioned as cross-cutting mechanisms. The study adopts Design Science Research, comprising problem identification, a systematic literature review, thematic analysis, framework development and literature-based validation against published empirical findings; no primary expert data were collected. The review indicates that existing reconstruction guidance treats technical resilience and humanitarian response separately from commercial decision-making, leaving Quantity Surveyors without a structured tool for linking cost, procurement and sustainability decisions during early recovery planning. The proposed framework positions the Quantity Surveyor as a coordinating actor connecting economic, environmental and social objectives throughout the reconstruction lifecycle, drawing on international examples including Ukraine, Indian Ocean tsunami recovery, the Türkiye earthquake response and post-conflict Sri Lanka. The study's contribution lies in synthesising previously fragmented commercial management practices into a single, Quantity Surveyor-centred construct. As a conceptual contribution, the framework requires empirical validation through industry case studies or practitioner evaluation before its practical effectiveness can be confirmed.

Keywords: resilient reconstruction; quantity surveying; post-conflict infrastructure; sustainable procurement; design science research

1 INTRODUCTION

Armed conflict and natural disaster damage critical infrastructure such as transport networks, schools, hospitals, water supply and energy systems, disrupting essential services for years after the triggering event (Mitoulis et al., 2023a). Reconstruction programmes that follow these events are usually under pressure to rebuild quickly, which can lead to decisions that restore previous capacity without improving long-term resilience or sustainability (Mitoulis et al., 2023b).
Decisions made early in recovery planning, particularly around procurement and cost planning, shape the resilience of rebuilt assets for decades. Cases such as the Ukraine infrastructure reconstruction effort, the 2004 Indian Ocean tsunami recovery, the Türkiye earthquake response and the post-conflict reconstruction of Northern and Eastern Sri Lanka illustrate how commercial decisions taken at the outset of reconstruction constrain or enable resilience outcomes long after physical rebuilding is complete.

Quantity Surveyors are commercial management professionals whose responsibilities include cost planning, procurement advice, risk management and life cycle costing across the project lifecycle (Chamikara et al., 2020). Their competencies are increasingly recognised as relevant to sustainable construction, positioning them to influence resilience outcomes at the point where reconstruction decisions are commercially committed.

Most existing studies, however, examine procurement, risk management, cost management and disaster reconstruction as separate fields of enquiry (Chandramohan et al., 2022). Limited research integrates these responsibilities into a single framework that positions the Quantity Surveyor as a central actor in resilient reconstruction of critical infrastructure, leaving practitioners without a structured basis for balancing economic, environmental and social objectives during recovery.

This gap is significant in the Sri Lankan context, where the construction industry has direct experience of both post-conflict reconstruction and disaster recovery. Yet professional guidance for Quantity Surveyors in this area remains limited, despite documented gaps in sustainable-construction competencies and an ongoing diversification of professional roles (Chamikara et al., 2020; Chandramohan et al., 2022).

Therefore, the aim of this study is to develop a conceptual Sustainable Quantity Surveying Framework that explains how Quantity Surveyors can support resilient reconstruction of critical infrastructure through commercial management practices that balance economic, environmental and social sustainability. Three objectives follow: (1) to identify, through a systematic review of recent literature, the commercial management responsibilities and resilience requirements most relevant to reconstruction of critical infrastructure; (2) to synthesise these findings into an integrated framework of components and layers that positions the Quantity Surveyor as a coordinating actor; and (3) to check the resulting framework against findings already reported in the published literature. These objectives address the study's guiding research question: how can Quantity Surveyors contribute to the resilient reconstruction of critical infrastructure in post-conflict and disaster contexts through sustainable commercial management?

2 METHODOLOGY

2.1 Research Design

This study adopts Design Science Research (DSR), since the objective is to design and refine a conceptual artefact rather than to test an existing theory (Hevner et al., 2004). DSR suits the development of practical frameworks while maintaining a clear connection to existing knowledge and has been used in construction management research to build conceptual and procedural artefacts (Peffers et al., 2007). The study follows five stages: problem identification, systematic literature review, thematic analysis, framework development and literature-based validation, each described below.

2.2 Systematic Literature Review

A systematic literature review was conducted to identify recent evidence relevant to resilient infrastructure reconstruction and the role of Quantity Surveyors in post-conflict and disaster

contexts. Literature published between 2020 and 2026 was searched using Google Scholar, Semantic Scholar and ResearchGate. The search used combinations of terms related to resilient reconstruction, post-disaster reconstruction, post-conflict reconstruction, critical infrastructure resilience, disaster recovery, Quantity Surveying, Quantity Surveyors, sustainable procurement, life-cycle costing, value engineering, resilience and infrastructure reconstruction.

Sources were included where they addressed infrastructure recovery or reconstruction in post-conflict or disaster contexts and covered at least one relevant area, including cost management, procurement, Quantity Surveying, resilience, risk management or sustainability. Only relevant English-language academic and authoritative sources published within the defined period were included. Sources were excluded where they were unrelated to post-conflict or post-disaster reconstruction, infrastructure or resilience, or the identified commercial and sustainability themes. Non-English sources, sources outside the 2020–2026 period, duplicates, sources without sufficient full-text information, and sources lacking direct relevance after title, abstract or full-text screening were also excluded.

The search identified 150 records. Following the removal of 20 duplicates, 130 records proceeded to title and abstract screening, of which 60 irrelevant records were excluded. The remaining 70 sources underwent full-text assessment, resulting in 60 studies being retained for thematic analysis.

2.3 Thematic Analysis

Thematic analysis was conducted using an inductive coding approach. Passages related to commercial management, resilience and sustainability were coded. Related codes were then grouped iteratively into candidate themes. The themes were refined by comparing them with the research problem and Quantity Surveying competency literature until a stable set of themes was reached. These themes were then translated into the twelve components of the proposed Sustainable Quantity Surveying Framework for Resilient Reconstruction. This process enabled recurring commercial management responsibilities and resilience requirements to be consolidated into an integrated framework.

2.4 Framework Development

The stabilised themes were translated into twelve framework components, each expressed as a specific commercial management practice rather than as an abstract theme, so that the framework communicates directly to practising Quantity Surveyors. The components were organised into three sequential layers (recovery planning, delivery and outcomes), reflecting the point in the reconstruction lifecycle at which each component is primarily exercised. Stakeholder collaboration and continuous monitoring and improvement were retained as cross-cutting mechanisms that operate across all three layers rather than at a single point in the sequence. The twelve components were retained specifically because each recurred across multiple sources within the 60 studies analysed, rather than appearing in only one or two; components mentioned by a single source were folded into the closest recurring theme rather than kept separately, which is why the framework contains twelve components and not a larger, more fragmented set. The three-layer structure follows directly from this evidence: the retained literature consistently distinguished an

early planning stage, a delivery stage and a longer-term outcomes stage, so the components were mapped onto these three stages rather than an arbitrary grouping. Stakeholder collaboration and continuous monitoring and improvement were separated out as cross-cutting mechanisms, rather than assigned to a single layer, because the reviewed literature associated them with activity at every lifecycle stage rather than with one stage in particular. Section 3.1 and Table 1 set out the basis on which each component was derived.

2.5 Literature-Based Validation

The developed framework was checked against findings reported in published empirical and case-based studies of quantity surveying practice and infrastructure reconstruction (e.g. Mitoulis et al., 2023a, 2023b; Iddamalgoda Pathiranage & Hadiwatte, 2020), to confirm that each component is supported by evidence already reported in the literature rather than by the authors' judgement alone. This constitutes literature-based validation. No primary data were collected from experts or practitioners for this study, and the framework has not yet been tested empirically. This single-method approach suits an extended abstract, since it presents the conceptual contribution within the available space, while primary validation, for example through industry case studies or expert interviews, is identified in Section 5 as necessary future research.

3 RESULTS AND DISCUSSION

3.1 Twelve Components and a Three-Layer Structure

The thematic analysis identified twelve components that the proposed Sustainable Quantity Surveying Framework for Resilient Reconstruction integrates: risk-informed cost planning, resilient procurement, life-cycle costing, value engineering, stakeholder collaboration, sustainable material selection, supply-chain resilience, community recovery, environmental sustainability, infrastructure resilience, long-term asset performance, and continuous monitoring and improvement. Table 1 summarises the function of each component in resilient reconstruction and the literature theme from which it was derived; components are not independently "proven" in isolation but are each supported by a broader theme recurring across the reviewed literature.

Table 1. Framework components and their basis in the reviewed literature

Component	Layer	Function in resilient reconstruction	Supporting literature theme
1. Risk-informed cost planning	Recovery planning	Incorporates hazard exposure and cost uncertainty into early cost estimates	Risk / cost (Mitoulis et al., 2023a)
2. Resilient procurement	Recovery planning	Select procurement routes that remain viable under supply and hazard disruption	Procurement continuity (Mitoulis et al., 2023a)
3. Life-cycle costing	Delivery	Evaluates cost decisions against whole life rather than initial capital cost	Lifecycle performance (Iddamalgoda Pathiranage & Hadiwatte, 2020)
4. Value engineering	Delivery	Balances cost, function and resilience requirements in design decisions	Value management (Chamikara et al., 2020)
5. Sustainable material selection	Delivery	Supports environmental performance and long-term durability objectives	Sustainability (Chamikara et al., 2020)
6. Supply-chain resilience	Delivery	Addresses material and logistics disruption during reconstruction	Supply chain (Mitoulis et al., 2023a)

Component	Layer	Function in resilient reconstruction	Supporting literature theme
7. Community recovery	Outcomes	Reflects social recovery needs in reconstruction outcomes	Social sustainability (Mitoulis et al., 2023b)
8. Environmental sustainability	Outcomes	Reduces environmental impacts of rebuilt infrastructure	Environmental sustainability (Mitoulis et al., 2023b)
9. Infrastructure resilience	Outcomes	Improves capacity of rebuilt assets to withstand future hazards	Resilience (Mitoulis et al., 2023a)
10. Long-term asset performance	Outcomes	Focus evaluation on performance across the asset life, not delivery alone	Lifecycle performance (Iddamalgoda Pathiranage & Hadiwatte, 2020)
11. Stakeholder collaboration (cross-cutting)	Cross-cutting	Coordinates reconstruction actors across the lifecycle	Governance (Chandramohan et al., 2022)
12. Continuous monitoring and improvement (cross-cutting)	Cross-cutting	Feeds performance data back into recovery-planning decisions	Monitoring / adaptive management (Mitoulis et al., 2023b)

The framework is organised in three layers, corresponding to the reconstruction stage at which each component is primarily exercised (Table 1). Recovery planning covers early risk and procurement decisions; delivery covers cost, value and material decisions; and outcomes cover the social, environmental and economic results of reconstruction. Stakeholder collaboration and continuous monitoring and improvement cut across all three layers, coordinating actors from planning through to outcome assessment and feeding performance data back into future recovery-planning decisions.

3.2 Positioning of the Quantity Surveyor

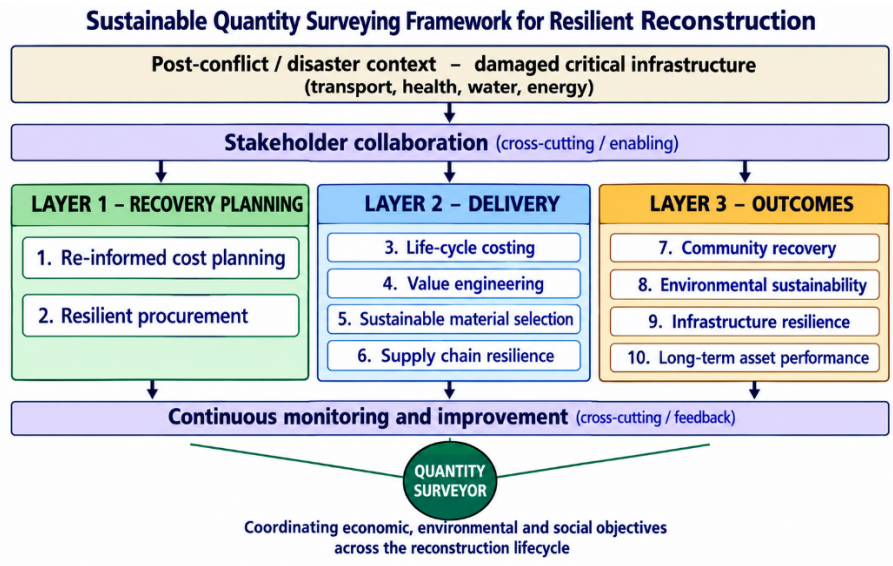


Figure 1. Sustainable Quantity Surveying Framework for Resilient Reconstruction, showing the three-layer structure, the twelve components, the cross-cutting mechanisms, the feedback loop and the coordinating role of the Quantity Surveyor.

Figure 1 presents the revised conceptual framework. The Quantity Surveyor is shown as the actor coordinating economic, environmental and social objectives across the three layers,

linking the cross-cutting mechanisms of stakeholder collaboration and continuous monitoring and improvement to each stage of the reconstruction lifecycle. This positioning reflects the commercial management responsibilities already established in the literature (Chamikara et al., 2020) and extends them explicitly into the resilience and sustainability dimensions of post-conflict and disaster reconstruction.

3.3 Originality and Comparison with Existing Frameworks

Existing literature addresses resilience, disaster recovery, procurement, cost management, sustainability, life-cycle costing and stakeholder management largely as separate strands of enquiry. Resilience and disaster-reconstruction frameworks (e.g. Mitoulis et al., 2023a, 2023b) focus primarily on technical and infrastructural resilience, with limited attention to the commercial mechanisms (procurement selection, cost planning, value engineering) through which resilience decisions are implemented. Sustainable procurement and life-cycle costing studies (Chamikara et al., 2020; Iddamalgoda Pathiranage & Hadiwatte, 2020) address specific commercial practices but do not situate them within a post-conflict or disaster-recovery timeline. Quantity Surveying competency, sustainable-construction and professional-role studies (Chamikara et al., 2020; Chandramohan et al., 2022) establish that the profession's responsibilities are diversifying toward sustainability but do not propose a reconstruction-specific structure for applying them.

The proposed framework does not claim to replace these existing bodies of work. Instead, its originality lies in integrating previously fragmented practices (cost, procurement, lifecycle, value, sustainability, supply-chain and stakeholder considerations) into a single Quantity Surveyor-centred commercial management layer that operates across the reconstruction lifecycle. This positions the contribution as a synthesis and reframing of established practices around a specific professional role and a specific delivery context, rather than as an entirely new body of theory.

3.4 International and Sri Lankan Relevance

Examples from international reconstruction programmes support the relevance of the framework. The conflict-resilience approach developed for critical infrastructure in Ukraine demonstrates the value of assessing resilience before committing to reconstruction sequencing (Mitoulis et al., 2023a). Transport-asset recovery research separately shows that resilience and sustainability metrics can be incorporated into cost and recovery decisions without separate parallel processes (Mitoulis et al., 2023b). In the Sri Lankan context, where Quantity Surveyors already report gaps in sustainable-construction competencies (Chamikara et al., 2020) and an increasing diversification of professional roles (Chandramohan et al., 2022), the framework offers a structured way to extend existing skills toward resilient reconstruction without requiring an entirely new professional role.

3.5 A Quantity Surveyor Decision-Making Workflow

To make the framework practically usable, Table 2 sets out an illustrative seven-stage workflow through which a Quantity Surveyor could apply the three-layer structure during an actual recon-

struction programme. The workflow is derived logically from the framework's layers and has not itself been tested in practice; it is presented as a conceptual decision-support structure rather than a validated operational procedure.

Table 2. Illustrative Quantity Surveyor decision-making workflow derived from the framework

Stage	Layer	Focus	Typical Quantity Surveyor actions
1. Context and damage assessment	Recovery planning	Understand the post-conflict/disaster situation	Identify damaged critical infrastructure, hazard exposure and urgency of intervention
2. Risk and cost assessment	Recovery planning	Establish cost and risk baseline	Assessing cost uncertainty, supply-chain vulnerability and sustainability constraints
3. Recovery planning	Recovery planning	Set the commercial strategy	Apply risk-informed cost planning, resilient procurement selection and stakeholder coordination
4. Option evaluation	Delivery	Compare delivery options	Apply life-cycle costing, value engineering, sustainable material selection and supply-chain resilience checks
5. Reconstruction delivery	Delivery	Deliver the works	Coordinate procurement, cost management, stakeholders, materials and resilience requirements
6. Outcome assessment	Outcomes	Evaluate results against objectives	Assess community recovery, environmental sustainability, infrastructure resilience and long-term performance
7. Monitoring and improvement	Cross-cutting	Sustain performance over the asset life	Monitor outcomes and feed lessons back into future recovery-planning decisions

4 PRACTICAL IMPLICATIONS

As a conceptual, literature-based contribution, the framework is intended to provide a structured basis for decision-making rather than a proven operational tool. Its practical significance can be considered separately for three audiences.

Policymakers. The framework could support the development of procurement policy, reconstruction standards and sustainability requirements for publicly funded recovery programmes and may provide a structured basis for long-term value-for-money decisions in public infrastructure investment.

Reconstruction agencies. The framework offers a decision-support structure for early-stage cost planning, procurement-route selection, risk assessment, supply-chain planning and coordination between stakeholders during delivery and could assist agencies in structuring monitoring activity across recovery programmes.

Quantity Surveyors. The framework is intended to assist practitioners in structuring risk-informed cost planning, procurement advice, life-cycle costing, value engineering, sustainable material assessment, supply-chain risk consideration, stakeholder coordination and performance monitoring within a single, reconstruction-specific reference structure.

These implications are expressed in deliberately cautious terms, since the framework has not yet been tested against outcomes in an active reconstruction programme.

5 LIMITATIONS AND FUTURE RESEARCH

This study is subject to several limitations. The framework is conceptual and literature-based; it has not been empirically tested, and no primary data were collected from experts or practitioners. The systematic review, while structured, relied on the sources available within the timeframe of this extended abstract, and the full search protocol will be reported in the subsequent full paper. The twelve components and three-layer structure represent the authors' synthesis of recurring themes in the literature and should be treated as a starting point for empirical enquiry rather than a settled classification.

Future research should validate and refine the framework through industry case studies, practitioner evaluation or expert interviews conducted with Quantity Surveyors and other professionals engaged in active post-conflict or disaster-reconstruction programmes. Such validation would allow the relative importance of the twelve components to be tested empirically and would allow the illustrative decision-making workflow presented in Table 2 to be assessed and refined against real reconstruction practice.

6 CONCLUSION

This study addresses the fragmentation of commercial management guidance available to Quantity Surveyors working on resilient reconstruction of critical infrastructure after conflict or disaster. It has developed a conceptual Sustainable Quantity Surveying Framework, organised around three layers (recovery planning, delivery and outcomes) and twelve components, that positions the Quantity Surveyor as a coordinating actor connecting economic, environmental and social objectives. The framework is relevant to Sri Lanka and to other post-conflict or disaster-affected regions rebuilding infrastructure for long-term performance. As a conceptual, literature-based contribution, it requires empirical validation through case studies, practitioner evaluation or expert interviews before claims about its practical effectiveness can be made.

7 REFERENCES

Chamikara, P. B. S., Perera, B. A. K. S., & Rodrigo, M. N. N. (2020). Competencies of the quantity surveyor in performing for sustainable construction. International Journal of Construction Management, 20(3), 237–251. https://doi.org/10.1080/15623599.2018.1484848

Chandramohan, A., Perera, B. A. K. S., & Dewagoda, K. G. (2022). Diversification of professional quantity surveyors' roles in the construction industry: The skills and competencies required. International Journal of Construction Management, 22(7), 1374–1381. https://doi.org/10.1080/15623599.2020.1720058

Hevner, A. R., March, S. T., Park, J., & Ram, S. (2004). Design science in information systems research. MIS Quarterly, 28(1), 75–105. https://doi.org/10.2307/25148625

Iddamalgoda Pathiranage, T. S., & Hadiwatte, C. (2020). Application of life cycle costing technique in Sri Lankan construction industry: Assessment by quantity surveyors. IQSSL Technical Research Proceedings 2020.

Mitoulis, S. A., Argyroudis, S., Panteli, M., Fuggini, C., Valkaniotis, S., Hynes, W., & Linkov, I. (2023a). Conflict-resilience framework for critical infrastructure peacebuilding. Sustainable Cities and Society, 91, Article 104405. https://doi.org/10.1016/j.scs.2023.104405

Mitoulis, S. A., Bompa, D. V., & Argyroudis, S. (2023b). Sustainability and climate resilience metrics and trade-offs in transport infrastructure asset recovery. Transportation Research Part D: Transport and Environment, 121, Article 103800. https://doi.org/10.1016/j.trd.2023.103800

Peffers, K., Tuunanen, T., Rothenberger, M. A., & Chatterjee, S. (2007). A design science research methodology for information systems research. Journal of Management Information Systems, 24(3), 45–77. https://doi.org/10.2753/MIS0742-1222240302

ISSN: 2773-7055
Proceedings of the 5th International Research Conference
Institute of Technology, University of Moratuwa
November 5, 2026

Paper ID: 65

HYDROLYSIS ROUTE AS A KEY DETERMINANT OF FISH-WASTE LIQUID FERTILIZER QUALITY: A METHOD-CENTRED REVIEW

K A D Thathsarani[1*], W V W H Wickramaarachchi[1], N M L Fernando[1]

[1]Division of Polymer and Chemical Engineering Technology, Institute of Technology, University of Moratuwa, Homagama, Sri Lanka

*Corresponding author: 22ch0044@itum.mrt.ac.lk

ABSTRACT: Fish processing generates 30-70% of the original biomass as waste, and conversion of this stream into liquid fertilizer is repeatedly proposed as a circular-economy solution for fisheries and aquaculture systems. However, the literature largely treats "fish waste liquid fertilizer" as a single product, when it is more accurately a platform with at least four distinct hydrolysis routes: enzymatic hydrolysis, microbial (lactic acid) silage, acid hydrolysis, and combined enzymatic-microbial processing. Each route produces a chemically and agronomically distinct material, and treating them as interchangeable obscures meaningful comparisons across studies. This review reframes the literature around a decision question: which hydrolysis route is most suitable for a given application. Drawing on raw material sourcing, hydrolysis chemistry, downstream stabilization, fertilizer performance, and scale-up considerations, a unified comparison framework is developed based on pH, degree of hydrolysis, nitrogen recovery, odour control, storage stability, dilution rate, and crop response. Direct matched-condition comparisons across routes remain limited; most studies report plant growth or nutrient content for a single processing or hydrolysis method. Where head-to-head data exist—notably a recent wheat trial comparing enzymatic, microbial, and combined hydrolysates on a nitrogen-equivalent basis, and a comparison of acid versus lactic-fermented silage—they indicate that route selection trades degree of hydrolysis and nitrogen recovery against odor, shelf stability, and capital cost, with no single route dominating across all use cases. The review proposes that future studies adopt a common reporting framework based on these variables and presents a provisional decision framework linking the hydrolysis route to the production context and intended use.

Keywords: fish waste valorization, hydrolysis route, liquid fertilizer, fish protein hydrolysate

1 INTRODUCTION

Globally, fish processing produces large amounts of heads, frames, viscera, skin, and other processing by-products, typically 30-70% of the catch, depending on species and degree of processing undertaken (Ahuja et al., 2020). With growing concerns for the environment and restrictions on conventional disposal methods, and given their high protein, lipid and mineral content, fish processing by-products are now being widely researched as feed stocks for resource recovery. Liquid fertilizers are one of the most commonly suggested valorization routes, along with fishmeal, fish oil and collagen (Arvanitoyannis & Kassaveti, 2008; Hopkins et al., 2025; Ozogul et al., 2021).

Though fish waste-derived liquid fertilizers are discussed generally, with reviews focusing on nutrient content, plant growth, and sustainability, the hydrolysis used to produce them is often not distinguished, an important variable when considering their relative effectiveness. The method of hydrolysis is not a minor processing detail: it shapes the resulting product's composition, stability, and downstream use, as detailed below (Hopkins et al., 2025; Toppe et al., 2018). This review will therefore focus on the influence of the method of hydrolysis on

the use of fish-waste liquid fertilizers in different agricultural systems. The literature describes four main approaches for hydrolysis: enzymatic hydrolysis, microbial (lactic acid) silage, acid hydrolysis and a combined enzymatic-microbial process. The hydrolysis methods are treated as the organizing variable across raw-material sourcing, process chemistry, downstream treatment, fertilizer performance, and industrial scale-up.

This type of literature review is needed because the current literature considers fish waste "liquid fertilizer" to be a homogeneous product category, despite the importance of key method-specific differences in determining agronomic effectiveness, safety, and up-scaling possibilities. Enzymatic, lactic microbial (silage), acid, and enzymatic-microbial (combined) hydrolysis yield chemically and functionally different products with varying degrees of protein degradation (peptide-based vs. free amino-acid profile); recoverability of soluble nitrogen; pH and solubilization of minerals; inherent odor and microbe content; and stability in storage (Toppe et al., 2018; Hopkins et al., 2025). Such hydrolysis-specific parameters will, in turn, influence the requirements for handling and stabilization of fish liquid fertilizer, its dilution and application rates, effect on crops, and cost of production and application (Ozogul et al., 2021; Ahuja et al., 2020); therefore, neglecting such method-specific differences in comparisons may lead to false conclusions regarding its efficacy, environmental implications, and economic viability. Thus, the re-evaluation of the literature based on the hydrolysis method used, along with suggestions of a unified report format, may allow for useful comparisons and inform the route choice for particular production settings and point out knowledge gaps for future studies (Toppe et al., 2018; Hopkins et al., 2025). Unlike prior reviews of fish-waste valorization (e.g., Ahuja et al., 2020; Hopkins et al., 2025), which discuss liquid fertilizer largely as a single product class, this review is, to our knowledge, the first to organize the literature explicitly by hydrolysis route and to propose a shared, route-agnostic comparison framework.

2 METHODOLOGY

This review synthesizes peer-reviewed studies, process-design reviews, and applied-agriculture sources addressing fish-waste hydrolysis and its agronomic use, identified through a structured literature search on enzymatic hydrolysis, microbial silage, acid hydrolysis, and combined hydrolysis routes for fish processing by-products. Studies were grouped by hydrolysis route rather than by reported outcome, consistent with the review framework. From each study, data were extracted, where reported, against seven comparison variables: pH and pH trajectory, degree of hydrolysis or equivalent measures of protein breakdown, nitrogen recovery, odor control mechanism, storage stability, dilution or application rate, and crop response. Studies reporting head-to-head comparisons across two or more routes under matched raw material, dose, or crop conditions were identified separately and treated as the primary evidence base for cross-route claims, given their relative scarcity in this literature (1983-2026).

3 RESULTS AND DISCUSSION

3.1 Raw Material and Route Selection

Hydrolysis route selection depends on raw material characteristics; the two cannot be chosen independently. Whole small pelagic fish naturally carry their own digestive enzymes and microbiota and are the traditional substrate for silage production, where proteolysis is initiated through autolytic and microbial activity once appropriate pH or fermentation conditions are established (Lindgren & Edlund, 1983). Processing by-products, in contrast, are compositionally more diverse: viscera carry concentrated digestive enzymes useful for autolysis, while frames and skin are comparatively enzyme-poor and depend more on added enzyme or acid for breakdown (Toppe et al., 2018). Mineral-rich residues such as carp scales are more resistant due to their collagen structure and associated calcium phosphate, and therefore generally require harsher hydrolysis such as acid or microwave-assisted acid (Long et al., 2025). In addition, fish waste is generally low in fermentable sugars; therefore, microbial silage routes require an external carbon source such as molasses to acidify the mass quickly (Toppe et al., 2018).

3.2 Hydrolysis Chemistry by Route

Enzymatic Hydrolysis- Enzymatic Hydrolysis utilizes external protease enzymes such as Alcalase, Flavourzyme, bromelain, or fruit-derived proteases under controlled temperature and pH to breakdown fish protein at a defined, measurable degree of hydrolysis (DH). Araujo et al. (2021) reported that using Alcalase 2.4 L at 50 °C and pH 8, the enzyme-to-substrate ratio is the dominant control variable and that DH scales linearly with recoverable hydrolysate, collagen, and oil; at DH 25%, roughly 430 g hydrolysate, 10 g collagen, and 350 g oil were recovered per kilogram of fish waste. This is one of the few quantitative process yield relationships reported in the literature, and DH is also the variable most consistently linked to downstream fertilizer performance. The route is controllable, but enzyme and energy costs remain dominant barriers to scale-up (Hopkins et al., 2025).

Microbial Silage- Fermenting fish silage with lactic acid bacteria typically *Lactiplantibacillus plantarum* depends on adding carbohydrates. The bacteria ferment these sugars into lactic acid, dropping the pH below 4.5 in under two days to effectively block spoilage microbes (Lindgren & Edlund, 1983). Notably, the fish's own internal enzymes drive protein break down, remaining active despite the acidic environment; hydrolysis therefore does not reach an abrupt endpoint but continues throughout storage. To examine how different preservation methods alter the final product, Özyurt et al. (2016) conducted a controlled trial on ponyfish silage using formic acid, a formic-sulfuric acid blend, and lactic fermentation. Because they held the source material constant while only changing the preservation chemical, their data demonstrated that the specific stabilization route creates distinct, measurable shifts in both fatty acid profiles and biogenic amine buildup over a 60-day storage window.

Acid Hydrolysis- Acid hydrolysis involves the addition of strong or organic acid, commonly formic acid alone or combined with sulfuric or phosphoric acid, to rapidly reduce pH below 4, halting microbial spoilage while activating endogenous proteases (ScienceDirect Topics, n.d.). Acid routes are typically the fastest to stabilize and the most cost-effective at small scale, but

the resulting product is highly acidic and must be diluted or neutralized before application. Microwave-assisted acid hydrolysis has been applied to harder substrates such as carp scales, with conditions optimized via response surface methodology to maximize amino-acid release (Long et al., 2025).

Combined Enzymatic-Microbial Routes- Combined routes sequence an enzymatic step with a microbial fermentation step, reasoning that the enzyme initiates protein breakdown while fermentation extends hydrolysis and enhances the stability of the product biologically. Solis et al. (2026) provided the most critical evidence for this review by executing a true head-to-head comparison-a rarity in this field of literature. They treated the exact same fish by-product stream with three distinct methods: an enzymatic route (Alcalase, 55 °C, pH 6.5), a microbial route (lactic culture, 40°C, pH 6.5, spanning 10 days), and a dual-action combined sequence. They then measured their performance as wheat fertilizers, balancing the applications on a nitrogen-equivalent basis. The data revealed a synergistic effect: single-route treatments underperformed, with enzymatic hydrolysis yielding 100 mM of α-amino groups and microbial fermentation reaching 170 mM, while the combined method produced 226 mM and achieved 33% protein recovery. Because it holds the raw material constant, this research offers the clearest demonstration of how these routes compare under matched conditions.

3.3 Comparison Framework and the Evidence Gap

Fish protein hydrolysate (FPH) is widely reported to improve germination, root development, and chlorophyll content across crops, with yield increases commonly cited in the 10–30% range relative to untreated controls (Dora Agri, 2022; HUMICO, 2025). A synthesis of FPH biostimulant trials found that a sardine-derived hydrolysate produced a significantly stronger yield response in tomato than in sorghum despite identical product and dose, directly contradicting the assumption that crop response is a generic property of "fish fertilizer" independent of crop type (Invenire, 2025). Table 1 summarizes the four hydrolysis families against the seven variable comparison framework; cells marked as having limited evidence reflect genuine gaps in the published comparative literature.

Table 1. Comparison of Fish-Waste Hydrolysis Routes Against Seven Performance Variables

Variable	Enzymatic	Microbial Silage	Acid Hydrolysis	Combined
Operating pH	Neutral–alkaline (6.5–8)	Falls to <4.5 in 24–48 h	Drops to <4 in minutes	Neutral, then microbial shift
Degree of hydrolysis	Controllable; scales linearly with yield	Progressive during storage	Rapid initial liquefaction	Highest: 226 mM α-amino groups
α-amino group concentration	Moderate (~100 mM)	Higher than enzymatic (~170 mM)	Limited matched data	Highest; synergistic effect
Odour control	Requires separate stabilization	Gradual pH-driven suppression	Fast acid-driven suppression	Limited comparative data
Storage stability	Lowest without added step	Moderate–high	Highest; storable for years	Limited long-term data
Crop response	Strong in horticulture; crop-specific	Positive; limited head-to-head data	Positive; limited matched-dose data	Positive in wheat (N-equivalent basis)

Variable	Enzymatic	Microbial Silage	Acid Hydrolysis	Combined
Dilution / Application Rate	Limited data	Limited data	Must be diluted or neutralized before application	Applied on nitrogen-equivalent basis

The recurring weakness across this literature is that most studies report outcomes for a single hydrolysis route at a single dose, on a single crop, without a matched comparison against alternative routes processing the same raw material. The few genuine head-to-head studies are limited to the pony fish acid-versus-silage comparison (Özyurt et al., 2016) and the wheat trial comparing enzymatic, microbial, and combined hydrolysates (Solis et al., 2026) and are disproportionately valuable precisely because they are rare. Future comparative work should report results against the seven-variable framework above, ideally on a nitrogen-equivalent basis across at least two crop types, given the demonstrated crop-specificity of response. The current seven-variable framework centres on chemistry, stability, and agronomic performance; processing time, energy requirement, production cost, capital requirement, and scalability are also relevant to route selection and are used qualitatively in the decision framework below, but were not tabulated in Table 1 because route-specific figures are rarely reported on a comparable basis across studies (Hopkins et al., 2025). Fish species and raw-material composition were likewise not treated as a formal framework variable: the studies reviewed here vary in species (e.g., ponyfish, sardine, carp) and by-product stream (whole fish versus viscera, frames, or scales), and the available evidence is too fragmented to isolate species effects from route effects. Extending the framework to explicitly capture raw-material variation is identified as a priority for future comparative work.

3.4 Provisional Decision Framework

Enzymatic hydrolysis is best suited to high-value horticultural biostimulant production, where controllable DH justifies the added enzyme cost. Microbial silage is best suited to low-cost, on-farm production where capital is constrained, and a carbohydrate co-substrate is available. Acid hydrolysis is best suited to applications prioritizing speed and long-term storage stability over peptide-profile control. Combined enzymatic-microbial routes are best suited to contexts where nitrogen recovery is the primary agronomic constraint, though limited scale-up evidence currently confines this route to research and pilot-scale applications rather than commercial-scale deployment.

4 CONCLUSION

Fish-waste liquid fertilizer is not a single product but a platform whose final chemistry, stability, and agronomic behavior are set by the hydrolysis route used to produce it. Enzymatic hydrolysis, microbial silage, acid hydrolysis, and combined enzymatic–microbial processing each occupy a distinct position on the trade-off space between degree of hydrolysis, nitrogen recovery, odour and stability, and cost, and the available evidence does not support establishing one route as universally superior. The literature's most significant gap is the scarcity of studies that hold raw material and crop constant while comparing routes directly; the few studies that do this should be treated as reference points for future comparative work. Organizing this literature

around hydrolysis route, rather than around an undifferentiated "fish fertilizer" category, gives researchers and practitioners a clearer basis for matching production method to agronomic and economic constraints.

5 REFERENCES

Ahuja, I., Dauksas, E., Remme, J. F., Richardsen, R., & Løes, A. K. (2020). Fish and fish waste-based fertilizers in organic farming - with status in Norway: A review. *Waste Management, 115*, 95–112.

Araujo, J., Sica, P., Costa, C., & Márquez, M. C. (2021). Enzymatic hydrolysis of fish waste as an alternative to produce high value-added products. *Waste and Biomass Valorization, 12*(2), 847–855.

Arvanitoyannis, I. S., & Kassaveti, A. (2008). Fish industry waste: Treatments, environmental impacts, current, and potential uses. *International Journal of Food Science and Technology, 43*(4), 726–745.

Dora Agri. (2022). Deep sea cold processed pure fish protein hydrolysate fertilizer. Dora Agri.

Hopkins, D. T., Berrué, F., Khiari, Z., & Hawboldt, K. A. (2025). Valorization of fisheries by-products via enzymatic protein hydrolysis: A review of operating conditions, process design, and future trends. *Process Biochemistry, 149*, 306–320.

HUMICO. (2025). Fish protein hydrolysate fertilizer: Benefits and application guide. HUMICO.

Invenire. (2025). Fish amino acids and protein hydrolysate as biostimulants. Invenire.

Lindgren, S., & Edlund, K. (1983). Silage fermentation of fish or fish waste products with lactic acid bacteria. *Journal of the Science of Food and Agriculture, 34*(10), 1057–1067.

Long, Y., Chen, M., Zhou, W., Xiao, N., & Cai, J. (2025). Process optimization and effectiveness verification of liquid amino acid-containing fertilizer prepared from hydrolysis of carp scales. *Waste and Biomass Valorization, 16*, 1411–1421.

Ozogul, F., Cagalj, M., Šimat, V., Ozogul, Y., Tkaczewska, J., Hassoun, A., Kaddour, A. A., Kuley, E., Rathod, N. B., & Phadke, G. G. (2021). Recent developments in valorisation of bioactive ingredients in discard/seafood processing by-products. *Trends in Food Science & Technology, 116*, 559–582.

Özyurt, G., Gökdoğan, S., Şimşek, A., Yuvka, I., Ergüven, M., & Kuley Boga, E. (2016). Fatty acid composition and biogenic amines in acidified and fermented fish silage: A comparison study. *Archives of Animal Nutrition, 70*(1), 72–86.

ScienceDirect Topics. (n.d.). Fish silage - an overview. Retrieved from `https://www.sciencedirect.com/topics/agricultural-and-biological-sciences/fish-silage`

Solis, T., Valdivia, S., Vergara, A., Carvajal, M., Seguel, I., & Valencia, P. (2026). Valorization of fish processing by-products through combined enzymatic and microbial hydrolysis: Nitrogen recovery and fertilizer efficiency in wheat. *Frontiers in Nutrition, 13*, 1757182.

Toppe, J., Olsen, R. L., Peñarubia, O. R., & James, D. G. (2018). *Production and utilization of fish silage: A manual on how to turn fish waste into profit and a valuable feed ingredient or fertilizer.* Food and Agriculture Organization of the United Nations.

ISSN: 2773-7055
Proceedings of the 5th International Research Conference
Institute of Technology, University of Moratuwa
November 5, 2026

Paper ID: 82

INFLUENCE OF BENTONITE INFILL ON THE SHEAR BEHAVIOUR OF BIOTITE GNEISS–CONCRETE INTERFACES UNDER CONSTANT NORMAL LOADING

Ayodya Bulathsinhala[1*], Anurudda Puswewala[2]

[1]Division of Civil Engineering Technology, Institute of Technology, University of Moratuwa, Homagama, Sri Lanka

[2]Department of Civil Engineering, Faculty of Engineering, Sri Lanka Institute of Information Technology, Sri Lanka

*Corresponding author: bulathsinhalau@itum.mrt.ac.lk

ABSTRACT: Rock-socketed piles in crystalline metamorphic rocks frequently exhibit higher mobilised shaft resistance than predicted by conservative empirical design guidelines. This study explicitly aims to quantify the influence of Bentonite filter-cake thickness (0.5 - 2.0mm) on the peak and residual shear strength of smooth Biotite Gneiss–concrete interfaces under Constant Normal Loading (CNL) at a normal stress of 306 kPa. Direct shear tests on Grade 30 self-compacting concrete cast against planar rock surfaces (JRC < 1) revealed that peak shear strength decreases rapidly up to a critical infill thickness (T) of 1.25 mm a 53.5 % reduction), whereas residual shear strength stabilizes at a critical thickness (T) of 1.75 mm (a 36.1 % reduction). Even under these weak, smooth boundary conditions, the measured interface shear strengths exceeded the conservative 200 kPa limiting value specified by Sri Lankan ICTAD guidelines. These experimental results provide fundamental baseline parameters for improving the design of rock-socketed piles in metamorphic geology.

Keywords: Biotite Gneiss, Bentonite infill, direct shear test, rock–concrete interface, rock-socketed piles

1 INTRODUCTION

The shear behaviour of rock–concrete interfaces plays a vital role in the design and stability assessment of geotechnical structures, including rock-socketed piles, concrete dams, and rock anchors (Bista et al., 2020; Hou et al., 2022; Sas et al., 2021). In regions underlain by crystalline metamorphic rock formations, design practice relies heavily on conservative empirical guidelines due to a lack of quantified interface parameters (Bulathsinhala and Puswewala, 2024). Field assessments of bored piles in Sri Lanka highlight this conservatism. Thilakasiri et al. (2015) evaluated mobilised skin friction from instrumented pile load tests and demonstrated that the upper limiting value of 200 kPa specified by the ICTAD guidelines (1997) is overly conservative, even for weak rock sockets. In contrast, design methods proposed by Hong Kong GEO (2006) and Williams et al. (1980) offer more realistic predictions when appropriate safety factors are applied.

While direct shear testing is widely recognized as the primary standard for characterizing interface strength (Malmgren et al., 2005), previous literature lacks systematic laboratory quantification regarding how Bentonite infill accumulation affects smooth Biotite Gneiss–concrete interfaces under Constant Normal Loading (CNL) conditions. To address this research gap, this study executes a systematic direct shear testing programme to isolate and quantify the effect of Bentonite infill thickness (0.0 - 2.0 mm) on both peak and residual interface shear strength under a constant normal stress of 306 kPa.

2 METHODOLOGY

2.1 Rock Sample Collection and Sizing

For this study, fresh Biotite Gneiss, a prevalent metamorphic rock type in regions characterized by the presence of metamorphic rocks, was specifically chosen from Kandy, Sri Lanka. Samples were cut into cuboids of the dimensions 150 mm x 150 mm x 75 mm and faces were made smooth (Joint Roughness Coefficient (JRC)< 1). The UCS of the selected rock sample varied between 140 – 170 MPa and the Poisson's ratio was 0.22.

2.2 Preparation of Concrete Samples for Shearing

Concrete samples were of Grade 30 self-compacting concrete which possessed high slump of 175+ 25mm. Concrete was casted over rock samples with and without the presence of Bentonite infill (12% moisture content) in between them. Different thicknesses of Bentonite infill starting from 0.5 mm up to 2 mm in the steps of 0.25 mm was placed over the rock surfaces prior to cast the concrete over it. A minimum of three replicate specimens were prepared for each of the seven infill thicknesses, as well as for the bonded condition without infill, to assess the repeatability of the test results. All cast assemblies were cured under controlled laboratory conditions for 28 days. In total, 24 test cases were evaluated, with three replicate tests conducted for each condition.

2.3 Direct Shear Tests on Biotite Gneiss-Concrete Interface

Direct shear tests were initially conducted using a purpose-built direct shear apparatus at the Institute of Technology, University of Moratuwa (ITUM), Sri Lanka. The test results were subsequently verified using the direct shear testing apparatus at the University of Wollongong (UOW), New South Wales, Australia. The results presented in this paper are based exclusively on the tests conducted at the University of Wollongong. The Samples were first placed in the shear box and subjected to normal stress 0.306 MPa, representing the typical lockdown normal stresses experienced by rock sockets due to the hydrostatic pressure of flowing concrete at depth 13.3 m respectively. Following this, the samples experienced shearing at a rate of 0.5 mm/min.

3 RESULTS

The variation of shear stresses with respect to shear displacement for different infill thicknesses are shown in Figure 1. Sudden brittle failure occurred for Biotite Gneiss – Concrete interface without infill as depicted in Figure 1. As the shear stress rises sharply with elastic behavior until 0.24 mm shear displacement and continues the plastic displacement thereafter until the bond breaks at 0.43 mm displacement achieving 607 kPa, leading to a rapid decrease in shear stress up to 395.7 kPa. Following this, there's another increase in shear stress until it reaches the friction strength. Once this point is reached, friction sliding begins, maintaining a nearly constant stress level 413 kPa while the displacement continues to rise.

The variation of peak shear strengths and residual shear strengths with respect to infill thicknesses are shown in Figure 2. Peak shear stress reduces significantly up to the infill thickness of 1.25 mm and thereafter the peak shear stress becomes stable. The peak shear stress decreases gradually

with the Bentonite infill thickness reaches 0.75 mm – 1 mm and there after the reduction in peak shear stress is insignificant. Residual shear stress also follows the identical behavior to the pattern of peak shear stress.

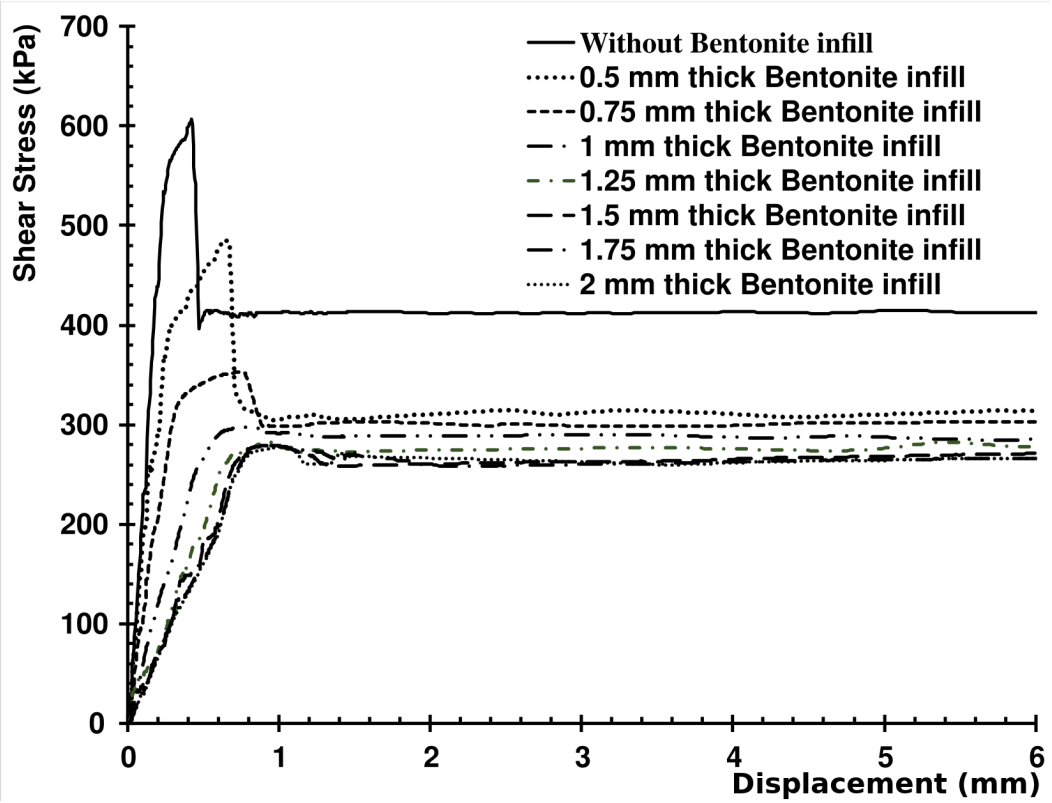


Figure 1. Variation of shear stresses for Biotite Gneiss – Concrete interfaces for different infill thickness at 306 kN/m2normal stress.

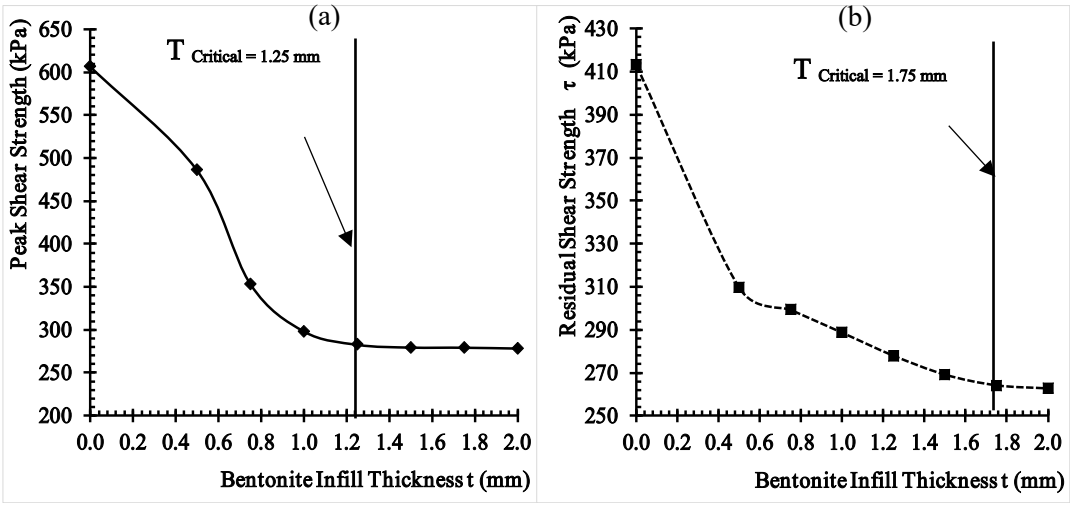


Figure 2. (a)Variation of Peak Shear strength with infill thickness, (b)Variation of Residual Shear strength with infill thickness

4 ANALYSIS

Figure 2 demonstrates the graphical method employed to determine the critical infill thickness in this study. Table 1 compares the shear stress values at these critical infill thicknesses with the shear stress of Bentonite infill at a 306 kPa normal stress level.

Table 1. Shear strengths of critical infill thicknesses at 306 kPa normal stress

Case	Shear stress (kPa)
Peak shear strength at critical infill thickness 1.25 mm	282.54
Residual shear strength at critical infill thickness 1.75mm	264.09
Bentonite infill (12% moisture content)	268.70

The reduction in peak shear stress was minimal, decreasing by only 4 kPa when the infill thickness reached 2 mm, following the critical infill thickness of 1.25 mm. In addition, beyond the critical infill thickness of 1.75 mm up to 2 mm, the residual shear stress decreased by 1.5 kPa. Notably, the residual shear stress at 1.75 mm shear displacement approached the shear stress of Bentonite infill, with a difference of only 4.61 kPa between these values. This highlights that upon reaching the critical infill thickness, the residual shear behavior becomes primarily influenced by the characteristics of the infill material. Table 2 depicts the percentage drop of the peak and the residual shear stresses with respect to infill thickness.

Table 2. Percentage reduction of shear stresses with infill thickness

Bentonite infill thickness (mm)	Peak shear strength (kPa)	(%) Reduction of peak shear strength	Residual Shear strength (kPa)	(%) Reduction of residual shear strength
0.00	607.03	0.00	413.19	0.00
0.50	485.90	19.95	309.43	25.11
0.75	352.98	41.85	299.17	27.60
1.00	298.00	50.91	288.54	30.17
1.25	282.54	53.46	277.84	32.76
1.50	279.35	53.98	269.04	34.89
1.75	279.22	54.00	264.09	36.08
2.00	278.18	54.17	262.67	36.43

The peak shear Strength is highly sensitive to thin infill layers. Introducing 1.00 mm of Bentonite reduces peak shear strength by 50.91 %. The critical infill thickness (t_{crit}) for peak shear strength occurs at 1.25 mm (53.46 % drop). Increasing infill thickness beyond 1.25mm up to 2.00 mm causes an additional reduction of less than 1%. Residual shear strength is less sensitive to initial infill thickness, reaching its critical threshold (t_{crit}) at 1.75 mm with a maximum reduction of 36.08 %. At t = 1.75 mm, Residual shear strength (264.09 kPa) closely approaches the pure shear strength of the Bentonite infill itself (268.70 kPa), indicating that residual behavior beyond t_{crit} is entirely governed by the internal shear strength of the infill matrix.

According to Bulathsinhala and Puswewala (2024), it takes less than 1 hour to form a 1 mm thick Bentonite infill over Biotite Gneiss. Further, when the pile idle time is 1.5 hours, the Bentonite infill reaches the critical infill thickness. Past studies found that the most frequent pile idling duration is between 3-6 hours range. Hence definitely the peak shear strength drops more than 50%. It takes 6.5 hours to reach the critical infill thickness of the residual shear stress 1.75 mm (Bulathsinhala and Puswewala,2024). However, it is more unlikely to idle a pile more than 6 hours unless there is a major break down or issue in the construction site. Nevertheless, for safe predictions, 30-37% reduction can be considered in the residual shear stress. Since the smooth surface represent the weakest conditions it possible to generalize this outcome and a valid result

and does not warrant to use the peak shear strength as the governing stress for the designing purposes because this bond between the rock and concrete can be affected largely by the infill material to a significant extent. From a design perspective, peak shear strength should not be relied upon as the governing design parameter because adhesive bonding breaks down at small displacements (< 1.0 mm). In contrast, bored cast-in-situ piles typically require larger shear displacements (up to 12 mm) to mobilise socket resistance, making residual shear strength the appropriate governing property.

5 CONCLUSION

Critical Infill Thicknesses: Under CNL conditions (n = 306 kPa), the critical infill thickness is 1.25 mm for peak shear strength (53.5 % reduction) and 1.75 mm for residual shear strength (36.1% reduction).

Governing Shear Behavior: Beyond critical infill thickness, residual shear behavior is governed by the shearing resistance of the Bentonite infill material itself. Because bond degradation occurs at displacements <1.0 mm, design practice should govern shaft capacity using residual shear strength rather than peak strength.

Comparison with Guidelines: The minimum measured residual shear strength (262.67 kPa) on smooth planar interfaces (JRC < 1) remains above the conservative 200 kPa limiting value specified by Sri Lankan ICTAD guidelines, confirming that current national guidelines remain conservative even under weak interface conditions.

Limitations & Future Outlook: These findings are strictly applicable to smooth planar interfaces under CNL conditions. Field pile sockets exhibit higher surface roughness (JRC approx. 4-12) and operate under Constant Normal Stiffness (CNS) conditions, which typically yield shear strengths 3-4 times higher than CNL conditions. This study serves as an essential preliminary baseline for future CNS interface testing on rough metamorphic rock sockets.

6 ACKNOWLEDGEMENT

Authors extend the gratitude to Prof. Jayan S. Vinod, senior lecturer in the School of Civil, Mining, and Environmental Engineering, at the University of Wollongong for letting use the Civil High Bay laboratory of University of Wollongong, NSW for testing program.

7 REFERENCES

Bista, D., Sas, G., Johansson, F., & Lia, L. (2020). Influence of location of large-scale asperity on shear strength of concrete-rock interface under eccentric load. *Journal of Rock Mechanics and Geotechnical Engineering*, 12(3), 449-460.

Bulathsinhala, A. U. V. B., & Puswewala, U. G. A. (2024). Formation of Bentonite Filter Cake over Crystalline Metamorphic Rocks by Means of a Pressure Chamber: A Laboratory Study. *Journal of Testing and Evaluation*, 52(1), 364-377. 10.1520/JTE20220322

Geotechnical Engineering Office. (2006). Foundation Design and Construction, Civil Engineering and Development, The Government of the Hong Kong Special Administrative Region (Vol. Geo Publication No.01).

Hou, J., Zhao, H., Peng, W., & Zhao, M. (2022). A limit solution for predicting side resistance on rock-socketed piles. *Journal of Engineering Mechanics*, 148(1), 1365–1609.

Institute for Construction Training and Development, Sri Lanka. (1997). Guidelines for Interpretation of Site Investigation Data for Estimating the Carrying Capacity of Single Piles for Design of Bored and Cast In-situ Reinforced Concrete Piles, (ICTAD /DEV/15).

Malmgren, L., Nordlund, E., & Rolund, S. (2005). Adhesion strength and shrinkage of shotcrete. *Tunnelling and underground space technology*, 20(1), 33-48

Sas, G., Popescu, C., Bista, D., Seger, A., Arntsen, B., Johansson, F., & Lia, L. (2021). Influence of large-scale asperities on the shear strength of concrete-rock interface of small buttress dams. *Engineering structures*, 245, 112952.

Thilakasiri, H.S., Abeyasinghe, R. M. & Peiris, T. A. Optimization of the Designing of Bored and Cast In-Situ Piles 368 in Sri Lanka", The International Conference on Geotechnical Engineering, Colombo, Sri Lanka, 369 August 11–15, 2015.

Williams, A. F., Johnstons, I. W., and Donald, I. B., 1980, The design of socketed piles in weak rock, *Int. Conf. structural foundations on rock*, Sydney Balkema

ISSN: 2773-7055
Proceedings of the 5th International Research Conference
Institute of Technology, University of Moratuwa
November 5, 2026

Paper ID: 2

META-CALIBRATED PROTOTYPE OPEN-SET ADAPTATION FOR CABLE-TERMINATION PARTIAL DISCHARGE DIAGNOSIS UNDER LABORATORY-TO-FIELD DOMAIN SHIFT

H P D S Madhuranga[1*], Wong Jee Keen Raymond[1], W L S Madhuranga[2]

[1]Department of Electrical Engineering, Faculty of Engineering, Universiti Malaya, 50603, Kuala Lumpur, Malaysia

[2]Division of Civil Engineering Technology, Institute of Technology, University of Moratuwa, Homagama, Sri Lanka

*Corresponding author: shiran.madhuranga90@gmail.com

ABSTRACT: Reliable partial discharge (PD) diagnosis in high-voltage cable terminations requires models that can classify known field patterns from limited labelled samples while rejecting unseen discharge patterns. This study formulates cable-termination PD diagnosis as a few-shot open-set field-adaptation problem under a laboratory-to-field domain shift. Related laboratory PD data from cable joints, oil-immersed transformers, and dry-type transformers are used as source reference data, while six field cable-termination PD classes form the target domain. A meta-calibrated prototype open-set adaptation framework is proposed. The method preserves an ImageNet-pretrained ResNet50 feature space, constructs K-shot target-domain field prototypes, and uses source open-set episodes to calibrate the unknown-rejection decision. Closed-set field evaluation achieves 94.69% accuracy and 94.24% macro-F1 using 20 labelled field samples per class. In leave-one-field-class-out testing, the cable-source meta-calibrated detector obtains 79.38% known-class accuracy, 91.21% unknown recall, 85.29% normalised accuracy, 82.76% open-set macro-F1, 93.05% AUROC, and 17.58% FPR@95TPR at K = 20. A source-calibrated prototype-distance threshold gives a comparable practical operating point, reaching 85.65% normalised accuracy at K = 10. The results suggest that, within the proposed framework, related laboratory PRPD data can support open-set calibration while preserving the target-domain prototype representation, and that limited field prototypes provide a practical basis for open-set PD diagnosis in field cable terminations.

Keywords: partial discharge diagnosis, cable termination, few-shot learning, open-set recognition, meta-calibration

1 INTRODUCTION

Partial discharge (PD) diagnosis is an important condition-monitoring task for high-voltage insulation systems because persistent discharge activity can indicate local insulation deterioration before severe failure occurs (Long *et al*., 2024). Many data-driven PD diagnosis studies are evaluated under a closed-set assumption, where each test sample must belong to one of the classes observed during training. Although open-set recognition (OSR) methods have been introduced to reject unseen fault patterns (Fei *et al*., 2024; Tuyet-Doan *et al*., 2021), and domain adaptation approaches have been investigated to reduce source–target distribution differences (Niu and Zhu, 2025), most existing studies still rely on sufficient labelled source or target data and often assume that laboratory and field conditions are closely aligned (Madhuranga *et al*., 2025a, 2025b). This assumption is restrictive for field operation because new or unfamiliar phase-resolved partial discharge (PRPD) patterns may appear after installation, and only a small number of labelled field samples may be available for a specific asset. Therefore, field cable-

termination diagnosis requires a model that can learn from limited target-domain examples while maintaining the ability to reject unfamiliar patterns as unknown.

The laboratory data available in this study were obtained from the authors' previous work (Madhuranga *et al.*, 2025b) and contain PRPD patterns from cable joints, oil-immersed transformers, and dry-type transformers. These data are useful, but they are not label-equivalent to field cable-termination data. Laboratory cable-joint measurements are related to cable accessories but should not be assumed to represent field cable terminations directly. This source–target mismatch creates a realistic laboratory-to-field domain-shift problem. Under such conditions, direct source training or source-only meta-learning may over-specialise the representation to laboratory morphology and reduce target-field transfer (Wang *et al.*, 2022).

This study therefore proposes a source-aware but field-adapted approach. Instead of using source data to replace the target representation, source data are used to calibrate open-set behaviour. The objective is to classify known field cable-termination PRPD classes using K labelled support samples per class and to reject a held-out field class as unknown. The main contribution is a meta-calibrated prototype open-set adaptation framework that preserves the transferable ImageNet feature space, constructs field prototypes from limited labelled target samples, and meta-calibrates the rejection boundary using source open-set episodes.

2 METHODOLOGY

As illustrated in Figure 1, the proposed Meta-Calibrated Prototype Open-Set Adaptation (MC-ProtoOSA) framework consists of four stages: feature extraction, field prototype construction, source-based meta-calibration, and open-set inference. First, each PRPD image is resized to the ResNet50 input size and mapped to a normalised deep feature vector using an ImageNet-pretrained ResNet50 encoder. The encoder is kept fixed to preserve a generic and transferable visual representation, while the laboratory source data are used for open-set calibration rather than direct feature retraining. For each known field class c, the prototype P_c is computed as the mean of the normalised support feature vectors z_i whose labels satisfy $y_i = c$, as expressed in (1). A query feature vector z is then compared with each prototype using cosine similarity s_c, as shown in (2), and the highest similarity score $s_{\max}$ in (3) is used for the open-set decision. If $s_{\max}$ satisfies the meta-calibrated acceptance criterion, the query sample is assigned to the nearest known field prototype; otherwise, it is rejected as an unknown PRPD pattern.

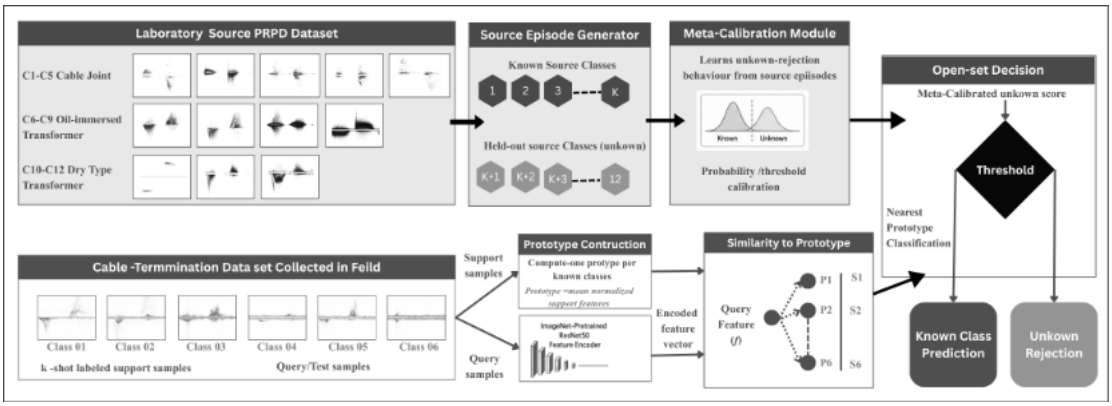


Figure 1. Proposed Model Architecture: Meta-Calibrated Prototype Open-Set Adaptation

$$P_c = \frac{1}{K} \sum_{y_i=c} z_i \tag{1}$$

$$s_c = \cos(z, P_c) \tag{2}$$

$$s_{\max} = \max_c s_c \tag{3}$$

Two deployable calibration modes are evaluated. The first uses a source-calibrated prototype-distance threshold, in which a query is rejected if its minimum distance to all known prototypes exceeds a threshold estimated from source open-set episodes. The second uses a learned meta-calibrator. In this study, the term cable-source refers specifically to calibration episodes generated from the five cable-joint classes in the laboratory source domain. The cable-source subset is used for the final calibration setting because cable-joint PRPD patterns are more closely related to field cable-termination measurements than oil-immersed or dry-type transformer PRPD patterns. However, these cable-joint source classes are still treated only as related source data and not as label-equivalent classes to the field cable-termination target data.

For each source episode, selected source classes are treated as known, other source classes are treated as unknown, and support–query statistics are extracted from the prototype similarity distribution. These statistics include maximum similarity, similarity margin, entropy, support compactness, inter-prototype separation, K-shot value, and known-way value. A logistic calibration model is trained to estimate the probability that a query is unknown. During field testing, the same calibration function is applied to field prototype statistics, enabling a more reliable unknown-decision process by adapting the rejection boundary to the support-set geometry rather than using a fixed confidence rule.

The experimental protocol follows a laboratory-source-to-field-target setting. The source domain includes cable-joint, oil-immersed transformer, and dry-type transformer defects, with 12 source classes and 600 images per class. The target domain consists of field PRPD images collected from a transformer manufacturing facility, covering six cable-termination classes under practical measurement conditions. For closed-set evaluation, all six target field classes are treated as known classes. For open-set evaluation, a leave-one-field-class-out protocol is adopted, where five target field classes are used as known classes and the remaining field class is treated as unknown. This process is repeated for all six unknown-class choices and three random seeds. The few-shot support sizes are set to K = 1, 3, 5, 10, 20, and 50. Model performance is evaluated using known-class accuracy, unknown-class recall, normalised accuracy, open-set macro-F1, AUROC, AUPR, and FPR@95TPR. The main evaluation metrics are defined as follows:

$$AKS = \frac{N_{KK}}{N_K}, \quad AUS = \frac{N_{UU}}{N_U} \tag{4}$$

$$NA = \frac{AKS + AUS}{2} \tag{5}$$

$$\mathrm{F1}_j = \frac{2 \times \mathrm{Precision}_j \times \mathrm{Recall}_j}{\mathrm{Precision}_j + \mathrm{Recall}_j}, \quad \text{Macro-F1} = \frac{1}{C+1} \sum_{j=1}^{C+1} \mathrm{F1}_j \tag{6}$$

where *AKS* denotes known-class accuracy, *AUS* denotes unknown-class recall, and *NA* provides a balanced measure between known-class classification and unknown-class rejection. N_{KK} is the number of known samples correctly classified into their corresponding known classes, N_K is the total number of known test samples, N_{UU} is the number of unknown samples correctly rejected, and N_U is the total number of unknown test samples. In the macro-F1 calculation, C denotes the number of known target classes, while the additional class represents the unknown category. AUROC, AUPR, and FPR@95TPR are further used to assess known–unknown separability across different rejection thresholds (Kong and Ramanan, 2025).

3 RESULTS AND DISCUSSION

All quantitative results are reported as mean ± standard deviation. For closed-set evaluation, the statistics are computed across three random seeds. For open-set evaluation, the statistics are computed across six leave-one-field-class-out settings and three random seeds, giving 18 runs for each K-shot condition.

3.1 Closed-Set Few-Shot Field Classification

Table 1 presents the closed-set field classification results using the ImageNet-pretrained ResNet50 prototype baseline. The model achieves strong performance even under very limited supervision. With only one labelled support sample per class, the model obtains 83.32 ± 0.51% accuracy and 83.30 ± 0.28% macro-F1. Performance improves as the number of support samples increases and reaches the best result at $K = 20$, with 94.69 ± 0.49% accuracy and 94.24 ± 0.56% macro-F1. Increasing the support size to $K = 50$ does not further improve the result, indicating that $K = 20$ provides an effective balance between labelling effort and closed-set diagnostic performance.

Table 1. Closed-Set Few-Shot Field Classification Results

K	1	3	5	10	20	50
Accuracy (%)	83.32±0.51	90.34±1.40	92.53±0.29	94.14±0.43	**94.69±0.49**	93.91±0.50
Macro-F1 (%)	83.30±0.28	90.24±1.20	92.23±0.33	93.73±0.33	**94.24±0.56**	93.43±0.44

3.2 Open-Set Performance of the Learned Meta-Calibrator

Table 2 reports the open-set performance of the learned cable-source meta-calibrated prototype detector. The results show that the proposed meta-calibration strategy provides meaningful unknown rejection while preserving known-class classification. At $K = 20$, the learned meta-calibrator achieves 79.38 ± 4.24% known-class accuracy, 91.21 ± 12.23% unknown recall,

85.29 ± 7.17% normalised accuracy, 82.76 ± 4.13% open-set macro-F1, and 93.05 ± 6.15% AUROC. The corresponding FPR@95TPR is 17.58 ± 15.15%, indicating strong known–unknown separability. Although $K = 50$ gives slightly higher unknown recall and AUROC, it reduces known-class accuracy. This shows that adding more support samples does not automatically improve the full open-set operating point, because a more conservative rejection boundary can improve unknown recall while rejecting more known samples. The larger standard deviations at low K, particularly for AUPR, indicate that open-set performance is more sensitive to support-sample selection and held-out unknown-class variation when only very limited field labels are available.

Table 2. Open-Set Results of the Learned Cable-Source Meta-Calibrated Detector

K	AKS (%)	AUS (%)	NA (%)	Open-F1 (%)	AUROC (%)	AUPR (%)	FPR@95TPR (%)
1	63.21±6.68	77.54±26.03	70.38±13.60	66.95±6.83	81.31±16.20	51.56±29.92	39.03±26.27
3	74.53±7.42	85.01±19.63	79.77±11.19	77.68±6.86	88.58±10.56	61.84±27.97	28.82±25.96
5	79.73±3.84	82.84±21.78	81.29±11.85	81.57±5.14	90.04±9.36	63.89±27.70	25.77±22.72
10	80.35±4.40	88.35±16.64	84.35±9.38	82.84±4.82	92.82±6.91	68.74±23.06	18.77±17.37
20	**79.38±4.24**	**91.21±12.23**	**85.29±7.17**	**82.76±4.13**	**93.05±6.15**	**68.61±22.66**	**17.58±15.15**
50	72.91±5.52	96.48±5.90	84.70±4.12	79.22±4.24	93.57±5.70	71.92±20.84	16.66±14.88

3.3 Practical Source-Calibrated Threshold Mode

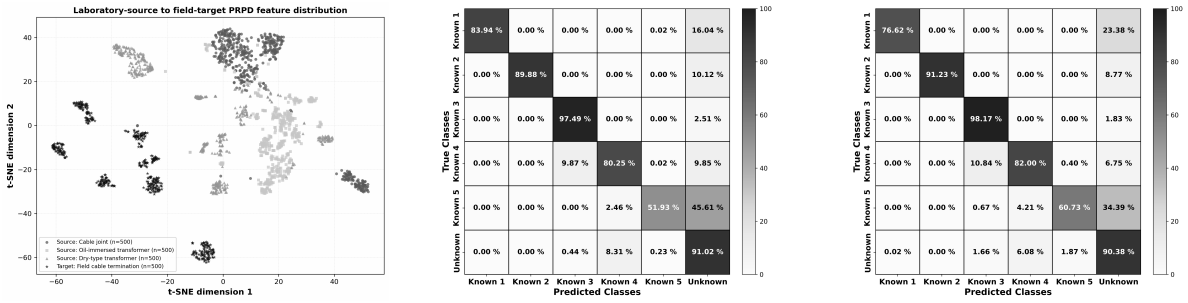
Table 3 shows the results of the source-calibrated prototype-distance threshold. This mode provides a simpler deployable alternative because it does not require a learned logistic calibration model. The threshold-based mode gives its strongest normalised accuracy at $K = 50$, reaching 85.84 ± 5.83% NA. However, the $K = 10$ setting is practically attractive because it requires only 10 labelled field samples per known class while achieving 79.85 ± 3.70% known accuracy, 91.45 ± 11.37% unknown recall, 85.65 ± 5.81% normalised accuracy, and 92.11 ± 7.18% AUROC. Compared with the learned meta-calibrator, the threshold mode gives slightly higher normalised accuracy at some K-shot settings, while the learned calibrator gives lower FPR@95TPR at $K = 20$. Therefore, the two modes support different deployment needs: the source-calibrated threshold is simpler and more robust, while the learned meta-calibrator provides stronger unknown-score separability.

Table 3. Open-Set Results of the Cable-Source Prototype-Distance Threshold

K	AKS (%)	AUS (%)	NA (%)	Open-F1 (%)	AUROC (%)	AUPR (%)	FPR@95TPR (%)
1	46.88±7.16	94.86±9.08	70.87±6.03	55.38±7.04	82.56±15.39	52.25±29.88	36.08±27.94
3	68.01±7.70	89.99±12.96	79.00±8.18	72.48±7.99	87.71±11.39	59.52±28.09	30.48±28.81
5	75.80±4.46	88.91±13.61	82.35±7.53	79.52±4.08	89.93±9.11	62.28±26.97	27.04±27.23
10	**79.85±3.70**	**91.45±11.37**	**85.65±5.81**	**82.89±3.06**	**92.11±7.18**	**66.21±23.34**	**23.09±26.88**
20	**80.72±3.12**	**90.28±11.41**	**85.50±5.63**	**83.45±2.55**	**92.08±6.98**	**66.22±23.11**	**22.81±25.13**
50	81.94±3.14	89.73±11.72	85.84±5.83	84.53±2.58	92.24±6.97	68.83±22.14	22.64±25.73

3.4 Domain-Shift Visualisation and Open-Set Confusion Analysis

Figure 2 jointly illustrates the laboratory-source-to-field-target feature shift and the open-set decision behaviour at $K = 20$. The t-SNE visualisation in Figure 2(a) shows that the field cable-termination samples occupy feature regions that are not fully aligned with the laboratory source groups, including cable-joint, oil-immersed transformer, and dry-type transformer PRPD data. This qualitative separation supports the experimental setting that the source and target domains are related but not label-equivalent. Therefore, direct source-to-target transfer may be unreliable, and field prototype adaptation with source-based calibration is more appropriate.



(a) (b) (c)

Figure 2. Domain-Shift Visualisation and Open-Set Confusion Analysis for Field Cable-Termination PD Diagnosis at $K = 20$: (a) t-SNE Visualisation of Laboratory Source and Field Target PRPD Samples; (b) Average Row-Normalised Confusion Matrix of the Learned Cable-Source Meta-Calibrator; (c) Average Row-Normalised Confusion Matrix of the Cable-Source Prototype-Distance Threshold

Figures 2(b) and 2(c) present the average row-normalised open-set confusion matrices for the learned cable-source meta-calibrator and the cable-source prototype-distance threshold, respectively. In both modes, the main error is the rejection of some known samples as Unknown, rather than confusion among known field classes. This indicates that the open-set boundary is conservative, which is desirable for field PD diagnosis because unfamiliar PRPD patterns should not be forced into known defect categories. The learned meta-calibrator provides slightly stronger unknown rejection, while the threshold mode offers a simpler deployable rule with better retention of some known classes.

4 CONCLUSION

This study proposed a Meta-Calibrated Prototype Open-Set Adaptation (MC-ProtoOSA) framework for few-shot field cable-termination PD diagnosis under laboratory-source-to-field-target

domain shift. The framework preserves an ImageNet-pretrained ResNet50 feature space, constructs target-domain prototypes from limited labelled field samples, and uses laboratory source episodes to calibrate unknown rejection. The results show that $K = 20$ provides a strong closed-set operating point, achieving 94.69% accuracy and 94.24% macro-F1. Under the leave-one-field-class-out evaluation, the learned cable-source meta-calibrator achieved 91.21% unknown recall, 85.29% normalised accuracy, and 93.05% AUROC, while the source-calibrated prototype-distance threshold provided a simple deployable alternative with 85.65% normalised accuracy at $K = 10$. These findings suggest that, within the proposed framework, related laboratory PRPD data can be used effectively for open-set calibration while preserving the target-domain prototype representation. The proposed framework therefore provides a practical basis for reliable field PD diagnosis when labelled field data are limited and unfamiliar PRPD patterns may emerge after deployment.

5 REFERENCES

Fei, Z., Li, Y., & Yang, S. (2024). Partial discharge pattern recognition based on an ensembled simple convolutional neural network and a quadratic support vector machine. *Energies*, *17*(11), 2443. https://doi.org/10.3390/en17112443

Kong, S., & Ramanan, D. (2025). OpenGAN: Open-set recognition via open data generation. *IEEE Transactions on Pattern Analysis and Machine Intelligence*, *47*(5), 3233–3243. https://doi.org/10.1109/TPAMI.2022.3184052

Long, J., Xie, L., Wang, X., Zhang, J., Lu, B., Wei, C., Dai, D., Zhu, G., & Tian, M. (2024). A comprehensive review of signal processing and machine learning technologies for UHF PD detection and diagnosis (II): Pattern recognition approaches. *IEEE Access*, *12*, 29850–29890. https://doi.org/10.1109/ACCESS.2024.3368866

Madhuranga, H. S., Raymond, W. J. K., Illias, H. A., & Mansor, N. N. B. (2025a). Hybrid latent space autoencoder and OCSVM framework for unknown class recognition in partial discharge diagnostics. *IEEE Access*, *13*, 198125–198141.

Madhuranga, H. S., Raymond, W. J. K., Illias, H. A., & Mansor, N. N. B. (2025b). Robust open-set partial discharge diagnosis based on hybrid supervised contrastive learning and SVM framework. *Ain Shams Engineering Journal*, *16*(12), 103762.

Niu, J., & Zhu, Y. (2025). Domain-adaptive transformer partial discharge recognition method combining AlexNet-KAN with DANN. *Sensors*, *25*(6), 1672. https://www.mdpi.com/1424-8220/25/6/1672

Tuyet-Doan, V. N., Pho, H. A., Lee, B., & Kim, Y. H. (2021). Deep ensemble model for unknown partial discharge diagnosis in gas-insulated switchgears using convolutional neural networks. *IEEE Access*, *9*, 80524–80534. https://doi.org/10.1109/ACCESS.2021.3084950

Wang, Y., Yan, J., Yang, Z., Jing, Q., Qi, Z., Wang, J., & Geng, Y. (2022). A domain adaptive deep transfer learning method for gas-insulated switchgear partial discharge diagnosis. *IEEE Transactions on Power Delivery*, *37*(4), 2514–2523. https://doi.org/10.1109/TPWRD.2021.3111862

ISSN: 2773-7055
Proceedings of the 5th International Research Conference
Institute of Technology, University of Moratuwa
November 5, 2026

Paper ID: 11

THERMAL-ACOUSTIC PERFORMANCE ANALYSIS OF A DOUBLE-ACTING THERMOACOUSTIC GENERATOR IN WASTE HEAT RECOVERY APPLICATIONS

R K A Rathnayake[1*], Malin Gunasekara[1]

[1]Division of Mechanical Engineering Technology, Institute of Technology, University of Moratuwa, Homagama, Sri Lanka

*Corresponding author: arunadulshan@gmail.com

ABSTRACT: This paper presents a theoretical model of thermoacoustic generators (TAGs), supported by experimental validation using a test rig. A double-acting thermoacoustic generator is capable of producing both travelling-wave and standing-wave thermoacoustic oscillations within a single generator. Thermo-acoustic generators can be used to generate electricity from acoustic power, which is produced from heat. When a temperature gradient is created across the stack, thermoacoustic oscillations are generated inside the resonator due to the thermoacoustic effect. The main components of the TAGs include a hot heat exchanger, a cold heat exchanger, a stack, a resonator, and an alternator. The critical design parameters identified for the design and fabrication of the TAG include the temperature difference across the stack, pressure-wave amplitude, sound level, and fluid velocity. In this experiment, the quarter-wavelength TAG was fabricated, and its elements were fabricated using a ceramic core as the stack/porous media, a nickel-chromium heating coil as the heat source, water as the coolant for the cold heat exchanger (heat sink) and a diaphragm as the linear alternator. Atmospheric air was used as the working fluid of the TAG. The experimental results demonstrated that the fabricated TAG was able to generate 31.3 W of acoustic power at a hot-end temperature of 250 °C while the maximum gauge pressure at the centre point of the stack was 666 kPa.

Keywords: heat recovery, thermo-acoustic generator, linear alternator, hot heat exchanger, stack

1 INTRODUCTION

Global energy consumption is escalating rapidly, driven primarily by population growth and accelerating industrialization. The U.S. Energy Information Administration (EIA) forecasts a 49% increase in total energy consumption between 2007 and 2035, representing an average annual growth rate of 2%. Over this period, the share of non-renewable energy sources is projected to decline from 92% to 85%, while renewable energy sources are expected to increase from 8% to 15% (Rathnayake et al., 2019). This shift highlights a growing global reliance on sustainable energy alternatives for the future.

Currently, internal combustion engines (ICEs) remain heavily dependent on fossil fuels to meet global power and transportation demands across automotive, aviation, rail, and maritime sectors (Wijewardana et al., 2012). However, the thermal efficiency of traditional ICEs rarely exceeds 25–30%, resulting in 70–75% of the fuel's chemical energy being dissipated as waste heat. To recover this low-grade thermal energy and utilise solar power, several advanced technologies are being developed, including thermoelectric generators (TEGs), turbo-compounding units, Organic Rankine Cycles (ORCs), and thermoacoustic generators (TAGs). While TEGs, ORC systems, and turbo-compounding units typically exhibit higher thermal efficiencies, TAGs offer a distinct advantage in their ability to effectively utilise low-grade waste heat without moving

parts. Within a TAG, this recovered thermal energy is converted into acoustic power, which is subsequently transformed into electrical energy via a linear alternator.

1.1 Thermo-Acoustic Generators

The key mechanism for converting thermal energy into acoustic energy is called a 'thermoacoustic effect'. The sound is generated (singing pipe) when a specific temperature gradient is applied across the porous core. Air serves as the compressible working fluid oscillating inside the porous stack. Using this phenomenon, current scientists have successfully designed and developed thermoacoustic generators which convert thermal energy into acoustic energy via the thermoacoustic effect (Zoontjens et al., 2005). The direction of energy conversion depends on the system (Ibrahim et al., 2012). called a 'thermoacoustic generator' (prime mover) or a 'refrigerator' (heat pump) (Swift et al., 1988). The two hot and cold heat sources maintain a temperature gradient within the porous media that is required to sustain and amplify the acoustic wave (Hariharan et al., 2018); this is generally referred to as a "stack" in standing-wave thermoacoustic devices and as a "regenerator" in travelling-wave devices (Backhaus et al., 2000 & Tsuda et al., 2017). Because acoustic vibrations are completely adiabatic in the absence of a solid substance in the acoustic field (Yang et al., 2018). Inside the porous stack, the thermodynamic cycle (compression, heating, expansion, and cooling) (Robert Stirling) undergoes when sound is generated.

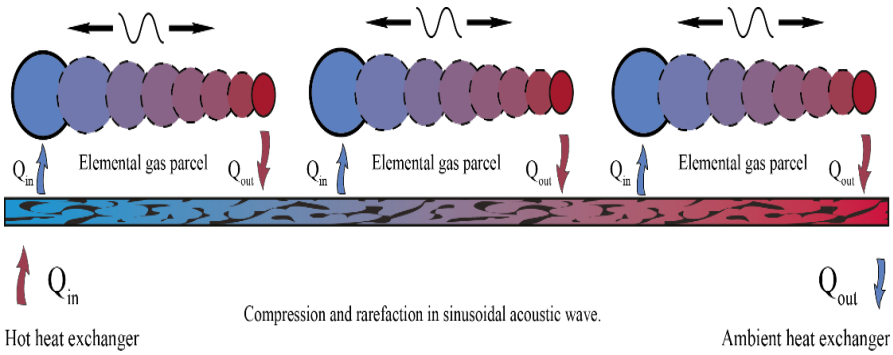


Figure 1. Thermoacoustic mechanism (Avent et al., 2015)

However, as shown in Figure 1, the presence of a solid surface causes viscous and thermal boundary layers to form in the acoustic field. Within these boundary layers, heat transfer occurs between the oscillating gas parcels and the solid surface (Soop et al., 2000). During the thermodynamic cycle, thermal expansion occurs at a higher pressure than thermal contraction$\oint p, dv > 0$. This indicates that the gas performs work on its surroundings, thereby producing acoustic power (Ceperley et al., 2012).

However, between 2018 and 2026, Thermo-acoustic generator (Engines) technologies have undergone significant changes. The thermo-acoustic field has moved beyond its initial stages. The simplified low-amplitude theoretical models are turning instead towards (Morgans et al., 2025). The sophisticated three-dimensional CFD simulations are applied to the multi-kilowatt (TAG) systems (Somu et al., 2021 and Morvayova et al., 2025), and also consider the electricity generation. But eliminate all mechanical parts (Cheng et al., 2025).

1.2 Mathematical Models

Acoustic power (W) can be determined using the following mathematical expression:

$$W = \ Re\ \{\frac{1}{2}\ PV\} \tag{1}$$

where P is acoustic pressure amplitude, V is volume flow rate is the complex conjugate of the acoustic volume flow rate amplitude, and {Re} denotes the real part of the product.
The average temperature gradient (dT/dx) along the axial direction (the x-direction) within the stack is defined as:

$$\nabla T_m = \frac{(T_h - T_c)}{\Delta x} \tag{2}$$

where T_h, T_C, and Δx are the hot-end temperature, cold-end temperature, and stack length, respectively.
These relations facilitate the design of TAG. Stack acoustic power powers a linear alternator to produce electricity (Sharify et al., 2016).

2 METHODOLOGY

2.1 Experimental Programme

A thermo-acoustic generator (TAG) was designed and fabricated as shown in Figure 2. The heart of the TAG is the regenerator or stack. A porous ceramic core was used to fabricate the designed TAG (Wu et al., 2018). It contains numerous straight holes parallel to the core's central axis. The length and the diameter of the stack are 55 mm and 95 mm, respectively. The resonator was designed to achieve a quarter-wavelength acoustic path length and was fabricated from stainless steel. The length and the diameter of the resonator are 620 mm and 98 mm, respectively. A nickel-chromium heating element was used to mimic a heat source, and a chilled water heat exchanger was used to mimic the heat sink of the TAG. The cold heat exchanger is made of copper because it has good thermal conductivity. The cold heat exchanger has a length of 185 cm and an internal diameter of 6 mm. The cooling medium can be used as normal water. The hot heat exchanger was powered by a transformer that could adjust the voltage in the range of 0–230 V. The regenerator/stack was sandwiched between the heat source and the heat sink. The alternator was mounted on the open end of the resonator tube. During these experiments, an audio speaker was used as the linear alternator to convert the acoustic power to electricity. The generated electrical energy was dissipated through a load resistor during testing.

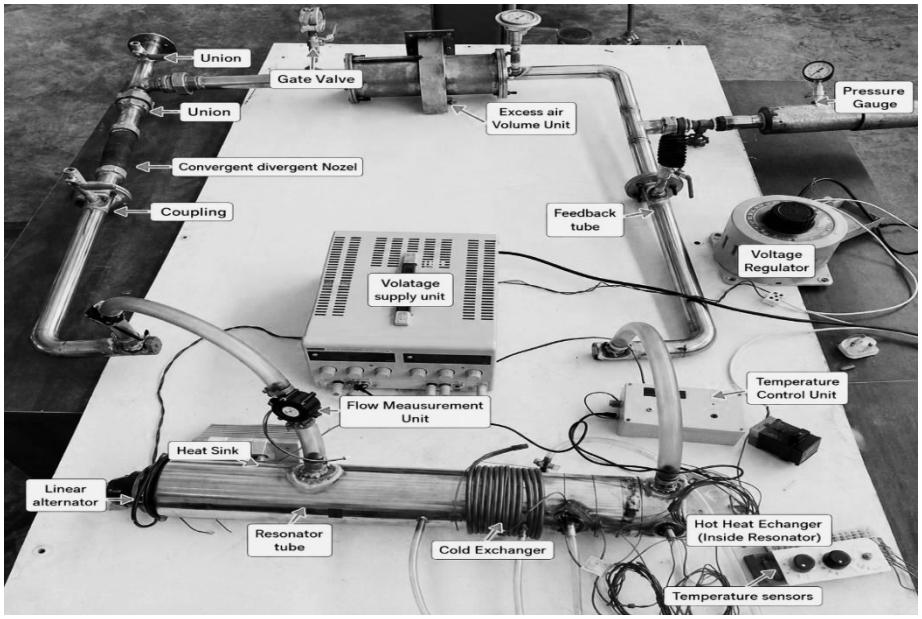


Figure 2. Experimental setup of the Thermoacoustic Generator

3 RESULTS AND DISCUSSION

The experimental results presented in Table 1 demonstrate a clear non-linear relationship between the stack hot-end temperature and the resulting thermoacoustic performance parameters. Ultimately, the data confirm that the thermoacoustic generator (TAG) successfully converts thermal energy into acoustic power. However, this power generation is strictly threshold-dependent; even though the working fluid expands smoothly and continuously as heat increases, the TAG will not produce measurable acoustic waves until a specific required temperature gradient is met. For this system, the critical onset threshold was determined to be 150 °C. Below this temperature, acoustic oscillations are not generated because the thermal gradient across the stack core is insufficient to overcome internal thermal dissipation and viscous losses.

Table 1. Measured acoustic and flow parameters under different operating temperatures

Temperature(°C)	**Volume flow rate at stack outlet (m^3s^{-1}) *10^{-5}**	**Pressure at stack outlet (KPa)**	**Acoustic Power(W)**
50	7.2	0.00	0.00
100	7.9	0.00	0.00
150	8.4	504	21.17
200	8.8	535	23.54
250	9.4	666	31.30

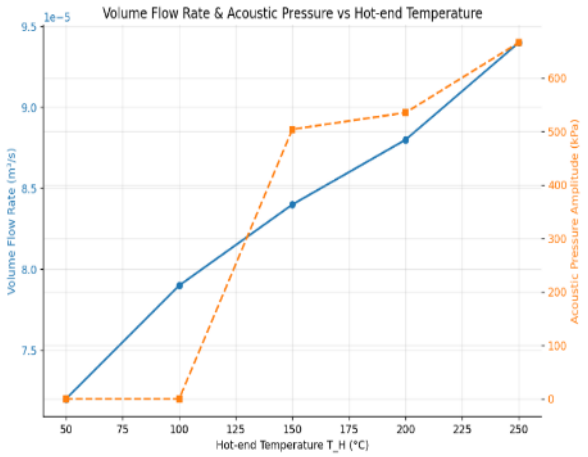


Figure 3. Volume Flow Rate and Acoustic Pressure Versus Hot-End Temperature

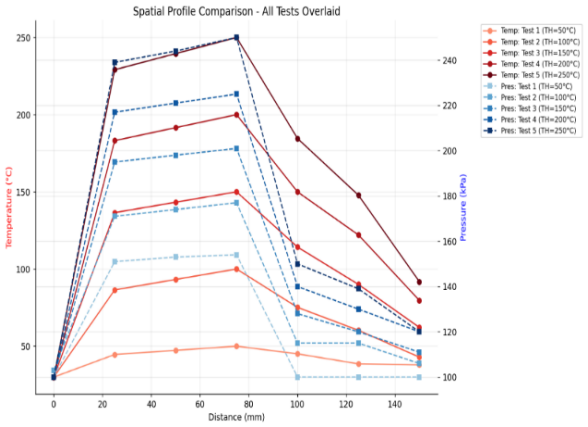


Figure 4. Temperature & Pressure Spatial Across the Stack

The volume flow rate (Figure 3) exhibits a highly linear and continuous upward trend across the entire testing temperature range. On the other hand, the acoustic pressure amplitude remains at zero until the threshold is reached. In Figure 4, the temperature graphs show a rapid increase along the stack region from the cold end to the hot end. Beyond the hot end, the temperature gradually decays as heat dissipates across the remaining length of the resonator.

4 CONCLUSION

A TAG was designed, fabricated and tested. This study successfully evaluated the performance and spatial characteristics of an experimental thermoacoustic generator (TAG) across the tested temperature range. The experimental results show that the system successfully turns thermal energy into acoustic power, describing a distinct non-linear operational relationship governed by a critical onset threshold.

5 ACKNOWLEDGEMENTS

The authors would like to express their sincere gratitude to the Department of Mechanical Engineering Technology at the Institute of Technology, University of Moratuwa, for providing the necessary facilities and resources to conduct this research. Special thanks are also extended to the staff of the automobile laboratories and all engineering workshops for their invaluable

assistance and technical support throughout the fabrication and testing phases of this project. The authors also thank D. V. Rathnayake for research assistance.

6 REFERENCES

Backhaus, S., & Swift, G. W. (2000). A thermoacoustic-Stirling heat engine: Detailed study. The Journal of the Acoustical Society of America, (February), 3148–3166. https://doi.org/10.1121/1.429343

Ceperley, P., & Korea, S. (2012). Background to Thermoacoustics Thermoacoustics - Layman ' s Explanation. 1–4.

Chen, H., Yang, Y., Wu, T., Zhu, S., Yu, G., Yang, R., & Luo, E. (2026). A thermoacoustically-driven liquid metal magnetohydrodynamic generation system with a thermal efficiency of 11%. The Innovation Energy, 3, 100139. https://doi.org/10.59717/j.xinn-energy.2026.100139

Hariharan, N. M., Arun, S., Sivashanmugam, P., & Kasthurirengan, S. (2018). CFD simulation on the performance of twin thermoacoustic prime mover for various resonator lengths and operating pressures. Heat Transfer - Asian Research, 47(2). https://doi.org/10.1002/htj.21306

Ibrahim, A., ElBeltagy, A., Emam, M., & Abdelrahman, E. (2012). Development and analysis of non-linearity in the pressure waves resulting from thermoacoustic heat engines. Acoustics 2012 . . . , (April), 1123–1129. http://hal.archives-ouvertes.fr/hal-00810609/

Morgans, A. S., & Yang, D. (2026). Thermoacoustic Instability in Combustors. Annual Review of Fluid Mechanics Downloaded from Www.Annualreviews.Org. Guest, 22, 45. https://doi.org/10.1146/annurev-fluid-121021

Morvayovà, A., Nobile, A., Bruno, M. E., Romano, A., Oresta, P., & Fabbiano, L. (2025). Efficiency of the Thermoacoustic Engine Induced by Stack Position, Pipe Aspect Ratio and Working Fluid. Energies, 18(18). https://doi.org/10.3390/en18184843

Rathnayake, M. M. I. D., Manthilake, M. D., & Wijewardane, M. A. (2019). Applicability of thermo-acoustic generators (TAGs) for low grade heat recovery and power generation. In 2018 8th International Conference on Power and Energy Systems (ICPES 2018) (pp. 161–165).

Sharify, E. M., Takahashi, S., & Hasegawa, S. (2016). Development of a CFD model for simulation of a traveling-wave thermoacoustic engine using an impedance matching boundary condition. Applied Thermal Engineering, 107, 1026–1035. https://doi.org/10.1016/j.applthermaleng.2016.07.028

Somu, S., Lacoste, D., Saxena, S., Roberts, W. L., & Keolian, R. M. (2020). Design optimization of a multi-kW thermoacoustic electric generator using deltaec model. Proceedings of the ASME Turbo Expo, 5. https://doi.org/10.1115/GT2020-15419

Tsuda, K., & Ueda, Y. (2017). Critical temperature of traveling- and standing-wave thermoacoustic engines using a wet regenerator. Applied Energy, 196, 62–67. https://doi.org/10.1016/j.apenergy.2017.04.004

Wijewardane, M. A. (2012). Exhaust System Energy Management of Internal Combustion Engines (Doctoral thesis). Loughborough University.

Yang, R., Wang, Y., Jin, T., Feng, Y., & Tang, K. (2018). Performance optimization of the regenerator of a looped thermoacoustic engine powered by low-grade heat. International Journal of Energy Research, 42(14), 4470–4480. https://doi.org/10.1002/er.4192

Zoontjens, L., Howard, C., Zander, A., & Cazzolato, B. (2005). Feasibility Study of an Automotive Thermoacoustic Refrigerator. Proceedings of ACOUSTICS 2005, (November), 363–371. https://doi.org/10.1109/ROBOT.2002.1013397

ISSN: 2773-7055
Proceedings of the 5th International Research Conference
Institute of Technology, University of Moratuwa
November 5, 2026

Paper ID: 89

SOCIO-ENVIRONMENTAL SUSTAINABILITY IN CROSS-BORDER ELECTRICITY TRADE OF NEPAL

Rajendra Singh[1*], Vinesh Agrawal[1], Shree Raj Shakya[2]
[1]Mewar University, Rajasthan, India
[2]Centre for Energy Studies, Nepal
*Corresponding author: rajendrasingh2000@gmail.com

ABSTRACT: Cross-border electricity trade (CBET) offers Nepal a strategic pathway to convert expanding hydropower generation into economic growth, energy security and regional cooperation. Existing Nepal-focused research has largely treated CBET economics, hydropower development, environmental impacts and social issues separately. This study integrates these dimensions through an ARDL export-performance model, Composite Sustainability Index (CSI), conditional forecasting and AHP-based multi-criteria decision analysis (MCDA). Annual data for 2000–2024 indicate a positive long-run elasticity of export revenue to hydropower generation (β=0.68, p=0.003) and a negative association with environmental stress (β=−0.29, p=0.017); the error-correction coefficient is −0.52 (p=0.001). The integrated assessment gives EPI=0.65, environmental condition=0.435, SAI=0.475 and CSI≈0.533, indicating moderate sustainability. Conditional 2030 export-revenue forecasts are NPR 77.6 billion under the baseline and NPR 100.2 billion under the high-growth scenario. The findings indicate that export expansion should be accompanied by environmental safeguards, stakeholder participation, resilient transmission and stronger regional governance.

Keywords: cross-border electricity trade, hydropower sustainability, environmental sustainability, composite sustainability index, MCDA

1 INTRODUCTION

Nepal's expanding hydropower capacity creates an opportunity to increase electricity exports and strengthen regional energy cooperation. Previous Nepal–India CBET studies emphasise economic prospects and institutional barriers (Dangal et al., 2022; Dhakal et al., 2019), while hydropower studies examine environmental compliance, environmental flows, public participation and community vulnerability (Bhattarai et al., 2021; Rijal et al., 2020; Munch-Petersen, 2017; Bhattarai et al., 2023). South Asian assessments further stress coordinated institutions and transmission infrastructure (ADB, 2021; World Bank, 2020). The research gap is therefore not a lack of evidence on individual dimensions, but the limited quantitative integration of export performance with environmental conditions and social acceptance in Nepal's CBET.

This study addresses the gap by linking an ARDL-based export model with a CSI, conditional 2025–2030 forecasts and AHP-MCDA. It asks whether hydropower generation supports export revenue, whether environmental stress constrains export performance, and whether project choices can be compared using economic, environmental and social criteria. The contribution is an integrated decision-support framework for sustainable CBET rather than an assessment based only on electricity-export volume.

2 METHODOLOGY

Annual secondary data for 2000–2024 (n=25) were compiled primarily from NEA, DoED, DHM and WECS, supplemented by published studies and sector reports. The dependent variable is CBET electricity-export revenue, Yt (NPR billion); Xt is hydropower generation (GWh); and ENVt is an environmental-condition/stress index. Export revenue is analysed in logarithmic form; generation is log-transformed, while the bounded ENV index is retained in level form. This parsimonious specification reflects the small sample.

$$\ln Y_t = \alpha + \beta_1 \ln X_1 + \beta_2 \mathrm{ENV}_t + \varepsilon_t \tag{1}$$

ADF tests establish integration order. Export revenue and generation are I(1), whereas ENV is I(0); no variable is I(2). AIC/BIC select ARDL(3,1,1). The general distributed-lag specification and ECM are:

$$Y_t = c + \sum_{i=1}^{3} \varphi_i Y_{t-i} + + \sum_{j=0}^{1} Y_j X_{t-j} + \sum_{k=0}^{1} \delta_k \mathrm{ENV}_{t-k} + \varepsilon_t \tag{2}$$

$$\Delta Y_t = \alpha + \sum_{i=1}^{2} \beta_i \Delta Y_{t-i} + \sum_{j=0}^{1} Y_j \Delta X_{t-j} + \sum_{k=0}^{1} \delta_k \Delta \mathrm{ENV}_{t-k} + \lambda \mathrm{ECT}_{t-1} + \varepsilon_t \tag{3}$$

The bounds-test F-statistic is 5.21 against a 5% upper bound of 4.85, supporting cointegration. The ECT coefficient is -0.52 (p=0.001), implying that about 52% of disequilibrium is corrected annually. Diagnostics indicate VIF<2, Durbin–Watson≈2.0, Breusch–Pagan p=0.27 and Ramsey RESET p=0.31.

For sustainability assessment, indicators are normalised to [0,1]. Positive indicators use:

$$N_i = (x_i - \min x_i)/(\max x_i - \min x_i) \tag{4}$$

and negative indicators use:

$$N_i = (\max x_i - x_i)/(\max x_i - \min x_i) \tag{5}$$

The economic performance index (EPI), environmental condition score (ENV=1−EII), and social acceptance index (SAI) are then combined as:

$$\mathrm{CSI} = 0.40\mathrm{EPI} + 0.30\mathrm{ENV} + 0.30\mathrm{SAI} \tag{6}$$

The reported values are EII=0.565, hence ENV=0.435; EPI=0.65; SAI=0.475; and CSI=0.533. Thus the weighting is explicitly economic 40%, environmental 30% and social 30%, rather than equal one-third weights. Forecasts for 2025–2030 are conditional on the estimated ARDL relationships under baseline and high-growth paths; uncertainty is represented by 95% intervals:

$$\hat{Y}_{t+h} \pm 1.96\,\mathrm{SE}(\hat{Y}_{t+h}) \tag{7}$$

For MCDA, project scores use the same three criteria. AHP weights (0.40, 0.30, 0.30) are reproduced by the consistent pair-wise comparison matrix:

Table 1. *AHP pair-wise comparison matrix for criterion weights*

	Economic	**Environmental**	**Social**
Economic	1	4/3	4/3
Environmental	¾	1	1
Social	¾	1	1

$$S_i = 0.40E_i + 0.30\text{ENV}_i + 0.30S_i \quad (8)$$

The matrix gives weights 0.40, 0.30 and 0.30 with CR=0, satisfying the AHP consistency requirement. Upper Tamakoshi scores 0.610 (=0.40×0.70+0.30×0.55+0.30×0.55); the comparative MCDA ranking places run-of-river options highest in sustainability.

3 RESULTS AND DISCUSSION

Table 2. Principal econometric results

Indicator/Test	Result	Interpretation
Export Revenue	I(1)	First-difference stationary
Generation	I(1)	First-difference stationary
ENV	I(0)	Level stationary
ARDL/Bounds	(3,1,1); F=5.21	Co-integration confirmed
Long-run coefficients	βX = 0.68; βENV = -0.29	Positive/ Negative, significant

Hydropower generation has a positive and statistically significant long-run relationship with export revenue (β=0.68, p=0.003), while environmental stress is negative and significant (β=$-$0.29, p=0.017). The magnitude of the generation elasticity indicates that a 1% long-run increase in generation is associated with about a 0.68% increase in export revenue, holding ENV constant. The -0.52 ECT indicates relatively rapid adjustment toward equilibrium. These results are consistent with the economic opportunity identified by Dangal et al. (2022), but extend it by quantifying an environmental constraint; they also complement Dhakal et al. (2019), whose stakeholder-based barrier analysis did not estimate export elasticities.

The sustainability results show a structural imbalance. EII=0.565 converts to ENV=0.435, while EPI=0.65 and SAI=0.475 produce CSI$\approx$0.533. Thus economic performance is stronger than the environmental and social dimensions. This pattern is consistent with evidence that Nepal's hydropower expansion can create local environmental and governance tensions (Bhattarai et al., 2021; Crootof et al., 2021) and that environmental flows and participation remain important for acceptance (Rijal et al., 2020; Munch-Petersen, 2017). Unlike these project-level studies, the present CSI links those dimensions to CBET performance.

Conditional forecasts indicate 2030 export revenue of approximately NPR 77.6 billion in the baseline and NPR 100.2 billion in the high-growth scenario. These values should be interpreted as conditional model projections, not unconditional forecasts: they require continued generation growth, transmission development, regional market access and effective environmental management. The MCDA result similarly shows why project selection should not be based solely on economic return; Upper Tamakoshi scores 0.610, while the overall ranking favours run-of-river alternatives on the combined criteria.

Policy implications follow directly from the results: diversify export markets and transmission corridors; strengthen environmental-flow and impact-management requirements; institutionalise stakeholder participation; and coordinate regional market rules and transmission investment. These priorities are aligned with regional energy-integration assessments that emphasise

institutions and infrastructure (ADB, 2021; World Bank, 2020).

4 LIMITATIONS AND CONCLUSION

The annual sample is small (n=25), environmental and social dimensions rely on secondary composite indicators, and the forecasts are conditional on assumed model relationships. MCDA outcomes are sensitive to criterion selection and weights, while future hydrological extremes, market rules, transmission constraints and geopolitical conditions may alter outcomes. Future work should use longer and higher-frequency data, project-level environmental and social indicators, stakeholder-derived weights and explicit climate and market scenarios.

The study demonstrates that hydropower generation can strengthen Nepal's CBET export earnings, but environmental stress and social acceptance constrain the sustainability of that pathway. With EII=0.565, ENV=0.435, SAI=0.475, EPI=0.65 and CSI≈0.533, sustainability is moderate and economically unbalanced. Sustainable CBET therefore requires simultaneous progress in export capacity, environmental safeguards, social participation, transmission resilience and regional governance.

5 REFERENCES

Asian Development Bank. (2021). Nepal energy sector assessment, strategy, and road map. ADB.

Bhattarai, S., Shrestha, S., & Karki, R. (2021). Environmental compliance of hydropower projects in Nepal. Environmental Challenges, 5, 100307. https://doi.org/10.1016/j.envc.2021.100307

Bhattarai, U., Devkota, R., Maraseni, T., Devkota, L., & Marahatta, S. (2023). Attaining multiple sustainable development goals through storage hydropower development amidst community vulnerabilities. Sustainable Development. https://doi.org/10.1002/sd.2634

Crootof, A., Shrestha, R., Albrecht, T., Ptak, T., & Scott, C. A. (2021). Sacrificing the local to support the national: Politics, sustainability, and governance in Nepal's hydropower paradox. Energy Research & Social Science, 80, 102206. https://doi.org/10.1016/j.erss.2021.102206

Dangal, D. N., Chapagai, S. D., & Ghimire, K. P. (2022). Economic prospects of cross-border electricity trade between Nepal and India. Economic Review of Nepal, 5(1).

Dhakal, S., Karki, P., & Shrestha, S. (2019). Cross-border electricity trade for Nepal: A SWOT-AHP analysis of barriers and opportunities based on stakeholders' perception. International Journal of Water Resources Development, 37(3), 559–580. https://doi.org/10.1080/07900627.2019.1648240

ICIMOD. (2023). Climate change impacts on Himalayan hydrology and energy systems. International Centre for Integrated Mountain Development.

Munch-Petersen, J. (2017). Public participation in environmental impact assessment of hydropower plants in Nepal: A context-specific approach (IWMI Working Paper No. 175). International Water Management Institute.

Rijal, N., Shrestha, H. K., & Bruins, B. (2020). Environmental flow assessment of Hewa Khola A and Lower Hewa Khola hydropower projects in Nepal. Hydro Nepal: Journal of Water, Energy and Environment, 23, 71–78.

World Bank. (2020). South Asia regional electricity cooperation and market integration. World Bank.

ISSN: 2773-7055
Proceedings of the 5th International Research Conference
Institute of Technology, University of Moratuwa
November 5, 2026

Paper ID: 47

REVIEW: PYROLYSIS OF BIOMASS AS A SUSTAINABLE ALTERNATIVE TO FOSSIL FUEL IN SRI LANKA

K A N I Kaluarachchi[1], O G D D M Jayawardhana[1], T G W M Kavinda[1], N K M S Karunarathna[1], G K Jayatunga[1*]

[1]Division of Polymer and Chemical Engineering Technology, Institute of Technology, University of Moratuwa, Homagama, Sri Lanka

*Corresponding author: gayanij@itum.mrt.ac.lk

ABSTRACT: Sri Lanka's dependence on fossil fuels has raised significant environmental and economic concerns, necessitating the exploration of sustainable energy alternatives. This review critically examines the application of pyrolysis for the conversion of forest biomass into value-added products, with particular emphasis on Pinus caribaea as a potential feedstock. The review synthesizes current literature on the physicochemical characteristics of Pine biomass, pyrolysis technologies, product distribution, and upgrading strategies. Existing evidence indicates that the high lignin content and widespread availability of Pinus biomass make it a suitable candidate for thermochemical conversion. Furthermore, the utilization of forest residues through pyrolysis offers opportunities for renewable energy generation, biochar production, and sustainable biomass management. Overall, the findings suggest that pyrolysis represents a promising approach for forest biomass valorization and could contribute to enhancing resource efficiency, supporting a circular economy, and reducing Sri Lanka's reliance on fossil fuels.

Keywords: biomass, bio-oil, biochar, pyrolysis, circular economy

1 INTRODUCTION

The rapid increase in global waste generation, driven by population growth, urbanization, and industrialization, has created significant environmental and public health challenges. Traditional disposal methods such as landfilling are becoming unsustainable due to land scarcity, greenhouse gas emissions, and long-term pollution risks. As a result, thermal treatment technologies namely incineration, pyrolysis, and gasification have emerged as effective alternatives for waste reduction and energy recovery (Sirimanna & Nadarajah, 2026). Among these, pyrolysis has gained particular attention for its ability to thermochemically decompose organic waste in the absence of oxygen, converting it into valuable byproducts such as bio-oil, syngas, and char. These outputs can be utilized as alternative fuels or raw materials in various industrial processes. By reducing waste volume, lowering environmental emissions, and enabling resource recovery, pyrolysis offers a sustainable and efficient approach to managing increasing volumes of solid waste, particularly biomass, and other carbon-rich materials.

According to these Primary Global Energy Consumption details ("Global Primary Energy Consumption in 2023," n.d.), fossil fuels (coal, oil, and natural gas) accounted for the highest percentage of global energy consumption, around 81%, showing the continued heavy reliance on non-renewable sources. The problem of nonrenewable fuel usage is multifaceted, involving environmental, economic and sustainability concerns. Traditional fuels such as gasoline, diesel and coal are fossil based and contribute significantly to air pollution, climate change, and the depletion of non-renewable resources.

Sri Lanka's dependence on imported non-renewable fossil fuels has resulted in recurring energy insecurity, most notably during the 1996 power crisis and the 2022 fuel shortage. This vulnerability has been further exacerbated by global geopolitical tensions and instability in key energy supply routes, including the Strait of Hormuz, leading to fuel price volatility and supply uncertainty in 2026. These challenges highlight the risks of fossil fuel dependency and reinforce the need to transition toward indigenous renewable energy resources to ensure long-term energy security and resilience.

Over time, this phenomenon has escalated into a pressing concern due to its far-reaching environmental and demographic consequences. The resultant impacts, such as rising temperatures and extreme weather events, threaten to displace large populations in developing regions and may incite socio-political instability shortly (Tadesse, 2010).

Materials suitable for pyrolysis include tires, sawdust, rice husk, plastic waste, municipal solid waste, agricultural residues, biomass resources, and forest wood. It can be used to produce both heat and electricity. In Sri Lanka, major biomass resources include firewood, agricultural residues such as coconut shells, and industrial residues from the tea, palm oil, timber industries, among others. These biomass resources store solar energy in the form of chemical energy through photosynthesis and can be converted into useful energy through thermochemical processes such as pyrolysis.

Pyrolysis from forest wood promotes efficient forest waste management by utilizing residues and deadwood, preventing wildfires and deforestation while promoting sustainable forestry practices. Economically, it fosters rural job creation in biomass collection, pyrolysis operations, and biochar production, contributing to a circular economy where waste materials are converted into valuable bio-based products.

Forest wood such as Teak and Mahogany, along with other biomass materials like coconut shells and sawdust, are used as feedstocks for the production of bio-oil and biochar through pyrolysis globally (Cusenza et al., 2021). In the context of Sri Lanka, Pinus wood presents a promising alternative feedstock for pyrolysis due to its availability and suitable composition.

A focused literature review was conducted on Pinus wood, with emphasis on pyrolysis technologies, operating conditions, product yields, and the characteristics of the outputs. Relevant studies were critically compared to assess the pyrolysis potential of Pinus biomass and its sustainable utilization in Sri Lanka, and the findings are presented and discussed in this paper.

2 PINUS WOOD

Pinus wood can be classified as a fast-growing tree in upcountry areas of Sri Lanka such as Nuwara Eliya, Bandarawela and Kandy. Pinus trees can be found in forests, and we can't get significant uses from it, and Pinus wood is highly flammable. So, these trees cause wildfire. Harvesting Pinus trees can involve land clearing and draining water tables. The most common Pinus species in Sri Lanka are Caribbean pine (Pinus caribaea) and Patula pine (Pinus patula), shown in Figure 1 and Figure 2 respectively (*Flora of Sri Lanka*, n.d.)



Figure 1. Caribbean pine



Figure 2. Patula Pine

Considering material availability and sourcing, it is preferable to use Caribbean Pine because 80% of the pine distribution in Sri Lanka consists of Caribbean pine. Hantana Range, upper Mahaweli catchment are areas with Caribbean pine plantations, while specific regions like Nuwara Eliya and Badulla Districts have limited plantations of Patula Pine (Jayawardena, 2023). Pinus wood can be used for this pyrolysis process because lignin decomposes over a broader temperature range such as 400–600 °C. Cellulose and hemicellulose are the main constituents in the wood. Depending on the type of wood, the content of cellulose can be up to 50 wt. %. Cellulose is a linear polymer consisting of 5,000–10,000 glucose units. The cellulose structure in wood has well-ordered crystalline regions that are separated by amorphous regions. Hemicellulose usually accounts for 25–35 wt.% in dry wood. Hemicellulose is a branched polymer that is built up from different C5 and C6 monomers. The average number of monomers is around 150, indicating a lower degree of polymerization for hemicellulose than for cellulose (Gao et al., 2025).

3 PYROLYSIS

Pyrolysis is an effective thermochemical process that converts biomass into bio-oil, syngas, and biochar through heating in an oxygen-limited environment, preventing combustion and enabling thermal decomposition (Cusenza et al., 2021). Pyrolysis can be conducted using slow, flash, and fast pyrolysis methods. Slow pyrolysis is a conventional type of pyrolysis. It involves a long residence time and a slow heating rate. The key differences among slow, fast, and flash pyrolysis in terms of operating conditions, product distribution, and major product yields are summarized in Table 1. Bio-oil is a liquid 60 -75% (dry basis), rich in oxygenated organics: acids, alcohols, aldehydes, ketones, phenols. It contains guaiacol, syringol, furfural, levoglucosan, etc. It has high energy content, but it is acidic and unstable. Therefore, bio-oil has to be upgraded using

cracking and reforming methods. Char is in solid form and has moisture content of around 10 - 25 %. It contains carbon-rich solid residue. It is used for soil amendment, carbon sequestration, or as a solid fuel and an adsorbent. Syngas from pyrolysis contains H_2, carbon oxides, light hydrocarbons, etc. (Bridgwater, 2007). Gas composition depends on biomass type and pyrolysis conditions. Hydrogen is formed by cracking hydrogen-carbon compounds at high temperatures.

Table 1. Comparison of slow, fast and flash pyrolysis methods

Feature	Slow Pyrolysis	Fast Pyrolysis	Flash Pyrolysis
Heating rate	0.1–1 °C/s (slow)	~1000 °C/s (very fast)	Very rapid heating
Temperature range	400 - 500 °C	~500 °C	(450–600 °C typical range)
Residence time	5 - 30 minutes (long)	short	Very short
Main Product	Biochar	Bio-oil	Bio-oil
Bio-oil yield	Low - moderate	60 - 70%	Up to 75%
By-products	Bio-oil, syngas	Biochar, syngas	Biochar, syngas
Key characteristics	Carbonization-focused	Bio-oil production focused	Maximum liquid fuel production
Major challenges	Lower liquid yield	Bio-oil instability	Catalyst degradation, stability issues

Figure 3 shows a typical process flow diagram for the production of bio-oil and biochar from pine wood. The production of bio-oil and biochar from forest wood involves a series of integrated unit processes designed to optimize yield and product quality. Initially, the biomass undergoes crushing and grinding to reduce particle size and ensure uniformity, which facilitates efficient heat transfer during subsequent processing.

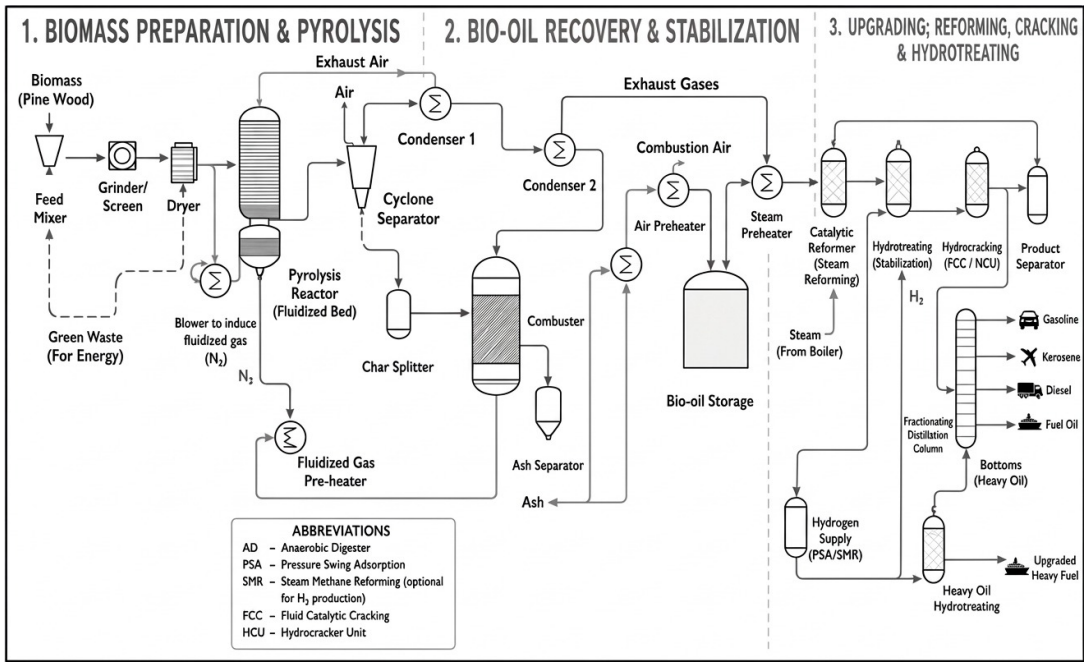


Figure 3. Process flow diagram of the production of bio-oil and biochar from forest wood

Drying carried out using dryers such as rotary drum dryers or packed bed dryers reduces the moisture content of biomass to below 15 %, thereby enhancing pyrolysis efficiency and improving the yield and quality of bio-oil. The dried biomass is fed to a fluidized bed reactor at 450–550

°C when fast pyrolysis is applied, where rapid thermal decomposition occurs, producing pyrolysis vapors and solid char. These vapors pass through a cyclone separator or particle entrained device to remove entrained particulates such as char and ash and are subsequently condensed in a heat exchanger to yield liquid bio-oil. Post-condensation upgrading is crucial due to the bio-oil's inherent instability, high oxygen content, and corrosiveness. Stabilization processes such as mild hydrogenation or catalytic treatment are employed to improve storage stability and reduce reactivity. Advanced upgrading steps include cracking, hydrotreating, and catalytic reforming. Cracking, often using zeolite-based catalysts, breaks down heavy oxygenated compounds into smaller, more volatile hydrocarbons, improving energy density (Bridgwater, 2007). Hydrotreating involves hydrogenating the bio-oil in the presence of metal catalysts such as Ni-Mo or Co-Mo, effectively removing oxygen and producing stable hydrocarbon fuels with higher calorific value (Grilc et al., 2014). Catalytic reforming further upgrades the oil by converting oxygenates and light hydrocarbons into synthesis gas or aromatic compounds, depending on catalyst choice and process conditions (Elliott et al., 2015). Collectively, these integrated unit operations offer an effective and systematic approach for converting forest biomass into renewable liquid fuels and carbon-rich biochar.

Sri Lanka has a wide variety of biomass resources such as agricultural residues, wood resources, plantation residues and industrial wastes, which have significant potential for sustainable production of energy and value-added products. These resources can reduce dependence on fossil fuels while promoting waste valorization and circular use of resources. However, sustainability in the long term depends on reliable availability of feedstock, sustainable resource management, efficient collection and transportation, and conversion efficiency. Table 2 presents selected biomass and waste feedstocks reported in the literature, together with their typical bio-oil and biochar yields and operating temperatures during pyrolysis.

Table 2. Typical bio-oil and biochar yields and operating temperatures reported for the pyrolysis of selected biomass and waste feedstocks

Biomass/Waste Source	**yield (wt%)**		**Temperature (°C)**	**References**
	Bio-oil	**Biochar**		
Coconut shell	~35-45	~30-40	~450-550	(Sarkar & Wang, 2020)
Gliricidia sepium	~35-45	~30-40	~700	(Keerthanan et al., 2020)
Rice husk	~40-56	~30-40	~450	(Park et al., 2014)
Rice straw / paddy residue	~30-50	~20-35	~450-550	(Park et al., 2014)
Coconut husk / fibre	~25-40	~30-45	~450-550	(Lubowa et al., 2024)
Sawdust / wood residues	~45-65	~20-30	~450-500	(Salehi et al., 2011)
Agricultural crop residues	~30-50	~20-35	~450-550	(Nithiya et al., 2019)
Waste sludge of Natural rubber process	~30-50	~20-40	~350	(Sirimanna & Nadarajah, 2026)

Life-cycle and techno-economic assessments should also be used to evaluate environmental performance and economic feasibility. In particular, the utilization of Pinus wood should be accompanied by proper management of existing Pinus plantations and controlled cultivation practices to ensure a sustainable and reliable supply of feedstock while minimizing potential

environmental impacts. Therefore, Sri Lanka needs to adopt a diversified biomass strategy focusing on sustainably available resources, responsible management of Pinus cultivation, efficient supply chains, advanced conversion technologies, and value-added utilization of pyrolysis products for a sustainable future.

4 CONCLUSION

Pyrolysis integrates both waste management and renewable energy generation, making it a sustainable solution. This review shows how forest biomass, particularly Pinus wood, serves as an excellent pyrolysis feedstock in Sri Lanka where it is abundant yet underutilized. Pinus species not only grow quickly but also aid in mitigating wildfire risks and have high lignin content, which makes it an attractive candidate for bio-oil and biochar production. In addition, adopting pyrolysis contributes towards sustainability by transforming waste materials into valuable products, fostering rural development, and decreasing greenhouse gas emissions. In the end, incorporating pyrolysis into Sri Lanka's strategy for biomass usage could greatly advance the country's circular and low-carbon energy initiatives.

5 REFERENCES

Bridgwater, A. V. (2007). The production of biofuels and renewable chemicals by fast pyrolysis of biomass. *International Journal of Global Energy Issues*, *27*(2), 160. https://doi.org/10.1504/IJGEI.2007.013654

Cusenza, M. A., Longo, S., Cellura, M., Guarino, F., Messineo, A., Mistretta, M., & Volpe, M. (2021). Environmental assessment of a waste-to-energy practice: The pyrolysis of agro-industrial biomass residues. *Sustainable Production and Consumption*, *28*, 866–876.

Elliott, D. C., Wang, H., Rover, M., Whitmer, L., Smith, R., & Brown, R. (2015). Hydrocarbon Liquid Production via Catalytic Hydroprocessing of Phenolic Oils Fractionated from Fast Pyrolysis of Red Oak and Corn Stover. *ACS Sustainable Chemistry & Engineering*, *3*(5), 892–902. https://doi.org/10.1021/acssuschemeng.5b00015

Flora of Sri Lanka. (n.d.). Retrieved July 20, 2025, from https://www.floraofsrilanka.com/species/1714

Gao, Q., Guo, L., Li, S., Wu, W., wei Ding, J., Xu, H., Luo, C., Li, J., Li, D., & Liu, Z. (2025). Biodegradation mechanism of cellulose, hemicellulose, and lignin in bacteria-dominant aerobic composting from agricultural biomass waste: A review. *Carbohydrate Polymer Technologies and Applications*, *11*, 100879.

Global primary energy consumption in 2023. (n.d.). *MSCI Sustainability Institute*. Retrieved July 20, 2025, from https://www.msci-institute.com/charts/global-primary-energy-consumption-generation-in-2023/

Grilc, M., Likozar, B., & Levec, J. (2014). Hydrodeoxygenation and hydrocracking of solvolysed lignocellulosic biomass by oxide, reduced and sulphide form of NiMo, Ni, Mo and Pd catalysts. *Applied Catalysis B: Environmental*, *150*, 275–287.

Jayawardena, M. (2023, September 22). The Grim Story behind 'Pines.' *Ceylon Today*. https://ceylontoday.lk/2023/09/23/the-grim-story-behind-pines/

Keerthanan, S., Rajapaksha, S. M., Trakal, L., & Vithanage, M. (2020). Caffeine removal by Gliricidia sepium biochar: Influence of pyrolysis temperature and physicochemical properties. *Environmental Research*, *189*, 109865.

Lubowa, P. S., Ndiritu, H., Oketch, P., & Mutua, J. (2024). Coconut fiber pyrolysis: Bio-oil characterization for potential application as an alternative energy source and production of bio-degradable plastics. *World Journal of Engineering and Technology*, *12*(2), 310–319.

Nithiya, K., Subramanian, P., Karthikeyan, S., & Sriramajayam, S. (2019). Laboratory estimation of bio-crude production potential from selected agricultural residues. *Journal of Agricultural Engineering (India)*, *56*(2), 72–89.

Park, J., Lee, Y., Ryu, C., & Park, Y.-K. (2014). Slow pyrolysis of rice straw: Analysis of products properties, carbon and energy yields. *Bioresource Technology*, *155*, 63–70.

Salehi, E., Abedi, J., & Harding, T. (2011). Bio-oil from Sawdust: Effect of Operating Parameters on the Yield and Quality of Pyrolysis Products. *Energy & Fuels*, *25*(9), 4145–4154. https://doi.org/10.1021/ef200688y

Sarkar, J. K., & Wang, Q. (2020). Different pyrolysis process conditions of South Asian waste coconut shell and characterization of gas, bio-char, and bio-oil. *Energies*, *13*(8), 1970.

Sirimanna, R., & Nadarajah, K. (2026). Status of Waste-to-Energy Technologies in Sri Lanka. *Multidisciplinary Approaches for National Development in Sri Lanka through Advances in Science and Green Technology*, 93.

Tadesse, D. (2010). The impact of climate change in Africa. *Institute for Security Studies Papers*, *2010*(220), 20.

ISSN: 2773-7055
Proceedings of the 5th International Research Conference
Institute of Technology, University of Moratuwa
November 5, 2026

Paper ID: 62

AN ETHICAL EVALUATION OF HYDROPOWER DEVELOPMENT USING AN ENERGY JUSTICE FRAMEWORK: BALANCING ECONOMIC, ENVIRONMENTAL AND SOCIAL IMPACTS

D H K Perera[1*], S S Morapitiya[1]

[1]Division of Electrical, Electronic and Telecommunication Engineering Technology, Institute of Technology, University of Moratuwa, Homagama, Sri Lanka

*Corresponding author: hirushikavi98@gmail.com

ABSTRACT: Hydropower is a significant source of renewable energy because of its capability to generate power continuously, promote grid stability and help in the energy transition. Even though hydropower is advantageous, it can also lead to river system modifications, biodiversity loss, community displacement, and unequal sharing of costs and benefits. Based on the literature search through the review of peer-reviewed academic articles, the ethical acceptance of hydropower has been assessed using environmental, social and economic evidence in combination with the energy justice framework. Different sources of literature in relation to hydropower were included based on certain criteria. Each source was analyzed based on social, environmental, and economic criteria, and those characteristics were compared through five ethical dimensions. Furthermore, information from different countries, especially Sri Lanka, was used to show the relevance of hydropower in the present context of energy transition. The findings of the research demonstrated that hydropower can generate significant effects on the provision of clean energy and energy independence, but the fact that it has different benefits does not mean that it is justified from an ethical point of view. The results demonstrate that hydropower development in Sri Lanka can be ethically justified if it complies with explicit environmental and social protections and if it undergoes transparent, participatory, and adaptive governance. Therefore, hydropower must be regarded as conditionally acceptable, rather than inherently good or bad.

Keywords: hydropower, environmental consideration, energy justice, sustainable development, renewable energy

1 INTRODUCTION

Hydropower has become one of the primary renewable forms of energy and continues to maintain significant relevance in the global energy systems. It offers reliable energy supplies, contributes to a stable grid system, and helps reduce the need for fossil fuels. In 2024, hydropower accounted for approximately 14% of global electricity generation, making it the largest individual renewable source of electricity (International Energy Agency, 2025). Nevertheless, the development of hydropower may impose a number of critical environmental and social challenges. In particular, hydropower development may cause changes in river systems, biodiversity loss, and displacement of local communities.

When it comes to the environmental and social consequences of hydropower, it has to be noted that they depend on the scale, localization, water reservoir features and operational conditions of the project. Hydropower projects can change the natural flow of rivers and affect aquatic ecosystems, as well as sediment transport. The larger the hydropower station is, the more land acquisition and relocation will be needed, leading to unequal distribution of profits and costs. Such issues naturally raise the question of ethics and the distribution of costs and benefits in

the hydropower industry. Energy justice can be used as a framework for dealing with the issues connected with hydropower concerns. It addresses the issues of distributive and procedural justice, as well as recognising affected communities (Siciliano et al., 2018).

Sri Lanka's energy consumption heavily relies on hydropower, which is still included in its renewable-energy plan. According to the Long-Term Generation Expansion Plan of the Ceylon Electricity Board for 2025–2044, renewable energy will be the primary resource for further capacity additions, with solar, wind, mini hydro and biomass being the contributors to the future generation mix. The usage of battery energy storage and pumped-storage hydropower will be added to the renewable energy plan of the Ceylon Electricity Board to facilitate energy integration (Ceylon Electricity Board, 2025). Thus, Sri Lanka must balance the positive effect of hydropower with protecting the environment, ensuring social justice and other renewable developments.

While previous studies have assessed the separate environmental, social, or economic impacts of hydropower, there are fewer studies which interrelate them within a specific ethical framework. Thus, the purpose of this paper is to assess the ethical viability of hydropower development through the application of the energy justice model. It intends to find out under what conditions hydropower can support the development of economic viability and energy security while limiting its negative ethical consequences.

This research is focused on principles of ethics of hydropower development and on defining the conditions under which it can be eco-friendly. The main objectives can be highlighted as follows, 1) exploration of the effects of hydropower on surroundings and on people in the country. 2) evaluation of the effects from the point of view of the following principles of justice: distributive, procedural, recognition, restorative, and intergenerational. 3) suggestions for the national hydropower development from the ethical and responsible point of view.

2 METHODOLOGY

The research used a systematic literature and secondary data review method to examine research, peer-reviewed articles, international energy reports and official documents of Sri Lanka. The findings of the research address the environmental, social and economic issues of hydropower development. The latest publications were given preference over previous publications due to the position of the reviewers regarding the researched evidence which is old, but older research works were used due to their importance in theory and methodology.

The search took place with the help of different combinations such as "hydropower", "hydropower environmental effects", "hydropower social consequences", "energy justice", "displacement due to hydropower", "biodiversity in hydropower", "greenhouse gas emissions in hydropower" and "hydropower in Sri Lanka". The material taken for the review has met the following requirements: it must include at least one aspect of hydropower such as environmental effects, social and livelihood effects, energy and economic effects, energy justice, governance in hydropower and renewable energy in Sri Lanka. The evidence obtained was examined thematically through four categories, which were environmental impacts, social effects, economic and energy system advantages, and ethical concerns. The findings were compared rather than

merely describing the material considered.

Furthermore, the energy justice framework has been applied for ethical assessment purposes. The framework considers distributive justice, analysing impacts of benefits and costs, procedural justice, focusing on participation and decision-making, recognition justice, addressing issues of rights, values and knowledge of the affected stakeholders; restorative justice, discussing compensation and restitution of the losses that may occur, and intergenerational justice, considering long-term aspects (Siciliano et al., 2018). The last step was extraction of the evidence from the literature available both on the global and Sri Lanka levels to determine whether they are relevant for the hydropower development.

3 LITERATURE REVIEW

3.1 Environmental Considerations

Hydropower has an important advantage because electricity generation does not require direct fossil-fuel combustion. Nevertheless, the environmental performance of hydropower depends on the particular project concerned. For example, in case of dams that have placed a large quantity of organic waste underwater, the water reserves can produce greenhouse gases such as carbon and methane. Some researchers observed recently that the amount of greenhouse emissions produced by water reserves varies due to the peculiarities of each reservoir, as well as climatic and geological conditions and management practices applied (Karambelkar et al., 2025).

Hydropower development can also lead to changes in river processes. Dams can change not only the water flow but also sediment movement, fish migration and aquatic habitat. A thorough literature survey on the consequences of hydropower on water flow revealed that the impacts vary from species to species and from river to river. Therefore, it is critical to conduct an environmental assessment for each project, taking into consideration such factors as requirements for environmental flow, biodiversity and ecological monitoring.

3.2 Social Considerations and Justice

The negative social effect of major hydropower projects highly relates to land acquisition, displacement, and changes in lifestyles. People who have been displaced may lose their agricultural land, jobs, natural resources, and social networks. An investigation of hydropower development in China indicated that displacement can cause distribution, recognition and procedural injustices since the displaced communities do not benefit from the projects and have little or no participation in the process (Zhao et al., 2020).

Also, large dams may introduce a difference between the national development aims and local community needs (Siciliano et al., 2018). Their framework of energy justice shows that hydropower development should be assessed taking into account not only the advantages for the state but also the way the power to make decisions, benefits, and drawbacks are distributed.

3.3 Economic and Energy System Benefits

Hydropower is capable of generating electricity over a long period of time, ensuring energy security and providing flexibility to the grid. The controllability of hydropower generation can

be used to balance the variability of renewable sources, such as solar energy and wind energy. Besides electricity generation, multipurpose hydropower plants may bring other benefits, like irrigation or flood protection.

At the same time, the economic benefits of the project need to be balanced with environmental and social costs. For instance, the project may have positive economic implications for the whole nation, leaving a small local population with the negative consequences of the project. Therefore, an economic analysis of the project is not sufficient to answer the question whether the project is ethical or not.

In the case of Sri Lanka, recent analysis by CEB indicates that the future development of electricity will be based on the combination of solar, wind, mini-hydropower and other renewable technologies, supported by battery and pumped-storage systems (Ceylon Electricity Board, 2025). This implies that hydropower is no longer regarded as the only renewable-energy technology and allows comparing different technologies when deciding on future projects.

In 2024, about 14% of total electricity production globally came from hydropower, making it the biggest single source of renewable electricity in the world. Meanwhile, renewable energy sources produced about 30% of total electricity production globally, with wind, solar photovoltaic, and bioenergy contributing their parts too (International Energy Agency, 2025). Figure 1 shows the relevance of hydropower for the global transition to low-carbon electricity systems.

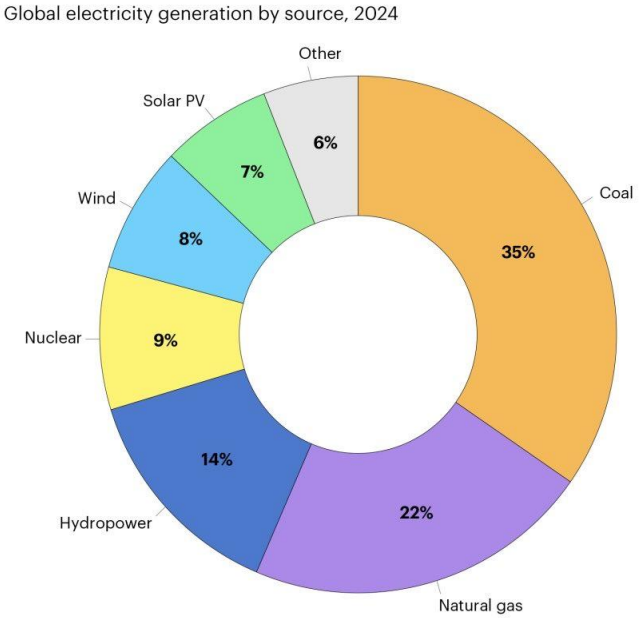


Figure 1. Global electricity generation by source, 2024 (International Energy Agency, 2025)

4 RESULTS AND DISCUSSION

The analysis demonstrates that hydropower cannot be classified either as purely beneficial or as an environmentally harmful energy source. The overall sustainability of hydropower depends on different aspects, such as the characteristics of the project, environmental conditions, standards of governance, and the allocation of profit and cost.

From the environmental standpoint, hydropower is a good source of low-carbon electricity, which contributes to electrification processes on the global level. It is reported that hydropower contributed around 14% of electricity generation in 2024 (International Energy Agency, 2025). However, the reservoirs can also emit greenhouse gas, whilst the construction of the dams can affect rivers' flows and the transportation of sediments as well as waterways (Karambelkar et al., 2025). From a procedural justice perspective, affected communities should have meaningful opportunities to participate in project planning and monitoring.

The analysis finds that restorative justice and recognition are significant aspects too. It is important to consider that cultural values and livelihoods are local knowledge aspects that must be considered in project planning. If impacts are unavoidable, compensation must go along with restoring one's livelihood, providing support for resettlement and monitoring. These steps matter, as the consequences of large infrastructure projects can carry on for years after they are built.

Economically, hydropower can produce a continuous supply of electricity and help increase integration of variable renewable technologies. According to Sri Lanka's latest LTGEP, 70% of electricity by renewable resources is a target by 2030 as well as solar, wind, mini-hydro and storage technologies considered important electricity generation techniques in the future (Ceylon Electricity Board, 2025). This indicates that decisions on hydropower should be made taking into consideration different renewable energy technologies and compared with other technologies.

Overall, the results indicate that hydropower is conditionally ethically sound rather than intrinsically sustainable. A project may be deemed ethically acceptable when it generates significant amounts of energy and creates economic benefits without exceeding certain thresholds of environmental damage. Simultaneously, it distributes the advantages and disadvantages fairly, involves affected parties, restores unavoidable losses, and secures the interests of the following generations. This viewpoint offers a better basis for making hydropower decisions in Sri Lanka than the traditional practice of evaluating projects based on the amount of energy produced or economic benefits created. Table 1 presents the analytical assessment of hydropower development based on environmental, economic, social, and energy justice dimensions, highlighting the key findings and ethical requirements identified from the reviewed evidence.

Table 1. Ethical assessment of hydropower development

Dimension	Main finding	Ethical requirement
Environmental	Low-carbon electricity but possible GHG emissions and river/ecosystem impacts	Project-specific EIA, environmental flows and monitoring
Economic	Reliable electricity, energy security and grid flexibility	Compare benefits with environmental/social costs
Distributive justice	National benefits may be greater than local benefits	Fair compensation and benefit sharing
Procedural justice	Communities can be excluded from major decisions	Early and meaningful participation
Recognition justice	Local livelihoods, culture and knowledge may be overlooked	Recognise affected communities and local values

Dimension	Main finding	Ethical requirement
Restorative justice	Compensation may not fully restore livelihoods	Long-term livelihood restoration and monitoring
Intergenerational justice	Long-term energy benefits but potentially long-term ecological impacts	Consider life-cycle and future-generation impacts

5 CONCLUSION

This research suggests that hydropower can greatly help renewable energy production, safeguarding energy, and assuring the flexibility of electricity systems. Nonetheless, its social acceptability depends on how its environmental consequences are controlled. The assessment of energy ethics indicates that developing hydropower means considering not just its value in terms of energy and money but also its potential to provide fair distribution, acknowledgment of the interests of all parties involved, and restorative justice. Hence, hydropower might be called conditionally acceptable. As for Sri Lanka, hydropower projects should be assessed in conjunction with solar, wind, and energy storage so that renewable energy development will be environmentally friendly and useful for both the present-day and future generations.

6 RECOMMENDATIONS

In the context of expanding hydropower generation in Sri Lanka and similar countries, it is important to take action for sustainable and equitable hydropower development. The environmental assessments need to be informed by river flow, biodiversity, sedimentation, and greenhouse gases emissions at reservoirs. Communities should be actively involved in the planning and implementation stages of projects through transparent information transfers and grievance mechanisms. The idea of compensation and restoration of livelihoods should be more efficient to the people impacted by hydropower projects. Benefit sharing mechanisms should be also improved to share the benefits fairly with local societies. Justice principles should act as a governing framework for hydropower planning and decision making. Project evaluations should be done in accordance with quality data and be updated to reflect new developments in renewable energies and shifts in energy demand. New hydropower projects should be compared with other alternative energy solutions.

7 ACKNOWLEDGEMENTS

The authors would like to express their gratitude to the Institute of Technology, University of Moratuwa for supporting this research. The ITUM and Division of Electrical, Electronic & Telecommunication Engineering are also acknowledged for their academic support.

8 REFERENCES

Ceylon Electricity Board. (2025). *Long-term generation expansion plan 2025–2044.* Ceylon Electricity Board.

International Energy Agency. (2025). *Global energy review 2025: Electricity.* IEA. Retrieved from https://www.iea.org/reports/global-energy-review-2025/electricity

Karambelkar, S., Fischer, M., & Ames, S. (2025). Hydropower reservoir greenhouse gas emissions: State of the science and roadmap for further research to improve emission accounting and mitigation. *Sustainability*, 17(13), 5794.

Siciliano, G., Urban, F., Tan-Mullins, M., & Mohan, G. (2018). Large dams, energy justice and the divergence between international, national and local developmental needs and priorities in the global South. *Energy Research & Social Science*, 41, 199–209.

Zhao, X., Wu, L., & Qi, Y. (2020). The energy injustice of hydropower: Development, resettlement, and social exclusion at the Hongjiang and Wanmipo hydropower stations in China. *Energy Research & Social Science*, 101366.

ISSN: 2773-7055
Proceedings of the 5th International Research Conference
Institute of Technology, University of Moratuwa
November 5, 2026

Paper ID: 71

DESIGN AND DEVELOPMENT OF AN AUTOMATED BULK FILLING SYSTEM USING A CARTESIAN ROBOT FOR COCONUT OIL PACKAGING

H M N C Herath[1*], D H K Perera[1], P T K Sachintha[1], S S Morapitiya[1]

[1]Division of Electrical, Electronic and Telecommunication Engineering Technology, Institute of Technology, University of Moratuwa, Homagama, Sri Lanka

*Corresponding author: chamani.edu@gmail.com

ABSTRACT: Industrial automation has become much more widely used over the last few years and is progressing toward becoming intelligent manufacturing systems. These systems will support companies in producing items with high levels of productivity, quality, and worker safety. A good example of this is in the coconut oil manufacturing industry. When manually filling 10 L bulk bags, workers must complete many tasks regarding the bag and contents such as bag handling, cap removal, filling with liquid coconut oil, capping, and many other tasks. All these tasks require a considerable number of workers and result in high labour costs, inconsistent amounts of liquid being filled into each bag, and reduced operating efficiencies. One significant objective of this research was to develop an Automated Bulk Filling System that meets all the above challenges via an entire filling cycle with little or no human intervention. To achieve this, a Cartesian robot was developed as the foundation for the automated bulk filling machine. The automated bulk filling machine has a pneumatic cap handling system, an Arduino Mega controller, an ESP32 Internet of Things (IoT) module and a flow sensor for measuring the amount of liquid used to fill the bulk bags. This paper presents a prototype of an automated bulk filling machine that produces greater accuracy, consistency, and operational efficiency than a traditional manual process. Additionally, this has greatly reduced the amount of labour needed to refill and handle bags and improved the safety of workers who handle materials due to using this automated material handling equipment. In addition, modular architecture allows for future integration of IIoT (Industrial Internet of Things) technologies, as well as machine vision and predictive maintenance systems.

Keywords: Cartesian robot, automated bulk filling, coconut oil packaging, industrial automation, Arduino Mega

1 INTRODUCTION

The rapid growth of industry has accelerated the use of automated processes and robotics in manufacturing to enhance productivity, the quality of products produced, and create safer work environments. Within the food processing industry, it is being reinforced by the use of robotics, smart sensors, Internet of Things (IoT) technology and intelligent control systems, which provide greater process monitoring and automation (Dadhaneeya, 2023) (Hassoun, 2023). Automated filling systems for liquid products are increasingly important within food and beverage manufacturing, as filling accuracy and consistency, and production efficiency directly impact the performance of the production process during manufacturing of those products. Recent advancements in food packaging have underscored the critical need for sensors and automation to optimize process control, product quality, and production efficiency (Palanisamy, 2025). Bulk coconut oil is still typically filled manually, as the current process requires multiple workers to perform different tasks including positioning the bags, removing the caps from the fill spouts, filling the bags with oil, and returning the caps onto the fill spouts. The manual methods of performing these tasks require significant labour, are time-consuming, have a high possibility

of human error, can result in variations in the volume of product that is filled into the bags, and raise the cost of labour while lowering productivity (Groover, 2020).

Because of the accurate positioning capabilities of the Cartesian robots, their simplistic, mechanical construction, and their low-cost implementation, they are effective solutions for industrial automation. The potential uses of robotic technologies in food manipulation and packaging are being explored due to their capabilities for repetitive manipulation with enhanced positioning and repeatability. (Derossi, 2023) (Vasudevan, 2024). Recent advancements in embedded control technology (e.g., Arduino Mega and ESP32) have also made robot-assisted automation systems a feasible option for real-time control, sensor integration, and wireless communications. In addition, IoT technologies can be used to enhance these aspects of real-time monitoring, data collection, and optimization in today's food processing settings (Dadhaneeya, 2023). Many studies have shown that automated systems for liquid filling will improve operational efficiencies and provide improved consistency of product. For example, recent efforts in automatic liquid filling have shown the potential for employing automatic control to enhance the performance of the filling process and optimization of the filling process has been recognized as having a beneficial impact on production efficiency (Arrasyid, 2024) (Cui, 2022). However, most existing systems focus on filling products into bottles and not on automating the bulk bag handling, cap removal, and cap replacement processes associated with the packaging of coconut oil (Craig, 2018; Liu et al., 2015).

To address this research gap, this study presents an automated bulk filling system integrating an Arduino Mega, an ESP32, flow sensing, pneumatic cap handling, and a Cartesian robot. The system can be automated with minimal human intervention, offering a compact and scalable solution for improved efficiency, accuracy, workplace safety, with provision for future IIoT integration.

2 METHODOLOGY

An automated bulk filling solution was created to automate the process of filling 10-litre coconut oil bulk bags. The bulk filling system comprises a Cartesian robotic arm, pneumatic cap-removal/installation mechanism, flow sensor, Arduino Mega board controller and ESP32 wireless communication module. The development process of the automated bulk filling system consisted of the mechanical design, development of the control system, integration of hardware components and validation of the prototype. All mechanical components were created in SolidWorks 2022, and all of the pneumatic circuits were designed using FluidSIM-Pneumatic, so that the operation of the cap-removal/installation mechanisms could be confirmed prior to building a prototype. The overall system was designed to function together (robot, fill unit, sensors & conveyor) in a synchronized manner.

The Cartesian robotic arm is made up of 3 linear axes (X, Y, Z), each driven by a stepper motor and screw-driven linear guide actuators, allowing for precise placement of the bulk bags during the filling procedure. A pneumatic suction mechanism was used to remove and replace the cap on the bulk bag. A linear actuator placed the filling nozzle directly above the opening of the bulk bag. The Arduino Mega was used as the master controller to synchronize the operation of

the robot, conveyor, pneumatic actuators and filling sequence. The system is designed with an ESP32 module which allows for wireless communication within the system. This will allow for future implementations of IIoT functions such as remote monitoring, data logging, and system diagnostics. A liquid flow sensor is utilized to continuously measure the volume of coconut oil during the filling process, thereby ensuring accurate dispensing and a reduction in product waste.

The operational sequence for the system begins with the conveyor transporting an empty bulk bag to the filling area, where an infrared sensor detects the presence of the empty bulk bag. The Cartesian robot utilizes the infrared sensor to position the empty bulk bag and then uses a pneumatic suction mechanism to remove the lid from the empty bulk bag before placing it in a placeholder location. Once the empty bulk bag is in place and the lid has been removed, the filling nozzle is lowered into the empty bulk bag, and coconut oil is dispensed into the bulk bag until the desired volume is achieved based on feedback from the flow sensor. Once the filling is complete, the robotic system withdraws the filling nozzle and replaces and tightens the lid on the filled bulk bag before transferring the filled bulk bag to the discharge conveyor. The prototype was experimentally evaluated based on filling accuracy, operational repeatability, and system performance. The automated filling process was also compared against traditional manual filling procedures to assess improvements in labour requirements, productivity, and consistency of the filling process. The operational sequence is shown in Figure 1.

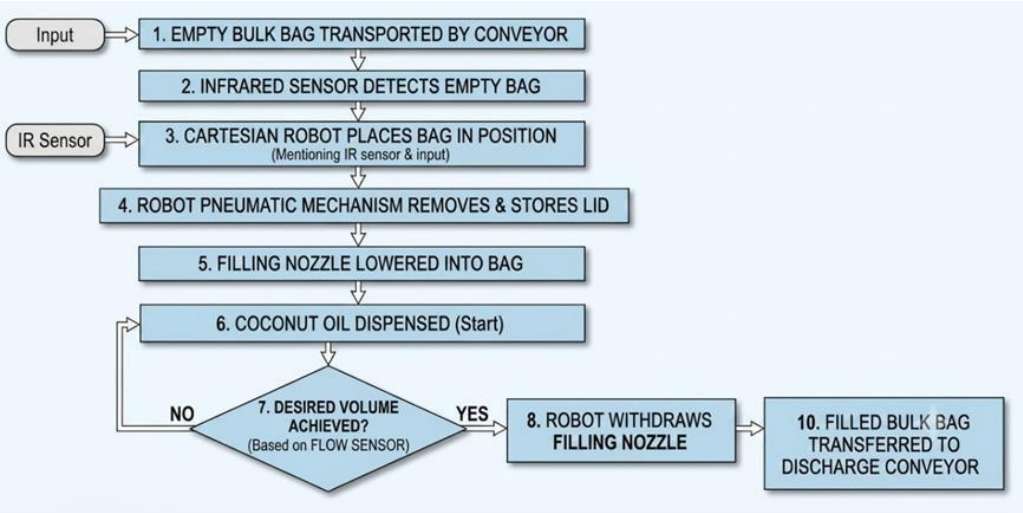


Figure 1. Operational sequence of the automated bulk filling system.

3 RESULTS AND DISCUSSION

The successful functioning of the prototype demonstrated the technical feasibility of automating the bulk filling operation using a Cartesian robot for 10 L coconut oil bags. The main aim of the integrated system was to carry out a series of operations with minimal manpower, such as the positioning of bulk bags, removal of caps, filling with liquid, replacing caps and transferring the finished product. Tests were conducted on the Arduino Mega, ESP32, flow sensor, stepper motors, conveyor system, IR break-beam sensor, and linear guide rail actuator modules to verify the proper integration of the major subsystems. The flow sensor was calibrated and tested

for coconut oil flow, and the Cartesian robot and conveyor mechanisms were tested to ensure coordinated movement in cap handling and pick and place operations.

To assess operating performance of the proposed system, quantitative analysis was done. The linear speed of screw-driven linear guide rail actuator was calculated as 255 mm/s. The total distance to be travelled by the Cartesian robots for one pick and place cycle was around 3000 mm, implying a motion time of 11.76 s to cover this distance. After including an additional 1.50 s for operational delays, the total Cartesian robot cycle time was calculated as 13.26 s. The travel distance for cap removal and filling-side movement was determined to be around 1100 mm, and a calculated movement time of 4.313 s was set for this travel distance. For the pneumatic operations, a time of 7 s was set.

The cycle-time analysis also suggests that the filling operation is about 89.4% of the total calculated cycle time of the machine. Hence, a higher flow rate of the liquid would have an even larger effect on the overall productivity than a further decrease in the Cartesian robot movement time. The project report had pointed out that the present filling rate was one of the serious limitations and it was suggested to install the appropriate pumping system to improve the filling rate and to shorten the overall cycle time.The developed hardware prototype of the proposed system is shown in Figure 2.

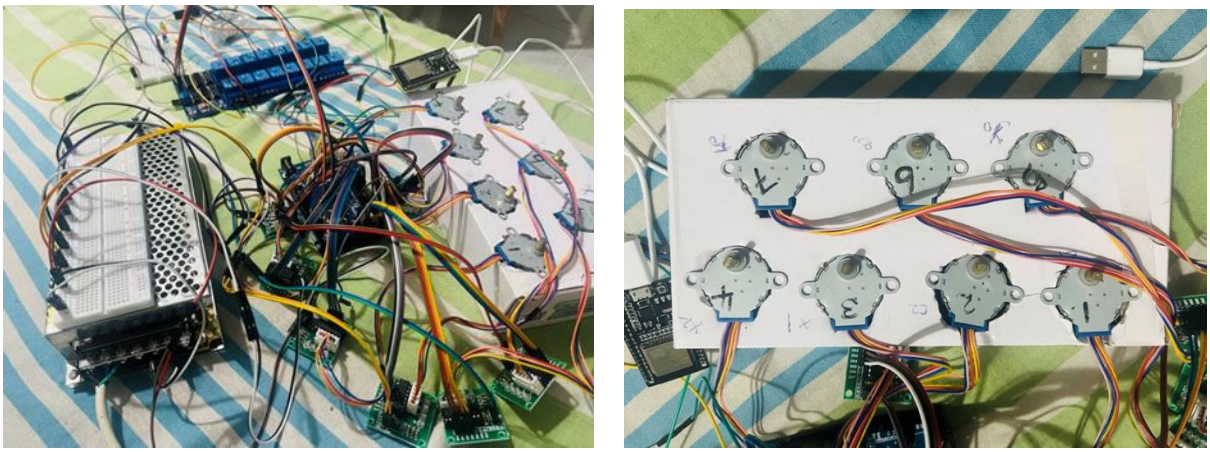


Figure 2. Prototype of an automated bulk filling system

The proposed system reduces the need for repetitive manual tasks like handling bags, removing caps, filling, and tightening the cap, which are the repetitive operations, compared with conventional manual filling methods. The Cartesian robot is used to automatically position and move the cap. The pneumatic cap-handling mechanism is designed to minimize the physical effort required for repetitive cap removal and replacement. Therefore, the automatic sequence offers a potential reduction of workload for the operator and a more consistent process. However, the present study does not include a sufficiently large experimental comparison between manual and automated production to quantify the percentage improvement in productivity or labour reduction. Thus, these benefits are presented as possible operating benefits and not as measurable gains. Conversely, the automated system has a significantly decreased need for the manual operation of all tasks, as each of these tasks can be accomplished sequentially with a coordinated robotic mechanism as shown in Figure 3.

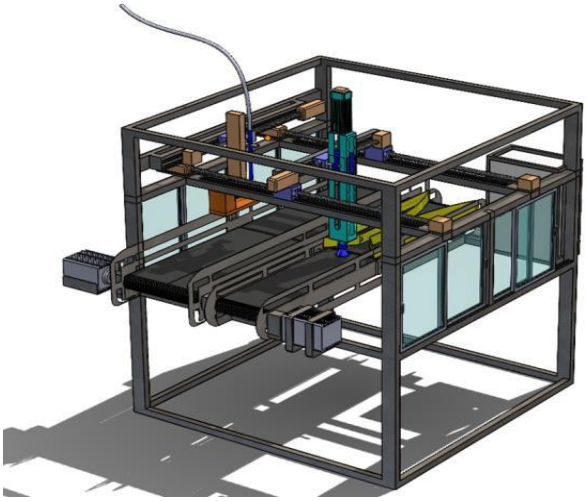


Figure 3. Machine mechanical structure design from SolidWorks

The cap-handling mechanism was also found to have a suitable force capacity in line with design calculations. The estimated force that would be needed to remove and fasten the caps was about 250 N while the force capacity of the selected Industrial Vacuum Suction Cup Pneumatic 400 N is about 400 N. This means that the available force is thus about 1.6 times the estimated required force, which means the force margin for cap handling is adequate from a theoretical point of view. At the prototype phase, however, a compressor was not available so an LED was used to represent the activation of a suction cup. Thus, for the intended industrial application, full pneumatic performance must be validated with the intended compressor and pneumatic system. During prototype testing, some limitations were identified that affected the final design. At first, the low cost 28BYJ-48 stepper motors were overheating and tending to run at low speeds. The voltage reduction fixed the overheating issue, but decreased torque. The tests therefore indicated the necessity of higher speeds and an adequately rated motor for actual industrial use. Furthermore, deformation of the mechanical holder was noticed during cap removal and cap fastening. Then a stress analysis was performed with SolidWorks to redesign the holder with a 15 mm thick galvanized iron plate. The modified design minimized the observed distortion and increased the holder's structural strength.

The S201C flow sensor was chosen as being inexpensive enough to use in the prototype, and was calibrated for the initial filling tests. The sensitivity is stated to be about 10% accurate over the specified flow range, though, which means that this sensor is not ideal for applications that demand highly accurate industrial filling. Thus, it is suggested to use a higher level of precision flow-measurement device in the future.

The quantitative analysis and prototype testing indicate that the Cartesian robotic motion, pneumatic cap handling, flow sensing, conveyor operation, and embedded control can be incorporated into a coconut oil bulk filling system. However, the findings of the current study must be taken in the context of a proof of concept prototype. A large number of repeated filling trials were not included in the study and thus it was not possible to calculate statistical parameters (mean filling error, standard deviation, repeatability). The 125 s cycle time and 28.8 bags/h throughput are also not validated with long duration industrial production tests. Thus, additional experimental testing under continuous operating conditions is needed in order to prove filling accuracy,

repeatability, reliability and actual production throughput.

The results have shown that the main potential improvement of system performance is the increase of the filling flow rate, and the improvement of the motion and sensing components to make the system suitable for an industrial application. Future development should then take into account an appropriate pumping system, flow metering with higher accuracy, higher speed motors, machine vision for bag positioning and cap checking, PLC-based industrial automation control and monitoring and predictive maintenance by Internet of Things. The enhancements made would overcome the restrictions that were observed during the prototype testing and give better grounds for the full-scale industrial implementation.

4 CONCLUSION

This research illustrates how to design and build an automated bulk fill system with a Cartesian robot to package coconut oil. The prototype achieved a functioning integration of robotic movement, pneumatic caps, flow detection and embedded controllers. This provided full automation of the process with very little contact by humans. When compared with traditional manual methods, the proposed system exhibited improved accuracy in filling, increased operational efficiency and greater safety in the workplace. Additionally, the system's modular design will allow for future enhancements that may include machine vision, PLC control and integration into an Industrial Internet of Things (IIoT). Consequently, the produced system represents an applicable, scalable means of promoting automation within a coconut oil manufacturing facility.

5 ACKNOWLEDGEMENTS

The authors would like to express their gratitude to the Institute of Technology, University of Moratuwa, for supporting this research, and to the Division of Electrical, Electronic & Telecommunication Engineering for its academic support.

6 REFERENCES

Arrasyid, M. R. (2024). Automatic filling machine for Metracide 1 liter product variant at Global Medipro Investama LLC. *International Journal on Robotics, Automation and Sciences*, 16-24.

Craig, J. J. (2018). *Introduction to Robotics: Mechanics and Control.* Pearson.

Cui, Y. Z. (2022). Filling process optimization through modifications in machine settings. *Processes*, 10(11).

Dadhaneeya, H. N. (2023). Internet of Things in food processing and its potential in Industry 4.0 era: A review. *Trends in Food Science & Technology*.

Derossi, A. D. (2023). Avenues for non-conventional robotics technology applications in the food industry. *Food Research International.*

Groover, M. P. (2020). *Automation, Production Systems, and Computer-Integrated Manufacturing*. Pearson.

Hassoun, A. J.-G. (2023). Food processing 4.0: Current and future developments spurred by the fourth industrial revolution. *Food Control*, 145.

Liu, Y., Zhang, H., & Wang, X. (2015). Design and realization of liquid filling machine intelligent control system. *IEEE International Conference on Mechatronics and Automation*, 1152–1157.

Palanisamy, Y. K. (2025). Recent technological advances in food packaging: Sensors, automation, and application. *Sustainable Food Technology*, 161-180.

Vasudevan, S. L. (2024). *Machine vision and robotics for primary food manipulation and packaging: A survey.* IEEE Access.

ISSN: 2773-7055
Proceedings of the 5th International Research Conference
Institute of Technology, University of Moratuwa
November 5, 2026

Paper ID: 45

EFFECT OF AGITATION STRATEGY ON BIODIESEL PRODUCTION FROM WASTE COCONUT OIL

W V W H Wickramaarachchi[1*], H C Dilshan[1], D M H M A Disanayaka[1], D M M D Dissanayaka[1], W M T M Dewdunu[1]

[1]Division of Polymer and Chemical Engineering Technology, Institute of Technology, University of Moratuwa, Homagama, Sri Lanka

*Corresponding author: wathsalav@itum.mrt.ac.lk

ABSTRACT: This study investigated the effect of agitation strategy on biodiesel production from single-use waste coconut oil (WCO) through alkali-catalyzed transesterification using virgin coconut oil (VCO) as a reference. Biodiesel was synthesized using a 5:1 methanol-to-oil volumetric ratio with sodium hydroxide (NaOH) as the catalyst at 60 °C for 90 min under four agitation strategies: constant stirring at 400 rpm and 700 rpm, and step-wise agitation profiles of 400–700 rpm and 700–400 rpm. The produced biodiesel was purified by wet washing and characterised in terms of yield, density, viscosity, flash point, and fire point. The highest biodiesel yield from WCO (63%) was achieved under continuous agitation at 700 rpm, while the 400–700 rpm agitation profile produced the lowest yield (47%). However, the highest flash point (113 °C) and fire point (126 °C) were obtained using the 400–700 rpm agitation strategy, indicating improved fuel safety characteristics. Density remained nearly constant (0.88–0.90 g/cm^3) for all agitation conditions, whereas viscosity varied with agitation strategy, suggesting differences in transesterification efficiency. The findings demonstrate that agitation strategy significantly influences biodiesel yield and selected fuel properties, providing useful information for optimising laboratory-scale biodiesel production from waste coconut oil.

Keywords: biodiesel, waste coconut oil, transesterification, agitation speed, fuel properties

1 INTRODUCTION

The increasing demand for renewable and sustainable energy sources has accelerated research on biodiesel as an environmentally friendly alternative to petroleum diesel. Biodiesel is commonly manufactured by the transesterification of triglyceride-rich feedstocks, including edible and non-edible vegetable oils, animal fats, waste cooking oils, and microalgal oils, with short-chain alcohols such as methanol or ethanol in the presence of an alkali catalyst such as sodium hydroxide (NaOH), potassium hydroxide (KOH), or sodium methoxide (CH_3ONa) (Nayab et al., 2022). Among these feedstocks, waste cooking oil (WCO), collected after one frying cycle, has gained considerable attention because it is an inexpensive and sustainable raw material that reduces waste disposal problems while avoiding competition with edible oils.

The efficiency of alkali-catalyzed transesterification is influenced by several operating parameters, including the alcohol-to-oil ratio, catalyst concentration, reaction temperature, reaction time, and mixing conditions (Ramos et al., 2019). Since oil and methanol are initially immiscible, adequate agitation is required to increase the interfacial contact area between the two phases, thereby enhancing mass transfer and promoting biodiesel formation. However, inappropriate mixing conditions may reduce conversion efficiency by limiting reactant dispersion or promoting undesirable side reactions such as soap formation, particularly when waste cooking oils containing elevated free fatty acid levels are used.

Previous studies have extensively investigated the optimisation of transesterification parameters, including catalyst concentration, methanol-to-oil ratio, reaction temperature, and reaction time, to maximize biodiesel conversion and fuel quality (Banerjee et al., 2018; Eevera et al., 2009; Garg & Jain, 2020). However, the efficiency of the transesterification process is also strongly influenced by the agitation speed, which governs mass transfer between the immiscible oil and methanol phases (Levenspiel, 1999; Noureddini & Zhu, 1997). In particular, the effects of constant and stage-wise agitation profiles on biodiesel yield and fuel quality from WCO have not been adequately investigated.

Therefore, this study evaluates the effect of different agitation strategies, including constant and step-wise mixing profiles, on biodiesel production from waste coconut oil. The produced biodiesel was characterised in terms of yield, density, viscosity, flash point, and fire point to identify suitable operating conditions for laboratory-scale biodiesel production.

2 METHODOLOGY

2.1 Raw materials

Single-use coconut oil, obtained from domestic sources after one frying cycle, and virgin coconut oil as a control were used as the main raw materials. Industrial-grade methanol with 99.8% purity was used as the alcohol medium for the transesterification reaction. Analytical-grade sodium hydroxide (NaOH, 98% purity) was used as the alkali catalyst for biodiesel production.

2.2 Procedure

The virgin coconut oil (VCO) and single-use waste coconut oil (WCO) were filtered to remove suspended impurities and preheated to 60 °C before transesterification. NaOH was dissolved in methanol to prepare the methoxide solution, which was then added to the preheated oil. The transesterification reaction was conducted in a batch reactor using a hot plate magnetic stirrer for 90 min. The methanol-to-oil volumetric ratio was 5:1, and NaOH was used at a concentration of 10 g L^{-1} in waste coconut oil. Four agitation strategies were investigated: constant stirring at 400 rpm, constant stirring at 700 rpm, and stepwise agitation profiles of 400–700 rpm and 700–400 rpm, with the stirring speed adjusted in 100 rpm increments at 22.5 min intervals. After the reaction, the mixture was allowed to settle for 20 h to separate the biodiesel and glycerol phases. The biodiesel layer was separated using a separating funnel and was purified by wet washing with distilled water.

2.3 Testing of Properties

The biodiesel yield was calculated using Equation (1).

$$Yield\ (\%) = \frac{Volume\ of\ biodiesel\ separated\ (ml)}{Total\ volume\ (ml)} \times 100 \quad (1)$$

The density of the biodiesel was determined using a pycnometer in accordance with ASTM D941. Dynamic viscosity was determined using a Digital Viscometer (Model: VR3000-L). Flash point

and fire point were measured using a Cleveland Open Cup Tester (Model: 13811-3P) according to ASTM D92.

3 RESULTS AND DISCUSSION

Figure 1 shows the effect of agitation strategy on the biodiesel yield. The highest yield (83%) was obtained from virgin coconut oil at a constant agitation speed of 700 rpm, indicating that fresh oil undergoes efficient transesterification under high-shear mixing. For waste coconut oil, continuous agitation at 700 rpm produced the highest yield (63%), whereas reducing the agitation speed to 400 rpm resulted in a slight decrease to 62%. The lowest yield (47%) was obtained using the step-wise agitation profile of 400–700 rpm, suggesting that insufficient mixing during the initial stage of the reaction limited mass transfer between the immiscible oil and methanol phases. In contrast, the 700–400 rpm profile produced a higher yield (58%), indicating that maintaining a high agitation speed during the early stages of transesterification promotes better reactant dispersion and enhances biodiesel formation (Noureddini & Zhu, 1997). Overall, continuous agitation at 700 rpm was found to be the most effective mixing strategy for biodiesel production from waste coconut oil under the investigated conditions.

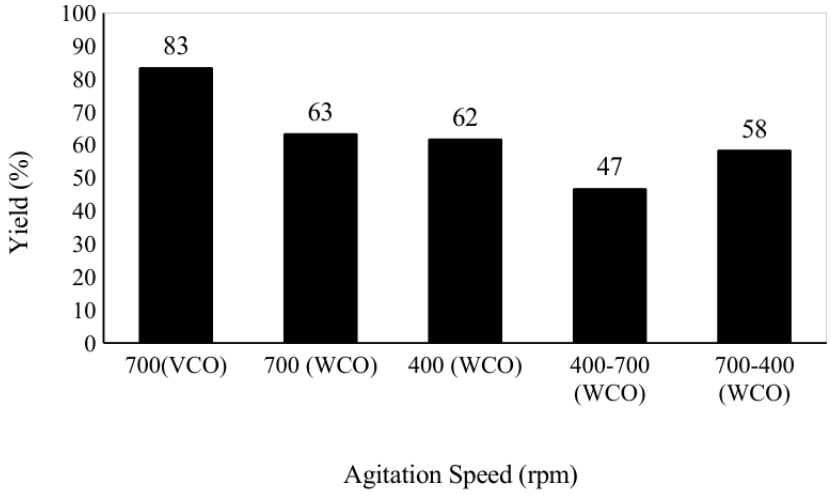


Figure 1. Effect of agitation strategy on the biodiesel yield obtained from virgin coconut oil (VCO) and waste coconut oil (WCO)

Figure 2 shows the effect of agitation strategy on the flash point and fire point of biodiesel produced from VCO and WCO. The biodiesel produced from VCO at a constant agitation speed of 700 rpm exhibited the lowest flash point (94 °C) and fire point (100 °C). For WCO, increasing the constant agitation speed from 400 rpm to 700 rpm slightly increased the flash point from 100 °C to 104 °C and the fire point from 108 °C to 110 °C. The highest flash point (113 °C) and fire point (126 °C) were obtained using the step-wise agitation profile of 400–700 rpm, indicating that gradually increasing the agitation speed during the reaction enhanced fuel quality. In contrast, the 700–400 rpm profile resulted in lower flash and fire points of 101 °C and 105 °C, respectively. These results suggest that the agitation strategy influences the extent of transesterification and the thermal ignition characteristics of the produced biodiesel (Meher et al., 2006). Higher flash and fire points indicate improved fuel quality and safer handling characteristics due to reduced volatile impurities (Knothe et al., 2015).

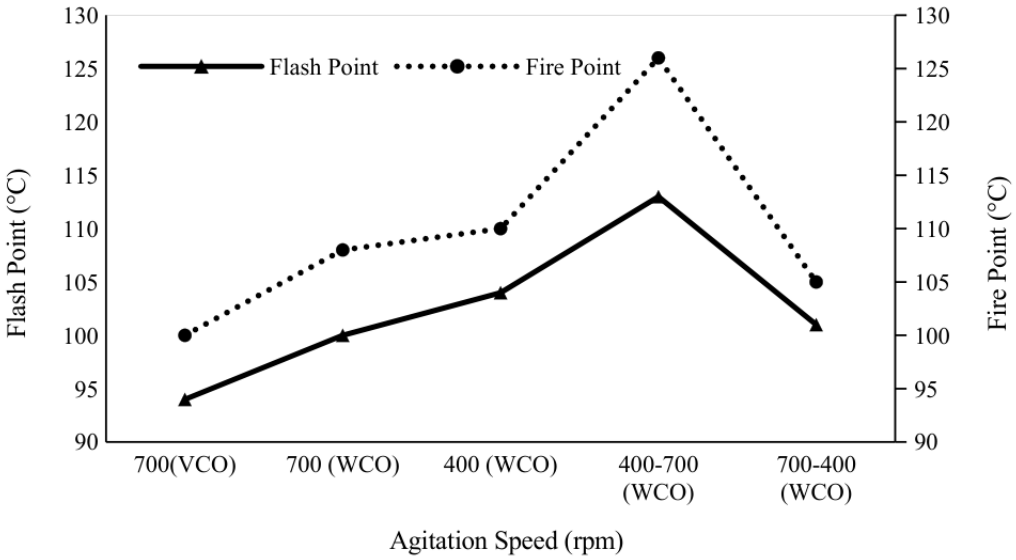


Figure 2. Effect of agitation strategy on the flash point and fire point

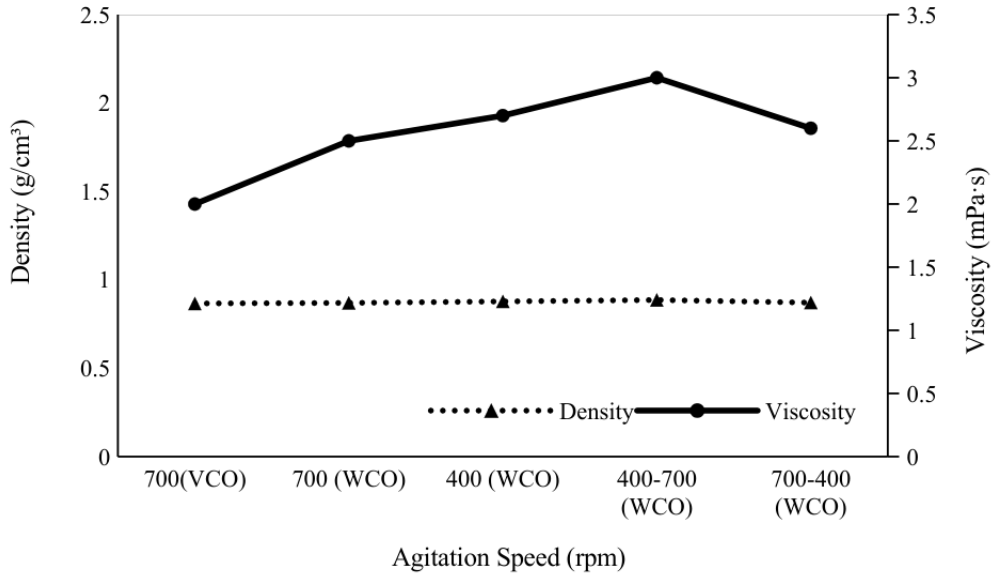


Figure 3. Effect of agitation strategy on the density and viscosity

Figure 3 illustrates the effect of agitation strategy on the density and viscosity of biodiesel produced from VCO and WCO. The density remained nearly constant at approximately 0.88–0.90 g/cm^3 for all agitation strategies, indicating that mixing conditions had little influence on the density of the final biodiesel. This observation suggests that the transesterification reaction produced biodiesel with similar chemical composition despite the differences in agitation profiles (Knothe et al., 2015). In contrast, viscosity showed noticeable variation with agitation strategy. Biodiesel produced from VCO exhibited the lowest viscosity (approximately 2.0 mPa·s), while viscosity gradually increased for WCO samples, reaching the highest value (approximately 3.0 mPa·s) under the 400–700 rpm agitation profile. The increase in viscosity may be attributed to incomplete transesterification or the presence of residual glycerides resulting from less efficient mixing during the initial stage of the reaction. The 700–400 rpm profile produced a slightly lower viscosity than the 400–700 rpm profile, indicating that maintaining a higher agitation speed

during the early stage of the reaction enhanced reactant dispersion and improved conversion (Noureddini & Zhu, 1997). Overall, the results demonstrate that the agitation strategy had a greater influence on biodiesel viscosity than on density.

4 CONCLUSION

This study demonstrated that agitation strategy has a significant influence on biodiesel production from waste coconut oil. Continuous agitation at 700 rpm produced the highest biodiesel yield (63%) among the waste coconut oil samples, indicating that sustained high-speed mixing enhanced mass transfer and transesterification efficiency. In contrast, the 400–700 rpm step-wise agitation profile resulted in the highest flash point (113 °C) and fire point (126 °C), suggesting improved fuel quality through more effective removal of volatile impurities. Density remained nearly constant for all agitation strategies, whereas viscosity showed noticeable variation, indicating that agitation had a greater influence on biodiesel viscosity than on density. Overall, the results demonstrate that selecting an appropriate agitation strategy is important for optimising biodiesel yield and fuel quality during laboratory-scale production from waste coconut oil.

5 ACKNOWLEDGEMENTS

The authors acknowledge the support of the Division of Polymer and Chemical Engineering Technology, Institute of Technology, University of Moratuwa, for providing the facilities and technical assistance for this study.

6 REFERENCES

Banerjee, N., Barman, S., Saha, G., & Jash, T. (2018). Optimisation of process parameters of biodiesel production from different kinds of feedstock. *Materials Today: Proceedings, 5*(11, Part 2), 23043–23050. https://doi.org/10.1016/j.matpr.2018.11.033

Eevera, T., Rajendran, K., & Saradha, S. (2009). Biodiesel production process optimisation and characterization to assess the suitability of the product for varied environmental conditions. *Renewable Energy, 34*(3), 762–765. https://doi.org/10.1016/j.renene.2008.04.006

Garg, A., & Jain, S. (2020). Process parameter optimisation of biodiesel production from algal oil by response surface methodology and artificial neural networks. *Fuel, 277*, 118254. https://doi.org/10.1016/j.fuel.2020.118254

Knothe, G., Krahl, J., & Van Gerpen, J. (2015). *The biodiesel handbook*. Elsevier.

Levenspiel, O. (1999). *Chemical reaction engineering* (3rd ed.). John Wiley & Sons.

Meher, L. C., Vidya Sagar, D., & Naik, S. N. (2006). Technical aspects of biodiesel production by transesterification—A review. *Renewable and Sustainable Energy Reviews, 10*(3), 248–268. https://doi.org/10.1016/j.rser.2004.09.002

Nayab, R., Imran, M., Ramzan, M., Tariq, M., Taj, M. B., Akhtar, M. N., & Iqbal, H. M. N. (2022). Sustainable biodiesel production via catalytic and non-catalytic transesterification of feedstock materials – A review. *Fuel, 316*, 125254. https://doi.org/10.1016/j.fuel.2022.125254

Noureddini, H., & Zhu, D. (1997). Kinetics of transesterification of soybean oil. *Journal of the American Oil Chemists' Society, 74*(11), 1457–1463. https://doi.org/10.1007/s11746-997-0254-2

Ramos, M., Dias, A. P. S., Puna, J. F., Gomes, J., & Bordado, J. C. (2019). Biodiesel production processes and sustainable raw materials. *Energies, 12*(23), 4408. https://doi.org/10.3390/en12234408

ISSN: 2773-7055
Proceedings of the 5th International Research Conference
Institute of Technology, University of Moratuwa
November 5, 2026

Paper ID: 14

ADOPTABILITY OF DUAL-COLOUR SOCKS FOR SCHOOL UNIFORMS: A STATISTICAL APPROACH

Aruna Ratnayake[1,2*], Ravindi Jayasundara[1], Prathibani Manthriratne[3]

[1]Department of Mathematics, Faculty of Engineering, University of Moratuwa, Moratuwa (10400), Sri Lanka

[2]Textile and Garments Section of Standardization Division, Sri Lanka Standards Institution, Colombo (00800), Sri Lanka

[3]Fashion Design & Product Development Degree Course, Department of Textile & Apparel Engineering, Faculty of Engineering, University of Moratuwa, Moratuwa (10400), Sri Lanka

*Corresponding author: arun.ou.lk@gmail.com

ABSTRACT: The mandatory use of white school socks in Sri Lanka creates significant maintenance challenges for parents and students. This study evaluates the feasibility of recommending dual-colour socks, consisting of a white leg section and a black sole, called "dual-colour" hereafter, as an alternative to completely white socks. Primary data were collected from 314 respondents, including parents and students. Hierarchical cluster analysis was applied to identify consumer segments based on usage behaviour, laundering practices and performance expectations. Cluster validation using a confusion matrix yielded an accuracy of 72.31%. Results indicate that respondents experience considerable difficulty in maintaining the appearance of white socks under local climatic and usage conditions. Dual-colour socks were perceived as a practical solution for improving aesthetic durability while reducing laundering frequency and replacement rates. The findings indicate that dual-colour socks can offer economic and environmental advantages while adhering to school uniform requirements and aligning with consumer preferences.

Keywords: dual-colour socks, cluster analysis, consumer preference, aesthetic durability, school uniforms

1 INTRODUCTION

School uniforms are a long-standing requirement in Sri Lanka and are intended to promote equality, discipline and social identity. White socks form an essential component of this uniform system. However, the tropical climate, dust, moisture and frequent use create rapid soiling and discolouration. As a result, parents must wash socks frequently using strong detergents and bleach. Previous studies have shown that compulsory clothing items generate dissatisfaction when functional performance does not match user expectations (Solomon, 2018; Entwistle, 2015). This study provides empirical evidence on consumer preferences and performance expectations for school socks in the Sri Lankan context, addressing a critical yet often overlooked component of the school uniform system. By statistically evaluating the feasibility of adopting dual-colour socks (white upper section with black sole) as in Figure 1, the research provides an evidence-based foundation for informed decision-making in product innovation, standard implementation, and uniform policy development.



Figure 1. Conceptual representation of a dual-colour sock

The school sock market represents a significant recurring consumer market. Although standards specify technical requirements, aesthetic durability remains a major concern. Dual-colour socks, featuring a white upper section and black sole, have been introduced as an innovative design solution. Previous research has addressed school uniforms, consumer behaviour, textile durability, and clothing performance from different perspectives (Lee et al., 2009; Forsythe et al., 1996; Kelley et al., 1986; Shim & Bickle, 1994). However, the reviewed literature shows limited empirical research specifically addressing school socks in tropical environments with mandatory uniforms, particularly regarding aesthetic durability, consumer preferences, and alternative sock designs. Therefore, an evidence-based assessment is needed to determine whether a dual-colour sock is an acceptable alternative to the conventional, completely white school sock. The objectives of this study were to assess the feasibility of recommending dual-colour socks for school uniforms based on consumer preferences and performance expectations.

2 METHODOLOGY

This study adopted a cross-sectional survey design to evaluate the feasibility of recommending dual-colour school socks (white leg with black sole) for use within the Sri Lankan school uniform system. Primary data were collected from parents and school-going students, who represent the principal purchasers and users of school socks. A structured questionnaire consisting of 36 questions was developed based on the literature review and research objectives. The questionnaire covered demographic characteristics, sock usage patterns, laundering practices, performance expectations, consumer perceptions, and acceptance of dual-colour socks. Prior to administration, the questionnaire was pre-tested with 20 respondents to assess clarity, relevance, and consistency, and minor modifications were made accordingly. Survey-based research is widely used in consumer and textile studies because it facilitates the systematic collection of perceptions, attitudes, and behavioural information from large respondent groups (Bryman, 2016).

A total of 314 valid responses were collected using a combination of convenience and snowball sampling techniques. These non-probability sampling methods were selected due to the absence of a comprehensive sampling frame and the exploratory nature of the study. Convenience sampling provided efficient access to appropriate respondents, while snowball sampling helped identify additional participants through social networks (Biernacki & Waldorf, 1981; Saunders et al., 2019). Data were collected primarily through an online Google Form distributed via per-

sonal contacts, schools, and community networks, supplemented by telephone and face-to-face responses. The collected data were analysed using descriptive statistics and hierarchical cluster analysis. Cluster analysis is an exploratory multivariate technique that groups observations by similarities across multiple variables and is widely used in consumer preference research (Hair et al., 2019; Everitt et al., 2011). Hierarchical clustering was employed to identify natural consumer segments based on sock usage patterns, preferences, and evaluations of performance parameters. The hierarchical clustering procedure was used to determine the underlying consumer segments without predefining the group membership. The resulting cluster assignments were subsequently compared with the observed sock-usage categories using a confusion matrix for external validation. The confusion matrix provided the basis for evaluating the agreement between the statistically derived clusters and the observed categories through measures including accuracy, precision, recall, and specificity (Everitt et al., 2011; Hair et al., 2019). Finally, the identified clusters were examined in relation to key sock-performance parameters to characterize differences in consumer expectations and perceptions and to assess the feasibility of recommending dual-colour socks within the Sri Lankan school-uniform context.

3 RESULTS AND DISCUSSION

The hierarchical cluster analysis identified two distinct consumer clusters based on similarities in sock usage patterns, preferences, and evaluations of performance parameters. Cluster 1 predominantly represented users of single-colour socks, including all-white and all-black socks, whereas Cluster 2 predominantly represented users of dual-colour socks or a combination of dual-colour and white socks. The two clusters therefore represented different patterns of sock usage and consumer preference. Hierarchical cluster analysis enabled these groups to be identified based on similarities across multiple variables rather than relying only on individual descriptive responses (Hair et al., 2019; Everitt et al., 2011). The identified clusters were subsequently evaluated using a confusion matrix by comparing the cluster assignments with the observed sock-usage categories. This provided an external assessment of the consistency of the cluster classification. The performance of the classification results is shown in Table 1.

Table 1. Classification performance of the identified consumer clusters

Metric	Value
Accuracy	72.31%
Precision	68.90%
Recall	76.87%
Specificity	68.13%

The 72.31% classification accuracy indicates that the identified cluster membership correctly matched with the reference sock-usage classification for approximately three-quarters of the observations. The precision of 68.90% indicates a high proportion of correctly identified cases among those assigned to the relevant category, while the recall of 76.87% indicates that a substantial proportion of cases belonging to the reference category were correctly captured. The specificity of 68.13% further indicates a reasonable ability to distinguish the alternative cate-

gory. Thus, the classification results provide quantitative support for the identified two-cluster solution. The use of external classification measures is especially valuable because hierarchical clustering is an unsupervised technique that does not provide inherent classification accuracy (Everitt et al., 2011; Hair et al., 2019). The identified clusters were then compared according to eight performance-related parameters: (1) convenient cuff, (2) cuff recovery, (3) leg length, (4) lengthwise recovery, (5) pilling resistance, (6) comfort during perspiration, (7) comfort of toe closure, and (8) abrasion resistance. These parameters were used to determine whether the two consumer groups differed in the aspects of sock performance that they valued or perceived positively. Figure 2 compares the positive perceptions of the eight selected performance parameters between single-colour and dual-colour sock users. Single-colour users showed particularly positive perceptions of leg-length precision (90.3%), convenient cuff performance (72.6%), abrasion resistance (60.2%), and cuff recovery (59.3%). In contrast, dual-colour users showed higher positive perceptions for abrasion resistance (67.7%), toe-closure comfort (41.2%), lengthwise recovery (29.4%), and perspiration comfort (26.5%). These differences indicate that the two consumer groups had distinct performance priorities. The results suggest that single-colour users were particularly satisfied with fit- and cuff-related characteristics, whereas dual-colour users showed relatively stronger perceptions of certain functional performance characteristics, particularly abrasion resistance and toe-closure comfort.

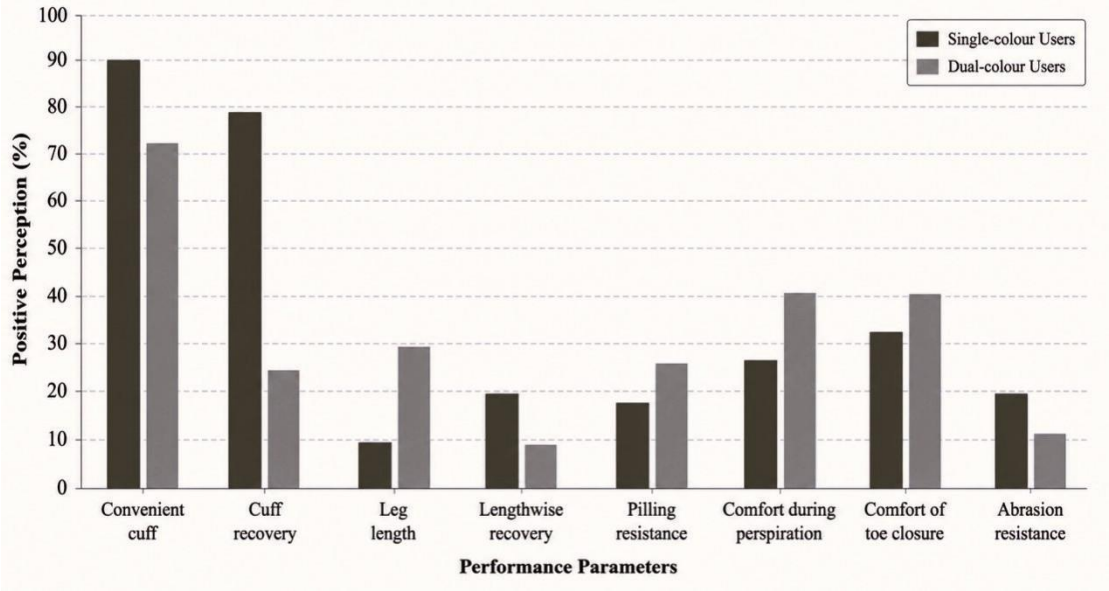


Figure 2. Comparison of performance parameters between single-colour and dual-colour sock user groups

In comparison, the dual-colour sock user group demonstrated a different pattern of performance perceptions, indicating that consumer acceptance cannot be explained solely by sock colour. Rather, the cluster results suggest that different user groups have different combinations of performance priorities. Figure 2 shows the crucial link between identified consumer clusters and their perceived sock performance characteristics. The findings demonstrate that aesthetic durability is an important consideration in school-sock use. Respondents reported difficulties in maintaining the appearance of white socks, particularly in areas exposed to frequent soiling. The black sole of the proposed dual-colour design could help conceal visible staining in high-soiling

areas while retaining a white leg section that matches the school uniform. The importance of physical and aesthetic performance in textile products is consistent with the principles discussed by Hatch (2011) and Saville (2007). Reducing laundering frequency can extend garment life and reduce resource consumption, as laundering significantly contributes to the environmental impact of clothing use (Laitala et al., 2011; McQueen et al., 2017). The critical performance assessment further revealed weaknesses in several performance characteristics of socks available in the market. Convenient cuff performance achieved the highest achievement level at 60.2%, followed by leg length at 50.0% and cuff recovery at 43.0%. Lower achievement levels were observed for lengthwise recovery (27.1%), toe-closure comfort (35.0%), abrasion resistance (38.2%), perspiration comfort (15.0%), and pilling resistance (11.8%). These findings indicate that although the dual-colour concept can address aesthetic deterioration, product development should simultaneously consider mechanical, dimensional and comfort-related properties. The findings therefore suggest that dual-colour socks should not be regarded merely as a change in colour configuration. They should also be considered a product-design alternative that addresses the performance expectations identified through consumer segmentation analysis. This is consistent with the product-development perspective that product design modifications can address identified user requirements (Ulrich & Eppinger, 2016).

The integration of hierarchical cluster analysis with confusion-matrix validation provides stronger support for assessing the adoptability of dual-colour school socks than descriptive statistics alone. The classification accuracy of 72.31%, together with a precision of 68.90%, recall of 76.87%, and specificity of 68.13%, indicates a moderate level of correspondence between the statistically identified consumer clusters and the observed sock-usage categories. The presence of false-positive and false-negative classifications also indicates some overlap in consumer behaviour. The results further indicate that consumer acceptance is associated with practical considerations including appearance retention, comfort, fit, recovery and durability. Therefore, the proposed dual-colour sock has potential as an alternative to the completely white school sock, provided that the identified performance requirements are adequately addressed.

4 CONCLUSION

This study investigated the feasibility of adopting dual-colour socks for school uniforms in Sri Lanka. Statistical analysis of responses from 314 participants demonstrated strong consumer support for a design incorporating a black sole. Cluster analysis identified distinct consumer groups and confirmed that aesthetic durability remains a major concern among users. The confusion matrix validation indicated acceptable clustering performance with an accuracy of 72.31%. The study concludes that dual-colour socks provide a practical and statistically supported solution to the maintenance challenges associated with white school socks. The design improves aesthetic durability, reduces laundering burden and may lower total ownership costs. Educational authorities, manufacturers and standards developers should consider the findings when reviewing future school uniform requirements. Further research should evaluate the physical and functional performance of dual-colour socks through laboratory testing and investigate their long-term economic and environmental benefits compared with conventional white socks.

5 ACKNOWLEDGEMENTS

The authors gratefully acknowledge all respondents who participated in the survey and contributed valuable insights to this study.

6 REFERENCES

Biernacki, P., & Waldorf, D. (1981). Snowball sampling: Problems and techniques of chain referral sampling. *Sociological Methods & Research, 10*(2), 141–163. https://doi.org/10.1177/004912418101000205

Brunsma, D. L. (2006). *School uniforms: A critical review of the literature*. R&L Education.

Bryman, A. (2016). *Social research methods* (5th ed.). Oxford University Press.

Entwistle, J. (2015). *The fashioned body: Fashion, dress and modern social theory* (2nd ed.). Polity Press.

Everitt, B. S., Landau, S., Leese, M., & Stahl, D. (2011). *Cluster analysis* (5th ed.). Wiley.

Forsythe, S., Presley, A. B., & Caton, K. W. (1996). Dimensions of apparel quality influencing consumers' perceptions. *Perceptual and Motor Skills, 83*(1), 299–305. https://doi.org/10.2466/pms.1996.83.1.299

Hair, J. F., Black, W. C., Babin, B. J., & Anderson, R. E. (2019). *Multivariate data analysis* (8th ed.). Cengage Learning.

Hatch, K. L. (2011). *Textile science* (2nd ed.). Fairchild Books.

Kelley, E., Strother, C. M., Blouin, D., & Crouch, C. (1986). Application of benefit segmentation to a generic product study in clothing and textiles. *Home Economics Research Journal, 14*(4), 363–370. https://doi.org/10.1177/1077727X8601400402

Laitala, K., Boks, C., & Klepp, I. G. (2011). Potential for environmental improvements in laundering. *International Journal of Consumer Studies, 35*(2), 254–264. https://doi.org/10.1111/j.1470-6431.2010.00968.x.

Lee, J. M., Koo, Y. S., & Lee, J.-R. (2009). Comparison of actual status and satisfaction of school uniform between middle and high school students. *Fashion & Textile Research Journal, 11*(5), 753–763.

McQueen, R. H., Batcheller, J. C., Moran, L. J., Zhang, H., & Hooper, P. M. (2017). Reducing laundering frequency to prolong the life of denim jeans. *International Journal of Consumer Studies, 41*(1), 36–45. https://doi.org/10.1111/ijcs.12311

Saunders, M., Lewis, P., & Thornhill, A. (2019). *Research methods for business students* (8th ed.). Pearson Education.

Saville, B. P. (2007). *Physical testing of textiles* (2nd ed.). Woodhead Publishing.

Shim, S., & Bickle, M. C. (1994). Benefit segments of the female apparel market: Psychographics, shopping orientations, and demographics. *Clothing and Textiles Research Journal, 12*(2), 1–12. https://doi.org/10.1177/0887302X9401200201.

Solomon, M. R. (2018). *Consumer behaviour: Buying, having, and being* (12th ed.). Pearson Education.

Ulrich, K. T., & Eppinger, S. D. (2016). *Product design and development* (6th ed.). McGraw-Hill Education.

ISSN: 2773-7055
Proceedings of the 5th International Research Conference
Institute of Technology, University of Moratuwa
November 5, 2026

Paper ID: 54

STUDY OF THE STRETCH AND RECOVERY PROPERTIES OF COTTON/SPANDEX SINGLE JERSEY FABRICS MADE WITH FULL PLATING TECHNIQUE

K D S Seneviratne[1*], C N Herath[2]

[1]Division of Textile and Clothing Technology, Institute of Technology, University of Moratuwa, Homagama, Sri Lanka

[2]Department of Textile & Apparel Technology, The Open University of Sri Lanka

*Corresponding author: k.d.s.senevirathne@gmail.com

ABSTRACT: In this research, variations in stretch and recovery properties of cotton/spandex and cotton single jersey fabrics were investigated. These fabrics were knitted at high, medium and low stitch lengths with four different fibre compositions: 100% cotton, 95% cotton/5% spandex, 93% cotton/7% spandex, 88% cotton/12% spandex, and subjected to finishing treatments in accordance with industry practices. It was found that the effect of spandex content in the knitted fabric is greater than that of stitch length of the fabric. Lengthwise elongation percentage increases with increasing stitch length and spandex content. Widthwise elongation percentage increases as stitch length increases. Widthwise elongation percentage decreases as the amount of spandex in the fabric increases. Widthwise recovery percentage slightly increases as the amount of spandex in the fabric increases. Stitch length has no significant effect on fabric recovery.

Keywords: cotton/spandex, single jersey, full plating, stitch length, stretch and recovery

1 INTRODUCTION

Weft-knitted fabrics are widely used in apparel because their looped structure provides softness, flexibility, and inherent stretchability. Although 100% cotton single jersey fabrics can extend through loop deformation and yarn movement, their recovery is limited because cotton is not an elastomeric fibre. Following extension, yarn slippage, loop distortion, and frictional locking at loop contact points may result in permanent deformation, reducing shape retention in body-fitted garments and sportswear. To improve elastic performance, spandex is commonly incorporated into knitted structures. In full plating, cotton and spandex yarns are fed simultaneously into every course, allowing the elastomeric yarn to store elastic energy during extension and generate a retractive force after unloading, thereby improving recovery and dimensional stability.

Previous studies have shown that stitch length and spandex-related parameters significantly influence the dimensional and elastic behaviour of plated knitted fabrics. Eltahan (2016) reported that increasing loop length increased fabric extension, whereas Lycra incorporation enhanced recovery while increasing course density and fabric thickness. Similarly, Senthilkumar et al. (2011) demonstrated that stitch length, spandex linear density, input tension, and loading direction significantly affected the elastic properties of plated cotton knitted fabrics. Abdessalem et al. (2009) further reported that increasing elastane consumption improved recovery and altered the dimensional characteristics of full-plated plain knitted fabrics. However, limited information is available on the combined influence of stitch length and cotton/spandex composition on directional stretch and time-dependent recovery in full-plated cotton/spandex single jersey fabrics produced under industrial processing conditions. Therefore, this study investigates the

effects of three stitch lengths and four cotton/spandex compositions on lengthwise and widthwise elongation and recovery after 30 s and 30 min to provide guidance for designing cotton-rich knitted fabrics with improved stretch, recovery, and dimensional stability.

2 METHODOLOGY

2.1 Materials

Ten sets of single jersey fabrics with full plating (100% cotton, 95% cotton/5% spandex, 93% cotton/7% spandex, and 88% cotton/12% spandex) were knitted on a circular knitting machine at high, medium, and low stitch lengths. Cotton (30 Ne) and spandex filaments of different denier counts were used to produce the cotton/spandex fabrics. Table 1 presents the fibre compositions and yarn characteristics used for the knitted structures. Knitting details are given in Table 2. All fabric samples were knitted in accordance with standard manufacturing practices employed in a textile mill in Sri Lanka.

The selected machine-set stitch lengths for all ten single jersey fabrics are given in Table 3. LSL, MSL, and HSL denote low, medium, and high stitch lengths, respectively. The corresponding LSL, MSL, and HSL values for the four fibre compositions are presented in Table 3. The stitch length values decreased after scouring, bleaching and finishing processes in all the cases. This reduction occurs because the tensions applied to the yarns during knitting are released during washing, drying, and subsequent relaxation. Consequently, the yarns tend to recover their extended length in the finished fabric state.

Table 1. Used Fiber Compositions, Yarn Counts and Loop Lengths of fabric sample

Notation	Fiber Percentage		Yarn count		Loop Length
	Cotton (%)	Spandex (%)	Cotton Yarn (Ne)	Spandex Yarn (Denier)	Cotton Yarn (mm)
C100	100	-	30	-	3.1
C95	95	5	30	30	3.1
C95	95	5	30	30	3.2
C95	95	5	30	30	3.3
C93	93	7	30	40	3.1
C93	93	7	30	40	3.2
C93	93	7	30	40	3.3
C88	88	12	30	70	3.1
C88	88	12	30	70	3.2
C88	88	12	30	70	3.3

Table 2. Specifications of the Machine used

Gauge	Diameter	No. of feeders	No. Of needles	Speed
28	32”	90	2815	30rpm

Table 3. Stitch Length variations after finishing the fabrics

	C100	C95			C93			C88		
	SL1	SL1	SL2	SL3	SL1	SL2	SL3	SL1	SL2	SL3
MC set SL (mm)	3.1	3.1	3.2	3.3	3.1	3.2	3.3	3.1	3.2	3.3
MC off SL (mm)	3.090	3.025	3.313	3.327	3.059	3.245	3.352	3.108	3.148	3.283
Finished fabric SL (mm)	3.056	2.954	3.2	3.214	3.004	3.149	3.253	2.979	3.018	3.147
Notation	L-SL	L-SL	M-SL	H-SL	L-SL	M-SL	H-SL	L-SL	M-SL	H-SL
SL reduction (%)	1.100	2.347	3.411	3.396	1.798	2.958	2.953	4.151	4.130	4.143

Note: MC-machine

The knitted cotton/spandex fabric samples were initially heat-set in a stenter machine at 200 °C. Thereafter, all samples underwent scouring and bleaching in a jet dyeing machine using sodium hydroxide (NaOH) and hydrogen peroxide (H_2O_2) at 95 °C for 45 minutes, followed by neutralization with acetic acid and sodium metabisulphite for 10 minutes each. Finally, the fabrics were hydro-extracted using a slitter machine and finished with a hydrophilic silicone softener, followed by drying in a stenter machine at 130 °C.

2.2 Experimental Procedure

All fabric samples were conditioned prior to testing in accordance with the respective test standards under the standard atmospheric conditions for textile testing; Temperature: 21 ± 2 °C, Relative humidity: 65 ± 2%

Stretch and recovery were measured according to ASTM D4964. A constant-rate-of-extension (CRE) tensile testing machine with Band clamps and a single-needle sewing machine were used for the test. To calculate the recovery percentage two length measurements were taken; one 30 s after removing the specimen from clamps and the other 30 min after removing the specimen from clamps. Recovery percentage was calculated as follows:

$$Recovery(\%) = \frac{Recovered\ length}{Extended\ length} \times 100 \quad (1)$$

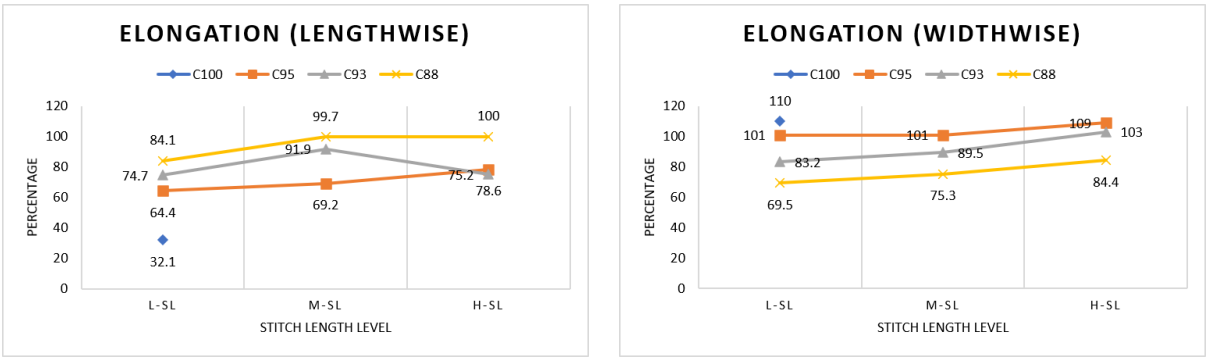
3 RESULTS AND DISCUSSION

The lengthwise and widthwise elongation percentages of the fabric samples are presented in Table 4 and Figures 1(a) and (b).

Table 4. Elongation Percentage

Stitch Length category	**Lengthwise direction (%)**				**Widthwise direction (%)**			
	C100	C95	C93	C88	C100	C95	C93	C88
L-SL	32.1	64.4	74.7	84.1	110	101	83.2	69.5
M-SL	NP	69.2	91.9	99.7	NP	101	89.5	75.3
H-SL	NP	78.6	75.2	100	NP	109	103	84.4

NP-Not Produced



(a) (b)

Figure 1. (a) Elongation percentage Lengthwise direction (b) Elongation percentage Widthwise direction

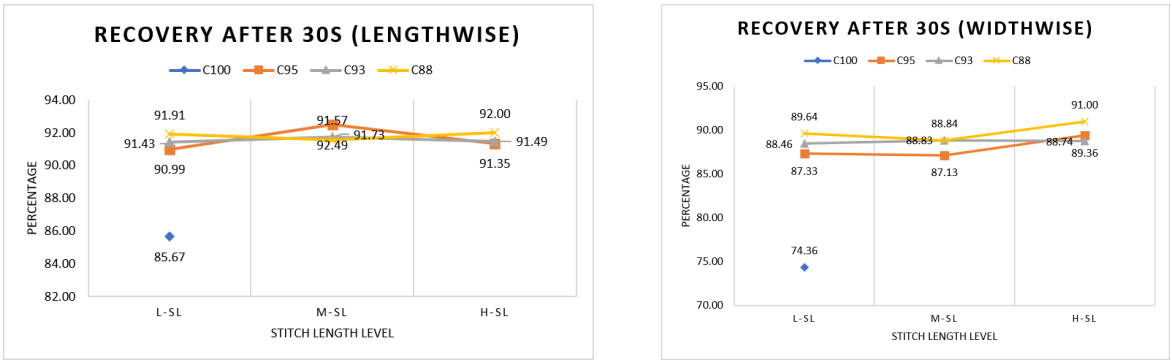
Table 4 and Figures 1(a) and 1(b) show that lengthwise elongation increased with both stitch length and spandex content, whereas widthwise elongation increased with stitch length but decreased as the spandex content increased. Increasing stitch length forms larger loops with lower loop density, allowing greater loop deformation and yarn mobility during tensile loading, thereby enhancing elongation in both directions. The increase in lengthwise elongation with spandex content is attributed to the high extensibility of the elastomeric filament, allowing the fabric to undergo greater tensile deformation. In contrast, increasing the spandex content reduced widthwise elongation because the recovery force of the spandex yarn pulled the loops closer together after relaxation, increasing course density and restricting loop opening during widthwise stretching. The resulting denser fabric structure offered greater resistance to transverse deformation despite its improved elasticity. These observations are consistent with the findings of Senthilkumar et al., who reported similar effects of stitch length and spandex content on the tensile behaviour of plated cotton knitted fabrics. The agreement suggests that loop geometry and the increased fabric compactness caused by the spandex yarn are the main factors affecting fabric elongation.

The lengthwise and widthwise recovery percentages of the fabric samples measured 30 s after unloading are presented in Table 5 and Figures 2(a) and 2(b).

Table 5. Recovery Percentage after 30 s

Stitch Length category	**Lengthwise direction (%)**				**Widthwise direction (%)**			
	C100	C95	C93	C88	C100	C95	C93	C88
L-SL	85.67	90.99	91.43	91.91	74.36	87.33	88.46	89.64
M-SL	NP	92.49	91.73	91.57	NP	87.13	88.83	88.84
H-SL	NP	91.35	91.49	92	NP	89.36	88.74	91

NP-Not Produced



(a) (b)

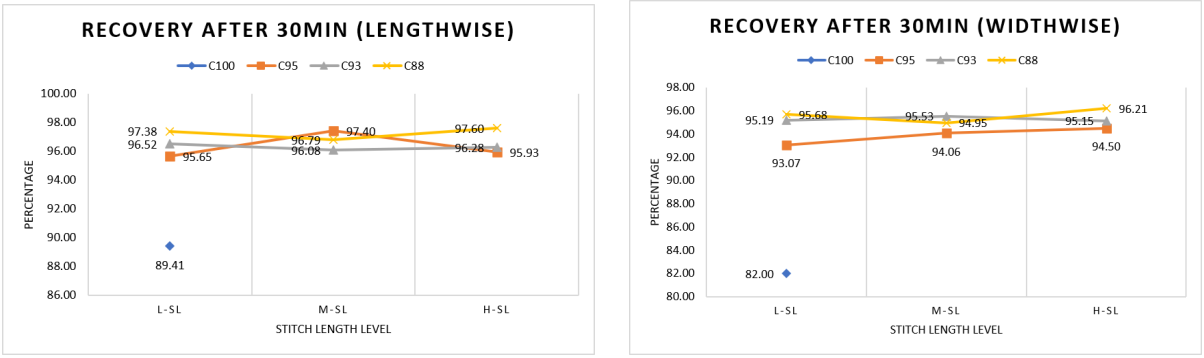
Figure 2. (a) Recovery after 30 s in lengthwise direction (b) Recovery after 30 s in width-wise direction

The lengthwise and widthwise recovery percentages of the fabric samples measured 30 min after unloading are presented in Table 6 and Figures 3(a) and 3(b).

NP-Not Produced

Table 6. Recovery Percentage after 30 minutes

Stitch Length category	Lengthwise direction (%)				Widthwise direction (%)			
	C100	C95	C93	C88	C100	C95	C93	C88
L-SL	89.41	95.65	96.52	97.38	82	93.07	95.19	95.68
M-SL	NP	97.40	96.08	96.79	NP	94.06	95.53	94.95
H-SL	NP	95.93	96.93	97.60	NP	94.50	95.15	96.21



(a) (b)

Figure 3. (a) Recovery after 30 min in lengthwise direction (b) Recovery after 30 min in width-wise direction

Tables 5 and 6 and Figures 2(a), 2(b), 3(a), and 3(b) show that the C100 fabric exhibited the lowest recovery percentages in both the lengthwise and widthwise directions after 30 s and 30 min of relaxation. In the absence of spandex, recovery depends primarily on the elastic bending of cotton yarns and the ability of the knitted loops to regain their original geometry. However, during extension, cotton loops experience yarn slippage, loop distortion, and frictional locking at loop contact points, resulting in greater permanent deformation and consequently lower recovery. The incorporation of spandex improved recovery because the elastomeric yarn stored elastic energy during extension and generated a retractive force after unloading, restoring the loop configuration and reducing residual deformation. The effect of spandex content was more

pronounced after 30 min than after 30 s, particularly in the lengthwise direction. Immediately after unloading, recovery remained incomplete owing to viscoelastic relaxation of the cotton component and friction between yarn segments, which delayed loop recovery. As the recovery period increased, the continued retraction of the spandex yarn further reduced the residual deformation, resulting in higher recovery percentages.

In the widthwise direction, recovery generally increased with increasing spandex content because the retractive force of the spandex yarn effectively restored the course structure by limiting permanent loop opening. In contrast, stitch length had no significant influence on recovery at either recovery time. Although longer stitch lengths increased fabric extensibility, recovery was governed mainly by the elastic retraction of the spandex yarn and frictional resistance between yarns. These findings agree with those reported by Senthilkumar et al., who observed that spandex content had a greater influence on fabric recovery than loop length, particularly in the widthwise direction.

4 CONCLUSION

Lengthwise elongation increased with increasing stitch length and spandex content. Widthwise elongation also increased with stitch length but decreased as the spandex content increased. These findings indicate that stitch length primarily influences fabric extensibility, whereas spandex content governs the directional elongation behaviour of the knitted structure.

The 100% cotton fabric exhibited the lowest recovery in both the lengthwise and width wise directions. Recovery percentage increased slightly with increasing spandex content after 30 min, while stitch length showed no significant effect on fabric recovery. Fabrics containing higher spandex content demonstrated greater recovery over time, highlighting the dominant role of spandex in improving the elastic recovery of single jersey fabrics.

5 REFERENCES

Abdessalem, S. B., Abdelkader, Y. B., Mokhtar, S., & Elmarzougui, S. (2009). Influence of Elastane Consumption on Plated Plain Knitted Fabric Characteristics. Journal of Engineering Fibers and Fabrics, 4(4), 30–35. https://doi.org/10.1177/155892500900400411

Eltahan, E. (2016). Effect of Lycra Percentages and Loop Length on the Physical and Mechanical Properties of Single Jersey Knitted Fabrics. Journal of Composites 2016. http://dx.doi.org/10.1155/2016/3846936

Senthilkumar, M., Anbumani, N. & Araujo, M. (2011). Elastic properties of spandex plated cotton knitted fabric. Journal of the Institution of Engineers (India) India), Part TX: Textile Engineering Division. 92. 9 13. Retrieved from https://www.researchgate.net/publication/290022352_Elastic_properties_of_spandex_plated_cotton_knitted_fabric

Paper ID: 33

IMAGE-BASED TURBIDIMETRIC DETERMINATION OF AVAILABLE SOIL POTASSIUM USING A CAPILLARY-DRIVEN MICROFLUIDIC DEVICE

H M C S Wijerathne[1,2], N D Tissera[3], G Priyadarshana[2], R N Wijesena[3*]

[1]Faculty of Graduate Studies, University of Sri Jayewardenepura, Nugegoda, Sri Lanka
[2]Department of Materials and Mechanical Technology, Faculty of Technology, University of Sri Jayewardenepura, Pitipana, Homagama, Sri Lanka
[3]Division of Textile and Clothing Technology, Institute of Technology, University of Moratuwa, Homagama, Sri Lanka

*Corresponding author: ruchiraw@itum.mrt.ac.lk

ABSTRACT: Rapid and on-site determination of soil potassium is essential for precision nutrient management and sustainable agricultural production. In this study, a capillary-driven microfluidic device was developed for image-based turbidimetric determination of available soil potassium using the sodium tetraphenylborate (NaTPB) precipitation reaction. The analytical conditions were optimised by evaluating the detection wavelength, NaTPB concentration, and reaction time. The optimum conditions were identified as 650 nm, 3% (w/v) NaTPB, and a reaction time of 5 min. Under these conditions, a spectrophotometric calibration curve exhibited good linearity within the concentration range of 0–30 mg/L (R^2 = 0.9913), with limits of detection and quantification of 0.047 mg/L and 0.143 mg/L, respectively. The optimised analytical protocol was successfully integrated into a PMMA-based capillary-driven microfluidic platform. Turbidity generated within the microchannels was quantified through smartphone image acquisition and grayscale analysis using ImageJ software. The microfluidic device demonstrated a strong linear relationship between blank-corrected grayscale intensity and potassium concentration over the range of 0–30 mg/L (R^2 = 0.9829). The developed platform exhibited limits of detection and quantification of 0.09 mg/L and 0.291 mg/L, respectively, demonstrating good analytical sensitivity. The applicability of the developed system was evaluated using soil extracts and spike recovery experiments. The microfluidic device produced potassium concentrations that were in good agreement with those obtained using the spectrophotometric method. Recovery values of 107.4% and 110.8% were obtained for 10 and 20 mg/L potassium spikes, respectively, confirming acceptable analytical accuracy. The proposed microfluidic platform provides a simple, low-cost, and portable approach for rapid soil potassium assessment and demonstrates considerable potential for field-based nutrient monitoring and precision agriculture applications.

Keywords: microfluidic device, turbidimetric analysis, sodium tetraphenylborate, soil nutrient assessment, precision agriculture

1 INTRODUCTION

Potassium (K) is one of the essential macronutrients required for plant growth and plays a vital role in enzyme activation, osmotic regulation, photosynthesis, and crop productivity (Leigh & Jones, 1984; Pettigrew, 2008). Since available potassium levels vary considerably with soil type, cropping history, and fertiliser management practices, periodic soil testing is necessary to optimise fertiliser application and ensure sustainable agricultural production. Conventional laboratory-based methods for potassium determination, such as flame photometry, atomic emission spectroscopy, and inductively coupled plasma techniques, provide accurate results but require expensive instrumentation, skilled personnel, and centralised laboratory facilities, making them unsuitable for rapid field-based analysis (Pereira et al., 2024).

Among the alternative approaches, sodium tetraphenylborate (NaTPB) turbidimetry has attracted considerable attention as a simple, low-cost, and portable method for potassium determination. In this method, potassium ions react with tetraphenylborate ions to form insoluble potassium tetraphenylborate, generating turbidity proportional to the potassium concentration. A limited number of previous studies have demonstrated that NaTPB-based turbidimetric methods provide satisfactory analytical performance. The pH of the reaction medium plays a critical role in the precipitation process. Under acidic conditions, hydrogen tetraphenylborate may form and interfere with potassium precipitation, leading to reduced analytical accuracy (Pereira et al., 2024). Therefore, an alkaline buffer is commonly employed to adjust the reaction medium to pH 9–10, ensuring selective formation of potassium tetraphenylborate and improving method reliability (Pereira et al., 2024). Recent advances in microfluidic technology have enabled the development of portable analytical devices capable of performing chemical analyses using small sample and reagent volumes with reduced cost and analysis time (Mishra et al., 2025). Integrating NaTPB turbidimetry with a capillary-driven microfluidic platform offers significant potential for rapid on-site soil potassium assessment. Therefore, this study aimed to develop and evaluate a microfluidic turbidimetric device for the determination of available potassium in soil using the NaTPB precipitation reaction and image-based detection.

2 METHODOLOGY

2.1 Reagents and materials

All chemicals used in this study, including potassium chloride (KCl), sodium carbonate (Na_2CO_3), sodium bicarbonate ($NaHCO_3$), and sodium tetraphenylborate (NaTPB), were of analytical grade and used without further purification. Spectral measurements were made using an Evolution 201 UV-Visible spectrophotometer (Thermo Scientific), with the samples analysed in quartz cuvettes having a 10 mm optical path length. The microfluidic device used for determining soil K levels was fabricated from poly(methyl methacrylate) (PMMA) using a laser micromachining technique. Potassium standard solutions were prepared from potassium chloride using distilled water. A carbonate–bicarbonate buffer solution (pH 9.5) was prepared using sodium carbonate and sodium bicarbonate. Sodium tetraphenylborate (NaTPB) solutions were prepared in distilled water and used as the precipitating reagent for potassium determination. For the analysis, soil samples were air-dried, sieved, and extracted using Mehlich-3 extractant at a soil-to-extractant ratio of 1:10 (w/v). The mixture was immediately shaken for 5 min and filtered, and the resulting extract was used for potassium analysis.

2.2 Optimisation of reaction conditions

The maximum absorbance wavelength/ analytical wavelength (λ_{max}) was determined using the UV–Visible spectrophotometer by scanning the absorbance spectrum of the potassium–NaTPB reaction product from 300 nm to 800 nm. The effect of NaTPB concentration was investigated by varying the reagent concentration from 1–5% (w/v). Blank-corrected absorbance values were used to identify the optimum reagent concentration. Reaction time optimization was performed by monitoring turbidity development at predetermined time intervals under optimised reagent

conditions. Unless otherwise stated, all subsequent measurements were carried out under the optimised experimental conditions.

2.3 Calibration curve development

Calibration standards ranging from 0–50 mg/L K were prepared and analysed under optimised conditions. The reaction mixture consisted of potassium standard solution, carbonate–bicarbonate buffer, and NaTPB reagent. Calibration curves were constructed by plotting absorbance against potassium concentration.

2.4 Recovery study

The accuracy of the developed method was evaluated using spike recovery experiments. Known concentrations of potassium standard solution were added to selected soil extracts at two concentration levels, 10 and 20 mg/L. The spiked samples were analysed under optimised conditions, and recovery percentages were calculated by comparing the measured and added potassium concentrations.

2.5 Microfluidic device evaluation

The optimised analytical protocol was integrated into a capillary-driven microfluidic device fabricated from poly(methyl methacrylate) (PMMA). Potassium standards and soil extracts were introduced into the device and reacted with the stored reagents. Images of the developed turbidity response were captured under controlled lighting conditions using a smartphone camera. Image analysis was performed using ImageJ software, and the obtained grayscale intensity values were correlated with potassium concentration to construct a microfluidic calibration curve. The performance of the microfluidic device was evaluated by comparing the obtained results with those generated by the spectrophotometric method.
The limit of detection (LOD) and limit of quantification (LOQ) were calculated from the standard deviation of blank measurements and the slope of the calibration curve.

3 RESULTS AND DISCUSSION

3.1 Optimisation of the reaction conditions

The absorbance spectrum of the potassium–sodium tetraphenylborate (K–NaTPB) reaction product was recorded to identify the optimum analytical wavelength. The maximum analytical response was observed at 650 nm and was therefore selected for all subsequent measurements. Selection of the wavelength corresponding to the maximum absorbance improves analytical sensitivity and enhances the reliability of quantitative measurements. The concentration of sodium tetraphenylborate (NaTPB) was optimised by evaluating concentrations ranging from 1–5% (w/v). As shown in Figure 1(a), the absorbance increased with increasing NaTPB concentration up to 4%, indicating enhanced formation of potassium tetraphenylborate precipitates. Although 4% NaTPB produced a slightly higher absorbance than 3%, the increase in analytical response was relatively small compared with the additional reagent required. Therefore, considering the negligible improvement in absorbance and the reduced reagent consumption, 3% (w/v) NaTPB was selected as the optimum concentration for subsequent experiments. A further increase to

5% resulted in a slight decrease in absorbance, indicating that increasing the NaTPB concentration beyond the optimum did not provide an analytical advantage. This is also supported by the literature (Pereira et al., 2024). The effect of reaction time on turbidity development was investigated under the optimised reagent conditions. The absorbance increased rapidly during the initial stages of the reaction and reached a stable value within 5 min, indicating completion of the precipitation reaction. The short reaction time obtained in this study is advantageous for rapid soil nutrient assessment and field-based applications.

3.2 Analytical Performance of the spectroscopy-based Method

Potassium standards in the concentration range of 0 –50 mg/L were prepared and analysed under optimised experimental conditions. Although the calibration study initially included the entire concentration range, only the linear response region (0 –30 mg/L) was selected for quantitative analysis and construction of the final calibration curve, which exhibited a strong linear relationship between potassium concentration and absorbance. A linear relationship was observed between potassium concentration and absorbance (Figure 1(b)), yielding a coefficient of determination (R^2) of 0.9913. The broad calibration range demonstrates the suitability of the developed method for potassium determination in soil extracts covering different fertility levels. The spectrophotometric method exhibited LOD and LOQ values of 0.047 mg/L and 0.143 mg/L, respectively.

3.3 Visual Turbidity Response and Microfluidic Device Performance

The visual turbidity increased progressively with potassium concentration, enabling clear differentiation of the standards within the investigated range (Figure 1(c), (d)). The turbidity resulted from the formation of insoluble potassium tetraphenylborate precipitates, supporting the feasibility of image-based quantification. A strong linear relationship between potassium concentration and blank-corrected grayscale intensity was obtained (Figure 1(c), R^2 = 0.9829), demonstrating the suitability of digital image analysis for quantitative potassium determination. The optimised reaction conditions were successfully integrated into the capillary-driven microfluidic device. Visible turbidity formation within the microchannels was observed following the potassium–NaTPB reaction (Figure 1(e), (f)). The microfluidic image-based method exhibited an LOD of 0.09 mg/L and LOQ of 0.291 mg/L, indicating good analytical sensitivity (ICH, 2005). The obtained LOD was comparable with that reported for a conventional NaTPB-based turbidimetric method for soil potassium determination by Pereira et al. (2024), while the present approach additionally provides microfluidic and image-based analysis. These results demonstrate the potential of the developed platform for rapid and portable potassium determination.

3.4 Soil Sample Validation and Recovery Study

The applicability of the developed method was evaluated using soil extracts and spike recovery experiments (Pereira et al., 2024). The original soil sample contained 2.07 mg/L potassium when determined using the spectrophotometric method, whereas the image-based microfluidic approach yielded a potassium concentration of 2.01 mg/L. To assess method accuracy, potassium

standards were spiked into the soil extract at concentration levels of 10 and 20 mg/L. The recovery values obtained using the spectrophotometric method were 109.5% and 106.2% for the 10 and 20 mg/L spikes, respectively. Corresponding recovery values obtained using the microfluidic image-based method were 107.4% and 110.8%. These results demonstrate acceptable analytical accuracy and confirm the applicability of the developed microfluidic platform for potassium determination in soil samples.

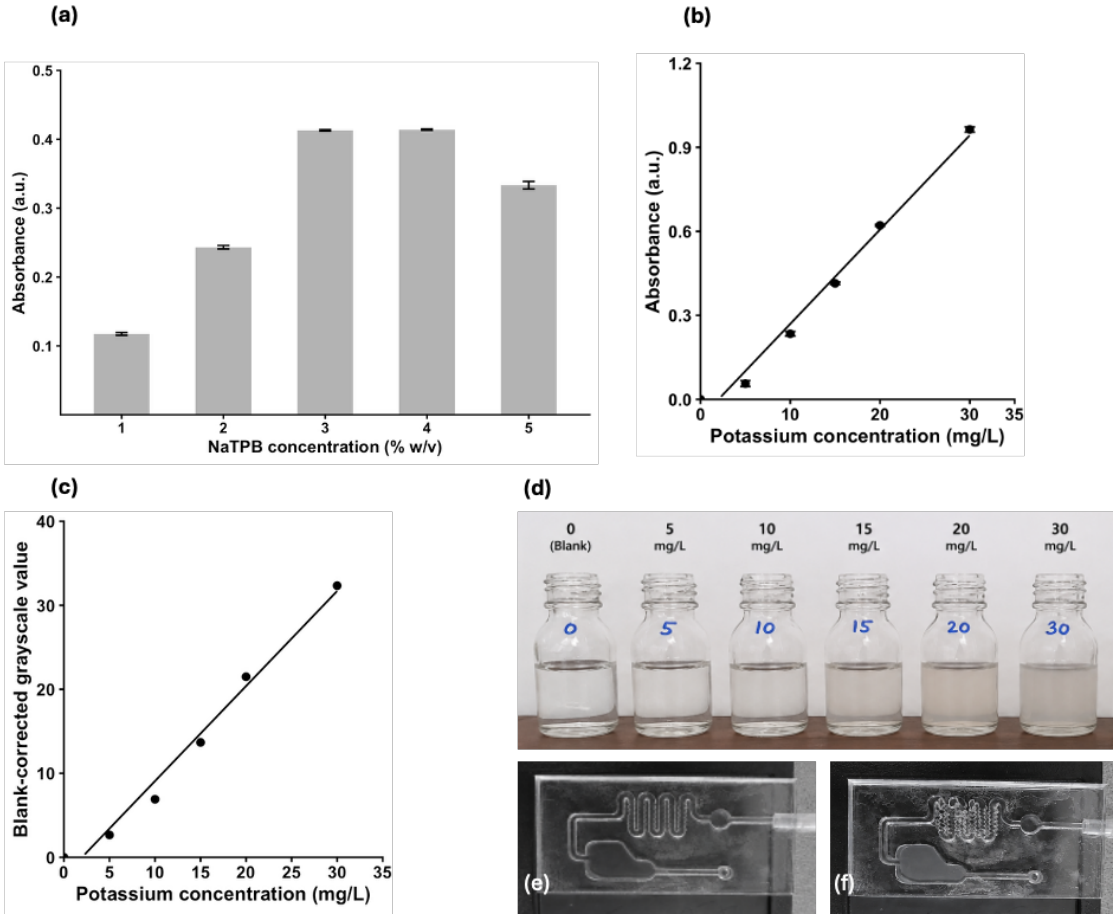


Figure 1. Development and evaluation of the NaTPB-based potassium sensing method and microfluidic platform. (a) Optimisation of sodium tetraphenylborate (NaTPB) concentration for potassium determination using a 20 mg/L potassium standard. (b) Calibration curve obtained under optimised reaction conditions for spectrophotometric determination of potassium in the concentration range of 0–30 mg/L (R^2=0.9913, n=3). (c) Relationship between blank-corrected grayscale intensity and potassium concentration obtained from image analysis (R^2=0.9829, n=3). (d) Visual turbidity response of potassium standards (0–30 mg/L) following reaction with NaTPB. (e) Fabricated PMMA-based capillary-driven microfluidic device before sample introduction (with the blank sample) (f) Turbidity formation within the microfluidic device after the potassium–NaTPB reaction, demonstrating on-chip potassium detection.

4 CONCLUSION

A capillary-driven microfluidic device coupled with NaTPB-based turbidimetric detection was successfully developed for available soil potassium determination. The optimised method exhibited good linearity ($R^2 > 0.98$), low detection limits, and satisfactory recovery values. Image-based grayscale analysis showed strong correlation with potassium concentration and enabled quantitative evaluation of turbidity within the microfluidic platform. The developed system

offers a simple, low-cost, and portable approach for rapid on-site soil potassium assessment and demonstrates potential for precision agriculture applications.

5 ACKNOWLEDGEMENTS

This study was funded by the National Science Foundation, Sri Lanka (NSF Grant No: RG/2023/AG/01).

6 REFERENCE

ICH. (2005, November). ICH Harmonised Tripartite Guideline, validation of analytical procedures: text and methodology Q2(R1). *International conference on harmonisation of technical requirements for registration of pharmaceuticals for human use*.

Leigh, R., & Jones, R. G. W. (1984). A hypothesis relating critical potassium concentrations for growth to the distribution and functions of this ion in the plant cell. *New Phytologist*, *97*(1), 113. https://doi.org/10.1111/j.1469-8137.1984.tb04103.x

Mishra, P., Gupta, P., Khanna, S., Singh, B. P., Mishra, P., Srivastava, S., Yadav, S., Kadian, S., Hwang, S. J., & Agrawal, V. V. (2025). Empowering agriculture: rapid on-site soil nutrient detection with microfluidic colourimetry. *Materials Advances*, *6*(9), 2942–2955. https://doi.org/10.1039/d4ma00971a

Pereira, C. K., Viana, A. B., Macedo, A. A., Pardinho, R. B., Vecchia, P. D., & Dressler, V. L. (2024). Exploring a low-cost turbidimetric sensor for available potassium determination in soil. *Analytical Methods*, *16*(46), 8037–8044. https://doi.org/10.1039/d4ay01190b

Pettigrew, W. T. (2008). Potassium influences on yield and quality production for maize, wheat, soybean and cotton. *Physiologia Plantarum*, *133*(4), 670–681. https://doi.org/10.1111/j.1399-3054.2008.01073.x

ISSN: 2773-7055
Proceedings of the 5th International Research Conference
Institute of Technology, University of Moratuwa
November 5, 2026

Paper ID: 38

FIRE PERFORMANCE OF GLYCEROL-BASED BIO-EPOXY SYSTEMS

G K B M Gannoruwa[1*], L H J Jeewantha[1], Allan Manalo[1], Omar Alajarmeh[2], Stephen Clarke[3], Sean Steed[3]

[1]Center for Future Materials, University of Southern Queensland, Toowoomba QLD 4350, Australia
[2]Department of Civil and Environmental Engineering, United Arab Emirates University, Al Ain P.O. Box 15551, United Arab Emirates
[3]Change Climate Pty Ltd, Adelaide, SA 5250, Australia

*Corresponding author: Gannoru.Gannoruwa@unisq.edu.au

ABSTRACT: Bio-based epoxy resins are emerging as sustainable alternatives to conventional petroleum-derived epoxy systems for advanced composite manufacturing. Among these, glycerol-based bio-epoxy (BE1) resin has demonstrated promising potential as a composite matrix owing to its favorable physical, mechanical, thermal, and durability properties. However, as a novel resin system, its fire performance remains largely unexplored and requires comprehensive evaluation before it can be adopted in widespread structural application. In this study, the fire performance of a glycerol triglycidyl ether-based bio-epoxy resin cured with an isophorone diamine hardener was systematically investigated using cone calorimetry and UL 94 flammability testing. The linear burning rate of the bio-epoxy resin was determined to be 31 mm/min from the horizontal burning test. Cone calorimetry results indicated an effective heat of combustion of 19 MJ/kg, a peak heat release rate of 2503 kW/m^2 and a total heat release of 78 MJ/m^2. These values are comparable to those reported for conventional diglycidyl ether of bisphenol A (DGEBA)-based epoxy systems, indicating similar fire performance. Accordingly, BE1 resins can be considered viable sustainable alternatives to DGEBA epoxy resin systems.

Keywords: fire retardancy, flammability, bio-epoxy, cone calorimetry

1 INTRODUCTION

Epoxy resins are extensively used in high performance engineering applications, including construction, aerospace, marine, mining and renewable energy, owing to their excellent mechanical properties, chemical resistance and lightweight attributes (Jian et al., 2019; Luo et al., 2020). However, the growing emphasis on environmental sustainability and the need to reduce dependence on fossil-derived materials have accelerated the development of bio-based epoxy resins as viable alternatives to conventional petroleum-based systems (Wan et al., 2016). As the adoption of bio-based epoxy resins continues to increase, it is essential to ensure that their fire performance meets the stringent safety requirements of these industries. Therefore, comprehensive evaluation of the fire behavior and flame-retardant characteristics of bio-based epoxy systems is critical to assess their suitability for high-performance structural applications and to facilitate their broader implementation in sectors where fire safety is a primary design consideration. Due to their relatively low limiting oxygen index (LOI), epoxy resins exhibit poor inherent flame resistance (Sun et al., 2023). Upon combustion, they generate significant heat release and dense smoke, both of which can be characterized using oxygen consumption calorimetry. In addition, the formation of burning molten droplets during combustion can promote rapid fire spread by igniting nearby combustible materials. This fire propagation behavior can be evaluated by determining the material's burning rate using standardized flammability testing methods.

The BE1 resin has emerged as a promising novel bio-based epoxy system for composite applications (Olatunbosun et al., 2025). The suitability of BE1 resin cured with isophorone diamine (IPDA) for composite manufacturing was demonstrated using sunn hemp fibers as reinforcement. The fabricated composites achieved tensile, flexural and interlaminar shear strengths of 70.4, 89.5 and 8.6 MPa respectively, which were attributed to effective fiber-matrix interfacial adhesion (Olatunbosun et al., 2025). The durability of the BE1 resin system was assessed following 3000 hours of hygrothermal exposure at 60°C and 98% relative humidity. The study reported a tensile strength of 52.3 MPa, corresponding to 90% property retention, a tensile modulus of 2.9 GPa with 86% retention and a glass transition temperature of 44.4°C with 105% retention (Iftikhar et al., 2025). These findings demonstrate the excellent hygrothermal durability of BE1 resin system.

These findings demonstrate the potential of the BE1-epoxy system for sustainable composite manufacturing. However, despite its promising mechanical performance and durability, the fire performance of this resin system has not yet been investigated. To address this knowledge gap, the present study evaluates the fire performance of the BE1 epoxy system to further establish its suitability for composite applications. The fire performance of the bio-epoxy resin system was evaluated by assessing key fire and flammability characteristics, including heat release rate (HRR), effective heat of combustion (EHC), specific extinction area (SEA) and specific mass loss rate (SMLR) as per ASTM E1354 standard and linear burning rate as per ASTM D635 standard. Collectively, these parameters provide a comprehensive understanding of the material's combustion behavior, thermal degradation, heat release, mass loss and smoke generation characteristics, which are critical for assessing its fire performance and suitability for engineering applications.

2 METHODOLOGY

2.1 Materials

Glycerol triglycidyl ether, a highly bio-based epoxy resin containing 98–99% renewable content, was used as the resin and combined with an isophorone diamine hardener at a mix ratio of 77:23 by weight according to the manufacturer's technical data sheet. The bio-epoxy and hardener supplied by Change Climate Pty Ltd, Adelaide, SA, Australia were used as received throughout the study.

Specimen Preparation

Neat epoxy specimens were prepared in the form of 3 mm thick flat sheets with dimensions of 300 mm by 300 mm. During sample preparation, the required quantities of epoxy and hardener were measured and blended. The mixture was manually stirred for 5 minutes to ensure a homogeneous blend and subsequently allowed to stand for 15 minutes at 23 °C to facilitate the release of entrapped air. The degassed resin system was subsequently poured into a 300 mm × 300 mm × 3 mm mold and cured at 23 °C for 7 days in accordance with the manufacturer's recommended curing cycle. The fabricated sheets, with calculated degree of cure exceeding 95% were subsequently water-jet cut into specimens of the required dimensions in accordance with the relevant testing standards.

Cone Calorimeter Test

The cone calorimeter test was conducted in accordance with ASTM E1354-25, the standard test method for heat and visible smoke release rates for materials and products using an oxygen consumption calorimeter. Square-shaped specimens with 100 mm × 100 mm and 3 mm thickness were used. Two replicate specimens were tested. Accordingly, the specimens had a nominal exposed surface area of 0.01 m^2, while the effective exposed surface area was 0.00884 m^2, calculated based on the configuration of the sample holder. The test environment was carefully controlled, maintaining a relative humidity of 50% and a temperature of $23 \pm 2°C$, to ensure consistency and accuracy across all tests. A heat flux rate of 50 kW/m^2 was applied during the test, a commonly used irradiance level representing severe fire exposure conditions in material fire performance studies.

UL 94 Chamber Test

The UL 94 chamber was used to determine the horizontal burning rate in accordance with ASTM D635-22, standard test method for rate of burning or extent and time of burning of plastics in a horizontal position. Rectangular-shaped specimens with 125 mm × 13 mm × 3 mm dimensions were used for linear burning rate determination, with five replicate test specimens. A 25 mm high flame was applied to the free end of the specimen at a 45° angle, using the laboratory gas burner as the ignition source. An important part of the test setup is the placement of a dry cotton indicator pad (approximately 50×50 mm^2) directly beneath the ignition point. This cotton serves two purposes:

- Detect Dripping of Flaming Particles: If burning drops from the specimen and ignites the cotton, it indicates ignition of flaming or burning drips due to dripping combustion.
- Enhance Safety Evaluation: Ignition of cotton signifies that the material not only burns but also produces flaming debris capable of spreading fire to surrounding materials in practical applications.

3 RESULTS AND DISCUSSION

Representative images of the specimen at different stages during the cone calorimeter test are presented in Figure 1.



(a) (b) (c)

Figure 1. Cone calorimeter test for bio-epoxy (a) Original specimen, (b) During burning, (c) Post burning

HRR is one of the most critical parameters for assessing a material's contribution to fire intensity. The HRR vs time curve presented in Figure 2 exhibits a typical three-stage combustion profile, comprising ignition and initial growth, rapid flame propagation and a final decay phase.

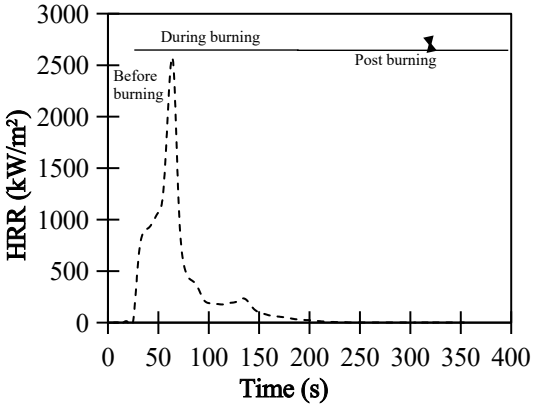


Figure 2. Heat release rate vs time

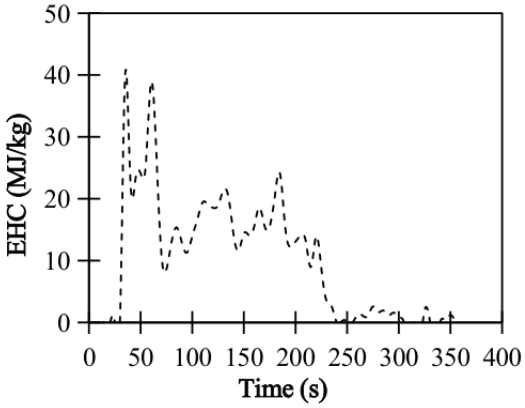


Figure 3. Effective heat of combustion vs time

The material ignited at approximately 25 s, after which the HRR increased progressively. Thereafter, a sharp increase in HRR was observed, reaching a peak value of 2503.83 kW/m^2 at 65 s, representing the rapid combustion and heat release. This pronounced rise suggests intense combustion associated with thermal degradation and pyrolysis of the polymer matrix. The high peak HRR indicates that, once ignited, the material releases a substantial amount of energy, highlighting a substantial heat-release intensity during the fully developed burning stage. Subsequently, the HRR gradually decreased, reflecting the depletion of combustible material and the transition toward flame decay and stabilization. Visual observations confirmed that no protective char layer formed and that the exposed combustible material remained essentially unchanged as burning progressed. The peak HRR of conventional diglycidyl ether of bisphenol A (DGEBA) epoxy resins cured with different hardeners has been reported to range from 1140 to 2590 kW/m^2 (Jian et al., 2019; Luo et al., 2020; Sun et al., 2023). The BE1 epoxy system investigated in the present study exhibited a peak HRR within this range, indicating comparable peak HRR to that of conventional DGEBA epoxy systems.

The EHC, Figure 3 reflects the energy content per unit mass of volatile gases. The EHC remained very low during the initial 30 s of combustion, indicating limited release of combustible gases during this period. Between 30 and 65 s, corresponding to the main combustion phase, the EHC increased substantially, reaching values in the range of 28-40 MJ/kg. The SEA is a measure of the smoke-producing propensity of the material per unit mass of material consumed, was

evaluated to assess the smoke generation characteristics of the bio-epoxy resin system. Smoke is a major contributor to fire-related fatalities due to reduced visibility and exposure to toxic combustion products. The maximum SEA value of 4082.38 m^2/kg was recorded at 315 s, indicating a high smoke-producing propensity per unit mass of material consumed during the later stages of combustion.

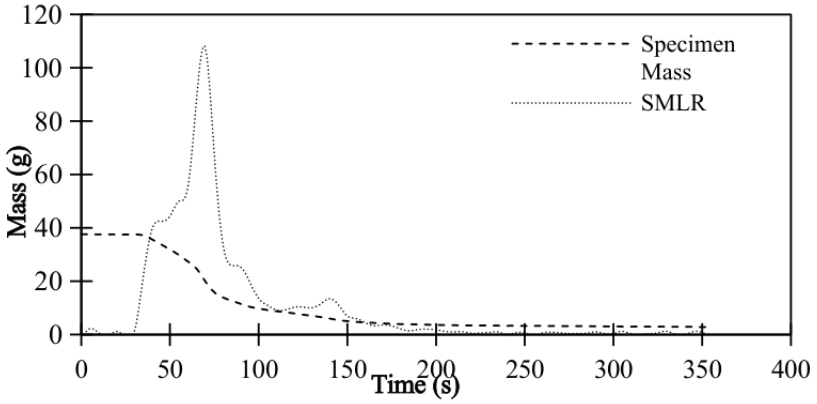


Figure 4. Specimen mass loss and specific mass loss rate vs time

A rapid decrease in specimen mass commenced at approximately 40 s and continued until around 75 s, after which the rate of mass loss gradually diminished and approached a plateau, indicating a depletion of combustible material (Dao et al., 2013). The SMLR reached its peak at approximately 70 s, corresponding to the maximum rate of thermal degradation and coinciding with the period of rapid mass loss. Subsequent fluctuations in the SMLR may be attributed to the continued decomposition of the residual char and thermally stable fractions of the polymer. The total heat release of DGEBA resin systems has been reported to range from 65 to 125 MJ/m^2 (Jian et al., 2019; Luo et al., 2020; Sun et al., 2023). The BE1 epoxy system investigated in the present study exhibited a THR of 78 MJ/m^2 as indicated in Table 1 which falls within the reported range for conventional epoxy systems.

Table 1. Cone calorimeter test results

Mass (g)	**Thickness** (mm)	**Time to ignition** (s)	**Heat release rate (kW/m^2)**				**Total heat released** (MJ/m^2)	**Mass remaining** (g)	**Mass loss rate** Average (g/(s m^2))	**Effective heat of combustion** Average (MJ/kg)
			Max	Average						
				60 s	180 s	300 s				
37.63	3.07	32	2503	1031	416	250	78	2.82	33	19

The horizontal burning behavior of the BE1 resin is presented in Figure 5.

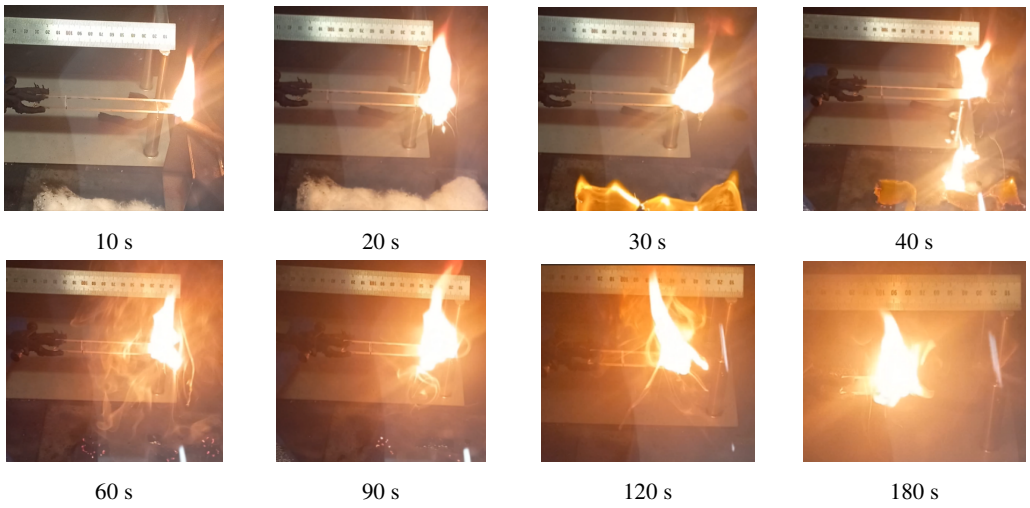


Figure 5. UL-94 horizontal burning test stages

During the horizontal burning test, the specimen ignited approximately at 10 s of flame exposure and continued to burn until the flame self-extinguished. At approximately 22 s, the cotton indicator positioned beneath the specimen ignited, confirming the occurrence of flaming molten drips from the burning sample. The measured linear burning rate was 31 mm/min. The observations indicate that the bio-epoxy resin readily sustains combustion and generates flaming drips under the applied test conditions.

4 CONCLUSION

This study evaluated the fire performance of a BE1 system using cone calorimeter and UL 94 flammability tests. The BE1 exhibited a peak heat release rate (PHRR) of 2503 kW/m^2 and a total heat release (THR) of 78 MJ/m^2, both of which fall within the range reported for conventional DGEBA epoxy resin systems. These findings demonstrate that BE1 epoxy provides fire performance comparable to that reported for conventional DGEBA epoxy system while offering the advantages of a renewable feedstock, highlighting its potential as a sustainable alternative.

5 ACKNOWLEDGEMENTS

The authors gratefully acknowledge the Centre for Future Materials, University of Southern Queensland, Australia, for the support provided during this study.

6 REFERENCES

Dao, D. Q., Luche, J., Richard, F., Rogaume, T., Bourhy-Weber, C., & Ruban, S. (2013). Determination of characteristic parameters for the thermal decomposition of epoxy resin/carbon fibre composites in cone calorimeter. *International journal of hydrogen energy*, *38*(19), 8167-8178.

Iftikhar, A., Manalo, A., Senselova, Z., Ferdous, W., Peerzada, M., Seligmann, H., Nguyen, K., & Benmokrane, B. (2025). Effects of resin types on the durability of single yarn polymer composites exposed to hygrothermal environment. *Available at SSRN 5291216*.

Jian, R.-K., Ai, Y.-F., Xia, L., Zhang, Z.-P., & Wang, D.-Y. (2019). Organophosphorus heteroaromatic compound towards mechanically reinforced and low-flammability epoxy resin. *Composites Part B: Engineering*, *168*, 458-466.

Luo, H., Rao, W., Zhao, P., Wang, L., Liu, Y., & Yu, C. (2020). An efficient organic/inorganic phosphorus–nitrogen–silicon flame retardant towards low-flammability epoxy resin. *Polymer Degradation and Stability*, *178*, 109195.

Olatunbosun, B., Manalo, A., Aravinthan, T., Chen, G., & Kiriella, S. (2025). Modelling of manufacturing parameters and characterisation on the mechanical properties of sunn hemp (Crotalaria juncea L.) bio-composites with different fibre forms. *Construction and Building Materials*, *489*, 142349.

Sun, S., Yu, Q., Yu, B., & Zhou, F. (2023). New progress in the application of flame-retardant modified epoxy resins and fire-retardant coatings. *Coatings*, *13*(10), 1663.

Wan, J., Gan, B., Li, C., Molina-Aldareguia, J., Kalali, E. N., Wang, X., & Wang, D.-Y. (2016). A sustainable, eugenol-derived epoxy resin with high biobased content, modulus, hardness and low flammability: Synthesis, curing kinetics and structure–property relationship. *Chemical Engineering Journal*, *284*, 1080-1093.

ISSN: 2773-7055
Proceedings of the 5th International Research Conference
Institute of Technology, University of Moratuwa
November 5, 2026

Paper ID: 39

DEVELOPING A SUSTAINABLE BLACK PRINT PIGMENT FROM COCONUT-COIR EXTRACT

M W M D Somarathna[1], K D S Senevirathne[1*], H A I Udeshika[1], D K A H J B Welikala[1], W P M S S Wijesooriya[1], H A S Wijewardhana[1], R N Wijesena[1]

[1]Division of Textile and Clothing Technology, Institute of Technology, University of Moratuwa, Homagama, Sri Lanka

*Corresponding author: k.d.s.senevirathne@gmail.com

ABSTRACT: This study investigated the development of a sustainable black print pigment for textile applications using tannins extracted from coconut coir and iron (Fe) ions. Coconut coir, a renewable waste product, was utilized as the primary source of tannins. The tannin extraction trials identified the following conditions as suitable for extracting tannins from coconut coir: an alkaline solution of NaOH at pH 12.24, a solid-to-solvent ratio of 1:16.66, and an extraction temperature of 78 °C. The extracted tannins were reacted with ferrous sulfate ($FeSO_4$) to form a black precipitate (ferric tannate). Experimental results indicated that direct addition of $FeSO_4$ crystals to the tannin extract was more efficient than using a $FeSO_4$ aqueous solution giving a more compact precipitate. A working dosage of 0.76 g $FeSO_4$ crystals per 50 mL tannin extract was selected from the trials to produce the black precipitate. The resulting black precipitate was centrifuged at 1200 rpm for 40 minutes, with the centrifugation conditions optimized according to the laboratory centrifuge model used, and subsequently oven-dried. The dried pigment was incorporated into a screen-printing paste and applied to cotton fabric with a binder. Wash fastness tests yielded gray scale values of 4, 3/4, and 3 for successive washes, indicating moderate durability. FTIR results showed spectral features consistent with tannic-acid-derived iron coordination; however, the measurements did not independently establish the Fe oxidation state. The findings demonstrate the feasibility of converting coconut-coir tannins into a black textile-printing pigment while highlighting the need for further improvement in wash fastness and chemical characterization.

Keywords: coconut coir, sustainable pigment, tannin extraction, iron ions, screen printing

1 INTRODUCTION

Pigments are essential in textile coloration, printing inks, and various industries. However, conventional black pigments made from carbon black, metal oxides, and synthetic chemicals rely on non-renewable resources and energy-intensive processes, which may cause environmental pollution and health risks. Recent research has increasingly focused on sustainable pigments from renewable natural resources (Basri, 2023), with tannin-based colorants gaining interest for their natural abundance, biodegradability (Basri, 2023) and ability to form stable-colored complexes with metal ions (Fragra-Corral M, 2020).

Tannins are naturally occurring polyphenolic compounds present in a wide range of plant materials and have historically been used in dyeing, leather tanning, and ink production (Fragra-Corral M, 2020). Previous studies have demonstrated that tannin extracts can produce dark shades when combined with iron salts, while their application as natural colorants has been reported in textile dyeing and traditional fabric coloration processes (Basri, 2023). Furthermore, advances in extraction technologies (Fragra-Corral M, 2020) have enabled the efficient recovery of tannins from agricultural and forestry residues, creating opportunities for waste valorization and sustainable material development.

Coconut coir is a lignocellulose by-product generated in large quantities by the coconut-processing industry, particularly in tropical regions such as Sri Lanka (Sirisangawansam R, 2023). Previous work has demonstrated the presence of appreciable amounts of extractable tannins in coconut coir and has investigated their extraction, characterization (Sirisangawansam R, 2023), and natural dyeing applications (Sari, 2023). The formation of dark-colored complexes between tannins and iron ions has been reported in literature (Hemingway, 1960) and forms the basis of several traditional dyeing (Basri, 2023) and ink-making processes (Wilson, 2007). However, there is a lack of research focused on developing a sustainable black pigment production route using coconut coir tannins and evaluating its suitability as a printing pigment for textile applications.

Therefore, this research aimed to produce a sustainable black print pigment using iron ions and tannins extracted from coconut coir. The objectives included investigating literature on tannin extraction from plant sources, developing a black pigment through characterized laboratory tests, checking its applicability in screen printing on cotton fabrics, and evaluating its wash fastness.

2 METHODOLOGY

2.1 Optimization of Tannin Extraction

Coconut coir was collected and shredded manually to increase surface area for efficient extraction. Experiments were conducted by solid–liquid extraction using an alkaline solution prepared with NaOH and water (Fragra-Corral M, 2020). NaOH alkaline solution was selected based on research paper (Basri, 2023). Based on literature (Sirisangawansam R, 2023), for the initial trial, the optimum conditions were established: pH 12, a 1:30 solid-to-solvent ratio, and a temperature of 78 °C. The extraction process was conducted for 2 hours. After extraction, the tannin solution was purified by filtration to remove insoluble coir components. The extraction apparatus is shown in Figure 1.

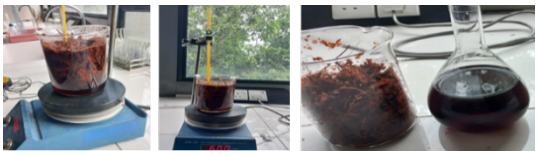


Figure 1. Extraction of tannin using coconut coir and NaOH alkali solution

2.2 Pigment Development and Characterization

Ferrous sulfate ($FeSO_4$) was selected as the iron salt for pigment development due to its effectiveness according to the literature (Hemingway, 1960) and local availability. The reaction involved tannins and Fe^{2+} to form ferric tannate, a black precipitate. The experiments compared different $FeSO_4$ concentrations and thermal conditions, followed by refinement of the tannin concentration and $FeSO_4$ dosage, reaction time and pH. Experiment 1 was conducted by adding 25 mL $FeSO_4$ solutions to 25 mL of extracted tannins as three separate samples as explained in Table 1.

Table 1. Experimental conditions and observed outcomes for Samples A–C in Experiment 1.

Sample	Condition of 25 mL $FeSO_4$ used	Tannin extract volume	Observed outcome
A	0.5 M aqueous $FeSO_4$; room temperature	25 mL	Dark-green supernatant, attributed to residual Fe^{2+} after reaction with tannin.
B	0.3 M aqueous $FeSO_4$; room temperature	25 mL	Dark precipitate with a lighter-green supernatant than Sample A; precipitate was separated by decanting.
C	0.3 M aqueous $FeSO_4$; heated to approximately 65 °C, then cooled to room temperature	25 mL	Red-brown residue after evaporation, attributed in the original observation to formation of Fe_2O_3 rather than the desired black precipitate.

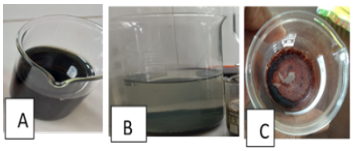


Figure 2. Observed Outcomes of sample A, B, C at the end of Experiment 1 as mentioned in Table 1; Label A: Sample A with Green Supernatant due to residue Fe^{2+}, Label B: After decanting the darker precipitate formed in Sample B, Label C: Red-brown residue formed in Sample C due to decomposition of residue Fe^{2+} into Fe_2O_3 during evaporation.

Experiment 1 showed that 0.5 M $FeSO_4$ was less suitable because residual green coloration remained after the reaction. Therefore, the $FeSO_4$ concentration was progressively reduced to 0.3 M and then 0.2 M, with 0.2 M (0.76 g $FeSO_4$ per 50 mL tannin extract) producing a more efficient reaction.

Experiment 1 also indicated that increasing the tannin concentration was necessary. Accordingly, in Experiment 3, the coconut coir mass was doubled for 500 mL of alkaline solution and the pH was increased to 12.24 using 0.35 g NaOH, resulting in a more concentrated tannin extract.

In Experiment 2, $FeSO_4$ crystals were added directly to the extracted tannin rather than as an aqueous solution. A total of 1.139 g $FeSO_4$ crystals, equivalent to the $FeSO_4$ content of 25 mL of 0.3 M $FeSO_4$ solution, was added to 75 mL of tannin extract, producing a more tightly packed precipitate.

Based on the experimental observations, 0.76 g $FeSO_4$ per 50 mL of tannin extract obtained under the selected conditions of Experiment 3 was used for subsequent pigment preparation. Fungal growth was observed in extracts and reaction mixtures exposed to air for prolonged periods; therefore, prompt processing or the use of suitable preservatives was recommended, with open-air exposure limited to less than 1.5 days.

The resulting black precipitate was separated by repeated decanting and centrifugation using a GEMMYCO PLC-025 laboratory centrifuge equipped with a T-5004 bucket (four 50 mL tubes; maximum speed 5000 rpm). Centrifugation at 1200 rpm for 40 min produced a denser and more compact precipitate, facilitating separation from the liquid phase. This condition was selected based on observational assessment rather than statistical optimization, as replicate experiments and statistical analysis were not performed. The decanting and centrifugation steps were repeated until no further visible precipitate was recovered.



Figure 3. Black precipitate separated by centrifugation of Tannin-FeSO4 solution mixtures.

The collected precipitate was then dried, with oven drying at 100 °C for 2 hours proving more effective than open-air drying in preventing fungal contamination and producing a finer powder as shown in Figure 4.

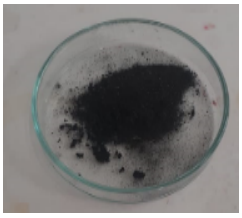


Figure 4. Black Pigment Powder collected by oven drying the black precipitate separated using centrifugation.

FTIR analysis was used to compare the synthesized pigment with a published reference spectrum of tannic acid and its Fe(III) complex (Rathnayake, 2022) to confirm ferric tannate formation by identifying characteristic functional groups responsible for its color.

2.3 Performance Evaluation

2.3.1 The dispersion and printability of the pigment on cotton fabrics

The black pigment's printability and dispersion were assessed by formulating it into a screen-printing ink for cotton fabric, with the recipe optimized through several trials. The first trial contained 10% binder, 5% thickener, 0.25% liquid ammonia, and 3% pigment, with water as the balance; insufficient pigment grinding and excessive thickener produced a poor paste and an ash-toned print. In Trial 2, a 2.5 g formulation contained 0.3 g thickener, 1–1.5 g binder, 0.5 g pigment, a few drops of NH_3, and water to the final mass. Since the precipitate had been thoroughly ground into a fine powder, the mixture formed a creamy paste and gave a black tone compared to trial 1. In Trial 3, a 3.5 g formulation contained 0.7 g pigment (20%), 0.632 g binder (18%), 0.3 g thickener, a few drops of NH_3, and water to balance the formulation. The Trial 3 formulation produced a creamier paste and greater apparent print color depth than Trial 2 during screen printing.



Figure 5. Printed sample in trial 3 with increased color depth compared to sample printed in trial 2

2.3.2 Wash-fastness evaluation

Wash fastness of the printed fabric was assessed following a procedure adapted from the ISO 105 C06 test method (textile learner, n.d.). Fabric specimens (4 cm × 10 cm) were sewn to multifibre fabric, immersed in a 4 g/L detergent solution for 30 minutes, rinsed with hot and cold water, and then air-dried at temperatures not exceeding 60 °C. Color change and staining were evaluated using grey scales after multiple wash cycles.

3 RESULTS AND DISCUSSION

3.1 Tannin Extraction and Pigment Formation

The experiments showed that the combination of tannin concentration and $FeSO_4$ dosage influenced the observed precipitate formation. The 0.5 M $FeSO_4$ condition produced residual green coloration, indicating that the iron salt was not fully consumed under that condition. Reducing the $FeSO_4$ concentration and increasing the tannin concentration produced a darker and more compact precipitate. Direct addition of $FeSO_4$ crystals was also visually more effective than addition of an aqueous $FeSO_4$ solution, producing a tighter precipitate and clearer supernatant. The working conditions selected from the trials were a coir-to-liquid ratio of 1:16.66, alkaline extraction at pH 12.24 and 78 °C for 2 h, followed by addition of 0.76 g $FeSO_4$ crystals per 50 mL tannin extract. After allowing approximately 24 h for precipitate formation, centrifugation at 1200 rpm for 40 min in the used model of lab centrifuge followed by decanting and then oven-drying at 100 °C for 2 h produced the final black pigment powder. These conditions should be regarded as trial-selected working conditions rather than statistically optimized process parameters, because the study did not include replicate trials or formal statistical optimization.

3.2 Performance Evaluation: Printability and Wash Fastness

Initial trials produced poor paste quality and ash-colored prints because of coarse pigment and excess thickener. The optimized formulation—20% pigment, 18% binder, 0.3% thickener, and ammonia—yielded a creamy paste and a black color screen print with improved color depth on cotton, confirming the pigment's potential for screen printing when appropriate grinding and formulation ratios are maintained. Wash-fastness testing conducted according to a method adapted from ISO 105-C06 method produced grey-scale ratings of 4, 3/4, and 3 after the first, second, and third washes, respectively. The progressive decline indicates moderate durability and highlights the need for further optimization of the binder system, post-treatment, or pigment structure to improve pigment–fiber bonding and meet industrial requirements.

3.3 Pigment Characterization

FTIR analysis confirmed the formation of the iron-tannate complex by identifying key functional groups consistent with reference spectra given in (Figure 6).

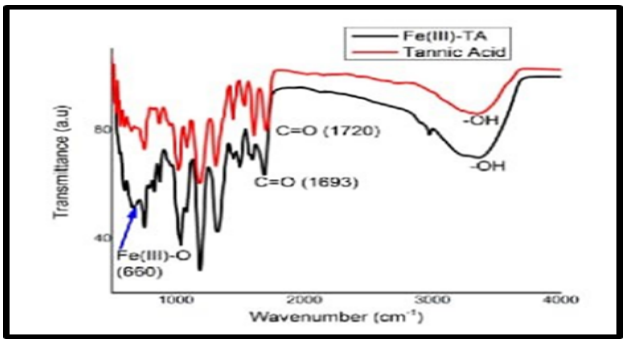


Figure 6. Reference FTIR spectrum of tannic acid and its Fe(III) complex, showing the reported carbonyl shift and Fe–O region (Source: https://doi.org/10.3390/suschem3020013)

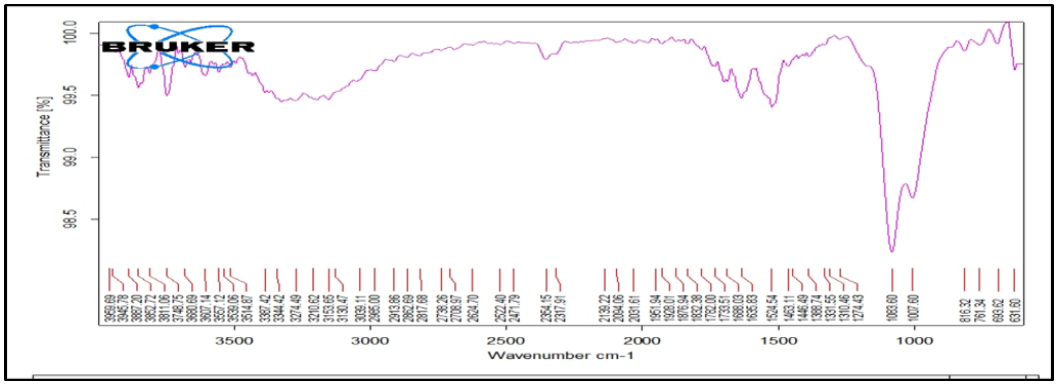


Figure 7. FTIR absorption spectra of synthesized black precipitate in this study

The FTIR spectrum of the synthesized black precipitate showed several absorption bands corresponding to functional groups present in tannic acid and its interaction with Fe(III). The synthesized black pigment showed FTIR bands in regions associated with hydroxyl, carbonyl, and C–O-containing groups. The reference Fe(III)-tannate spectrum reported by (Rathnayake, 2022) also contains features in these regions and a low-wavenumber band near 660 cm^{-1} attributed to Fe–O stretching. The carbonyl band in the reference material shifts from approximately 1720 to 1693 cm^{-1} after Fe(III) coordination, indicating a change in the carbonyl environment.

Table 2. FTIR regions used to interpret the synthesized pigment in comparison with the reference spectrum

Region (cm^{-1})	Assignment	Reference evidence	Interpretation in this study
3300–3500	O–H stretching	Broad hydroxyl band reported for tannic-acid-derived structures.	Consistent with phenolic hydroxyl groups in the extracted tannin material.
~1635	C=O stretching	Carbonyl region present in tannic-acid/Fe(III) reference spectra.	Consistent with carbonyl-containing structures; the assignment is supportive, not unique.
1000–1100	C–O stretching	Bands associated with oxygen-containing groups.	Consistent with phenolic/alcohol/ether C–O groups that may participate in coordination.
~660	Fe–O stretching	Reference Fe(III)-tannate band near 660 cm^{-1}.	A similar low-wavenumber feature supports iron–oxygen interaction.

Overall, the synthesized pigment exhibited a spectral pattern similar to the reference in the hydroxyl, carbonyl, C–O, and low-wavenumber regions. These similarities support the presence of an iron–tannate-type interaction in the product. However, FTIR alone cannot establish whether the iron in the synthesized material is exclusively Fe(III) or determine the exact coordination structure. Independent oxidation-state or elemental characterization would therefore be required to confirm formation of a specific ferric tannate phase.

4 CONCLUSION

A black textile-printing pigment was developed from coconut-coir tannins and $FeSO_4$ through alkaline extraction and controlled precipitation and drying. The selected extraction conditions were a 1:16.66 coir-to-liquid ratio, pH 12.24, and 78 °C for 2 h, with 0.76 g $FeSO_4$ crystals per 50 mL tannin extract. Centrifugation at 1200 rpm for 40 min followed by drying at 100 °C for 2 h produced a fine pigment powder suitable for screen printing. The pigment produced black prints on cotton, with wash-fastness ratings of 4, 3/4, and 3 after successive

washes. FTIR results supported iron–oxygen interactions and an iron–tannate-type structure, but did not independently confirm Fe(III) formation. The lack of replicate trials and statistical optimization limits the findings, highlighting the need for further process optimization, chemical characterization, and improvement of pigment–binder bonding and wash fastness.

5 REFERENCES

Basri, E. (2023). Utilization of tannin as renewable natural pigment in the culture of Indonesian batik fabrics: A review. *Journal of Positive School Psychology*, 7(4).

Fraga-Corral, M., G.-O., & P.-L. (2020). Technological application of tannin-based extracts. *Molecules*, 25(3), 614.

Hemingway, J. (1960). Complexes of ferrous iron with tannic acid. *U.S. Geological Survey Water-Supply Paper*, 1459-D, 16.

Rathnayake, H., Dawood, S., Pathiraja, G., Adrah, K., & Ayodele, O. (2022). Green synthesis of de novo bioinspired porous iron-tannate microstructures with amphoteric surface properties. *Sustainable Chemistry*, 3(2), 192–204. https://doi.org/10.3390/suschem3020013

Sari, Y. (2023). Tannin determination in young coconut coir (Cocos nucifera L.) by FTIR and UV-Vis spectroscopy. *Jurnal Matematika dan Ilmu Pengetahuan Alam LLDIKTI Wilayah 1 (JUMPA)*, 3(1), 8–13.

Sirisangawansam, R. (2023). Optimization of tannin extraction from coconut coir through response surface methodology. *Heliyon,* 9(2), e13377. https://doi.org/10.1016/j.heliyon.2023.e13377

Textile Learner. (n.d.). *Colour fastness to washing procedure.* https://textilelearner.net/colour-fastness-to-washing-procedure/

Wilson, H. (2007). Analysis of the current research into the chemistry of iron gall ink and its implications for paper (Master's thesis). https://doi.org/10.13140/2.1.4803.2000

ISSN: 2773-7055
Proceedings of the 5th International Research Conference
Institute of Technology, University of Moratuwa
November 5, 2026

Paper ID: 44

DEVELOPMENT OF CHEMICALLY MODIFIED WOOL-BASED SUSTAINABLE ADSORBENTS FOR REMOVAL OF SYNTHETIC DYES FROM AQUEOUS SYSTEMS

M M Suraweera[1,2], N D Tissera[3], R N Wijesena[3], K A A Dilhari[4], G Priyadarshana[1*]

[1]Department of Materials and Mechanical Technology, Faculty of Technology, University of Sri Jayewardenepura, Homagama 10200, Sri Lanka

[2]Faculty of Graduate Studies, University of Sri Jayewardenepura, Gangodawila, Nugegoda 10250, Sri Lanka

[3]Division of Textile and Clothing Technology, Institute of Technology, University of Moratuwa, Homagama, Sri Lanka

[4]Department of Basic Sciences, Faculty of Allied Health Sciences, University of Sri Jayewardenepura, Gangodawila, Nugegoda 10250, Sri Lanka

*Corresponding author: gayanp@sjp.ac.lk

ABSTRACT: The discharge of dye-containing wastewater from textile and related industries poses a significant environmental challenge. Wool, a renewable natural fiber, can serve as a low-cost adsorbent, and its performance can be enhanced through chemical modification. This study evaluated the acid dye adsorption performance of wool fibers through chemical modification by alkaline hydrolysis. Hydrolyzed and untreated wool fibers were characterized using Fourier Transform Infrared Spectroscopy (FT-IR) and Thermogravimetric Analysis (TGA), while their adsorption performance was evaluated using UV–Visible spectrophotometry (λmax = 540 nm). FT-IR analysis indicated that the alkaline hydrolysis altered the secondary structure of keratin, suggesting partial disruption of β-sheet-rich cuticle structures surrounding the intermediate filaments. TGA results also showed a slight reduction in thermal stability of hydrolyzed wool due to weaker intermolecular hydrogen bonds. Hydrolyzed wool showed higher adsorption capacity (44.72 ± 0.17 mg g^{-1}) with higher dye removal (50.82 ± 0.10%) than untreated wool (4.78 ± 0.21 mg g^{-1} and 5.44 ± 0.15%, respectively) after 10 min. The enhanced adsorption is attributed to the increased exposure of functional groups in hydrolyzed wool, which promoted strong dye–fiber interactions. These findings demonstrate the potential of chemically modified wool as a sustainable, biodegradable adsorbent for dye-contaminated wastewater treatment.

Keywords: wool fibers, alkaline hydrolysis, acid dye adsorption, keratin, wastewater treatment

1 INTRODUCTION

Wool is a biodegradable natural fiber composed of keratin, a sulfur-rich structural protein with a molecular weight of up to approximately 60 kDa (Bhavsar et al., 2017). Globally, there is growing interest in natural fibers as a replacement for synthetic fibers to produce composite materials. The projected increase in the global sheep population from 1.7 to 2.7 billion between 2000 and 2050, together with the resulting generation of low-value waste wool, creates opportunities for value-added applications of wool (Allafi et al., 2022). However, wool remains an underutilized sustainable material despite its potential for diverse industrial applications. It has been used as a raw material in the textile industry since ancient times, and it has gained attention for use in other industries due to its abundance, recyclability, and low environmental impact. Conversion of waste wool into a functional adsorbent for dye removal from wastewater represents a waste-to-resource approach that supports circular economy principles.

Chemical modification of wool through alkaline hydrolysis alters the natural structure of the keratin fiber by partial cleavage of peptide bonds and the formation of low molecular weight proteins and peptides (Rajabinejad et al., 2018). This modification increases the accessibility of free amine groups and other surface functional groups, thereby enhancing the interactions with dye molecules (Tissera et al., 2020). Wool, as a keratin-derived material, has been investigated for various applications, including oil removal and dye adsorption (Sulyman et al., 2017; Tissera et al., 2020). A recent study by Cretescu et al. (2017) used wool powders for acid-dye removal, while hydrolyzed wool-derived keratin has demonstrated adsorption capacities of 235.02 and 122.83 mg g^{-1} for Acid Red 337 and Acid Blue 349, respectively. However, the latter approach involved extracted keratin rather than the direct use of chemically modified wool fibers. Tissera et al. (2020) also investigated alkaline-hydrolyzed Merino wool fibers for the removal of Rhodamine B dye. However, Rhodamine B is a cationic dye and therefore does not represent the adsorption behavior of anionic acid dyes. The present study addresses this gap by comparing untreated and alkaline-hydrolyzed wool fibers for acid-dye removal and relating the adsorption performance to hydrolysis-induced changes in keratin structure.

2 METHODOLOGY

2.1 Reagents and Materials

Merino wool fibers were used as raw material for the preparation of the adsorbent. Analytical-grade sodium hydroxide (NaOH) was used for the alkaline hydrolysis treatment of wool fibers. A commercial acid red dye was used as the model dye for adsorption studies, while glacial acetic acid (99% purity) was used to prepare the adsorption medium. Distilled water was used for all experiments. All chemicals were used as received without further purification.

2.2 Preparation of Adsorbents

The wool fibers were washed with distilled water to remove surface impurities and dust particles. The cleaned wool fibers were subjected to alkaline hydrolysis following Tissera et al. (2020) with slight modifications to their optimized treatment conditions. Approximately 0.125 g of wool fibers were treated with 40 mL of 0.5 M NaOH solution for 10 minutes at room temperature. After 10 minutes, the resulting dispersion was centrifuged at 9000 rpm. The resulting precipitate was continuously washed with distilled water until a neutral pH was reached in the precipitate. Both the hydrolyzed and untreated wool samples were dried at 60 °C to remove excess moisture. Prepared samples were stored for further analysis as adsorbent material.

2.3 Physicochemical Characterization of Adsorbents and Acid Dye Removal Study

Following the procedure reported by Tissera et al. (2020), FT-IR spectra of both wool fibers and hydrolyzed wool fibers were recorded using a Nicolet iS10. The attenuated total reflectance (ATR) measurement mode was used with the sample positioned on a ZnSe crystal. Absorption spectra were recorded over 32 scans within the wavenumber range of 800 cm^{-1} to 4000 cm^{-1}, with 4 cm^{-1} resolution. The thermal stability of untreated and hydrolyzed wool fibers was evaluated using a TA SDT 650 thermogravimetric analyzer. Approximately 3 mg of each sample was placed in Al_2O_3 crucibles and heated from 25 to 500 °C at a heating rate of 5 °C min^{-1} under

a nitrogen atmosphere. The resulting thermograms were used to assess the effect of alkaline hydrolysis on the thermal degradation behavior of wool fibers.

The adsorption performance of hydrolyzed wool fibers was evaluated using an acid red dye solution, while untreated wool fibers were used as the control. Approximately 0.05 g of hydrolyzed wool fibers and untreated wool fibers were added separately to 40 mL of 110 ppm acid red dye solution containing 3% acetic acid. The resulting dispersions were stirred at room temperature for 10 min to facilitate dye adsorption. After 10 minutes, the suspensions were centrifuged, and the supernatants were analyzed using a UV–Visible spectrophotometer. Residual dye concentrations were determined from absorbance measurements at the maximum absorption wavelength (λmax = 540 nm) using a calibration curve. This procedure was done in triplicate.

3 RESULTS AND DISCUSSION

3.1 Physicochemical Characterization of Adsorbents

FT-IR analysis was performed to investigate the structural modifications induced by alkali hydrolysis in hydrolyzed wool fibers compared to untreated wool (Figure 1). The absence of new absorption bands or significant peak shifts in the spectra of the hydrolyzed wool sample compared with untreated wool indicates that alkaline hydrolysis did not introduce new functional groups or alter the main macromolecular bonds of keratin. Both samples showed characteristic absorption bands including amide I (approximately 1630 cm^{-1}), amide II (approximately 1515 cm^{-1}), and amide III (approximately 1238 cm^{-1}) regions, which are attributed to peptide bonds (-CONH-) of keratin (Rajabinejad et al., 2018; Tissera et al., 2020). Amide-A (3271 cm^{-1}) and Amide-B (3065 cm^{-1}) bands are related to N-H bond stretching, while the 2920 cm^{-1} band corresponds to C-H bond stretching vibrations in both samples. Second-derivative FT-IR analysis was obtained for untreated and hydrolyzed wool fibers to enhance the separation of overlapping peaks and provide more specific structural information. It showed differences between untreated and hydrolyzed wool samples, particularly in the Amide I, II, and III regions (Figure 2). The peak assignments indicated that the observed bands were associated with α-helix structure, β-sheets, β-turns, and disordered structures (Jiang et al., 2022). Compared with the untreated wool sample, the hydrolyzed wool sample exhibited reduced intensities of β-sheet-associated bands and a relative increase in α-helix-associated bands across the Amide I, Amide II, and Amide III regions. The β-sheet is a constituent of cuticle cells of wool fibers, which helps to cover the intermediate filament structure made up of α-helix protein structure in the wool fibers (Tissera et al., 2020). These observations suggested that alkaline hydrolysis preferentially disrupts β-sheet-rich cuticle structure while preserving the α-helix structure of the intermediate filaments.

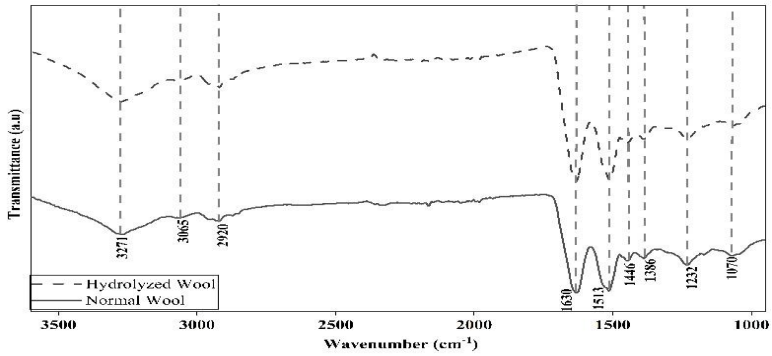


Figure 1. FT-IR spectra (4000–800 cm^{-1}) of Untreated wool and hydrolyzed wool fiber samples.

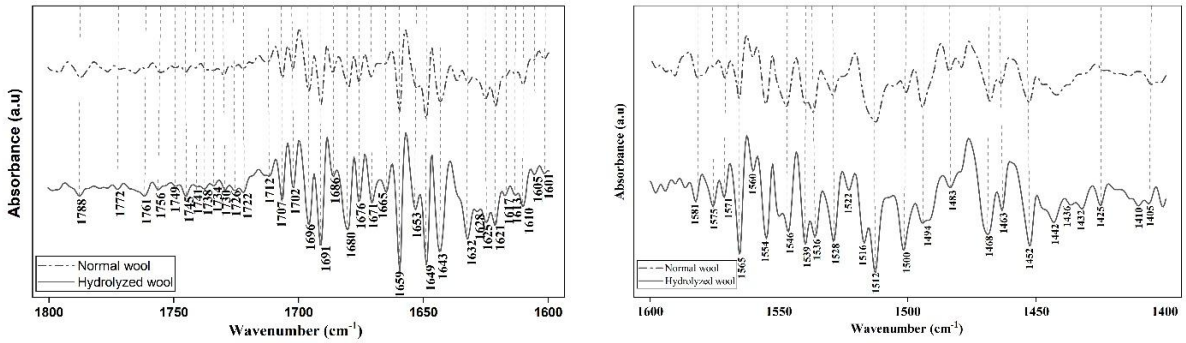
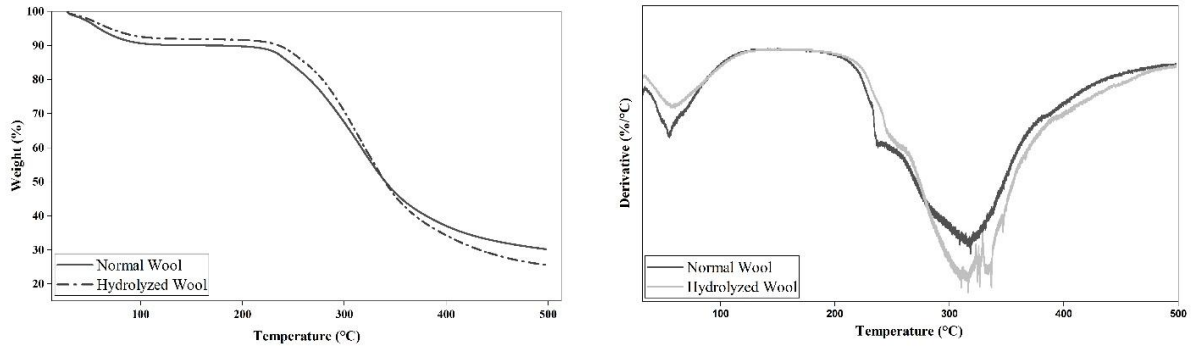


Figure 2. FT-IR spectra (4000–800 cm^{-1}) of Untreated wool and hydrolyzed wool fiber samples.

The TG curves and the first derivatives of both samples are shown in Figure 3(A) and (B), respectively, as the results of the Thermogravimetric analysis. The initial weight loss at 100-150 °C was attributed to moisture loss (Aluigi et al., 2007). The main thermal degradation region was observed at 200 - 400 °C, and higher thermal stability of untreated wool than hydrolyzed wool was observed. The difference may be associated with the β-sheet structure and intermolecular hydrogen bonding between amino and carbonyl groups of the protein chains. Since both FT-IR and TGA results indicated that alkaline hydrolysis disrupted the β-sheet-rich cuticle and weakened intermolecular hydrogen bonding, the effect of these structural changes on acid dye uptake was then investigated, particularly in relation to the increased availability of polar and ionizable side-chain groups.



(A) (B)

Figure 3. TGA thermograms of samples (A) and their first derivatives (B)

3.2 Acid Dye Removal Study

The adsorption performance showed that hydrolyzed wool reduced the residual dye concentration to 54.10 ± 0.10 ppm, compared with 104.02 ± 0.17 ppm for untreated wool after 10 min. Accordingly, dye removal increased from 5.44 ± 0.15% for untreated wool to 50.82 ± 0.10% for hydrolyzed wool (Figure 4), while the calculated adsorption capacity increased from 4.78 ± 0.21 to 44.72 ± 0.17 mg g^{-1}. Therefore, alkaline hydrolysis led to around a 9.4-fold improvement in adsorption capacity compared to untreated wool. This performance is lower than the 294 mg g^{-1} reported for alkaline-hydrolyzed wool by Tissera et al. (2020) for Rhodamine B, likely reflecting differences in dye type, initial dye concentration, contact time and adsorption conditions.

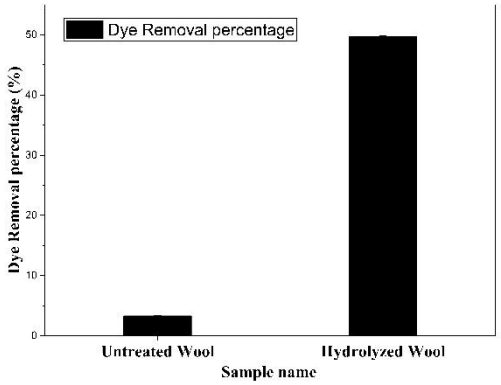


Figure 4. Dye removal percentage of untreated wool and hydrolyzed wool samples

This enhanced adsorption is attributed to partial disruption of the β-sheet-rich cuticle, which increased the accessibility of surface functional groups, including free amine and carboxyl groups, thereby strengthening interactions between the wool surface and acid dye molecules. The considerably lower residual dye concentration after the treatment shows that alkaline modification led to higher accessibility of adsorption sites within the wool fiber framework.

4 CONCLUSION

Alkaline hydrolysis significantly enhanced the adsorption performance of wool fibers for acid dye removal from aqueous systems. Structural characterization using FT-IR analysis and TGA analysis indicated partial disruption of the β-sheet-rich cuticle structure while preserving the α-helix keratin framework of the intermediate filaments. These structural modifications increased the accessibility of surface functional groups, improving dye removal from 5.44 ± 0.15% for untreated wool to 50.82 ± 0.10% for hydrolyzed wool after 10 min of dye adsorption. The corresponding dye adsorption capacity increased from 4.78 ± 0.21 to 44.72 ± 0.17 mg g^{-1}, indicating the potential of chemically modified wool as a biodegradable adsorbent for dye-contaminated wastewater treatment.

5 ACKNOWLEDGEMENTS

This study was funded by the Research Council of the University of Sri Jayewardenepura (Grant No: RC/UGR/TEC/2026/66), Sri Lanka

6 REFERENCES

Allafi, F., Hossain, M. S., Lalung, J., Shaah, M., Salehabadi, A., Ahmad, M. I., & Shadi, A. (2022). Advancements in Applications of Natural Wool Fiber: Review. *Journal of Natural Fibers*, *19*(2), 497–512. https://doi.org/10.1080/15440478.2020.1745128

Bhavsar, P., Zoccola, M., Patrucco, A., Montarsolo, A., Rovero, G., & Tonin, C. (2017). Comparative study on the effects of superheated water and high temperature alkaline hydrolysis on wool keratin. *Textile Research Journal*, *87*(14), 1696–1705. https://doi.org/10.1177/0040517516658512

Cretescu, I., Lupascu, T., Buciscanu, I., Balau-Mindru, T., & Soreanu, G. (2017). Low-cost sorbents for the removal of acid dyes from aqueous solutions. *Process Safety and Environmental Protection*, *108*, 57–66. https://doi.org/10.1016/j.psep.2016.05.016

Jiang, Z., Li, W., Wang, Y., & Wang, Q. (2022). Second-Order Derivation Fourier Transform Infrared Spectral Analysis of Regenerated Wool Keratin Structural Changes. *AATCC Journal of Research*, *9*(1), 43–48. https://doi.org/10.1177/23305517211060778

Rajabinejad, H., Zoccola, M., Patrucco, A., Montarsolo, A., Rovero, G., & Tonin, C. (2018a). Physicochemical properties of keratin extracted from wool by various methods. *Textile Research Journal*, *88*(21), 2415–2424. https://doi.org/10.1177/0040517517723028

Rajabinejad, H., Zoccola, M., Patrucco, A., Montarsolo, A., Rovero, G., & Tonin, C. (2018b). Physicochemical properties of keratin extracted from wool by various methods. *Textile Research Journal*, *88*(21), 2415–2424. https://doi.org/10.1177/0040517517723028

Sulyman, M., Namiesnik, J., & Gierak, A. (2017). Greener Cleaner: Sheep Wool Fiber as Renewable Sources for Oil Spill Cleanup. *International Journal of Advances in Science Engineering and Technology*, 5(2), 84-92.

Tissera, N. D., Wijesena, R. N., Yasasri, H., de Silva, K. M. N., & de Silva, R. M. (2020). Fibrous keratin protein bio micro structure for efficient removal of hazardous dye waste from water: Surface charge mediated interfaces for multiple adsorption desorption cycles. *Materials Chemistry and Physics*, *246*. https://doi.org/10.1016/j.matchemphys.2020.122790

ISSN: 2773-7055
Proceedings of the 5th International Research Conference
Institute of Technology, University of Moratuwa
November 5, 2026

Paper ID: 18

FERMENTATION PERFORMANCE OF SELECTED SRI LANKAN HERITAGE GRAINS FOR SPIRIT PRODUCTION UNDER ENZYME-FREE PROCESSING CONDITIONS

R H R W Lakshana[1], W M Y B Wanninayake[1], M L L Madhushan[1], D G Mallawaarachchi[1], W D M P L Malshan[1], G K Jayatunga[1*]

[1]Division of Polymer and Chemical Engineering Technology, Institute of Technology, University of Moratuwa, Homagama, Sri Lanka

*Corresponding author: gayanij@itum.mrt.ac.lk

ABSTRACT: This study investigated the fermentation performance of various Sri Lankan heirloom grains, namely, Batapolalla, Ran Kahawanu, Suwandel, Heenati, Pachchaperumal, Kuruluthuda, Kurakkan, Thana Hal, Madanamaalu, and Kollu, to identify suitable substrates for spirit production. Experiments were conducted using cereal samples for thermal gelatinization at 65 °C without adding any external amylase enzymes, followed by fermentation with *Saccharomyces cerevisiae* and supplemental sucrose. Alcohol level and pH kinetics were monitored over six days to assess fermentation efficiency. Results indicated significant variations in alcohol yield based on cereal type, with Suwandel, Batapolalla, and Ran Kahawanu demonstrating the highest ethanol production. The observed decline in pH across the samples further confirmed the progression of yeast activity and the development of an acidic environment. The findings highlight that cereal selection is a critical factor in optimizing ethanol yield under low-input fermentation conditions, with Suwandel, Batapolalla and Ran Kahawanu emerging as the most promising candidates for spirit production.

Keywords: heritage grains, pH variation, alcohol production, fermentation, spirits

1 INTRODUCTION

The global alcoholic beverage industry is a rapidly growing sector consisting of beer, wine, and distilled spirits. Among these categories, the spirits industry has experienced significant expansion due to increasing consumer demand for premium alcoholic beverages and innovative products. Spirits are produced using various raw materials such as grains, fruits, sugarcane, and coconut sap through fermentation and distillation processes. Globally, cereal-based spirits such as whiskey and vodka dominate industrial production because of their scalability, process efficiency, and consistent product quality. At the same time, traditional spirits such as coconut arrack continue to gain international recognition due to their unique cultural identity and distinctive flavor profiles *(Alcoholic Beverages Industry Worldwide - Statistics & Facts | Statista, n.d.) - Google Search*, n.d.).

Modern alcohol production industries increasingly adopt advanced technologies such as simultaneous saccharification and fermentation (SSF), continuous distillation systems, and sustainable wastewater treatment methods to improve production efficiency and reduce environmental impacts. Overall, the global alcoholic beverage industry presents strong market opportunities for both traditional and modern spirit products, supported by technological advancements, growing international demand, and the expansion of premium alcoholic beverage markets. (*Alcoholic Beverages Industry Worldwide - Statistics & Facts | Statista*, n.d.)

Ethanol production relies on the fermentation of simple sugars by *Saccharomyces* yeasts, but complex grain starches made of amylose and amylopectin must first undergo a multi-step transformation consisting of hydration, cooking, enzymatic hydrolysis, and fermentation. Heating is required to gelatinize the starch, allowing enzymes to efficiently break the alpha-1,4 glycosidic bonds and incorporate a water molecule at each split to release fermentable glucose. While this intensive conversion makes starch-based distillation more operationally expensive than fermenting simple sugars like coconut sap, it yields an exceptionally neutral, high-purity alcohol that is highly valued for premium beverages, pharmaceuticals, and cosmetics (Cereda & de Almeida Lima, 2025).

Although considerable research has been conducted on spirit production using conventional cereals such as barley, maize, wheat, and rye, limited information is available on the suitability of Sri Lankan heritage grains as feedstocks for distilled spirits. Sri Lanka possesses a rich diversity of traditional rice varieties, finger millet (*Eleusine coracana*), and horse gram (*Macrotyloma uniflorum*), which are valued for their nutritional composition, climate resilience, and cultural significance. However, their fermentation characteristics, alcohol-producing potential, and suitability for spirit production have received little scientific attention. Furthermore, comparative studies evaluating the fermentation behavior of different heritage grain varieties under identical processing conditions are scarce. This lack of information limits the utilization of these indigenous grains in the development of value-added alcoholic beverages and sustainable grain-based distilling industries.

Therefore, the objective of this study was to evaluate the fermentation performance of selected Sri Lankan heritage rice varieties, finger millet, and horse gram for spirit production without the addition of commercial hydrolytic enzymes. Fermentation performance was assessed by monitoring alcohol production and pH changes throughout fermentation. The findings provide baseline information on the natural fermentability of Sri Lankan heritage grains and their potential as alternative raw materials for sustainable premium spirit production.

2 METHODOLOGY

Bulk samples of the traditional Sri Lankan heritage rice (*Hela Wee*), finger millet (*Kurakkan*), and horse gram (*Kollu*) were collected from traditional chena cultivation and wetland paddy fields in Monaragala, Sri Lanka (6°40′–6°52′ N, 81°20′–81°34′ E).

First, 40 g representative cereal samples (*KERN ABJ-NM/ABS-N* analytical balance) were prepared for fermentation to compare ethanol production among different cereal types. Each 40 g sample was ground to a fine powder and transferred to a 250 mL Erlenmeyer flask. Then 200 mL of water were added to each flask, and the contents were mixed by shaking. The flasks were placed in a water bath at 65 °C for 1 hour to promote starch gelatinization, then removed and allowed to cool to 30 °C. After cooling, 1 g of yeast (*Saccharomyces cerevisiae*) and 10 g of table sugar (sucrose) were aseptically added to each flask. The mouth of each flask was covered with aluminum foil to minimize contamination while permitting gas exchange. Fermentation proceeded at ambient laboratory temperature. Alcohol level (alcohol meter) and pH (*EUTECH Instruments* pH meter) were measured starting after three days and then daily up to day 6 to

monitor the progress of fermentation and identify the cereal producing the highest spirit yield.

3 RESULTS AND DISCUSSION

The variations in alcohol concentration and pH observed during the fermentation of the selected traditional grain varieties are summarized in Tables 1 and 2, respectively. Different cereal substrates showed distinct fermentation performance when processed only with water, yeast, and added sugar, without the use of amylase enzyme. Therefore, the observed spirit production mainly indicated the natural fermentability of each cereal, the effect of heat treatment at 65 °C, and the availability of the added sucrose rather than enzymatic starch hydrolysis.

Table 1. Alcohol percentage of different grain samples over time

No.	Substrate Variety	Alcohol amount % (v/v)					
		Day 1	Day 2	Day 3	Day 4	Day 5	Day 6
1	Suwandel	2	10	4	5	5	5
2	Thana Hal	0	2	2	0	0	0
3	Madanamaalu	0	2	2	0	0	0
4	Heenati	3	3	1	0	0	0
5	Pachchaperumal	4	4	0	0	0	0
6	Ran Kahawanu	5	3	3	4	4	5
7	Batapolalla	6	5	6	5	5	5
8	Kollu (horse gram)	3	0	0	0	0	0
9	Kurakkan (finger millet)	2	3	2	0	4	4
10	Kalu Heenati	0	0	3	0	0	0
11	Suwandel (without sugar)	1	0	0	0	0	0
12	Pachchaperumal (without sugar)	0	0	0	0	0	0

Table 2. pH changes of different grain samples over time

No.	Substrate Variety	pH					
		Day 1	Day 2	Day 3	Day 4	Day 5	Day 6
1	Suwandel	5.02	4.82	4.12	3.98	3.86	4.44
2	Thana Hal	4.50	4.41	3.81	3.43	3.32	4.10
3	Madanamaalu	4.80	4.00	3.76	3.4	3.20	3.82
4	Heenati	4.05	3.96	3.68	3.24	2.91	3.11
5	Pachchaperumal	3.60	3.58	3.14	3.68	3.46	3.91
6	Ran Kahawanu	4.95	4.56	4.23	4.04	3.83	3.67
7	Batapolalla	4.98	4.31	3.89	3.78	3.52	4.35
8	Kollu (horse gram)	5.18	4.96	4.54	4.18	3.99	3.20
9	Kurakkan (finger millet)	4.81	4.72	4.40	4.09	3.92	4.27
10	Kalu Heenati	4.63	4.12	3.82	3.46	3.15	3.72
11	Suwandel (without sugar)	4.32	4.28	3.73	3.50	3.13	3.64
12	Pachchaperumal (without sugar)	4.33	4.12	4.00	2.96	2.69	3.83

Starch gelatinization can be improved using heat; it helps to make the cereal matrix more accessible to fermentation. However, in the absence of commercial amylolytic enzymes, starch hydrolysis was expected to be limited, and fermentation depended largely on readily available fermentable sugars, any naturally occurring hydrolytic activity within the grains, and the uniform

sucrose supplementation. Consequently, cereals that provided a more favorable environment for yeast growth and metabolism produced higher alcohol concentrations.

Alcohol production varied considerably among the grain varieties, indicating significant differences in their fermentation performance under identical enzyme-free processing conditions (Table 1). Among the substrates evaluated, Suwandel produced the highest alcohol concentration, increasing from 2% (v/v) on Day 1 to a maximum of 10% (v/v) on Day 2 before declining and stabilizing at approximately 5% (v/v) during the remaining fermentation period. The rapid increase in alcohol concentration suggests that Suwandel provided readily fermentable carbohydrates that supported vigorous yeast activity during the initial stages of fermentation. The subsequent decline may reflect changes in fermentation dynamics, including depletion of readily available fermentable sugars, ethanol loss during sampling or measurement, or reduced yeast activity as fermentation progressed. Batapolalla also exhibited excellent fermentation performance, maintaining consistently high alcohol concentrations between 5 and 6% (v/v) throughout the six-day fermentation period, indicating stable and sustained yeast activity. Similarly, Ran Kahawanu demonstrated relatively stable alcohol production, with concentrations ranging from 3 to 5% (v/v), while Kurakkan produced moderate alcohol levels that reached 4% (v/v) by the end of fermentation.

In contrast, Thana Hal, Madanamaalu, Heenati, Pachchaperumal, and Kalu Heenati produced comparatively low alcohol concentrations, indicating less favorable fermentation performance under the conditions employed. Kollu exhibited only limited alcohol production during the initial stage of fermentation, after which no detectable alcohol was observed, suggesting that this substrate provided limited fermentable carbohydrates for sustained yeast metabolism. The sugar-free control prepared from Suwandel produced only 1% (v/v) alcohol on the first day, whereas the Pachchaperumal sugar-free control produced no detectable alcohol throughout the experiment. These observations demonstrate that, in the absence of commercial amylolytic enzymes, the selected grains possessed limited capacity to generate fermentable sugars from starch alone. Because identical amounts of sucrose and yeast were added to all experimental treatments (except the sugar-free controls), the differences in alcohol production are primarily attributable to the intrinsic physicochemical properties of the grain varieties, including starch accessibility, grain composition, and their ability to support yeast fermentation under low-input, enzyme-free conditions.

The observed fermentation pattern in the alcohol measurements can also be understood using pH measurements. In most samples, pH gradually decreased during the six-day fermentation period, which is consistent with the production of acidic metabolites by yeast and associated microbial activity. This reduction is attributed to the formation of organic acids, dissolved carbon dioxide and other acidic metabolites generated during active yeast metabolism. A moderate decrease in pH is generally favorable because it suppresses contaminating microorganisms and supports yeast dominance; however, excessive acidification can inhibit yeast growth and reduce ethanol productivity. Therefore, the relationship between pH and alcohol level in this study was likely influenced by the balance between beneficial acidification and pH-related yeast stress. Similar decreases in pH have been widely reported during cereal fermentation and

are considered beneficial because acidic conditions suppress spoilage microorganisms while maintaining favorable conditions for yeast growth (Chan, 1997).

Grain pericarp color alone did not show a consistent relationship with fermentation performance. Among the white rice varieties, Suwandel and Ran Kahawanu produced relatively high alcohol concentrations, whereas among the red rice varieties, Batapolalla also exhibited high alcohol production while Pachchaperumal showed comparatively lower alcohol concentrations. These findings suggest that fermentation efficiency depends more on the biochemical characteristics of individual varieties than on grain color itself. Red rice varieties generally contain higher concentrations of phenolic compounds, tannins, dietary fibre, and antioxidant pigments than white rice, which can influence enzyme accessibility, starch digestibility, and yeast metabolism (Tiozon et al., 2021). However, the effect of these compounds varies among cultivars and may either inhibit or promote fermentation depending on their concentration and interaction with starch.

Overall, the results indicate that Suwandel, Batapolalla, Ran Kahawanu and Kurakkan possess favorable fermentation characteristics for spirit production, whereas the remaining varieties exhibited lower fermentative efficiency under the conditions employed. The observed variations in pH and alcohol production emphasize the importance of grain composition, and yeast metabolic activity in determining the suitability of Sri Lankan heritage grains for alcohol production. Therefore, this study has been able to determine which of the cereals can give the best ethanol output under low-input fermentation conditions.

4 CONCLUSION

The study demonstrated significant differences in the fermentation performance of selected Sri Lankan heritage grain varieties under enzyme-free processing conditions. Among the tested substrates, Suwandel, Batapolalla, Ran Kahawanu, and Kurakkan showed comparatively favorable alcohol production, with Suwandel recording the highest alcohol concentration of 10% (v/v) on Day 2, while Batapolalla showed the most consistent fermentation performance. The overall decrease in pH observed in most samples indicated the formation of acidic metabolites during fermentation and the development of conditions favorable for yeast activity. The low alcohol production observed in several varieties and the sugar-free controls further indicated that, without commercial amylolytic enzymes, starch hydrolysis and the release of fermentable sugars were limited. Overall, the results confirm that fermentation efficiency depended more on the intrinsic biochemical characteristics, starch accessibility, and fermentability of individual grain varieties than on grain color alone. Therefore, Suwandel, Batapolalla, Ran Kahawanu, and Kurakkan can be considered promising Sri Lankan heritage grains for further investigation in spirit production, while optimization of enzyme-assisted hydrolysis and fermentation conditions is recommended to improve ethanol yield.

5 ACKNOWLEDGEMENTS

Authors acknowledge the Division of Polymer and Chemical Engineering Technology, ITUM for providing the laboratory facilities for the experimentation. Also, authors wish to acknowl-

edge assistance given by Mrs. H.H. Galagedara of Energy Engineering and Environmental Engineering Laboratories.

6 REFERENCES

Alcoholic beverages industry worldwide—Statistics & Facts | Statista. (n.d.). Retrieved May 16, 2026, from https://www.statista.com/topics/1709/alcoholic-beverages/

(Alcoholic Beverages Industry Worldwide—Statistics & Facts | Statista, n.d.)—Google Search. (n.d.).

Briggs, D. E., Brookes, P. A., Stevens, R., & Boulton, C. A. (2004). *Brewing: Science and practice*. Elsevier.

Cereda, M. P., & de Almeida Lima, U. (2025). Etanol, spirits and beer produced from underground starchy raw materials. In *Traditional Starch Food Products* (pp. 205–236). Elsevier. https://www.sciencedirect.com/science/article/pii/B9780323908443000226

Chan, L. H. (1997). *Handbook of indigenous fermented foods: 2nd edn. edited by Keith H. Steinkaus. Marcel Dekker Inc., NY. 1996. ISBN 0-8247-9352-8*. Elsevier.

Etanol, spirits and beer produced from underground starchy raw materials—ScienceDirect. (n.d.). Retrieved May 16, 2026, from https://www.sciencedirect.com/science/chapter/edited-volume/abs/pii/B9780323908443000226

Tiozon, R. J., Sartagoda, K., Fernie, A., & Sreenivasulu, N. (2021). The nutritional profile and human health benefit of pigmented rice and the impact of post-harvest processes and product development on the nutritional components: A review. *Critical Reviews in Food Science and Nutrition*, *63*, 1–28. https://doi.org/10.1080/10408398.2021.1995697

ISSN: 2773-7055
Proceedings of the 5th International Research Conference
Institute of Technology, University of Moratuwa
November 5, 2026

Paper ID: 27

TERRABOT: ENHANCED MODULAR PLATFORM WITH ON-DEVICE AI FOR PRECISION AGRICULTURE

Chanuka Jayasooriya[1*], Pasandul Kasthuri[1], Ravishan Hapukotuwa[1], Thosantha Thirandi[1], Heshadi Gayasha[1], A W C K Atugoda[1]

[1]Division of Electrical, Electronic and Telecommunication Engineering Technology, Institute of Technology, University of Moratuwa, Homagama, Sri Lanka

*Corresponding author: 23ET0394@itum.mrt.ac.lk

ABSTRACT: In Sri Lankan paddy and vegetable cultivation, traditional weed management relies heavily on indiscriminate herbicide spraying, which degrades soil quality, contaminates local water sources, and drastically increases agricultural production costs. While commercial robotic solutions exist, their high initial investment often exceeding one million rupees per machine creates an insurmountable barrier for regional smallholder farmers. To resolve this, our research proposes "TerraBOT" a low-cost, CNC type autonomous robotic platform utilising an ESP32-S3 microcontroller to deploy on-device TinyML model with Time-of-flight sensor for real-time field operations. This research aims to develop an affordable, modular, and autonomous robotic platform that localises plant care and weed management without cloud-dependent networks. A key innovation is its Universal Modular Interface (UMI), allowing rapid physical and software reconfiguration between tasks like laser weeding and precision fertilising. By pairing Time-of-Flight (TOF) sensors and multi-spectral imaging, the robot tracks crop rows, establishes baseline heights to isolate ground noise, and maps variances to accurately classify weeds. Experimental validation demonstrates that deploying on-device AI via the ESP32-S3 eliminates cloud processing delays, achieving real-time plant classification with an edge inference time under 200 milliseconds. Mechanically, the CNC-grade gantry paired with TOF sensing theoretically guarantees sub-millimeter mapping precision, successfully neutralizing weed candidates via a targeted laser while preventing collateral crop damage. Ultimately, this targeted actuation provides a highly sustainable, robust alternative to broad-spectrum chemical application, drastically optimising resource efficiency. This ongoing research outlines a highly practical engineering framework that successfully transitions regional weed management from an inefficient, toxic manual process to a proactive, automated defence system.

Keywords: precision agriculture, modular robotics, TinyML, autonomous weed management, Sri Lanka

1 INTRODUCTION

Access to safe, uncontaminated food sources is critical; however, current agricultural practices rely heavily on manual weed removal and broad-spectrum chemical applications (Kanchalwar et al., 2024). This over-reliance directly degrades environmental health, contaminates water sources, and limits overall crop yield. Although automated robotic solutions exist, basic sensor-based systems struggle to distinguish crops from weeds across varying lighting conditions and growth stages. Furthermore, modern AI-driven agricultural robots heavily depend on cloud computing, introducing high latency and severe connectivity issues in rural farming areas (Chen & Kumar, 2025). To address these critical limitations, this research introduces TerraBOT, a low-cost, autonomous robotic platform. The primary aim of this study is to develop an affordable, modular edge-computing solution that localises plant care and weed management. By eliminating reliance on cloud networks and GPS, TerraBOT ensures high-precision crop protection with zero human intervention directly in the field. Unlike commercial weeding robots that are

cost-prohibitive (often exceeding 1 million LKR) and cloud-dependent, TerraBOT provides an open-source, ultra-low-cost (<50,000 LKR) modular platform capable of autonomous edge execution via dual ESP32-S3 microcontrollers.

1.1 Literature Review

Recent research highlights a critical shift from cloud-dependent deep learning toward edge-computing frameworks for real-time agricultural plant classification in resource-constrained environments (Silva et al., 2025). While complex neural networks historically achieved high accuracy, they required substantial computational power, rendering them unsuitable for remote farming. Addressing this limitation, the transition toward decentralised Tiny Machine Learning (TinyML) has demonstrated significant potential in agricultural IoT by enabling completely offline, on-device inference (Heydari & Mahmoud, 2025; Terziyska et al., 2025). Practically, deploying quantized TinyML models on low-cost microcontrollers such as the ESP32 has proven highly effective for real-time weed recognition and agricultural object classification (Donskoy et al., 2025). These advancements underline the necessity for lightweight, modular edge architectures in precision agriculture.

1.1.1 Identification of the Research Gap

Despite these technological advancements, existing robotic systems present several core limitations when deployed in regional smallholder contexts. High implementation costs, architectural rigidity, and a heavy reliance on stable cloud infrastructure remain prominent issues. Most existing solutions feature single-purpose chassis designs that restrict farmers from utilising multiple actuation tools, forcing separate investments for weeding and fertilising hardware. Furthermore, computationally heavy edge-cloud deep learning frameworks introduce high processing latency and fail entirely in rural fields lacking robust Wi-Fi networks (Silva et al., 2025). The identified research gap is the lack of a fully open-source, low-cost autonomous dosing robot with a modular plug-and-play architecture tailored specifically for regional smallholder farming. TerraBOT directly addresses this gap by combining an affordable physical interface with a dual-core firmware configuration capable of localised execution without external network dependencies.

2 METHODOLOGY

The proposed system design is categorised into three primary domains: mechanical architecture, electronic logic, and actuation frameworks. The underlying structural blueprint focuses on minimising production costs while maintaining structural flexibility for smallholder farming environments. Furthermore, the platform integrates localised data processing pipelines with sensory feedback mechanisms to completely isolate core navigation routines from external server networks.

2.1 Proposed Mechanical Design: Universal Modular Interface (UMI)

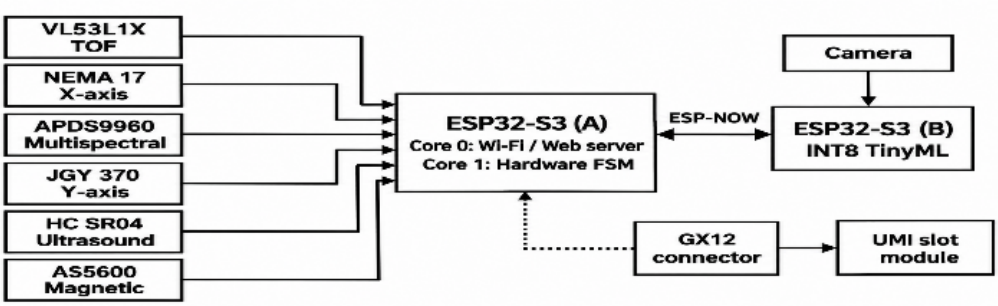


Figure 1. Universal Modular Interface (UMI) Hardware Connections and Chassis Tracking Geometry

Drawing inspiration from traditional tractor Power Take-Off (PTO) systems (Srivastava et al., 2024), the Universal Modular Interface (UMI) acts as the central mechanical nexus of the proposed platform. It facilitates the seamless interchangeability of task-specific end-effectors, such as the targeted weed-eradication module, thereby eliminating the need for complete system replacement across diverse agricultural operations. This architecture physically decouples the primary navigation chassis from the actuation modules using quick-release mounts and industrial-grade GX12 connectors to ensure rapid reconfiguration. To strictly maintain the ultra-low-cost objective while ensuring high torque, the longitudinal (Y-axis) locomotion utilizes off-the-shelf JGY-370 DC gear motors paired with an AS5600 absolute magnetic encoder. By eliminating the need for expensive proprietary servomotors, this closed-loop combination effectively reinforces the platform's economic viability and successfully mitigates odometry errors caused by wheel slip in unpredictable agricultural terrains (Gonzalez & Iagnemma, 2025). This setup guarantees precise chassis advancement synchronized with the camera's Field of View (FoV) per row pass. Additionally, an HC-SR04 ultrasonic array is implemented for perimeter boundary detection. As illustrated in Figure 1, the entire electromechanical framework interfaces directly with the primary ESP32-S3 microcontroller, establishing a robust command and telemetry loop.

2.2 Electronic Design and Logic Framework

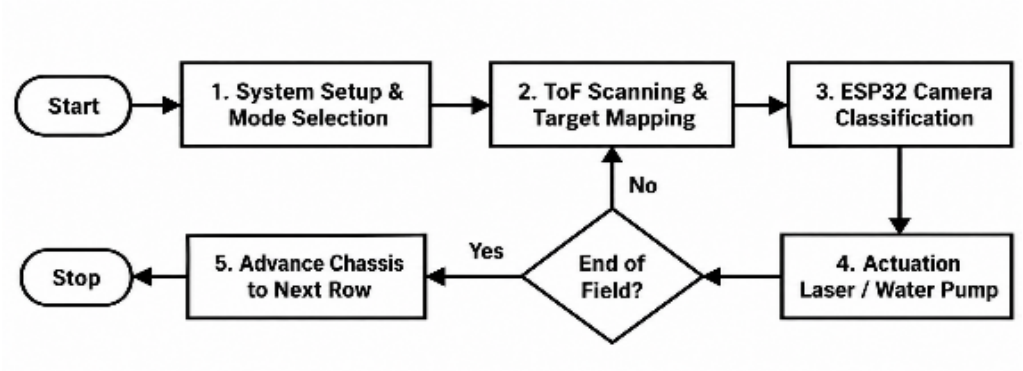


Figure 2. Sequential Execution Flow of the Hardware State Machine

The computational architecture of the proposed system leverages a distributed processing model utilising two separate ESP32-S3 microcontrollers interconnected via the low-latency ESP-NOW peer-to-peer wireless protocol (Sharma & Lee, 2025). The primary controller operates on a

dual-core FreeRTOS framework to ensure deterministic execution. Core 0 is exclusively assigned to asynchronous tasks, hosting a continuous Wi-Fi web server and aggregating sensor telemetry every 500ms to guarantee that remote dashboard updates remain unaffected by mechanical blocking functions. Core 1 is dedicated to hardware state machine execution, governing kinematics calibration, gantry translation, and end-effector actuation.

During a row pass, the X-axis gantry utilizes a NEMA 17 stepper motor to sweep a VL53L1X TOF sensor, an ESP32-S3 camera module, and an APDS-9960 multispectral sensor across the crops (Patel et al., 2025). To support the modular physical design, the electronics include a plug-and-play detection protocol utilising a resistor-based ID system. This allows the ESP32-S3 to automatically detect the attached module and dynamically reconfigure the software state machine in real time. The complete sequential flow of this operating logic, from initial system setup to chassis advancement, is illustrated in Figure 2.

2.3 Proposed Edge AI Actuation and Dynamic Model Deployment

Table 1. Input Dataset Configurations and Local Feature Mapping Thresholds

Target Feature	Sensor Modality	Input Dimensions	End Effector Response	Decision Criteria/ Threshold
Ground Base	TOF (VL53L1x)	1D Depth(mm)	System Idle / Navigation	Measured Depth ≈ Dynamic Baseline
Weed Candidate	Esp32 S3 camera + TOF	RGB Image + 1D Depth	UMI Action (e.g., Targeted Laser Fire)	INT8 Inference Confidence > 70% & Depth Valid
Target Crop	Esp32 S3 camera + TOF	RGB Image + 1D Depth	UMI Action (e.g. Nutrient supply)	INT8 Inference Confidence > 70% & Depth Valid

The system employs an adaptive Edge AI framework, utilising Edge Impulse for Microcontrollers on the ESP32-S3. To optimize memory and latency, trained models are quantized to INT8 format (Donskoy et al., 2025). Enhancing agricultural versatility, the robot dynamically downloads crop-specific ML models (e.g., tomato, chili) from a cloud server via Wi-Fi based on current operational needs. Locally, the ESP32-S3 fuses onboard camera imagery with Time of Flight (ToF) spatial data to classify targets (Patel et al., 2025). Upon detection, the system halts and activates the appropriate end-effector, such as a precision laser or nutrient pump, dynamically determined by the attached UMI module's resistor ID (detailed in Table 1). Simultaneously, a live Wi-Fi dashboard broadcasts real-time inference data, ToF height graphs, and row-scan maps for remote facility management.

3 RESULTS AND DISCUSSION

A custom dataset of 600 images, captured via the ESP32-S3 camera, was utilised to train a quantized INT8 MobileNetV2 architecture using transfer learning and data augmentation within Edge Impulse. Initial validation of the TerraBOT platform confirmed the viability of its mechanical architecture and real-time sensor fusion capabilities. The Universal Modular Interface (UMI) and CNC-grade gantry were successfully assembled, enabling rapid end-effector interchangeability while maintaining structural integrity. Simultaneously, the dual ESP32-S3 electronic framework established seamless, stable communication and successfully initialised the

onboard sensor array.

Table 2. Real-Time Sensor Fusion Telemetry and Dynamic Actuation Results

Scan point (X-Axis mm)	TOF Distance (mm)	APDS-9960 (Green Intensity)	APDS-9960 (Red Intensity)	System Classification	Actuation Trigger
0	400	25	45	Ground Base	System Idle
20	395	30	50	Ground Base	System Idle
40	150	180	60	Crop	Precision NPK Dosing
60	145	190	65	Crop	Precision NPK Dosing
80	405	22	42	Ground Base	System Idle
100	210	140	90	Weed Candidate	Targeted Laser Fire
120	205	145	85	Weed Candidate	Targeted Laser Fire
140	390	28	48	Ground Base	System Idle

To evaluate the system's target classification capabilities, a test dataset was generated dynamically without manual measurements. As the X-axis gantry traversed the canopy, the primary ESP32-S3 automatically logged ToF depth and APDS-9960 multispectral intensities at precise 20 mm intervals (Table 2). These real-time readings were transmitted via ESP-NOW to construct the dataset, as illustrated in the plotted scan sequence (Figure 3). The ToF sensor successfully established a ground baseline distance averaging between 390 mm and 405 mm, reliably flagging any spatial variances as potential plant structures. For instance, distance measurements dropped significantly to the 145–150 mm range (at X-axis points 40–60 mm) and the 205–210 mm range (at X-axis points 100–120 mm), effectively isolating plants from the ground base. However, relying solely on ToF height data is insufficient for accurate target identification. This limitation was resolved through sensor fusion with the APDS-9960, which measured specific colour channel intensities. As the data in Table 2 indicates, the first detected structure exhibited a high green channel intensity (180–190) and a lower red intensity (60–65), leading the system to classify it as a crop. In contrast, the second structure displayed a lower green intensity (140–145) alongside a proportionately higher red intensity (85–90), accurately triggering the weed candidate classification.

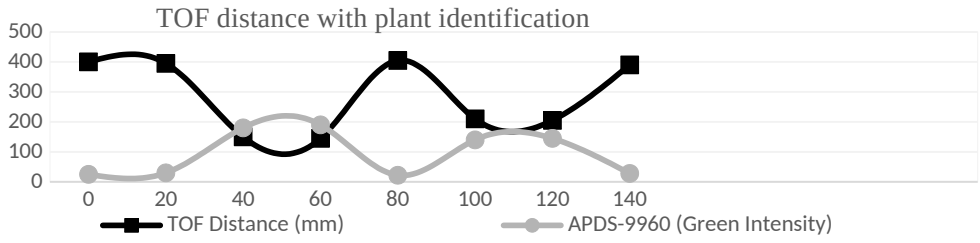


Figure 3. Real-Time Spatial and Optical Data Variation Across the Scan Sequence

This early-stage sensor fusion efficiently pre-filters targets based on spatial and optical thresholds, significantly reducing the computational load on the INT8 TinyML model. Theoretical benchmarks based on this architecture indicate that the platform can reliably achieve the 200-millisecond edge inference times required for real-time, cloud-independent actuation. Ultimately, this logic allows TerraBOT to seamlessly toggle between fertiliser mode for crops and weed mode for identified weeds, demonstrating the robustness of the automated system.

3.1 Impact of Model Quantisation for Edge Deployment

To enable real-time execution on the resource-constrained ESP32-S3 microcontroller, the baseline neural network was quantized from a standard Float32 architecture to an INT8 format. An analysis was conducted to evaluate the impact of this TinyML optimisation on classification performance. As detailed in Table 3, the unoptimised Float32 model achieved a baseline validation accuracy of 96.0% with a loss of 0.208. Following INT8 quantisation, the model maintained a highly robust accuracy of 94.0%.

This negligible accuracy reduction of 2.0% is highly acceptable, given the significant reduction in RAM and Flash memory requirements. Furthermore, the system exhibited excellent sensitivity in identifying invasive plants, maintaining a recall rate of 0.98 for the weed class across both optimised and unoptimised versions. This ensures that the platform rarely misses a weed candidate, successfully validating the reliability of the edge AI actuation framework.

Table 3. Impact of INT8 Quantisation on Edge Classification Metrics

Performance Metric	Unoptimised Model (Float32)	Edge-Optimised Model (INT8)
Overall Accuracy	96.0%	94.0%
Model Loss	0.208	0.230
Crop Class F1-Score	0.957	0.935
Weed Class F1-Score	0.962	0.944
Weed Class Recall	0.981	0.981

4 LIMITATIONS AND FUTURE WORKS

While the current prototype successfully validates core modular navigation and edge classification, several technical limitations must be acknowledged. Environmental factors, such as extreme sunlight glare and dynamic lighting variations, can occasionally impact optical sensor and camera precision under field conditions. Furthermore, the data set utilised in this initial phase is constrained by limited sample variance. Future work will focus on expanding the training dataset to encompass diverse crop species and growth stages across varying outdoor illumination conditions. Additionally, research will be directed toward optimising on-board inference speeds, refining physical actuation mechanisms, and conducting long-term agricultural field trials to rigorously evaluate mechanical endurance in muddy and unstructured terrains.

5 CONCLUSION

This research successfully designed and integrated the foundational hardware and electronic architecture for TerraBOT, a modular robotic platform tailored for regional smallholder farmers. By engineering a system centred around dual ESP32-S3 microcontrollers and a Universal Modular Interface (UMI), this study demonstrated that complex agricultural tasks can be effectively localised without reliance on cloud infrastructure. While future work will focus on extensive field deployment and the rigorous training of crop-specific TinyML models, the current integration phase establishes that low-cost, multifunctional chassis designs present a viable alternative to rigid, commercial single-purpose robots.

6 ACKNOWLEDGEMENTS

The authors gratefully acknowledge the support and facilities provided by the Division of Electrical, Electronic and Telecommunication Engineering Technology, Institute of Technology, University of Moratuwa.

7 REFERENCES

Chen, Y., & Kumar, S. (2025). Overcoming latency in agricultural robotics: A transition from cloud to TinyML inference on microcontrollers. Computers and Electronics in Agriculture, 230, 108431.

Donskoy, D., Gvindjiliya, V., & Ivliev, E. (2025). TinyML classification for agriculture objects with ESP32. Digital, 5(1), 48–61.

Gonzalez, R., & Iagnemma, K. (2025). Slip compensation and odometry correction for autonomous agricultural rovers on unstructured terrains. IEEE Robotics and Automation Letters, 10(2), 845–852.

Heydari, S., & Mahmoud, Q. H. (2025). Tiny machine learning and on-device inference: A survey of applications, challenges, and future directions. Sensors, 25(10), 3191.

Kanchalwar, B., Dhobale, V., Chandurkar, M., Marne, S., Chavan, S., & Patil, P. (2024). Crop weed detection to improve the crop yield using AI and IoT. In Proceedings of International Conference on Smart Agriculture and Artificial Intelligence Systems (pp. 257–272). Springer.

Patel, N., Kim, Y., & Zhao, H. (2025). Real-time crop and weed differentiation utilising Time-of-Flight and multispectral sensor fusion at the edge. Sensors and Actuators A: Physical, 368, 115022.

Sharma, A., & Lee, K. (2025). Low-latency wireless communication in decentralised agricultural IoT using the ESP-NOW protocol. IEEE Internet of Things Journal, 12(4), 4150–4158.

Silva, A., Martinez, J., & Wang, L. (2025). Edge-computing frameworks for real-time weed recognition in resource-constrained farming environments. IEEE Access, 13, 45210–45222.

Srivastava, A. K., Goering, C. E., & Buckmaster, D. R. (2024). Engineering principles of agricultural machines (3rd ed.). American Society of Agricultural and Biological Engineers.

Terziyska, M., Ilieva, I., Terziyski, Z., & Komitov, N. (2025). A review of the transition from Industry 4.0 to Industry 5.0: Unlocking the potential of TinyML in industrial IoT systems. Science, 8(1), 10–28.

ISSN: 2773-7055
Proceedings of the 5th International Research Conference
Institute of Technology, University of Moratuwa
November 5, 2026

Paper ID: 52

IDENTIFICATION OF THE EFFECTIVENESS OF USING STRUCTURED REFLECTION AND FLIPPED LEARNING TO MITIGATE MISCONCEPTIONS IN UML MODELLING

Pathini Lankika[1*], Chalini Silva[1], Shashika Ruwanmini[1]

[1]Division of Information Technology, Institute of Technology, University of Moratuwa, Homagama, Sri Lanka

*Corresponding author: pathinil@itum.mrt.ac.lk

ABSTRACT: UML (Unified Modelling Language) modelling is a core component of software engineering education. Even in the era of AI-driven development and evolving educational practices, UML remains a crucial abstraction tool for designing complex systems. However, students frequently experience conceptual confusion when constructing UML diagrams. This study examines the relationship between structured reflective learning within a flipped classroom approach and students' reflective and conceptual performance in UML diagram modelling among undergraduate diploma students enrolled in an Object-Orientated Analysis and Design module. Although both quantitative and qualitative data were collected, this paper reports only the quantitative findings from weekly reflection and UML mind-map assessment scores. A seven-week intervention was implemented involving pre-class learning, teacher-led instruction, in-class modelling activities, structured reflective-writing exercises, discussion sessions, and diagram correction and redrawing. Of the 92 students enrolled, 83 (90.2%) completed all seven weekly reflective-writing assessments and the final UML mind-map assessment and were included in the analysis. Weekly mean reflection scores generally increased from 4.02 (SD = 1.38) in Week 06 to 7.31 (SD = 1.64) in Week 12, despite a temporary decline in Week 10. Because the weekly activities addressed different UML topics, this pattern represents a descriptive change in reflective performance rather than direct evidence that all UML misconceptions were reduced. A weak positive correlation was observed between average reflection performance and UML mind-map scores (r = .309, p = .004), indicating that students with stronger reflective performance tended to obtain higher mind-map scores. Simple linear regression showed that average reflection performance significantly predicted UML mind-map scores, although the model explained only 9.6% of the variance (R^2 = .096, p = .004). These findings suggest that reflection performance is positively associated with students' conceptual organisation but has limited explanatory power. Structured reflection may therefore serve as a useful complementary strategy within flipped learning, rather than as a sufficient approach on its own, for supporting reflective reasoning and conceptual development in UML modelling.

Keywords: Unified Modelling Language, reflective learning, flipped classroom, reflective reasoning, conceptual organisation

1 INTRODUCTION

Even with the dynamic changes of AI-assisted software tools and models, UML (Unified Modelling Language) continues to play a fundamental role in designing complex systems to provide better communicational understanding for stakeholders (Al-Ahmad et al., 2025). Furthermore, some scholarly research studies report that UML is still a foundational representation used for validating system design (Wang et al., 2026). Therefore, it can be concluded that diagrammatic modelling is an important skill in software engineering education, allowing students to represent system structures and behaviours visually. Research in various computing education fields have

highlighted that diagrammatic modelling tasks, such as those involving Unified Modelling Language (UML), impose significant cognitive challenges for learners. A key challenge arises from two levels of understanding: the conceptual domain of the software system being modelled and the graphical notation system used to represent it. This dual processing requirement increases cognitive load and often leads to misunderstandings in diagram construction and interpretation (Amálio et al., 2019; Chren et al., 2019; Reuter et al., 2020). Reflective and feedback-orientated learning practices can support error recognition, iterative refinement, and metacognitive awareness during learning (Ardimento et al., 2026; Merkebu et al., 2024). This study is motivated by observations from these similar studies and classroom observations where students demonstrated difficulties in constructing UML diagrams. To address this issue, a structured reflective learning intervention was introduced within a flipped UML teaching context. The purpose of this study is to examine students' reflective-writing performance and its relationship with UML conceptual organisation within a structured reflective learning intervention integrated with a flipped classroom approach. The research questions in the study are

1. What is the level of students' engagement in weekly reflective writing activities during the intervention?
2. How does reflective learning contribute to students' conceptual organisation and performance in UML modelling tasks?
3. To what extent does reflective writing predict students' conceptual understanding in UML diagram modelling?

2 METHODOLOGY

This study employed a one-group intervention design to examine the relationship between students' structured reflective-writing performance and their UML conceptual performance within a flipped classroom learning environment. Although the overall study adopted a mixed-methods design, this paper reports only the quantitative findings. The participants in this study were diploma students enrolled in the Object-Oriented Analysis and Design module (IT1206) in the National Diploma Technology in Information Technology programme. The study was conducted with a class of 92 students. However, only students who completed all weekly reflective writing activities and the UML mind map assessment were included in the final analysis. Consequently, data from 83 students were analysed, while nine records with incomplete submissions were excluded. A flipped classroom approach was implemented as part of the instructional design. Pre-class learning materials were distributed one week in advance to enable students to develop preliminary conceptual understanding before attending classroom sessions. Each weekly session followed by a structured instructional sequence. First, the lecturer conducted a teacher-led session introducing a specific UML diagram type and relevant application scenarios. Students then completed a structured handwritten reflective writing assessment in which they documented their understanding of UML diagram elements, explained their reasoning, and completed a short modelling task. To ensure that the reflections represented students' own understanding and metacognitive processes, the use of AI-assisted tools and other

external resources was not permitted during the assessment. These reflections were collected and reviewed by the lecturer and supporting teaching assistant. After the reflection phase, a teacher-led discussion and redrawing session were conducted. During this stage, students revisited the same modelling task, compared their initial diagrams with corrected versions, discussed alternative modelling decisions, and identified conceptual gaps. This process helped students recognise errors in their initial thinking and supported the development of metacognitive awareness through guided discussion. In Week 13, students were asked to construct conceptual mind maps to represent their understanding of UML modelling concepts. Reflective writing was selected because it provided evidence of students' conceptual understanding, reasoning, error recognition, and reconsideration of modelling decisions. Mind mapping was selected as a complementary measure because it enabled students to organise UML concepts and demonstrate meaningful relationships among them.

All reflective writings and the quality of mind maps were evaluated using a standardised rubric to minimise subjective bias. The weekly reflective-writing assessments were marked out of 10 using criteria related to conceptual understanding, justification of modelling decisions, identification and correction of errors or conceptual gaps, and reflection on future improvement. These criteria were selected to capture students' reflective reasoning, misconception recognition, self-correction, and metacognitive awareness. The UML mind maps were marked out of 100 based on the accuracy of UML concepts and relationships, completeness, conceptual organisation, appropriate terminology and notation, and overall clarity. These criteria were selected because an effective UML mind map should demonstrate not only knowledge of individual concepts but also the student's ability to organise them and represent technically meaningful relationships. A detailed rubric formalising these assessment criteria is provided as supplementary material to improve measurement transparency.

3 RESULTS AND FINDINGS

The quantitative data were analysed using descriptive statistics to summarise students' weekly reflective-writing performance and final UML mind-map scores. Pearson's correlation and simple linear regression were used to examine the relationship between average reflection performance and UML mind-map performance.

Table 1. Descriptive Statistics of Students' Reflection Scores and UML Mind Map Performance

Statistic	Average reflection score	Mind Map Score (out of 100)
Standard deviation	0.92	16.21
Minimum	3.29	23.00
Mean	5.39	69.31
Maximum	7.43	96.00
Count	83	83
75th percentile	6.14	81.00
Median	5.57	72.00
25th percentile	4.71	62.00

Note: The average reflection score represents each student's mean performance across seven weekly reflective-writing assessments, each scored out of 10. The UML mind-map assessment

was scored out of 100.

Students obtained a mean reflection score of 5.39 (SD = 0.92), with scores ranging from 3.29 to 7.43. The median score (5.57) was close to the mean, indicating an approximately symmetric distribution. All 83 students included in the analysis completed the seven weekly reflection-writing assessments, indicating sustained participation throughout the intervention. The UML mind-map assessment yielded a mean score of 69.31 (SD = 16.21). The median score (72.00) indicated a slight negative skew, while scores ranging from 23.00 to 96.00 demonstrated considerable variation in students' conceptual organisation. Weekly mean reflection scores generally increased from 4.02 (*SD* = 1.38) in Week 06 to 7.31 (*SD* = 1.64) in Week 12, despite a temporary decline in Week 10. However, because the weekly activities addressed different UML topics, this pattern represents a descriptive change in reflective performance rather than direct evidence that all UML misconceptions were reduced.

Table 2. Correlation Between Average Reflection and UML Mind-Map Scores

	Average Reflection Score	**Mind Map Score (Out of 100)**
Average Reflection Score	1.000	.309
Mind Map Score (Out of 100)	.309	1.000

A weak positive correlation was observed between students' average reflection scores and UML mind-map performance, r = .309, p = .004. This indicates that students who demonstrated stronger reflective performance tended to obtain higher mind-map scores. However, the modest strength of the relationship suggests that reflective performance was only one of several factors associated with students' conceptual organisation.

OLS Regression Results

Dep. Variable:	MindMap_100	R-squared:	0.096
Model:	OLS	Adj. R-squared:	0.084
Method:	Least Squares	F-statistic:	8.556
Date:	Sat, 27 Jun 2026	Prob (F-statistic):	0.00447
Time:	11:15:15	Log-Likelihood:	-344.33
No. Observations:	83	AIC:	692.7
Df Residuals:	81	BIC:	697.5
Df Model:	1		
Covariance Type:	nonrobust		

	coef	std err	t	P>|t|	[0.025	0.975]
const	40.0009	10.165	3.935	0.000	19.776	60.226
Reflection_Avg	5.4393	1.860	2.925	0.004	1.739	9.139

Omnibus:	5.002	Durbin-Watson:	1.925
Prob(Omnibus):	0.082	Jarque-Bera (JB):	4.781
Skew:	-0.588	Prob(JB):	0.0916
Kurtosis:	2.977	Cond. No.	33.7

Figure 1. Linear Regression Analysis Predicting UML Mind Map Performance from Reflection Scores

Simple linear regression showed that average reflection performance significantly predicted UML mind-map scores, $F(1, 81) = 8.56$, p = .004. The model explained 9.6% of the variance in mind-map performance (R^2 = .096). The positive unstandardised coefficient (B = 5.44) indicates that a one-point increase in the average reflection score was associated with an estimated 5.44-point increase in the mind-map score. Although statistically significant, the model had limited explanatory power. The remaining variation may be related to factors not measured in this study, such as prior UML knowledge, spatial reasoning, diagrammatic literacy, pre-class preparation, and individual learning differences.

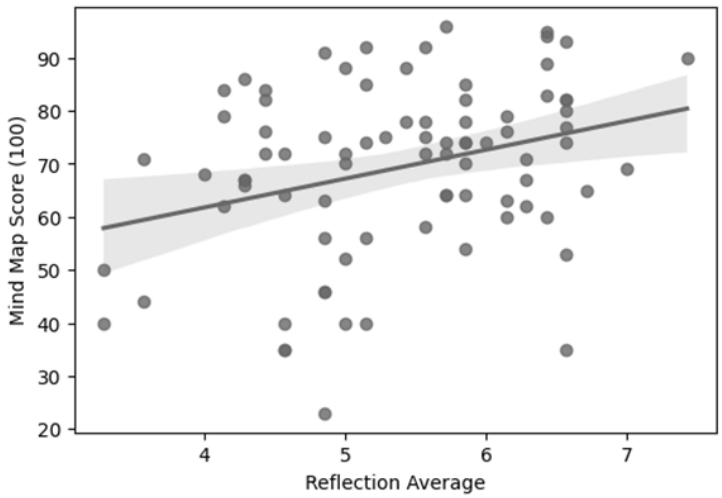


Figure 2. Scatter Plot of Average Reflection and UML Mind-Map Scores

The scatter plot shows a general upward trend, indicating a positive association between average reflection and UML mind-map scores. The regression line confirms this pattern, suggesting that students with higher reflection scores tended to achieve higher mind-map scores. However, the spread of data points around the regression line indicates considerable variability among students, meaning that reflection performance alone did not fully explain differences in mind-map performance.

4 CONCLUSION

The results indicate that using a reflective learning strategy within a flipped classroom environment was positively associated with students' understanding of UML modelling. The weak positive relationship between reflection and mind-map performance (r = .309, p = .004) and the significant regression model (R^2 = .096) suggest that students with stronger reflective performance tended to obtain higher mind-map scores. However, these results also indicate that reflection explained only a small proportion of the variation in conceptual organisation. The remaining variation may be related to factors not measured in this study, including prior UML knowledge, spatial reasoning, diagrammatic literacy, pre-class preparation, and individual learning differences. The flipped classroom structure, which combined pre-class preparation, in-class modelling, and iterative reflection activities, appeared to support students' reflective reasoning and conceptual development. Overall, structured reflection can be used as a complementary classroom strategy that encourages students to explain their modelling decisions, identify conceptual gaps, compare alternative solutions, and correct and redraw UML diagrams. However, it should be combined with other instructional approaches rather than treated as a sufficient strategy on its own. The study involved one intact class at a single institution, used a complete-case analytical sample of 83 students, and did not include a control group or a pre-intervention measure of UML conceptual understanding. Accordingly, the findings should not be generalised beyond similar educational settings without further investigation. Future research should employ controlled or pre-test–post-test designs to compare structured reflection with alternative instructional strategies and examine the long-term retention and transfer of UML modelling skills. The

findings contribute to computing education research by providing quantitative evidence on the role of structured reflection within a flipped UML learning environment.

5 REFERENCES

Al-Ahmad, B., Alsobeh, A., Meqdadi, O., & Shaikh, N. (2025). A student-centric evaluation survey to explore the impact of LLMs on UML modelling. *Information, 16*(7), Article 565. https://doi.org/10.3390/info16070565

Amálio, N., Briand, L., & Kelsen, P. (2020). An experimental scrutiny of visual design modelling: VCL up against UML+OCL. *Empirical Software Engineering, 25*(2), 1205–1258. https://doi.org/10.1007/s10664-019-09784-9

Ardimento, P., Bernardi, M. L., Cimitile, M., & Scalera, M. (2026). A conversational tool for AI-driven feedback for UML modelling. *Software and Systems Modelling*. Advance online publication. https://doi.org/10.1007/s10270-026-01373-x

Chren, S., Buhnova, B., Macak, M., Daubner, L., & Rossi, B. (2019). Mistakes in UML diagrams: Analysis of student projects in a software engineering course. In *2019 IEEE/ACM 41st International Conference on Software Engineering: Software Engineering Education and Training (ICSE-SEET)* (pp. 100–109). IEEE. https://doi.org/10.1109/ICSE-SEET.2019.00019

Merkebu, J., Veen, M., Hosseini, S., & Varpio, L. (2024). The case for metacognitive reflection: A theory integrative review with implications for medical education. *Advances in Health Sciences Education, 29*, 1481–1500. https://doi.org/10.1007/s10459-023-10310-2

Reuter, R., Stark, T., Sedelmaier, Y., Landes, D., Mottok, J., & Wolff, C. (2020). Insights in students' problems during UML modelling. In *2020 IEEE Global Engineering Education Conference (EDUCON)* (pp. 592–600). IEEE. https://doi.org/10.1109/EDUCON45650.2020.9125110

Wang, C., Wang, B., Liang, P., & Liang, J. (2026). Assessing UML diagrams by GPT: Implications for education. *Journal of Systems and Software, 234*, Article 112709. https://doi.org/10.1016/j.jss.2025.112709

ISSN: 2773-7055
Proceedings of the 5th International Research Conference
Institute of Technology, University of Moratuwa
November 5, 2026

Paper ID: 56

ADAPTIVE DEEP REINFORCEMENT LEARNING FOR MISINFORMATION MANAGEMENT: A CRISIS-RESPONSE SIMULATION FRAMEWORK

L A S S S Samadhi[1*], P N T Pathirana[1]

[1]Division of Information Technology, Institute of Technology, University of Moratuwa, Homagama, Sri Lanka

*Corresponding author: sanayasamadhi@gmail.com

ABSTRACT: In times of crisis, misinformation often proliferates, creating serious challenges to public trust and information management. Current misinformation detection systems are mostly based on supervised learning models focused on classification accuracy, with limited ability to support adaptive intervention decisions. This study introduces the concept of adaptive misinformation management and designs and implements a Deep Reinforcement Learning (DRL) framework to simulate an intervention environment. Articles from the Fake and Real News dataset were preprocessed and represented using Term Frequency–Inverse Document Frequency (TF-IDF). A Logistic Regression (LR) detector was used as a baseline misinformation detector, achieving 99% classification accuracy. A Deep Q-Network (DQN) agent was designed to make adaptive intervention decisions in a custom simulated environment that includes four possible intervention actions: Ignore, Flag, Fact-Check, and Escalate. A reward system was developed to encourage appropriate interventions while reducing missed interventions and unnecessary responses to legitimate content. Experimental results showed that policy learning took place successfully in the simulated environment, with cumulative rewards increasing from 164.8 to 988.9 over 50 training episodes. The results demonstrate the feasibility of using reinforcement learning to augment traditional misinformation classification with adaptive intervention decision-making under controlled simulated conditions. The framework was evaluated using a dataset applicable to a wide range of contexts rather than crisis- or conflict-specific data. Therefore, its effectiveness in real-world crisis and conflict environments has not yet been validated.

Keywords: misinformation management, deep reinforcement learning, deep Q-network, fake news detection, adaptive intervention, crisis response

1 INTRODUCTION

The rapid growth of digital communication platforms has accelerated the spread of misinformation, particularly during crises such as pandemics, natural disasters, and armed conflicts, where false information can undermine public trust and emergency response efforts (Bondielli, 2019). Consequently, automated misinformation detection has become an important research area within Natural Language Processing (NLP), Machine Learning (ML), and Artificial Intelligence (AI). Traditional approaches rely on supervised learning algorithms such as Logistic Regression, Support Vector Machines, and Random Forests to classify news as genuine or misleading (Bondielli, 2019). More recently, deep learning models, including CNNs, LSTMs, and BERT, have significantly improved classification performance (Devlin, 2019), including domain-specific variants such as FakeBERT, which combines BERT-based embeddings with convolutional layers for social media fake-news detection (Kaliyar et al., 2021). However, existing fake news detection systems primarily function as static classifiers and focus only on identifying whether news is fake or real, whereas crisis management also requires intelligent decision-making that adapts intervention strategies according to misinformation severity and

the evolving crisis context. Reinforcement Learning (RL) addresses this limitation by enabling agents to learn adaptive decision-making policies through continuous interaction with the environment (Sutton & Barto, 2018). Prior research has applied reinforcement learning to misinformation-related tasks: Mosallanezhad et al. (2022) proposed a reinforcement-learning approach for domain-adaptive fake news detection, while more recent studies have combined RL with large language models for stance detection and rumor debunking (Yang et al., 2024) and for reinforced sampling in fake news detection pipelines (Tong et al., 2025). In particular, Deep Q-Networks (DQNs) have demonstrated strong performance in sequential decision-making tasks (Mnih, 2015). Building on this line of work, this study proposes a Deep Reinforcement Learning framework that complements traditional misinformation detection with a DQN-based decision-making mechanism capable of dynamically selecting intervention strategies, including Ignore, Flag, Fact-Check, and Escalate, within a simulated intervention environment.

2 METHODOLOGY

This study proposes a hybrid framework integrating supervised machine learning and Deep Reinforcement Learning (DRL) for adaptive misinformation management during crises. The overall methodology consists of data preprocessing, misinformation classification using Logistic Regression, and adaptive intervention through a Deep Q-Network (DQN) agent.

2.1 Dataset and Data Preprocessing

Experiments were conducted using the Kaggle Fake and Real News Dataset, consisting of 44,898 news articles, including 23,481 fake news samples and 21,417 real news samples. The dataset has been widely used in misinformation detection studies due to its suitability for benchmarking machine learning algorithms (Shu, 2017). The dataset is general-purpose rather than crisis-specific; therefore, it was used to establish and evaluate the mechanics of the proposed DRL framework under controlled conditions. Validation using crisis- and conflict-specific datasets is an important direction for future research. Textual data were preprocessed prior to model training to improve classification performance. Preprocessing steps included lowercase conversion, removal of punctuation and special characters, stop-word removal, and text normalisation. Subsequently, the cleaned text was transformed into numerical feature vectors using the Term Frequency–Inverse Document Frequency (TF-IDF) technique, which is commonly employed in text classification tasks (Bondielli, 2019). A Logistic Regression classifier was implemented as a baseline misinformation detection model. The classifier was trained using TF-IDF feature vectors and evaluated using accuracy, precision, recall, and F1-score metrics. The predicted class labels were subsequently used as the basis for the reinforcement learning environment, enabling the DQN agent to determine the most appropriate intervention strategy.

2.2 Problem Formulation

Misinformation management during crises can be formulated as a sequential decision-making problem. Rather than merely determining whether a news article is fake or real, an intelligent system must decide how to respond to the information in a manner that minimises misinformation

propagation while preserving information accessibility. The proposed framework models the misinformation management process as a Markov Decision Process (MDP), represented by the tuple $M = (S, A, P, R, \gamma)$,where: S denotes the state space, A denotes the action space, P represents state transition probabilities, R denotes the reward function and γ denotes the discount factor.

State Space - Each state corresponds to a TF-IDF representation of a news article: $S_t = \{x_1, x_2, ..., x_n\}$ where $x_i$represents a TF-IDF feature.

Action Space - The action space comprised four intervention actions, namely Ignore (A0), Flag (A1), Fact-Check (A2), and Escalate (A3), representing the possible responses to detected misinformation.

Reward Function – The reward mechanism was designed to encourage stronger interventions for misinformation while penalizing unnecessary intervention on legitimate content. Reward magnitudes increase with action severity (Ignore < Flag < Fact-Check < Escalate) when applied to misinformation, reflecting the assumption that stronger interventions carry greater value against confirmed fake content during a crisis. Conversely, the same actions receive penalties that also scale with severity when applied to legitimate content, discouraging unnecessary intervention that could suppress accurate crisis information. Table 1 summarizes the reward values used.

Table 1. Reward values assigned per (action, true label) pair

Agent Action	True Label: Fake / Misinformation	True Label: Real / Legitimate
Ignore (A0)	−5.0 (missed intervention)	+1.0 (correctly left alone)
Flag (A1)	+2.0 (partial mitigation)	−1.0 (unnecessary friction)
Fact-Check (A2)	+5.0 (verified correction)	−2.0 (wasted verification effort)
Escalate (A3)	+8.0 (severity-appropriate response)	−4.0 (over-escalation penalty)

These values were set manually based on the relative cost of under- and over-intervention in a crisis-response context, rather than learned or elicited from domain experts.

Objective Function – The agent seeks to maximise cumulative discounted rewards, $G_t = \Sigma$ (k=0 to ∞) γ^k R_{t+k+1}.

2.3 Deep Reinforcement Learning Environment

A custom misinformation management environment was designed to simulate decision-making scenarios. Each news article was treated as an environment state, while intervention actions represented possible responses to misinformation.

2.3.1 System Architecture

The proposed framework integrates supervised learning and reinforcement learning components to create an adaptive misinformation management system, as shown in **Figure 1.**

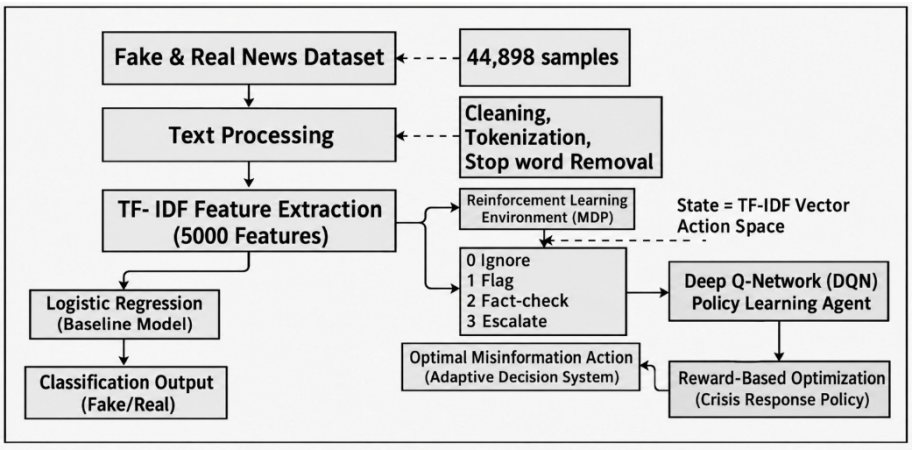


Figure 1. System architecture of the proposed hybrid detection–intervention framework.

Deep Q-Network Architecture- The DQN architecture comprised an input layer (5,000 neurons), two fully connected hidden layers (128 and 64 neurons), and an output layer with four neurons representing Q-values for the available intervention actions.

Experience Replay and Target Network - To improve training stability, Experience Replay Memory was employed to store historical transitions:(s_{t+1}). A separate Target Network was periodically updated to reduce Q-value oscillations during training.

Loss Function -The Mean Squared Error (MSE) loss function was utilised to minimise the difference between predicted and target Q-values: - $L(\theta) = E[(Q(s,a;\theta) - y)^2]$. The target Q-value was computed using: - $y = r + \gamma maxQ(s^{'}, a^{'}, \theta^{-})$

Experimental Setup -The DQN model was trained for 50 episodes using a learning rate of 0.001, a discount factor (γ) of 0.99, a batch size of 64, and a replay memory capacity of 5,000. The exploration rate (ε) was gradually decayed from an initial value of 1.0 to a final value of 0.01.

Evaluation Metrics - The Logistic Regression model was evaluated using Accuracy, Precision, Recall and F1-score. The DQN model was evaluated using Cumulative Reward, Learning Curve Convergence and Action Distribution Analysis.

3 RESULTS AND DISCUSSION

The Logistic Regression classifier demonstrated excellent performance on the misinformation dataset, achieving an overall classification accuracy of 99%. The confusion matrix shown in **Figure 2(a)** indicates that the model correctly classified 23,260 fake news articles and 21,278 real news articles. Only 221 fake news instances were misclassified as real news, while 139 real news articles were incorrectly identified as fake news. The results demonstrate that the combination of TF-IDF feature extraction and Logistic Regression provides an effective approach for misinformation classification. The high accuracy (99%) and balanced precision, recall, and F1-score values (0.99) indicate strong classification performance with minimal bias between classes. As shown in **Figure 2(b)**, the trained DQN agent predominantly selected the Escalate action (53.6%), indicating that it learned to favour this intervention strategy under the defined reward structure. This extends conventional classification by adding an adaptive decision-making layer. However, the action distribution is directly influenced by the manually

specified reward weights in Table 1 and should therefore be interpreted as evidence of the learned policy within the simulated environment rather than as an independently validated crisis-response recommendation.

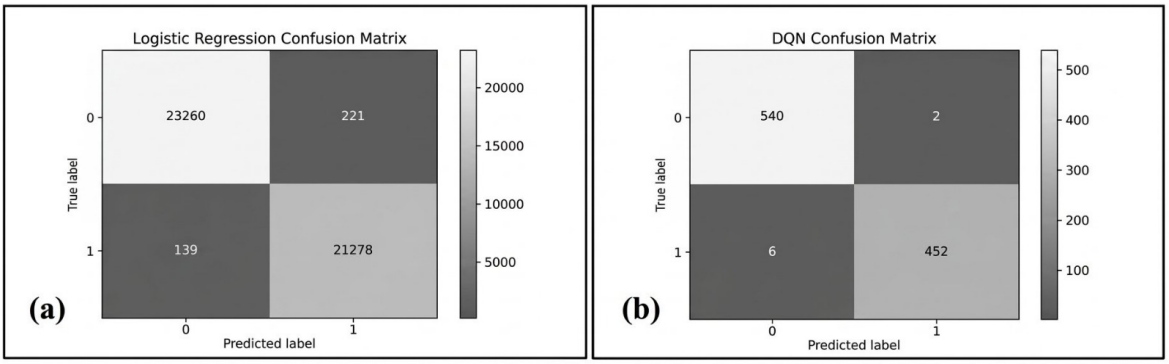


Figure 2. (a) Confusion matrix for the Logistic Regression classifier; (b) action distribution of the trained DQN agent.

As shown in **Figure 3**, the DQN agent exhibited a steady increase in cumulative reward over 50 training episodes, increasing from an initial reward of approximately 164.8 to a maximum reward of 988.9. This upward trend indicates that the agent learned policies that increased cumulative reward within the simulated environment. The reward curve suggests that the DQN agent learned an adaptive intervention policy under the defined simulation and reward structure.

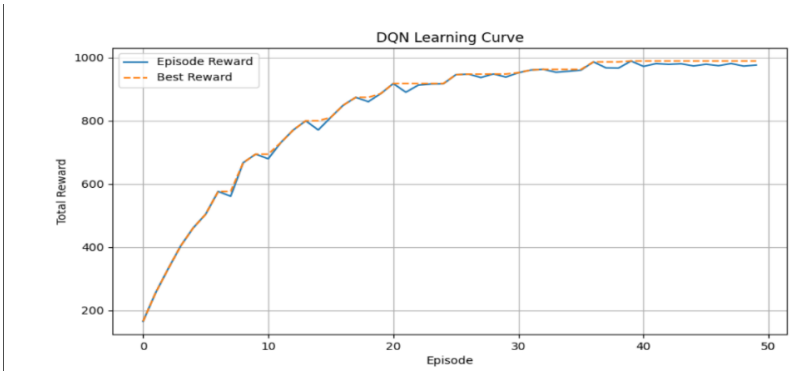


Figure 3. DQN learning curve illustrating the cumulative reward obtained during the learning process.

3.1 Adaptive Decision-Making Analysis

Compared with recent work, transformer-based classifiers such as FakeBERT (Kaliyar et al., 2021) and progressive-training BERT approaches (Raza et al., 2025) achieve comparable or higher classification accuracy than the Logistic Regression baseline but do not generate intervention policies. RL-based approaches, including Mosallanezhad et al. (2022) and Tong et al. (2025), are closer to this study because they use reinforcement signals for detection or sampling, but they are also mainly evaluated on static benchmark datasets. The contribution of this framework is therefore its decision layer rather than improved classification accuracy, as Logistic Regression already achieves 99% accuracy. The DQN developed a preference for Escalate under the specified reward structure, while the increase in cumulative rewards indicates policy learning within the simulated environment. Thus, the DQN extends misinformation classification with adaptive intervention decision-making.

4 LIMITATIONS

Several limitations should be considered when interpreting these results. First, the framework was evaluated using the general-purpose Kaggle Fake and Real News Dataset rather than crisis- or conflict-specific data. Thus, the study's title and framing describe an intended application domain, not one already validated, and the results should not be interpreted as evidence of performance during an actual pandemic, disaster, or conflict. Second, the reward function (Table 1) was manually defined based on the authors' judgement of intervention severity rather than crisis-response expert input or observed outcomes; different weightings could produce different policies. Third, the four intervention actions (Ignore, Flag, Fact-Check, Escalate) and their consequences were simulated in a custom environment rather than tested in an operational emergency-response or content-moderation system, leaving real-world effectiveness untested. Fourth, no direct empirical comparison was conducted with recent transformer-based (Fake-BERT, Raza et al., 2025) or reinforcement-learning-based (Mosallanezhad et al., 2022; Tong et al., 2025) systems using the same dataset and protocol; comparisons in Section 3 are conceptual. Future work should address these limitations through crisis-specific data, expert-informed reward design, human-in-the-loop or live evaluation, and head-to-head benchmarking.

5 CONCLUSION

This work introduces an Adaptive Misinformation Management framework based on Deep Reinforcement Learning (DRL) in a simulated intervention environment. The proposed framework extends the traditional misinformation detection system, which is mainly a classification process, by adding a Deep Q-Network (DQN) agent to learn intervention decisions through interaction with the simulated environment. The experimental results demonstrated that the Logistic Regression baseline achieved 99% classification accuracy, while the DQN agent learned an intervention policy over 50 training episodes, resulting in a cumulative reward that increased from 164.8 to 988.9. The results show that it is possible to use reinforcement learning to support adaptive intervention decision-making under controlled simulation conditions as a complement to traditional misinformation classification. The evaluation was not conducted using crisis- or conflict-specific data, but rather the general-purpose Fake and Real News dataset, and the intervention actions were simulated rather than validated in an actual crisis-response setting. Thus, the findings should be understood as evidence of policy learning within the proposed simulation rather than as evidence of effectiveness in real-world crisis or conflict contexts. Future work will involve testing the framework with datasets from specific crisis and conflict contexts to evaluate the framework under more realistic conditions. It will also extend the representation of misinformation propagation to include temporal information and social network dynamics, while exploring transformer-based representations and multi-agent reinforcement learning for more realistic and scalable evaluation.

6 REFERENCES

Bondielli, A., & Marcelloni, F. (2019). A survey on fake news and rumour detection techniques. *Information Sciences, 497*, 38–55. https://doi.org/10.1016/j.ins.2019.05.035

Devlin, J., Chang, M. W., Lee, K., & Toutanova, K. (2019). BERT: Pre-training of deep bidirectional transformers for language understanding. *Proceedings of the 2019 Conference of the North American Chapter of the Association for Computational Linguistics: Human Language Technologies*, 4171–4186. https://doi.org/10.18653/v1/N19-1423

Kaliyar, R. K., Goswami, A., Narang, P., & Sinha, S. (2021). FakeBERT: Fake news detection in social media with a BERT-based deep learning approach. *Multimedia Tools and Applications, 80*(8), 11765–11788. https://doi.org/10.1007/s11042-020-10183-2

Mnih, V., Kavukcuoglu, K., Silver, D., Rusu, A. A., Veness, J., Bellemare, M. G., Graves, A., Riedmiller, M., Fidjeland, A. K., Ostrovski, G., et al. (2015). Human-level control through deep reinforcement learning. *Nature, 518*, 529–533. https://doi.org/10.1038/nature14236

Mosallanezhad, A., Karami, M., Shu, K., Mancenido, M. V., & Liu, H. (2022). Domain adaptive fake news detection via reinforcement learning. *Proceedings of the ACM Web Conference 2022 (WWW '22)*, 3632–3640. https://doi.org/10.1145/3485447.3512258

Raza, N., Abdulkadir, S. J., Abid, Y. A., Albouq, S. S., Alwadain, A., Rehman, A. U., et al. (2025). Enhancing fake news detection with transformer-based deep learning: A multidisciplinary approach. *PLOS ONE*. https://doi.org/10.1371/journal.pone.0330954

Shu, K., Sliva, A., Wang, S., Tang, J., & Liu, H. (2017). Fake news detection on social media: A data mining perspective. *ACM SIGKDD Explorations Newsletter, 19*(1), 22–36. https://doi.org/10.1145/3137597.3137600

Sutton, R. S., & Barto, A. G. (2018). *Reinforcement learning: An introduction* (2nd ed.). MIT Press. http://incompleteideas.net/book/the-book-2nd.html

Tong, Z., Gu, Y., Liu, H., Liu, Q., Wu, S., Shi, H., & Zhang, X.-Y. (2025). Generate first, then sample: Enhancing fake news detection with LLM-augmented reinforced sampling. *Proceedings of the 63rd Annual Meeting of the Association for Computational Linguistics (Volume 1: Long Papers)*, 24276–24290.

Yang, R., Gao, W., Ma, J., Lin, H., & Wang, B. (2024). Reinforcement tuning for detecting stances and debunking rumors jointly with large language models. *arXiv preprint arXiv:2406.02143*.

ISSN: 2773-7055
Proceedings of the 5th International Research Conference
Institute of Technology, University of Moratuwa
November 5, 2026

Paper ID: 66

DEVELOPMENT AND EVALUATION OF PHARMAAI: A HUMAN-CENTRED RULE-BASED EXPERT SYSTEM FOR MEDICATION SAFETY IN COMMUNITY PHARMACY

W S Kodippili[1*], K A D P Lankika[1], M P C M Silva[1]

[1]Division of Information Technology, Institute of Technology, University of Moratuwa, Homagama, Sri Lanka

*Corresponding author: waruni323@gmail.com

ABSTRACT: Medication safety remains a significant challenge in community pharmacy due to increasing prescription complexity, polypharmacy, and the growing risk of medication-related errors, including drug–drug interactions, inappropriate dosing, allergies, contraindications, and therapeutic duplication. Although Clinical Decision Support Systems (CDSS) have demonstrated potential to improve medication safety, most existing systems are designed for hospital settings and do not adequately support the workflow and clinical decision-making processes of community pharmacists. Furthermore, limited adoption of Human-Centred design principles has reduced the transparency, explainability, and acceptance of automated decision support tools. This study aimed to develop and evaluate PharmaAI, a human-centred, deterministic rule-based expert framework for improving medication safety in community pharmacy. A Design Science Research (DSR) methodology was employed to guide the design, development, and evaluation of the framework. The evaluation was conducted using 30 structured, hypothetical outpatient prescription scenarios adapted from published medication safety literature and evidence-based clinical guidelines, distributed evenly across six distinct risk domains to ensure balanced evaluation difficulty. The scenarios and expected outcomes were independently reviewed and validated by three registered pharmacists, whose consensus classifications served as the reference standard for performance evaluation. PharmaAI correctly identified 19 medication-related risk scenarios and 7 clinically appropriate prescriptions, achieving an overall accuracy of 86.7% (95% CI: 69.3% to 96.2%), precision of 90.5% (95% CI: 69.6% to 98.8%), recall of 90.5% (95% CI: 69.6% to 98.8%), specificity of 77.8% (95% CI: 40.0% to 97.2%), and an F1-score of 90.5%. The findings provide preliminary evidence that the proposed rule-based framework can identify clinically relevant medication risks while providing transparent and explainable recommendations intended to support pharmacist decision-making without replacing professional judgement. PharmaAI provides an ethical, scalable, and human-centred foundation for automated clinical decision support in community pharmacy and offers a basis for future validation using larger real-world clinical datasets.

Keywords: deterministic expert system, clinical decision support system, medication safety, community pharmacy, human-centred computing

1 INTRODUCTION

Medication safety is a critical component of healthcare quality, with community pharmacists playing a key role in preventing medication-related harm during the dispensing process. Increasing prescription complexity, the growing prevalence of chronic diseases, and the widespread use of multiple medications have increased the risk of medication errors, requiring pharmacists to make timely and accurate clinical decisions. As the final point of contact before medicines reach patients, community pharmacies are well positioned to identify potential medication-related problems, including drug–drug interactions, dosage errors, allergies, contraindications, and therapeutic duplications. However, manual prescription review alone may not be sufficient

to consistently detect these risks, particularly in busy pharmacy environments. The National Institute for Health and Care Excellence (NICE, 2023) emphasises that effective medicines optimisation and systematic medication review are essential to improve patient outcomes and reduce preventable medication-related harm. Recent advances in automated decision systems have created new opportunities to support clinical decision-making by analysing clinical information and providing evidence-based recommendations. Kim et al. (2024) reported that explainable clinical decision support systems (CDSS) can improve the transparency and interpretability of generated recommendations, thereby increasing user confidence in clinical decision-making. Within community pharmacy, automated CDSS can enhance prescription review, improve workflow efficiency, and support safer medication use while preserving the pharmacist's professional judgement. Moon et al. (2023) found that CDSS can support community pharmacists in identifying medication-related problems and improving dispensing safety; however, many existing systems are primarily designed for hospital settings and do not adequately support the workflow and decision-making requirements of community pharmacies. Furthermore, limited transparency, poor explainability, and usability challenges reduce user trust and hinder the adoption of automated systems in routine pharmacy practice. Xu et al. (2023) similarly concluded that improving the interpretability of rule-based CDSS is essential for increasing their acceptance and practical implementation in healthcare. Human-centred design principles address these challenges by promoting collaboration between healthcare professionals and intelligent computing systems through transparency, explainability, and human oversight. Schoonderwoerd et al. (2021) demonstrated that incorporating human-centred explainability into clinical decision support systems improves users' understanding of recommendations and supports safer clinical decision-making. Similarly, Van Dort et al. (2025) highlighted that explainable rule logic integrated into clinical decision support interfaces enhances usability, transparency, and user trust while enabling healthcare professionals to remain responsible for final clinical decisions. Despite these advances, limited research has focused on developing human-centred, rule-based clinical decision support frameworks specifically tailored to the workflow and decision-making requirements of community pharmacy. Therefore, this study aimed to develop and evaluate PharmaAI, a human-centred clinical decision support framework that supports medication safety in community pharmacy by integrating rule-based prescription validation, medication risk detection, and explainable decision support. The framework was developed using the Design Science Research methodology and evaluated through simulated prescription scenarios to assess its functionality and potential contribution to medication safety while supporting pharmacists' clinical decision-making. The present evaluation is intended as an initial proof-of-concept assessment rather than evidence of established clinical effectiveness or readiness for routine clinical deployment.

2 METHODOLOGY

This study adopted the Design Science Research (DSR) methodology to develop and evaluate PharmaAI, a human-centred, deterministic rule-based expert framework for improving medication safety in community pharmacy practice. DSR was selected because it provides a systematic

approach for designing, developing, and evaluating technological artefacts that address practical healthcare problems. The research followed six DSR phases: (1) problem identification, (2) objective definition, (3) design and development, (4) demonstration, (5) evaluation, and (6) communication. The framework was designed by integrating evidence from published studies on medication safety, clinical decision support systems, explainable interfaces, and human-centred design principles. The Medication Knowledge Base forms the clinical foundation of the framework and contains evidence-based medication-safety knowledge used to assess prescriptions. The deterministic clinical rules address prescription validation, drug–drug interaction detection, dosage verification, allergy screening, contraindication assessment, therapeutic duplication detection, and patient-specific risk identification. To ensure complete transparency and reproducibility, these rules were manually encoded into logical IF-THEN conditional structures based on source selection criteria derived directly from established national clinical guidelines and peer-reviewed medication-safety literature. Rule conflicts are handled via a rigid priority-ranking system, where absolute contraindications override mild interaction alerts. Version control and regular knowledge-based updates are maintained using systematic manual entry tables linked to quarterly guideline releases. The decision process strictly combines these evidence-based clinical rules with deterministic reasoning logic; no separate machine-learning model, large language model, or external drug database is utilised in this architecture. The conceptual data-flow architecture consists of seven interacting components, as shown in Figure 1:

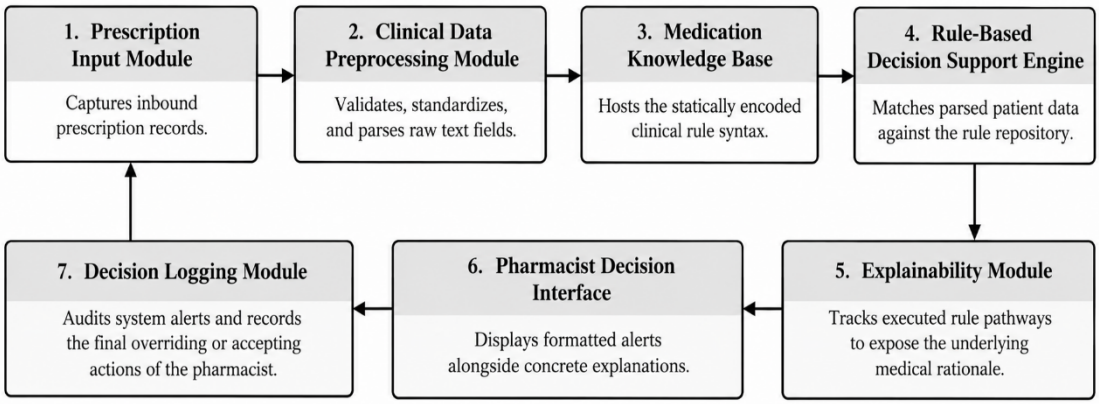


Figure 1. Conceptual architecture and data-flow components of PharmaAI.

This structured framework clarifies that the primary contribution of PharmaAI is the seamless operational integration of evidence-based medication-safety reasoning, deterministic rule checking, explainability, pharmacist oversight, and decision auditing within a community pharmacy environment, rather than the invention of a novel machine-learning algorithm. The framework was evaluated using a simulation-based experimental design to ensure ethical compliance while avoiding the use of patient-identifiable information. A dataset of 30 structured, hypothetical outpatient prescription scenarios was developed by adapting medication safety cases reported in published literature and evidence-based clinical guidelines. The 30-case set serves as an initial proof-of-concept evaluation. To provide a transparent and balanced distribution of difficulty, the evaluation dataset was structured into five distinct clinical test scenarios for each of the six

targeted risk categories: (1) drug–drug interactions, (2) dosage errors, (3) allergy-related prescribing risks, (4) contraindications, (5) therapeutic duplication, and (6) clinically appropriate baseline controls. The study did not use a real-world patient dataset. Because only 30 scenarios were evaluated, the resulting performance percentages are highly sensitive to individual classification changes and must be interpreted as preliminary evidence of framework performance rather than definitive clinical effectiveness.

To ensure clinical validity, the scenarios and their expected outcomes were independently reviewed and validated by three registered pharmacists with experience in community pharmacy practice. Each expert assessed the prescriptions for potential medication-related risks. Any differences in expert opinion were resolved through discussion until 100% consensus was achieved. These consensus classifications served as the reference standard. Because the original evaluation protocol utilised consensus agreement rather than recording independent pre-consensus ratings, inter-rater agreement statistics (such as Fleiss' kappa) cannot be computed retrospectively. Each simulated prescription was processed by the framework, and the system-generated recommendations were compared with the expert-validated reference outcomes using a confusion matrix comprising True Positives (TP), True Negatives (TN), False Positives (FP), and False Negatives (FN). Classification performance measures were calculated using standard mathematical definitions for Accuracy, Precision, Recall, Specificity, and F1-Score.The following evaluation metrics were calculated:

$$\text{Accuracy} = (TP + TN) / (TP + TN + FP + FN) \quad (1)$$

$$\text{Precision} = TP / (TP + FP) \quad (2)$$

$$\text{Recall (Sensitivity)} = TP / (TP + FN) \quad (3)$$

$$\text{Specificity} = TN / (TN + FP) \quad (4)$$

$$\text{F1-Score} = (2 \times \text{Precision} \times \text{Recall}) / (\text{Precision} + \text{Recall}) \quad (5)$$

To satisfy strict reporting requirements for statistical uncertainty, 95% binomial confidence intervals (Exact Clopper-Pearson method) were computed for each metric based on the sample population (n=30). Since only expert-validated simulated prescription scenarios were used, no real patient data were processed. Consequently, the research posed minimal ethical risk and complied with accepted research ethics principles regarding confidentiality, privacy, and responsible software development.

3 RESULTS AND DISCUSSION

The proposed PharmaAI framework was evaluated using 30 expert-validated simulated outpatient prescription scenarios representing common medication safety situations encountered in community pharmacy practice, including drug–drug interactions, dosage errors, allergy-related prescribing risks, contraindications, therapeutic duplication, and clinically appropriate prescriptions. The prescription scenarios were developed from published medication safety literature and evidence-based clinical guidelines, and their expected outcomes were independently reviewed and validated by three registered pharmacists.The expert consensus served as the reference standard for evaluating the framework's performance. The classification results are summarized in Table 1.

Table 1. Confusion Matrix and Performance Metrics of PharmaAI

Category	Count
True Positives (TP)	19
False Positives (FP)	2
True Negatives (TN)	7
False Negatives (FN)	2
Total Scenario	30

Note: TP = True Positives; FP = False Positives; TN = True Negatives; FN = False Negatives.
As shown in Table 1, PharmaAI correctly identified 19 medication-related risk scenarios and 7 clinically appropriate prescriptions, with 2 false-positive and 2 false-negative classifications, indicating strong agreement with expert-validated classifications.

Table 2. Performance Metrics with 95% Confidence Intervals

Metric	Value	95% Confidence Interval (CI)
Accuracy	86.7%	69.3% to 96.2%
Precision	90.5%	69.6% to 98.8%
Recall	90.5%	69.6% to 98.8%
Specificity	77.8%	40.0% to 97.2%
F1-score	90.5%	—

Note: Metrics were calculated by comparing PharmaAI predictions with the expert-validated reference outcomes. Binomial confidence intervals were computed using the exact Clopper–Pearson method (n = 30).
The performance metrics presented in Table 2 indicate that PharmaAI achieved an accuracy of 86.7%, with precision and recall of 90.5%. These findings suggest that the framework was able to identify a substantial proportion of clinically relevant medication-related risks within the simulated evaluation set. Nevertheless, the results should be interpreted as preliminary, given the limited number of expert-validated scenarios included in the evaluation.The two false-positive cases indicate that PharmaAI occasionally generated alerts for clinically appropriate prescriptions. While minimising missed medication-related risks remains an important objective, excessive false-positive alerts may increase alert burden and potentially contribute to alert fatigue in practice. Conversely, the two false-negative cases demonstrate that some medication-related risks were not detected. These findings highlight the need for further refinement of the clinical knowledge base and decision rules to improve the balance between sensitivity and specificity. The appropriate balance between detecting risks and limiting unnecessary alerts should ultimately be determined through evaluation involving practicing pharmacists and realistic dispensing workflows.An important feature of PharmaAI is its human-centred design. The framework is intended to support, rather than replace, pharmacist professional judgement by presenting medication-safety assessments together with clinically relevant explanations. This approach promotes transparency in the decision-support process and allows pharmacists to review the rationale underlying an alert before making a dispensing decision. However, the present study evaluated the technical classification performance of the framework and did

not empirically assess usability, trust, explanation quality, cognitive workload, or intention to use. Therefore, these aspects should be considered potential benefits of the design rather than demonstrated outcomes.The use of expert-validated prescription scenarios provided a clinically informed reference standard and strengthened the internal validity of the simulation-based evaluation. However, agreement with expert-derived classifications does not demonstrate that PharmaAI performs better than pharmacists or existing medication-safety technologies. In particular, the absence of a comparison with conventional drug-interaction checkers, existing CDSS platforms, or pharmacist assessment limits conclusions regarding the incremental value of the proposed framework. Future studies should therefore incorporate appropriate baseline systems and pharmacist-based comparisons to determine whether PharmaAI provides measurable advantages over established approaches.The findings indicate that PharmaAI has potential as a community pharmacy-oriented clinical decision-support framework, particularly through its integration of medication-risk detection with explainable recommendations. Its focus on community pharmacy requirements differentiates the framework from approaches primarily developed for hospital-based clinical environments. However, translation into routine practice would require consideration of workflow integration, knowledge-based maintenance, alert management, and pharmacist acceptance. These factors are particularly important in community pharmacy settings, where decision-support interventions must provide clinically useful information without imposing unnecessary cognitive or operational burden.Overall, the results provide preliminary evidence supporting the feasibility of the PharmaAI framework for medication-safety decision support in simulated community pharmacy scenarios. However, the findings should not be interpreted as evidence of clinical effectiveness or superiority over existing systems. The limited simulation-based evaluation, absence of direct baseline comparison, and lack of pharmacist-centred usability and workflow assessment restrict the generalisability of the findings. Further research should therefore focus on larger and more diverse clinical scenarios, comparative evaluation against established decision-support approaches, and prospective assessment with practicing pharmacists to determine the framework's clinical utility, usability, and acceptability in real-world community pharmacy practice.

4 CONCLUSION

This study developed and evaluated PharmaAI, a human-centred, deterministic rule-based expert clinical decision support framework for medication safety in community pharmacy. The simulation-based evaluation demonstrated its feasibility in identifying medication-related risks and providing transparent, explainable decision support based on expert-validated reference classifications. However, the small simulated dataset limits generalisability and does not establish clinical effectiveness or deployment readiness. Future research will focus on larger real-world evaluations, comparison with existing decision-support approaches, automated knowledge-base parsing, and pharmacist-centred assessment of usability, trust, explanation quality, cognitive workload, and workflow integration.

5 REFERENCES

Kim, S. Y., Kim, D. H., Kim, M. J., Ko, H. J., & Jeong, O. R. (2024). *XAI-based clinical decision support systems: A systematic review*. *Applied Sciences, 14*(15), 6638. https://doi.org/10.3390/app14156638

Moon, J., Chladek, J. S., Wilson, P., & Chui, M. A. (2023). *Clinical decision support systems in community pharmacies: A scoping review*. *Journal of the American Medical Informatics Association, 31*(1), 231–239. https://doi.org/10.1093/jamia/ocad208

National Institute for Health and Care Excellence. (2023). *Medicines optimisation: The safe and effective use of medicines to enable the best possible outcomes.*

Schoonderwoerd, T. A. J., Jorritsma, W., Neerincx, M. A., & van den Bosch, K. (2021). *Human-centred XAI: Developing design patterns for explanations of clinical decision support systems*. *International Journal of Human–Computer Studies, 154*, 102684. https://doi.org/10.1016/j.ijhcs.2021.102684

Van Dort, B. A., López Cañizares, J., Marcilly, R., Peute, L., & Sent, D. (2025). *Enhancing clinical decision support: A heuristic evaluation of explainable AI in healthcare dashboards*. *Studies in Health Technology and Informatics, 326*. https://doi.org/10.3233/SHTI250341

Xu, Y., et al. (2023). *Interpretability of clinical decision support systems based on artificial intelligence from technological and medical perspective: A systematic review*. *Journal of Healthcare Engineering, 2023*, Article 9919269. https://doi.org/10.1155/2023/9919269

ISSN: 2773-7055
Proceedings of the 5th International Research Conference
Institute of Technology, University of Moratuwa
November 5, 2026

Paper ID: 78

MULTI-PARAMETER IOT SYSTEM FOR DISTRIBUTION TRANSFORMER CONDITION MONITORING: DESIGN AND PRELIMINARY VALIDATION

W M P L Nanayakkara[1*], M M K Munasinghe[1], H D O Tharinda[1], S M S N Rathnayake[1], Ms. Dinushi Ganepola[1], K W D C I Koswaththa[1]

[1]Division of Electrical, Electronic and Telecommunication Engineering Technology, Institute of Technology, University of Moratuwa, Homagama, Sri Lanka

*Corresponding author: 23ee0310@itum.mrt.ac.lk

ABSTRACT: The reliability of distribution transformers is essential for ensuring stable electrical power grids; breakdowns that occur due to thermal stress, insulation degradation, overloading and the deterioration of the oil can result in major power outages and high maintenance expenses. In many power utilities that are developing, maintenance is generally carried out on a time-based and reactive basis, which means that faults are only discovered after considerable damage has taken place. This paper describes the design and the initial experimental verification of a low-cost, multi-parameter Internet of Things (IoT) condition-monitoring system for distribution transformers, the aim being to lay the groundwork for future predictive maintenance capabilities. The system's architecture is based on an ESP32 microcontroller which is connected to a range of sensors measuring seven parameters: winding temperature, oil temperature, load current, voltage, oil level, gas-sensor response screening and mechanical vibration. The sensor readings are locally compared with preset threshold values and the status information is sent via a Wi-Fi link to a local gateway to a cloud-based dashboard. If there is poor network connectivity, a GSM module sends SMS alerts directly to the maintenance staff when the critical threshold values are reached, and a local LCD screen shows the on-site status. At this stage, the winding/oil-temperature and oil-level subsystems have been put into place and have been experimentally tested in the laboratory: the temperature measurements were accurate to within ±0.5 °C of a reference thermometer, the oil-level measurements had a standard deviation of less than 0.3 cm in repeated trials, and the local web server responded to requests in less than 500 ms. The other subsystems involving current, voltage, gas sensing and vibration have been implemented in hardware and are now waiting to be integrated and validated. These findings show that the proposed hardware and the threshold-based alerting method are feasible and represent a step towards the full validation of a multi-parameter predictive-maintenance platform for distribution transformers.

Keywords: internet of things (IoT), condition monitoring, distribution transformers, multi-parameter analysis, ESP32 microcontroller

1 INTRODUCTION

Distribution transformers form an important component of electrical power grids. They are responsible for reducing high transmission voltages to lower, usable voltages for both industries and households. Transformers operate continuously under changing loads and varying environmental conditions, which makes them vulnerable to gradual wear over time. Common causes of unexpected transformer failure include thermal stress from overloading, insulation deterioration, harmonic interference, voltage stress, and degradation of the cooling oil.

In Sri Lanka, distribution-system maintenance is structured around preventive inspection, follow-up maintenance, and remedial maintenance, with condition information commonly collected through periodic field inspections and checklists rather than continuous online monitoring

(Public Utilities Commission of Sri Lanka, 2012). This periodic approach can allow developing faults between inspection intervals to remain undetected. As a result, unplanned transformer failures can lead to outages, damage to adjacent equipment, emergency-repair costs, and reduced transformer service life.

The incorporation of Internet of Things (IoT) technologies presents an opportunity to transition from reactive maintenance approaches toward condition-based and predictive maintenance. A substantial body of literature supports the use of IoT in this field. Kore et al. (2019) demonstrated IoT/GSM-based distribution-transformer monitoring using low-cost embedded hardware, but the approach remained primarily monitoring and threshold based. Aizpurua et al. (2019) applied machine-learning and uncertainty modelling to transformer remaining-useful-life prediction, illustrating a substantially more computationally sophisticated prognostic approach. Mina and Kartika (2023) implemented ESP8266-based monitoring of voltage, current, temperature, methane, carbon monoxide, and hydrogen in distribution transformers, focusing on remote parameter monitoring. Kwarteng et al. (2021) developed an Arduino/Blynk condition-monitoring system using current, oil-level/moisture, and loading-related information, demonstrating a low-cost remote-monitoring approach.

More recent work has explored gas-sensing approaches specifically: Equbal et al. (2022) applied an electronic-nose sensor array combined with an adaptive neuro-fuzzy inference system (ANFIS) to classify transformer faults from gas signatures, showing that low-cost gas sensing can support fault classification without laboratory-grade equipment. On the connectivity side, Bajwa et al. (2025) reviewed IoT-enabled transformer condition-monitoring approaches and identified LoRaWAN and NB-IoT as prominent communication options for remote substations. Commercially, the Qualitrol Intelligent Transformer Monitor family provides remote/local monitoring of transformer parameters and industrial communication interfaces (Qualitrol Corp., n.d.), which underscores both the industrial relevance of this problem and the cost gap that low-cost IoT approaches such as this one aim to address.

Despite this progress, a research gap remains. Current state-of-the-art low-cost systems generally measure a limited set of parameters (one or two variables), operate through fixed threshold alerts without a predictive multi-parameter algorithm, or require levels of investment that are difficult to justify at the local distribution-network level. To help address this gap, this paper presents the design of a low-cost, integrated IoT-based condition-monitoring system for distribution transformers and reports the experimental validation completed to date. The design targets seven parameters: winding temperature, oil temperature, load current, voltage, oil level, gas-sensor response screening, and vibration-measured using an ESP32 microcontroller, with data uploaded to a cloud server and evaluated against configurable multi-variable threshold logic to flag possible developing faults.

2 METHODOLOGY

2.1 System Architecture

The architecture of the proposed monitoring system consists of three levels: the sensor acquisition level, the edge processing level, and the cloud communication/visualisation level (Figure

1). Central processing is performed using an ESP32 DevKit V1, selected for its processing capability, built-in Wi-Fi support, and sufficient number of GPIO pins for sensors covering the seven monitored parameters.

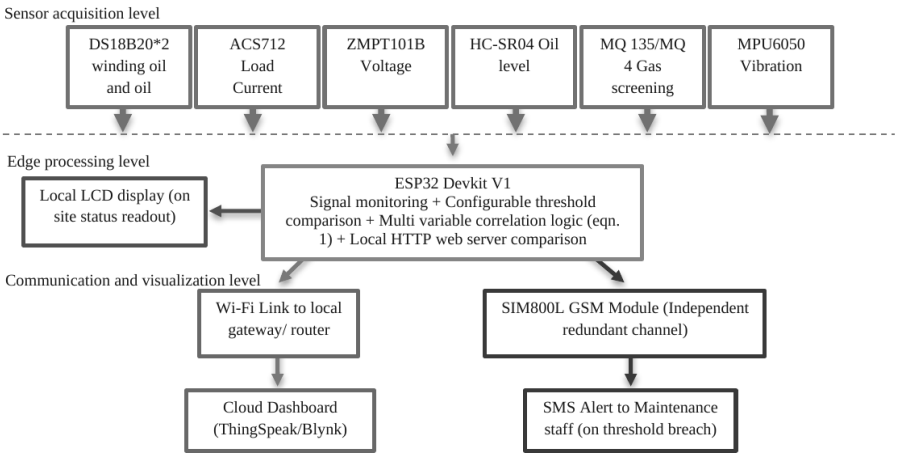


Figure 1. System Architecture of the Multi-Parameter IoT Transformer Monitoring Platform

2.2 Monitored Parameters and Sensor Selection

The design takes into account seven transformer-condition parameters, the temperature and oil level subsystems having been validated by experimental means, while the current, voltage, gas-screening, and vibration subsystems are implemented in hardware and are waiting for further validation.

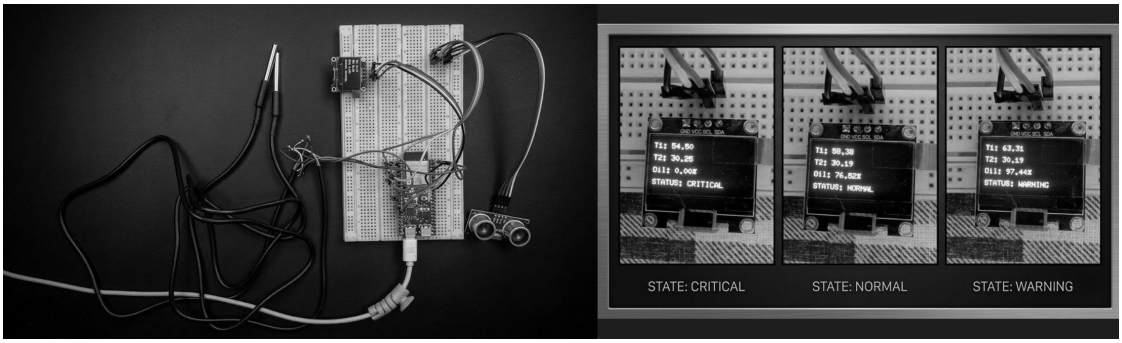


Figure 2. Developed Prototype of the IoT-Based Transformer Condition-Monitoring System: (a) Hardware Prototype and (b) LCD Display Showing Critical, Normal, and Warning States.

The winding and oil temperatures are measured by means of two DS18B20 sensors (range: -55 °C to 125 °C). The load current and voltage are monitored with the help of ACS712 and ZMPT101B modules, and the oil level is determined by means of an HC-SR04 ultrasonic sensor. Gas-sensor response screening is carried out using MQ-135/MQ-4 sensors, and a MPU6050 accelerometer is used to monitor mechanical vibration. Since True Dissolved Gas Analysis requires specialized techniques such as gas chromatography or photoacoustic spectroscopy (Wani et al., 2021), the MQ sensors are employed only as a low-cost method for detecting changes in gas-sensor response rather than as a replacement for full DGA (Equbal et al., 2022).

2.3 Communication Framework and Dashboard Development

The Arduino environment was used to develop the embedded C firmware for the ESP32, with the sensor inputs being processed and compared against predetermined thresholds, and at the same time a lightweight HTTP server supplies a dashboard which is refreshed about every five seconds and sends the data to a cloud service such as ThingSpeak or Blynk.
Wi-Fi connectivity is made available by means of a local gateway or router at substations or distribution hubs; in the case of remote transformers where Wi-Fi is not available, NB-IoT or LoRaWAN (Bajwa et al., 2025) is more appropriate and will therefore be considered for future use. A SIM800L GSM module supplies an independent SMS alert channel when threshold breaches occur, and the local LCD ensures that on-site status can be monitored.

2.4 Multi-Variable Threshold Correlation Logic

Rather than relying on a single static threshold as in conventional reactive systems, the proposed logic evaluates the rate of change together with the status of multiple variables simultaneously. For example, the combination of a rapid rise in load current and winding temperature together with a detected rise in gas-sensor output is treated as a higher-risk condition than a gradual rise in temperature alone. The basic rule used to trigger a high-risk alarm is expressed in (1):

```
IF (Temp > Temp_Threshold) AND (Current > Rated_Current) OR
(d(Gas)/dt > Rate_Threshold) -> HIGH RISK WARNING
```
(1)

The thresholds given in (1) and in Table 1 were chosen by referring to IEEE C57.91-2011 (IEEE, 2012) and IEC 60076-7 (International Electrotechnical Commission, 2018). For mineral-oil transformers, the winding hot-spot limits are generally in the range of 98–110 °C; on this basis Warning and Critical thresholds of 65 °C and 75 °C were selected in order to allow for an early intervention margin. During the laboratory tests the oil-level thresholds were fixed at 50% for Warning and at 30% for Critical. Equation (1) describes the proposed multi-variable logic; in this study only the temperature and oil-level threshold functions were verified experimentally. The method enables condition-based alerts and is not at this stage a trained predictive model.

3 RESULTS AND DISCUSSION

At the current stage, hardware implementation, calibration, and software validation have been completed for the winding/oil-temperature and oil-level subsystems; validation of the current, voltage, gas-sensing, and vibration subsystems is planned for the next phase of testing and is not yet reported here. The test setup used an ESP32 microcontroller connected to the DS18B20 temperature sensors and the HC-SR04 ultrasonic sensor, with sensor accuracy validated against reference calibrated instruments. The DS18B20 sensors returned temperature readings within ±0.5 °C of a reference thermometer across a hot-water-bath test series. The ultrasonic sensor produced stable distance measurements, with a standard deviation below 0.3 cm across ten consecutive readings at varying fluid levels.

3.1 System Performance and Threshold Validation

The threshold-based alerting logic was evaluated by simulating abnormal environmental and operating conditions. A heat gun was used to artificially raise sensor temperatures, while the oil level was reduced manually to simulate leakage. The firmware correctly detected each anomalous condition and transitioned the system status from Normal to Warning or Critical according to the configured thresholds. When the winding temperature exceeded 65 °C, the firmware raised a Winding Temperature Warning; when it exceeded 75 °C, the status escalated further. Similarly, when the oil level fell below 50%, the firmware raised an Oil Level Warning. The ESP32 web server remained responsive throughout testing, processing HTTP requests in under 500 ms. Table 1 summarizes the test conditions and corresponding system responses.

Table 1. Experimental Test Results and System Response

Parameter	Measured Value	Threshold	System Status
Winding Temperature	42.5 °C	65.0 °C	**Normal**
Oil Temperature	38.2 °C	60.0 °C	**Normal**
Oil Level	70%	50%	**Normal**
Winding Temp (Heat Test)	68.1 °C	65.0 °C	**Warning**
Oil Level (Drain Test)	20%	30%	**Critical**

Note: The threshold values shown are the configured laboratory test limits.

3.2 Discussion

The findings show that the proposed low-cost, multi-sensor method for monitoring is feasible with respect to the parameters that have so far been validated. Different from systems which depend primarily on GSM alerts (Kore et al., 2019) or remote Blynk monitoring (Kwarteng et al., 2021), the present design includes a local LCD, a web dashboard, and GSM as a backup feature in order to ensure that monitoring can continue when there are network limitations. Moreover, the low cost of the hardware offers an alternative to industrial systems such as the Qualitrol ITM range (Qualitrol Corp., n.d.) and to computationally demanding machine-learning methods (Zahra et al., 2025). The fact remains, though, that only two of the seven target parameters have been experimentally verified. A comparison of the proposed system with some academic and commercial solutions is given in Table 2, and future work will involve verifying the remaining current, voltage, gas-sensing, and vibration subsystems.

Table 2. Comparison of Proposed System with Reviewed Literature and Commercial Solutions

Study / Product	Parameters Monitored	Predictive Capability	Connectivity	Approx. Cost Tier
Kore et al. (2019)	Temperature, voltage, current	None (threshold monitoring)	IoT + GSM	Low
Kwarteng et al. (2021)	Current, oil level/moisture, load-related data	Health-index / life-assessment support	Wi-Fi (Blynk)	Low
Mina and Kartika (2023)	Voltage, current, temperature, CH4, CO, H2	None; parameter monitoring	ESP8266 Wi-Fi / Blynk	Low

Study / Product	Parameters Monitored	Predictive Capability	Connectivity	Approx. Cost Tier
Aizpurua et al. (2019)	Hot-spot temperature, load, RUL inputs	Machine-learning RUL prediction	Data-driven prognostic framework	High (computational)
Bajwa et al. (2025)	Transformer monitoring (review)	Reviews AI/ML approaches	LoRaWAN / NB-IoT discussed	N/A (review)
Qualitrol ITM family (Qualitrol Corp., n.d.)	Temperature, pressure/oil level, cooling	Rule/control-based monitoring	DNP3 / Modbus / industrial	High (industrial)
Proposed system (this paper)	7 designed; 2 validated (Temp., Oil level)	Threshold / multi-variable correlation; ML extension planned	Wi-Fi (local gateway) + GSM SMS backup	Low

4 CONCLUSION

The paper describes the design and initial validation of a low-cost IoT condition-monitoring system for distribution transformers, the system making use of an ESP32 and sensors that cover seven different parameters. Validation has been carried out for the temperature and oil-level subsystems, resulting in a temperature accuracy of ±0.5 °C, a standard deviation for the oil level below 0.3 cm, and web-server response times that are under 500 ms. The other subsystems relating to current, voltage, gas sensing, and vibration still need further validation. In future work, the threshold-based logic will be extended towards predictive fault analysis and the LoRaWAN/NB-IoT connectivity will be evaluated for use in remote deployments.

5 ACKNOWLEDGEMENTS

The authors would like to thank the project advisors and the Division of Electrical and Electronic Engineering Technology, Institute of Technology, University of Moratuwa (ITUM), for their continuous guidance, technical support, and feedback throughout this research.

6 REFERENCES

J. I. Aizpurua, S. D. J. McArthur, B. G. Stewart, B. Lambert, J. G. Cross, and V. M. Catterson, "Adaptive power transformer lifetime predictions through machine learning and uncertainty modelling in nuclear power plants," IEEE Transactions on Industrial Electronics, vol. 66, no. 6, pp. 4726–4737, Jun. 2019, doi: 10.1109/TIE.2018.2860532.

A. Bajwa, A. A. R. Tonoy, and M. A. M. Khan, "IoT-enabled condition monitoring in power transformers: A proposed model," Review of Applied Science and Technology, vol. 4, no. 2, pp. 118–144, 2025, doi: 10.63125/3me7hy81.

M. D. Equbal, M. M. Nezami, H. Hashem, M. Bajaj, T. Khurshaid, S. S. M. Ghoneim, and S. Kamel, "IOT based classification of transformer faults using emerging techniques of E-nose and ANFIS," Frontiers in Energy Research, vol. 10, Art. no. 1020040, 2022, doi: 10.3389/fenrg.2022.1020040.

IEEE Guide for Loading Mineral-Oil-Immersed Transformers and Step-Voltage Regulators, IEEE Std C57.91-2011, 2012.

P. S. Kore, G. N. Amane, A. N. Dalne, V. R. Ambare, S. N. Kapse, and S. Bhavarkar, "IoT based distribution transformer monitoring and controlling system," International Journal of Advance Research and Innovative Ideas in Education, vol. 5, no. 2, pp. 122–126, 2019.

A. Kwarteng, S. K. Okrah, B. Asante, P. A. Bediako, and P. A. A. Baidoo, "Design and construction of an IoT based distribution transformer condition monitoring system," The International Journal of Engineering and Science, vol. 10, no. 5, pp. 20–44, 2021, doi: 10.9790/1813-1005032044.

M. Mina and K. Kartika, "Monitoring system for levels of voltage, current, temperature, methane, and hydrogen in IoT-based distribution transformers," International Journal of Engineering, Science and Information Technology, vol. 3, no. 1, pp. 22–27, 2023, doi: 10.52088/ijesty.v3i1.414.

Power transformers-Part 7: Loading guide for mineral-oil-immersed power transformers, IEC 60076-7:2018, International Electrotechnical Commission, 2018.

Public Utilities Commission of Sri Lanka (PUCSL), Distribution Code of Sri Lanka, Jul. 2012. [Online]. Available: https://www.ceb.lk/front_img/img_reports/1532500020Distribution_Code.pdf

Qualitrol Corp., "ITM 507 Intelligent Transformer Monitor," [Online]. Available: https://www.qualitrolcorp.com/products/ITM507. [Accessed: Aug. 28, 2026].

S. A. Wani, A. S. Rana, S. Sohail, O. Rahman, S. Parveen, and S. A. Khan, "Advances in DGA based condition monitoring of transformers: A review," Renewable and Sustainable Energy Reviews, vol. 149, Art. no. 111347, 2021, doi: 10.1016/j.rser.2021.111347.

S. T. Zahra, S. K. Imdad, S. Khan, S. Khalid, and N. A. Baig, "Power transformer health index and life span assessment: A comprehensive review of conventional and machine learning based approaches," Engineering Applications of Artificial Intelligence, vol. 139, Part A, Art. no. 109474, 2025, doi: 10.1016/j.engappai.2024.109474.

ISSN: 2773-7055
Proceedings of the 5th International Research Conference
Institute of Technology, University of Moratuwa
November 5, 2026

Paper ID: 80

EVALUATION OF OPEN-ACCESS AI TRANSLATION SYSTEMS FOR PRESERVING CULTURAL HERITAGE EXPRESSIONS

P N T Pathirana*

Division of Information Technology, Institute of Technology, University of Moratuwa, Homagama, Sri Lanka

*Corresponding author: nadeesha8thamali@gmail.com

ABSTRACT: During periods of global conflict and geopolitical uncertainty, preserving intangible cultural heritage, such as traditional narratives and local idioms, is critical to maintaining human values and community resilience. Displaced populations rely heavily on digital information systems and artificial intelligence tools for cross-border communication and localised crisis assistance. However, standard automated translation models often struggle to capture deep cultural nuances. This study evaluates the efficacy of three widely used open-access translation platforms such as Google Translate, ChatGPT (GPT-4o), and Microsoft Translator in preserving the cultural context and emotional intent of minority language narratives. A mini dataset consisting of 200 localised historical idioms and cultural proverbs from Sinhala and Tamil (100 phrases per language) was subjected to a round-trip back-translation framework (Local Language → English → Local Language). The translated outputs were analysed using a structured mixed-method evaluation framework consisting of two five-point Likert-scale criteria, Semantic Accuracy and Cultural Nuance Preservation supplemented by categorical Error Classification. The results demonstrate that while conventional neural machine translation systems achieve high literal or semantic accuracy, they exhibit substantial limitations on cultural preservation metrics, often stripping historical context or introducing misleading, tonally flat terms. In contrast, Large Language Model-driven systems such as ChatGPT showed higher descriptive performance than the conventional tools in the evaluated dataset by more effectively preserving cultural sentiment and contextual nuance. The study concludes that further development of translation systems should consider culturally diverse and localised datasets to improve the preservation of intangible cultural heritage, particularly in low-resource language contexts.

Keywords: cultural heritage, machine translation, artificial intelligence, information systems, minority languages

1 INTRODUCTION

In times of global conflict and socio-economic uncertainty, the preservation of human values and cultural heritage extends beyond physical monuments to encompass intangible traditions, localised oral histories, and linguistic nuances. The safeguarding of intangible cultural heritage has been recognised as a fundamental component of preserving cultural identity and community resilience, particularly during periods of crisis and displacement (UNESCO, 2003). When humanitarian crises force populations to relocate, digital technologies and online information systems become essential tools for communication, access to humanitarian assistance, and the preservation and dissemination of cultural knowledge (United Nations, 2023). Consequently, machine translation (MT) systems are increasingly relied upon by international aid organisations, refugees, and cultural preservation initiatives to facilitate multilingual communication and overcome language barriers in humanitarian contexts (Costa-jussà et al., 2022; Hendy et al., 2023).

Machine translation has advanced considerably with the introduction of neural architectures. Early neural approaches used attention-based encoder–decoder models to improve alignment between source and target sequences (Bahdanau et al., 2014), and this line of work was later extended by fully attention-based transformer architectures that now underpin most modern translation and language systems (Vaswani et al., 2017). Despite these advances, mainstream translation systems continue to exhibit performance disparities across languages, with low-resource languages generally facing greater challenges than high-resource languages (Zhu et al., 2024; NLLB Team et al., 2024). Idiomatic expressions, historical proverbs, and crisis-related cultural phrases carry distinct emotional weight and historical value that literal, word-for-word translation often fails to retain. Mistranslations during crises can lead to a degradation of intangible heritage and, in critical situations, severely compromise the delivery of psycho-social support. While extensive research addresses neural machine translation performance for technical prose, a notable research gap remains regarding how effectively open-access AI tools handle localised cultural narratives under stressful societal conditions. This study addresses this gap by providing a comparative evaluation of Google Translate, ChatGPT (GPT-4o), and Microsoft Translator using culturally significant Sinhala and Tamil expressions. Unlike conventional translation evaluations that primarily emphasise linguistic or semantic accuracy, this study distinguishes between Semantic Accuracy (SA) and Cultural Nuance Preservation (CNP), thereby examining whether a translation can preserve the literal meaning of an expression while simultaneously retaining its historical, idiomatic, emotional, and cultural significance. The study further incorporates Error Classification (EC) to identify patterns of cultural and contextual loss. By focusing on underrepresented Sinhala and Tamil cultural expressions, the study contributes empirical evidence on the ability of contemporary AI translation systems to support the preservation of intangible cultural heritage.

The primary objective of this study is to evaluate and compare the linguistic and cultural preservation capabilities of three major open-access Platforms-Google Translate, ChatGPT, and Microsoft Translator using a back-translation methodology.

2 METHODOLOGY

This study employed a rapid empirical evaluation framework using a manually curated dataset comprising 200 culturally significant expressions, including 100 Sinhala and 100 Tamil expressions. The expressions were selected from published Sinhala and Tamil proverb books and collections of traditional idioms using a purposive selection approach based on predefined cultural relevance criteria. The selection focused on traditional proverbs, idiomatic expressions, historical references, metaphorical expressions, and localised socio-cultural expressions reflecting regional values, customs, interpersonal relationships, emotional meanings, and intangible cultural heritage. Expressions that were duplicated, incomplete, unclear, or culturally neutral were excluded. The final dataset consisted of 100 Sinhala and 100 Tamil expressions to maintain a balanced representation of the two language groups and enable comparable evaluation across the language pairs. As the size of the initial candidate pool was not recorded during data collection, the selection process is reported as a purposive selection procedure rather than as a

quantified screening process.

2.1 Experimental Framework

The assessment utilised a round-trip back-translation protocol, in which each phrase was translated from the source language into English and back again for comparison against the original. This approach was chosen because it does not require extensive parallel corpora, making it suitable for under-resourced language pairs such as Sinhala and Tamil. Round-trip fidelity alone is known to correlate poorly with translation quality (Somers, 2005). To address this, three bilingual evaluators independently assessed both the intermediate English translation and the final back-translated output against the original phrase, rather than relying on round-trip agreement alone. Figure 1 illustrates the round-trip back-translation workflow adopted in this study. Each of the 200 source phrases was processed through the public web interfaces of Google Translate, ChatGPT (GPT-4o), and Microsoft Translator. The intermediate English translations were recorded and subsequently translated back into the original language using the same translation platform.

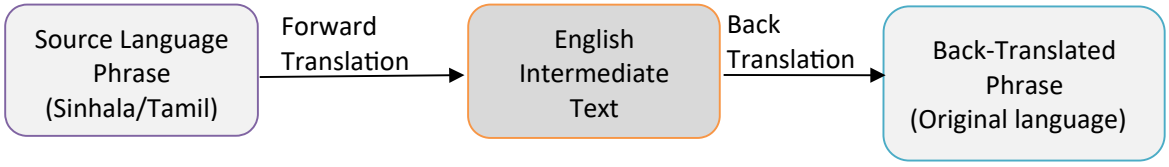


Figure 1. Back-translation workflow

2.2 Evaluation Metrics

The final back-translated outputs were evaluated using a human-centred mixed-method evaluation framework. Three independent bilingual evaluators with expertise in translation and language education, each possessing more than five years of professional experience and proficiency in Sinhala, Tamil, and English, independently assessed every phrase by reviewing the original phrase, the intermediate English translation, and the corresponding back-translated output. Evaluations were conducted independently, with no communication or discussion among the evaluators during the assessment process. The evaluation procedure did not include documented system-level blinding, and therefore the evaluators' awareness of the translation system identities could not be excluded. The evaluation was based on two primary criteria: Semantic Accuracy (SA) and Cultural Nuance Preservation (CNP). Both criteria were assessed using a five-point Likert scale (1 = Very Poor, 2 = Poor, 3 = Fair, 4 = Good, and 5 = Excellent).

Semantic Accuracy (SA) - The extent to which the back-translated phrase preserves the semantic meaning of the original phrase.

Cultural Nuance Preservation (CNP) - The extent to which the translation retains the historical, idiomatic, emotional, and cultural meaning embedded in the original phrase.

This process produced 600 individual ratings per translation platform for Semantic Accuracy and 600 individual ratings for Cultural Nuance Preservation (200 phrases × 3 evaluators). For each phrase, the final SA and CNP scores were calculated as the arithmetic mean of the ratings assigned by the three evaluators. The overall performance of each translation platform was then

determined by averaging the phrase-level scores across all 200 evaluated phrases. Standard deviations were calculated from the 200 phrase-level mean scores for each translation platform to quantify variability. In addition to the quantitative ratings, Error Classification (EC) was performed to identify the predominant translation error for each phrase. The final error category was determined using majority voting among the three evaluators. Error categories included Literal Distortion (LD), Cultural Flattening (CF), Omission of Context (OC), Robotic or Out-of-Context Terms (RT), and No Significant Error (NSE).

2.3 Statistical Analysis

The evaluation results were analysed using descriptive statistics. For each translation system, the mean and standard deviation of the Semantic Accuracy (SA) and Cultural Nuance Preservation (CNP) ratings were calculated across the evaluated expressions. The Error Classification (EC) results were summarized according to the frequency of the identified error categories. These descriptive results were used to compare the performance of the three translation systems within the evaluated dataset.

3 RESULTS AND DISCUSSION

3.1 Comparative Performance of AI Translation Systems

The performance of the three open-access AI translation systems was evaluated using the proposed mixed-method evaluation framework based on Semantic Accuracy (SA), Cultural Nuance Preservation (CNP), and Error Classification (EC). Three bilingual evaluators independently assessed the translated outputs generated through the round-trip back-translation process. The reported SA and CNP scores represent the mean of the phrase-level scores calculated from the three evaluator ratings across all 200 evaluated cultural expressions.

Table 1. Performance Comparison of AI Translation Systems

Translation System	Semantic Accuracy (Mean ± SD)	Cultural Nuance Preservation (Mean ± SD)	Dominant Error
Google Translate	4.42 ± 0.39	2.81 ± 0.47	Cultural Flattening
ChatGPT (GPT-4o)	4.78 ± 0.26	4.63 ± 0.31	No Significant Error
Microsoft Translator	4.08 ± 0.45	2.65 ± 0.56	Omission of Context

As shown in Table 1, the three translation systems achieved relatively high descriptive mean scores for Semantic Accuracy. ChatGPT obtained the highest mean Semantic Accuracy score (M = 4.78, SD = 0.26), followed by Google Translate (M = 4.42, SD = 0.39) and Microsoft Translator (M = 4.08, SD = 0.45). A larger difference was observed in Cultural Nuance Preservation. ChatGPT obtained the highest mean CNP score (M = 4.63, SD = 0.31), while Google Translate and Microsoft Translator obtained lower mean scores of 2.81 (SD = 0.47) and 2.65 (SD = 0.56), respectively. These descriptive results indicate that the differences among the systems were more pronounced for Cultural Nuance Preservation than for Semantic Accuracy. Within the evaluated dataset, the higher CNP score observed for ChatGPT is consistent with a greater degree of retention of culturally embedded meanings, idiomatic elements, and contextual information in the evaluated outputs. However, descriptive differences in mean scores alone do not establish

whether the observed differences between the systems are statistically significant. The error classification analysis provided additional information about the types of translation problems observed. Google Translate most frequently received the Cultural Flattening classification, indicating cases in which culturally meaningful expressions were represented in a more literal or culturally neutral form. Microsoft Translator was most frequently classified as Omission of Context, indicating cases in which contextual, historical, or emotional information was not fully retained. ChatGPT most frequently received the No Significant Error (NSE) classification within the evaluated dataset.

Overall, the descriptive results indicate differences among the evaluated systems in their ability to preserve culturally embedded information. In particular, the larger differences observed in CNP scores suggest that semantic accuracy alone may not fully capture the quality of translations involving culturally significant expressions. Therefore, evaluating cultural and contextual preservation alongside semantic accuracy may provide a more comprehensive assessment of AI translation quality for culturally significant content. These findings highlight the importance of considering cultural and contextual preservation when evaluating AI translation systems for culturally significant content. Maintaining contextual meaning alongside semantic accuracy may be particularly relevant when translation technologies are used for cultural documentation, communication, or the digital preservation of oral traditions. Translation systems that better retain cultural nuances may support future efforts to document and preserve aspects of intangible cultural heritage while facilitating cross-cultural communication. However, the findings of this study are limited to the 200 purposively selected Sinhala and Tamil expressions and should not be generalised to broader humanitarian or cultural contexts. Future research could expand the dataset to include additional regional dialects, folklore, historical narratives, and other culturally specific expressions from low-resource language contexts. Further studies could also incorporate automatic evaluation metrics such as BLEU, COMET, and BERTScore alongside expert human assessment to provide a broader evaluation of translation quality.

4 CONCLUSION

This study evaluated the capability of open-access AI translation systems to preserve cultural narratives and human values during times of uncertainty. The empirical findings indicate differences in the evaluated dataset: conventional NMT platforms (Google Translate and Microsoft Translator) achieved relatively high semantic accuracy but showed lower descriptive scores for cultural nuance preservation, whereas the LLM-based system ChatGPT showed higher descriptive performance in retaining historical and idiomatic context. These findings suggest the importance of considering cultural and contextual preservation alongside semantic accuracy when evaluating AI translation systems for culturally significant content. To support future digital heritage preservation, AI translation systems should incorporate culturally aware training data and localised linguistic resources, particularly for low-resource languages.

5 REFERENCES

Bahdanau, D., Cho, K., & Bengio, Y. (2014). *Neural machine translation by jointly learning to align and translate* [Preprint]. arXiv. https://doi.org/10.48550/arXiv.1409.0473

Costa-jussà, M. R., Cross, J., Çelebi, O., Elbayad, M., Heafield, K., Heffernan, K., Kalbassi, E., Lam, J., Licht, D., Maillard, J., Sun, A., Wang, S., Wenzek, G., Youngblood, A., Akula, B., Barrault, L., Bhosale, S., Casas, N., Clark, J., . . . Fan, A. (2022). *No language left behind: Scaling human-centred machine translation* [Preprint]. arXiv. https://doi.org/10.48550/arXiv.2207.04672

Hendy, A., Abdelrehim, M., Sharaf, A., Raunak, V., Gabr, M., Matsushita, H., Kim, Y. J., Afify, M., & Awadalla, H. H. (2023). *How good are GPT models at machine translation? A comprehensive evaluation* [Preprint]. arXiv. https://doi.org/10.48550/arXiv.2302.09210

NLLB Team. (2024). Scaling neural machine translation to 200 languages. *Nature, 630*, 841–846. https://doi.org/10.1038/s41586-024-07335-x

Somers, H. (2005). Round-trip translation: What is it good for? In *Proceedings of the Australasian Language Technology Workshop* (pp. 127–133). Australasian Language Technology Association.

United Nations. (2023). *Our common agenda: Policy brief on global digital cooperation*. https://www.un.org/

United Nations Educational, Scientific and Cultural Organisation. (2003). *Convention for the safeguarding of the intangible cultural heritage*. https://ich.unesco.org/en/convention

Vaswani, A., Shazeer, N., Parmar, N., Uszkoreit, J., Jones, L., Gomez, A. N., Kaiser, Ł., & Polosukhin, I. (2017). *Attention is all you need*. In *Advances in Neural Information Processing Systems* (Vol. 30, pp. 5998–6008). Curran Associates, Inc. https://doi.org/10.48550/arXiv.1706.03762

Zhu, W., Liu, H., Dong, Q., Xu, J., Huang, S., Kong, L., Chen, J., & Li, L. (2024). Multilingual machine translation with large language models: Empirical results and analysis. *Findings of the Association for Computational Linguistics: NAACL 2024*, 2765–2781. https://doi.org/10.18653/v1/2024.findings-naacl.176

Paper ID: 84

PREDICTING UNIVERSITY DROPOUT RISK USING MACHINE LEARNING

Y R C Ariyathilaka*

Division of Information Technology, Institute of Technology, University of Moratuwa, Homagama, Sri Lanka

*Corresponding author: rasikac@itum.mrt.ac.lk

ABSTRACT: University dropout is expensive, both for students and for the institutions they leave. OECD data show that only 39% of bachelor's students graduate on time, and roughly a fifth never finish at all. If institutions could flag at-risk students early, they could intervene before the situation becomes unrecoverable. We test this idea on the UCI "Predicting Student Dropout and Academic Success" dataset (4,424 students, 36 attributes), recoding the original three-class target into a binary dropout indicator (1,421 dropout cases against 3,003 non-dropout cases) and splitting the data 80:20 for training and testing. We trained Logistic Regression (scaled), Decision Tree, and Random Forest, then validated the comparison with stratified 5-fold cross-validation, a McNemar's test on paired predictions, full per-class precision/recall/F1 for every model, ROC-AUC and PR-AUC, a randomised hyperparameter search over Random Forest, and a HistGradientBoosting baseline. On a single 80:20 split, Logistic Regression appeared to lead (86.67% against 85.42% for Random Forest and 78.42% for Decision Tree), but this did not hold up: cross-validated accuracy for Logistic Regression (87.64% +/- 0.62%) and Random Forest (87.50% +/- 0.80%) shows no statistically significant difference (McNemar's p = 0.118), and tuning Random Forest or adding a boosting baseline narrowed the gap further without reversing it (p = 0.188 and p = 0.349). Decision Tree, in contrast, was significantly and consistently the weakest model (80.70% +/- 1.54%). Curricular units approved and average grades in the first two semesters, together with tuition-fee status, were by far the strongest predictors, matching prior studies on this dataset. We do not claim a new best algorithm. The more useful, and more honest, finding is that once the comparison is properly validated, algorithm choice matters far less than it first appeared to, and we report this correction transparently rather than keep an earlier, more dramatic-sounding claim that did not survive testing.

Keywords: student dropout, machine learning, logistic regression, higher education, predictive analytics

1 INTRODUCTION

Dropout is a global problem in higher education, and its costs fall on everyone involved. Only 39% of full-time bachelor's students graduate within the normal duration of their programme; 12% leave before the second year even starts; 21% never finish at all (Hoca & Dimililer, 2025). Every student who leaves also represents lost tuition revenue for the institution and a loss of public or private investment in that student's education (Villegas-Ch et al., 2023). Most of this attrition happens early. That is precisely why early identification matters: an institution that can flag a struggling student in their first or second semester still has time to act.

1.1 Literature Review

Ensemble methods lead this field. A review of 75 dropout-prediction studies published between 2019 and 2024 found Random Forest and XGBoost typically reaching 86-88% accuracy, ahead of simpler baselines like logistic regression and decision trees at 79-81% (Lopez-Muñoz et al., 2026). A separate PRISMA review of 23 studies reached a similar conclusion: Random Forest was both the most commonly used algorithm and the most frequent best-performer,

which the authors attribute to its bagging structure reducing overfitting relative to a single tree (Andrade-Girón et al., 2023).

The dataset we use comes from Realinho et al. (2022), who assembled records for 4,424 students at the Polytechnic Institute of Portalegre, Portugal. It has since become something of a standard benchmark, and two studies in particular use it the same way we do. Ridwan et al. (2024) trained XGBoost across five different train-test splits and got 86-87% accuracy throughout, with the best precision-recall balance, 88% precision and 81% F1, at an 80:20 split, the same split we use here. Villar and de Andrade (2024) went further and compared seven algorithms on this dataset: LightGBM and CatBoost came out on top, beating Decision Tree, SVM, and Random Forest with F1-scores of 0.86-0.88. Their SHAP analysis pointed to one variable above all others, curricular units approved in the second semester, as the dominant predictor of dropout. That matches what Realinho et al. (2022) had already found using a completely different importance method.

Results from other institutions tell a broadly similar story, though not an identical one. Palacios et al. (2021) worked with 6,656 students in Chile and, using a Friedman test across four different dropout-timing models, found Random Forest reliably came out on top. But their accuracy fell once they got to predicting later-year dropout, where class imbalance grew severe. Hoca and Dimililer (2025) compared eight classifiers on registration data from a Cypriot university and found CatBoost, Random Forest, and a multilayer perceptron the most dependable performers there. Across this literature, a few gaps keep showing up. Lopez-Muñoz et al. (2026) report that 68% of dropout studies rely on a single institution, 71% never check whether their predictions actually change retention outcomes, and fewer than 10% include any psychosocial or equity-related variable at all. There is also a recurring complaint about interpretability: the ensemble and boosting models that perform best are frequently criticised as black boxes that give little insight into why a particular student was flagged (Andrade-Girón et al., 2023). Dietz-Uhler and Hurn (2013), writing from the perspective of a working faculty member rather than a data scientist, add a caution worth keeping in mind: analytics should support an instructor's judgement, not replace it, and flagging students by algorithm raises ethical questions an institution cannot outsource to the model.

1.2 Contribution of This Study

Villar and de Andrade (2024) and Ridwan et al. (2024) have already benchmarked several tuned algorithms, boosting included, on this exact dataset, so we are not trying to beat them, and a fourth comparison of classifiers would not by itself tell anyone much new. What we think is useful here is narrower and more methodological: we start from a fully untuned baseline, of the kind a small institution without a dedicated data-science team might realistically run on a first attempt, and then show concretely what changes, and what does not, once that baseline is properly validated with cross-validation, significance testing, and a fairer, tuned comparison. That progression is the contribution: not a new best algorithm, but a demonstration of how much an unvalidated single-split comparison can mislead, and what it takes to find that out.

With that in mind, this study has three aims: first, to compare Logistic Regression, Decision

Tree, and Random Forest on binary dropout prediction using the UCI dataset, starting from default configurations; second, to see which variables Random Forest ranks as the strongest predictors of dropout; and third, to test whether the resulting algorithm ranking survives cross-validation, significance testing, and a fairer comparison against a tuned Random Forest and a boosting baseline, and to report honestly if it does not.

2 METHODOLOGY

Our pipeline is a standard one: load the data, recode the target, split 80:20, scale where necessary, train each model in its default configuration, and evaluate mainly on accuracy, with a closer look at one model's class-wise performance. Everything was done in Python, using pandas, scikit-learn, and matplotlib.

2.1 Dataset and Preprocessing

The dataset is the UCI "Predicting Student Dropout and Academic Success" dataset built by Realinho et al. (2022) from records held by the Polytechnic Institute of Portalegre, Portugal: 4,424 students and 36 attributes, covering demographics (marital status, nationality, age at enrolment), academic history (admission grade, units enrolled, evaluated, approved, and graded per semester), and a handful of macroeconomic indicators (unemployment, inflation, GDP). There are no missing values. Students originally fall into three categories, shown in Table 1.

Table 1. Student Status Distribution in the UCI Dataset Prior to Binary Recoding

Status	Number of Students	Percentage
Graduate	2,209	49.9%
Dropout	1,421	32.1%
Enrolled	794	18.0%
Total	4,424	100.0%

We recoded this into a binary target: Dropout = 1, Graduate and Enrolled both = 0, following the same approach as Ridwan et al. (2024). That gives 3,003 non-dropout cases against 1,421 dropout cases, an imbalance of roughly 2.1:1. This is mild compared with the up to 33:1 imbalances reported elsewhere in the literature (Palacios et al., 2021), so we did not apply any resampling technique such as SMOTE. We come back to that choice as a limitation later, since even a moderate imbalance like this one can still drag down recall on the minority class. The data were split 80:20 into training (3,539 records) and testing (885 records) sets, with random_state = 42 fixed so the split can be reproduced exactly. We standardised features (zero mean, unit variance) before fitting Logistic Regression, but left the Decision Tree and Random Forest models on the raw, unscaled data, since tree-based models don't need scaling to begin with.

2.2 Models and Evaluation

The three original models ran with scikit-learn's defaults, apart from two small adjustments: Logistic Regression was allowed up to 1,000-2,000 iterations to ensure convergence, and Random Forest used 100 trees. Test accuracy on the original 80:20 split was our headline comparison,

but we did not stop there: we additionally ran stratified 5-fold cross-validation (reporting mean +/- SD) for all three models, computed a full per-class precision, recall, and F1 report plus ROC-AUC and PR-AUC for every model, and applied a McNemar's test to the paired test-set predictions to check whether any accuracy difference was statistically significant. To address the concern that comparing a scaled linear model against untuned tree ensembles is not a fair fight, we also ran a 30-iteration randomised hyperparameter search over Random Forest and added a HistGradientBoosting model as a boosting baseline neither of the original three models had to compete against. Finally, we pulled Random Forest's feature importances (mean decrease in Gini impurity) to rank the ten variables that mattered most.

3 RESULTS AND DISCUSSION

3.1 Model Comparison

Table 2 gives test-set accuracy, 5-fold cross-validated accuracy, and threshold-free ranking metrics (ROC-AUC, PR-AUC) for all three models, plus a tuned Random Forest and a boosting baseline added specifically to make the comparison fairer. On the original single 80:20 split, Logistic Regression (scaled) reached 86.67%, Random Forest 85.42%, and Decision Tree 78.42%, reproducing our earlier reported figures exactly. But that single-split ranking does not survive scrutiny. Under stratified 5-fold cross-validation, Logistic Regression and Random Forest show no statistically significant difference, 87.64% +/- 0.62% against 87.50% +/- 0.80%, well within one standard deviation of each other, while Decision Tree trails clearly at 80.70% +/- 1.54%. A McNemar's test on the original test set's paired predictions confirms this: Logistic Regression and Random Forest disagreed on 41 of 885 cases (26 in Logistic Regression's favour, 15 in Random Forest's), giving chi-square = 2.44, p = 0.118, not significant at the conventional 0.05 threshold. In other words, the 1.25-point gap we originally reported was noise, not signal.

Table 2. Model Performance: Single-Split Accuracy, 5-fold Cross-Validated Accuracy (mean +/- SD), and Ranking Metrics

Model	Test Acc. (%)	5-fold CV Acc. (%)	ROC-AUC	PR-AUC
Logistic Regression (scaled)	86.67	87.64 +/- 0.62	0.913	0.881
Random Forest (default)	85.42	87.50 +/- 0.80	0.905	0.869
Random Forest (tuned)	85.65	-	0.908	0.873
HistGradientBoosting	85.88	-	0.910	0.871
Decision Tree (default)	78.42	80.70 +/- 1.54	0.760	0.593

Tuning did not change this picture. A 30-iteration randomised search over Random Forest's hyperparameters (n_estimators, max_depth, min_samples_split/leaf, max_features) improved its test accuracy only marginally, from 85.42% to 85.65%. A HistGradientBoosting model, added as a boosting baseline, reached 85.88%, close to but still short of Logistic Regression's 86.67%. Neither difference from Logistic Regression was significant by McNemar's test (tuned Random Forest: chi-square = 1.73, p = 0.188; HistGradientBoosting: chi-square = 0.88, p = 0.349). Table 3 gives the full per-class precision, recall, and F1-score for the three originally compared models. Decision Tree's weakness is concentrated in the dropout class (recall 0.674);

Logistic Regression and Random Forest are close across both classes, with Logistic Regression recalling dropout cases slightly better (0.722 against 0.677).

Table 3. Full Per-Class Classification Report for Logistic Regression, Decision Tree, and Random Forest

Model	Class	Precision	Recall	F1-score	Support
Logistic Regression	0 (Non-dropout)	0.860	0.947	0.901	569
Logistic Regression	1 (Dropout)	0.884	0.722	0.794	316
Decision Tree	0 (Non-dropout)	0.824	0.845	0.834	569
Decision Tree	1 (Dropout)	0.708	0.674	0.690	316
Random Forest	0 (Non-dropout)	0.842	0.953	0.894	569
Random Forest	1 (Dropout)	0.888	0.677	0.768	316

3.2 Feature Importance

Figure 1 shows the ten variables Random Forest ranked as most important, by Gini-based importance. Curricular units approved in the second semester came out on top (0.154), followed closely by the second-semester grade average (0.142). Further down: first-semester units approved (0.080), first-semester grade (0.064), and whether tuition fees were up to date (0.063). Age at enrolment, the number of second-semester evaluations, admission grade, previous-qualification grade, and course of study rounded out the list, each between 0.033 and 0.040. None of this is a surprise, exactly: Realinho et al. (2022) found the same top variables using permutation importance across four different algorithms, and Villar and de Andrade (2024), using SHAP on boosting models, also put second-semester units approved firmly in first place. Three different importance methods, on three different kinds of models, none of them Logistic Regression, landing on the same answer is a reasonably strong signal that this ranking is not just an artefact of how Random Forest happens to split its trees.

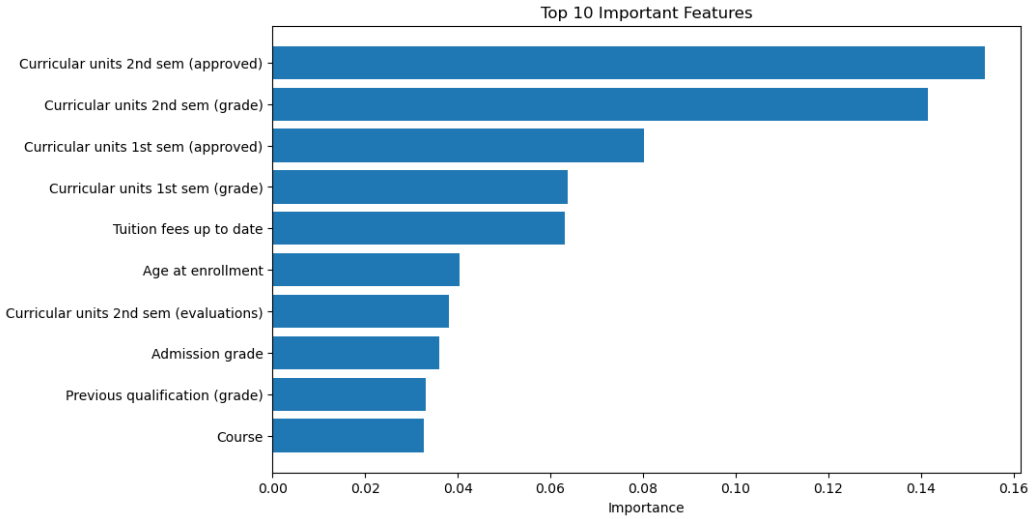


Figure 1. Top 10 Important Features Identified by the Random Forest Model

3.3 Discussion

Our original claim that Logistic Regression outperformed Random Forest does not hold up. Once evaluated properly, with cross-validation and a significance test rather than a single split, no

statistically significant difference was detected between Logistic Regression and Random Forest at the 0.05 significance level. Similarly, no statistically significant differences were detected between Logistic Regression and the tuned Random Forest or HistGradientBoosting models. The Decision Tree showed the lowest observed performance among the evaluated models. This is a more honest and, we think, still a useful finding: for this dataset, algorithm choice among Logistic Regression, Random Forest, and HistGradientBoosting matters far less than getting the basics right, using all available semesters of academic data and, ideally, addressing class imbalance. Decision Tree is the one model that is genuinely and significantly worse, which fits the general pattern in the literature that a single tree, with no ensembling or regularisation, is the weakest choice available (Andrade-Girón et al., 2023). Our results sit slightly below the 86-88% ceiling that tuned XGBoost and CatBoost reach on this exact dataset elsewhere (Ridwan et al., 2024; Villar & de Andrade, 2024); the gap could reflect differences between boosting libraries, or simply that 30 iterations of random search is a modest tuning budget.

One more thing worth noting: the strongest predictors we found only exist once a student has finished at least one semester. That makes this a within-programme early-warning tool, not a pre-enrolment screen, which fits the minimal-feature, first-year approach that Hoca and Dimililer (2025) also took.

Dropout is not only a modelling problem; it is a resilience problem. Institutions working under tight budgets are usually the ones who can least afford to lose a student, yet least able to fund the tuned, continuously validated systems the literature says are needed to flag risk reliably (Villegas-Ch et al., 2023). A flag generated by a model like this could misdirect scarce support, or become self-fulfilling if a student is treated differently once labelled "at risk" — concerns Dietz-Uhler and Hurn (2013) raise from a faculty perspective without resolving. In practice, such a model should not be used to decide who gets real support without a clear institutional policy on how flagged students are told and helped.

4 CONCLUSION

We compared Logistic Regression, Decision Tree, and Random Forest for predicting dropout on the UCI dataset, then validated the comparison properly. On a single 80:20 split, Logistic Regression appeared to lead (86.67% against 85.42% for Random Forest and 78.42% for Decision Tree), but 5-fold cross-validation and a McNemar's test showed the Logistic Regression/Random Forest gap is not statistically significant ($p = 0.118$), and this held even after tuning Random Forest ($p = 0.188$) and adding a HistGradientBoosting baseline ($p = 0.349$). Decision Tree, in contrast, is significantly and consistently the weakest of the three. Curricular performance in the first two semesters, units approved and grades above all, was confirmed as the strongest predictor of dropout, matching prior studies on this and related datasets. Because stronger, tuned benchmarks already exist for this exact dataset, we do not present this as a new best algorithm; the useful finding is instead that algorithm choice matters much less here than whether the comparison is validated properly in the first place.

Two limitations remain, both genuine and both still open. First, we did not address the moderate class imbalance (about 2.1:1) through resampling; recall on the dropout class stayed below 73%

for every model tested, and it is not yet clear how much of that is attributable to imbalance as opposed to the predictors themselves being imperfect. Applying and comparing resampling strategies such as SMOTE is a natural next step. Second, and this is a gap our own literature review points to but does not close: this work leans on a single, already well-studied dataset, leaves out psychosocial and equity variables, and does not check whether acting on its predictions would actually improve retention. That last question cannot be answered by another offline benchmark, however carefully validated; it needs a real institutional trial. Closing the validation gap in this revision changed our headline result. We would rather report that honestly than keep a more dramatic-sounding claim that did not survive testing.

5 REFERENCES

Andrade-Girón, D., Sandivar-Rosas, J., Marín-Rodriguez, W., Susanibar-Ramirez, E., Toro-Dextre, E., Ausejo-Sanchez, J., Villarreal-Torres, H., & Angeles-Morales, J. (2023). Predicting student dropout based on machine learning and deep learning: A systematic review. EAI Endorsed Transactions on Scalable Information Systems, 10(5), 1-11. https://doi.org/10.4108/eetsis.3586

Dietz-Uhler, B., & Hurn, J. E. (2013). Using learning analytics to predict (and improve) student success: A faculty perspective. Journal of Interactive Online Learning, 12(1), 17-26.

Hoca, S., & Dimililer, N. (2025). A machine learning framework for student retention policy development: A case study. Applied Sciences, 15(6), 2989. https://doi.org/10.3390/app15062989

Lopez-Muñoz, G. L., Gonzalez Serrano, C., & Sanchez-Ferreira, C. (2026). Student dropout prediction in higher education: A systematic review of machine learning methods and risk factors [Preprint]. ResearchGate.

Palacios, C. A., Reyes-Suárez, J. A., Bearzotti, L. A., Leiva, V., & Marchant, C. (2021). Knowledge discovery for higher education student retention based on data mining: Machine learning algorithms and case study in Chile. Entropy, 23(4), 485. https://doi.org/10.3390/e23040485

Realinho, V., Machado, J., Baptista, L., & Martins, M. V. (2022). Predicting student dropout and academic success. Data, 7(11), 146. https://doi.org/10.3390/data7110146

Ridwan, A., Priyatno, A. M., & Ningsih, L. (2024). Predict students' dropout and academic success with XGBoost. Journal of Education and Computer Applications, 1(2), 1-8. https://doi.org/10.69693/jeca.v1i2.13

ISSN: 2773-7055
Proceedings of the 5th International Research Conference
Institute of Technology, University of Moratuwa
November 5, 2026

Paper ID: 9

IDENTIFYING DOMINANT FACTORS ASSOCIATED WITH TUBERCULOSIS TREATMENT OUTCOMES IN THE KALMUNAI REGION, SRI LANKA: A LOGISTIC REGRESSION APPROACH

S A I M Samaraweera[1*], Hemalika T K Abeysundara[1]

[1]Department of Computer Science, University of Peradeniya, Sri Lanka

*Corresponding author: ishanimdsamaraweera@gmail.com

ABSTRACT: Tuberculosis remains a major public health challenge in Sri Lanka despite the implementation of control programmes and treatment strategies. Identifying factors associated with treatment outcomes is important for improving patient management and strengthening disease control efforts. This study aimed to identify the dominant factors associated with tuberculosis treatment outcomes among patients registered in the Kalmunai Regional Director of Health Services area, Sri Lanka, in 2016. Retrospective patient records data from 165 tuberculosis patients were analyzed using descriptive statistics, Chi-square tests, and binary logistic regression. The Chi-square analysis revealed significant associations between treatment outcome and age group, smoking status, betel chewing, and alcohol consumption. Binary logistic regression identified age, body weight, TB type, treatment category, smoking status, and betel chewing as significant independent predictors of treatment outcome. Increasing age was associated with higher odds of unsuccessful treatment outcomes, whereas higher body weight was associated with lower odds. Smoking had the largest estimated odds ratio for unsuccessful treatment outcomes (OR = 447, p = 0.036); however, the estimate was imprecise and should be interpreted cautiously because of the small number of relevant observations and its wide confidence interval. As the study was based on patient records from 2016, the findings are interpreted as a historical regional baseline and require validation using contemporary TB data.

Keywords: nutritional status, predictive factors, risk factors, smoking, treatment outcomes

1 INTRODUCTION

Tuberculosis (TB) remains one of the leading infectious diseases worldwide and continues to be a major public health challenge, particularly in developing countries. According to the World Health Organization (WHO, 2024), TB causes significant morbidity and mortality despite the availability of effective treatment and prevention strategies. In Sri Lanka, tuberculosis remains a concern for the public health sector, with new cases being reported annually across different regions (WHO, 2024). Early identification of factors associated with treatment outcomes is important for improving disease management and reducing the burden of TB.

The Kalmunai Regional Directorate of Health Services (RDHS) area is one of the regions where tuberculosis cases have been reported regularly. Understanding the demographic and clinical characteristics of TB patients in this region is essential for developing targeted interventions and strengthening existing control programmes. Although treatment success rates have improved over the years, unsuccessful treatment outcomes continue to occur among certain patient groups, highlighting the need for further investigation into the factors influencing treatment outcomes.

Several studies have reported factors associated with tuberculosis treatment outcomes. A study conducted in Pakistan by Atif et al. (2022) found that age, previous treatment history, and drug resistance significantly influenced unfavorable treatment outcomes among tuberculosis patients. Similarly, it was reported that older age, low body weight, and treatment category were important

predictors of unsuccessful treatment outcomes in Ethiopia (Tola et al., 2019). However, limited research has examined the factors associated with tuberculosis treatment outcomes at the regional level in Sri Lanka, particularly in the Kalmunai region. Furthermore, there is limited evidence regarding the dominant factors associated with tuberculosis treatment outcomes in the Kalmunai region.

Although the data used in this study were collected in 2016, they provide useful information about the factors related to TB treatment outcomes in the Kalmunai RDHS area at that time. Since then, TB treatment and monitoring practices in Sri Lanka have been updated, including changes in diagnosis, treatment procedures, and the management of drug-resistant and extra-pulmonary TB. Therefore, the findings of this study should be understood in relation to the situation in 2016 and should not be considered as a direct representation of current TB treatment outcomes.

Therefore, this study aims to identify the dominant factors associated with tuberculosis treatment outcomes among patients registered in the Kalmunai RDHS area in 2016. Specifically, the study seeks to (i) describe the socio-demographic and clinical characteristics of tuberculosis patients, (ii) identify factors associated with treatment outcomes, (iii) determine significant predictors of treatment outcomes using logistic regression. The findings of this study are expected to contribute to evidence-based decision-making and support the development of targeted public health interventions for tuberculosis control in Sri Lanka.

2 METHODOLOGY

This study was conducted using TB patient records obtained from the Regional Director of Health Services (RDHS) office in Kalmunai, Sri Lanka. The study area covers the Kalmunai health region, where tuberculosis remains an important public health concern. Secondary data collected through the National Tuberculosis Control Programme were used for the analysis.

The dataset consisted of 165 tuberculosis patients who were registered in the Kalmunai RDHS area during 2016. The treatment outcome of each patient was considered as the response variable and categorized as cured and non-cured. Several socio-demographic and clinical variables, including age, gender, body weight, disease classification, and patient category, were considered as explanatory variables (Hosmer et al., 2013).

Descriptive statistical methods were initially employed to summarize the demographic and clinical characteristics of the TB patients. Frequency distributions, percentages, and graphical representations were used to describe the distribution of tuberculosis cases according to the selected variables. The Chi-square test of independence was applied to examine the association between categorical explanatory variables and TB treatment outcomes (Agresti, 2019). For descriptive and categorical association analyses, continuous variables such as age and weight were grouped into appropriate categories. However, age and weight were retained as continuous variables in the binary logistic regression analysis to preserve their quantitative information. The response variable was TB treatment outcome, categorized as cured and non-cured, and was coded as 0 for cured and 1 for non-cured in the binary logistic regression analysis. Potential explanatory variables were subsequently evaluated using binary logistic regression to identify

independent predictors of unsuccessful treatment outcomes. The general form of the binary logistic regression model was expressed as:

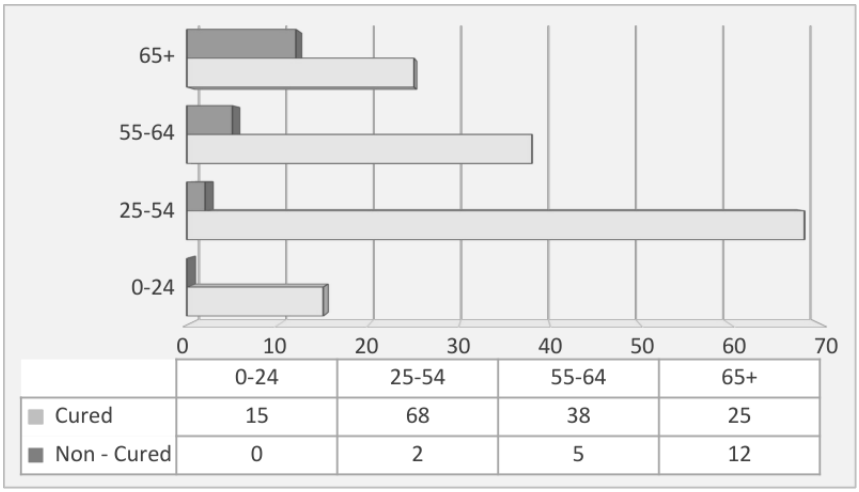
$$\log\left(\frac{p}{1-p}\right) = \beta_0 + \beta_1 x_1 + \beta_2 x_2 + \ldots + \beta_n x_n \quad (1)$$

where p represents the probability of a non-cured treatment outcome, β_0 is the intercept, β_i are the regression coefficients, and x_i are the explanatory variables. The significance of the explanatory variables was assessed at the 5% significance level.

3 RESULTS AND DISCUSSION

3.1 Distribution of Tuberculosis Patients

A total of 165 tuberculosis (TB) patients registered in the Kalmunai RDHS area during 2016 were included in this study. The distribution of patients according to age group is presented in Figure 1. Most TB patients belonged to the middle-aged and older age groups, while relatively fewer cases were reported among younger individuals.



	0-24	25-54	55-64	65+
Cured	15	68	38	25
Non - Cured	0	2	5	12

Figure 1. Distribution of TB Patients by Age Group

3.2 Factors Associated with Treatment Outcome

The association between selected patient characteristics and tuberculosis treatment outcome was examined using the Chi-square test of independence. The results revealed that age, smoking status, betel chewing, and alcohol consumption were significantly associated with treatment outcome at the 5% significance level (Table 1). Among these factors, age showed the strongest association with treatment outcome ($p = 0.020$). The findings suggest that behavioural and demographic factors may influence the likelihood of successful tuberculosis treatment. Therefore, these significant variables were considered for further investigation in the logistic regression analysis to identify the dominant predictors of treatment outcome.

Table 1. P-values for the Association Between Selected Factors and Tuberculosis Treatment Outcome

Variable	*p*-value	Variable	*p*-value
Age group	0.02	Gender	0.19
Smoking	0.04	Referral type	0.26
Betel chewing	0.02	Marital status	0.60
Alcohol consumption	0.04	Income level	0.97
		Occupation	0.10

3.3 Logistic Regression Analysis

Binary logistic regression identified age, body weight, TB type, treatment category, smoking status, and betel chewing as significant independent predictors of unsuccessful treatment outcome Table 2.

Table 2. Significant Predictors of Tuberculosis Treatment Outcomes Identified by Binary Logistic Regression

Variable	Coefficient (β)	OR	*p*-value	95% CI
Age	0.23	1.26	0.006	(1.07, 1.48)
Weight	-0.14	0.87	0.044	(0.76, 1.00)
TB Type (Pulmonary)	-3.05	0.047	0.049	(0.002, 0.99)
Treatment Category (2)	4.10	60.34	0.041	(1.18, 3079.16)
Smoking (Yes)	6.10	447	0.036	(1.49, 133475.82)
Betel (Yes)	2.25	9.49	0.047	(1.03, 87.37)

Note: OR = Odds Ratio, CI = Confidence Interval

Increasing age was associated with a higher likelihood of unsuccessful treatment outcomes, whereas higher body weight reduced this risk. Pulmonary TB patients showed lower odds of unsuccessful treatment outcomes compared with the reference group. Treatment Category 2 patients were more likely to experience unsuccessful outcomes. In addition, betel chewing was significantly associated with increased odds of unsuccessful treatment outcomes. Smoking had the largest estimated odds ratio for unsuccessful treatment outcomes (OR = 447, p = 0.036), although the estimate was imprecise and should be interpreted with caution. The final model had a Nagelkerke pseudo-R^2 of 0.61, with an AIC of 58.85 and a BIC of 98.75. Two-way interaction terms were tested; however, none were statistically significant at the 5% significance level and were therefore excluded from the final model. These findings indicate that demographic, clinical, and behavioral factors play important roles in determining tuberculosis treatment success.

3.4 Contemporary Relevant Findings

Although the data used in this study were collected in 2016, some factors identified in this study, particularly age, nutritional status, and smoking, have also been reported in more recent studies of TB treatment outcomes. Age has been associated with treatment outcomes in recent studies, with older age being linked to less favourable outcomes (Umayorubhagom & Baliga, 2024). Nutritional status also remains an important factor, as recent studies have reported that undernutrition is associated with an increased risk of unsuccessful TB treatment outcomes (Sinha et al., 2023). Smoking has also continued to be identified as a factor associated with adverse TB outcomes (Vidyasagaran et al., 2024). However, the results from this study may

not be directly applicable to TB patients today, as treatment guidelines, diagnostic methods, monitoring systems, and TB control practices have changed over time (NPTCCD, 2022). The NPTCCD has subsequently introduced updated guidance, including the National Manual for Tuberculosis Control 2022 Update and newer guidelines for extra-pulmonary and drug-resistant tuberculosis (NPTCCD, 2024). Therefore, the findings should be considered in the context of the 2016 Kalmunai RDHS population. Further studies using recent patient data would be useful to determine whether these factors are still important and whether their effects have remained similar.

4 LIMITATIONS

The use of data collected in 2016 is one of the limitations of this study. Since then, TB treatment guidelines, diagnostic methods, and surveillance systems in Sri Lanka have been updated. The National Programme for Tuberculosis Control and Chest Diseases (NPTCCD) has also introduced updated guidance, including the National Manual for Tuberculosis Control 2022 Update, which incorporates revised guidelines and updated definitions of TB treatment outcomes (NPTCCD, 2022). TB notification and reporting patterns have also changed over the years. Therefore, the predictors identified in this study may not have the same importance or effect among TB patients today. Further studies using more recent patient data are needed to confirm whether these findings are still applicable. The study also had a relatively small number of non-cured patients compared with cured patients. This imbalance may have affected the stability of the estimated effects in the logistic regression model. In addition, some categorical comparisons contained small, expected frequencies, which may affect the reliability of the Chi-square results. Therefore, the statistical findings, particularly the large odds ratios, should be interpreted with caution.

5 CONCLUSION

This study investigated factors associated with tuberculosis treatment outcomes among 165 patients registered in the Kalmunai RDHS area in 2016 using descriptive statistics, Chi-square analysis, and binary logistic regression. The findings revealed significant associations between treatment outcome and age group, smoking, betel chewing, and alcohol consumption. Binary logistic regression further identified age, body weight, TB type, treatment category, smoking status, and betel chewing as significant predictors of treatment outcome. Older age and selected behavioral factors were associated with higher odds of unsuccessful treatment, whereas higher body weight was associated with lower odds of unsuccessful treatment. Given the historical nature of the data and the relatively small number of non-cured patients, the findings should be interpreted cautiously and validated using contemporary TB data.

6 REFERENCES

Agresti, A. (2019). *An introduction to categorical data analysis* (3rd ed.). John Wiley & Sons.

Atif, M., Mukhtar, S., Sarwar, S., Naseem, M., Malik, I., & Mushtaq, A. (2022). Drug resistance patterns, treatment outcomes and factors affecting unfavourable treatment outcomes among extensively drug-resistant tuberculosis patients in Pakistan: A multicentre record review.

Saudi Pharmaceutical Journal, 30(4), 462–469. https://doi.org/10.1016/j.jsps.2022.01.015

Hosmer, D. W., Jr., Lemeshow, S., & Sturdivant, R. X. (2013). *Applied logistic regression* (3rd ed.). John Wiley & Sons. https://doi.org/10.1002/9781118548387

National Programme for Tuberculosis Control and Chest Diseases. (2022). *National manual for tuberculosis control: 2022 update*. Ministry of Health, Sri Lanka.

National Programme for Tuberculosis Control and Chest Diseases. (2024). *Patient management guidelines with BPaLM/BPaL: 2024: A supplement to PMDT guidelines–2021*. Ministry of Health, Sri Lanka.

Sinha, P., Ponnuraja, C., Gupte, N., Babu, S. P., ... Hochberg, N. S. (2023). Impact of undernutrition on tuberculosis treatment outcomes in India: A multicenter, prospective, cohort analysis. *Clinical Infectious Diseases, 76*(8), 1483–1491. https://doi.org/10.1093/cid/ciac915

Tola, A., Minshore, K. M., Ayele, Y., & Mekuria, A. N. (2019). Tuberculosis treatment outcomes and associated factors among TB patients attending public hospitals in Harar Town, Eastern Ethiopia: A five-year retrospective study. *Tuberculosis Research and Treatment, 2019*, Article 1503219. https://doi.org/10.1155/2019/1503219

Umayorubhagom, A., & Baliga, S. S. (2024). Factors affecting tuberculosis treatment outcome among newly diagnosed tuberculosis patients: A longitudinal study. *The Indian Journal of Tuberculosis, 71*(3), 337–343. https://doi.org/10.1016/j.ijtb.2023.06.007

Vidyasagaran, A. L., Readshaw, A., Boeckmann, M., Jarde, A., Siddiqui, F., Marshall, A.-M., Akram, J., Golub, J. E., Siddiqi, K., & Dogar, O. (2024). Is tobacco used associated with risk of recurrence and mortality among people with TB? *Chest, 165*(1), 22–47. https://doi.org/10.1016/j.chest.2023.08.021

World Health Organization. (2024). *All for health, health for all: Investment case 2025–2028*

ISSN: 2773-7055
Proceedings of the 5th International Research Conference
Institute of Technology, University of Moratuwa
November 5, 2026

Paper ID: 25

STRIKING THE RIGHT NOTE: ENHANCING FOUNDATIONAL CALCULUS LEARNING THROUGH ACTIVE LYRIC COMPOSITION AND PERFORMANCE

K K T S Bandara*

Division of Interdisciplinary Studies, Institute of Technology, University of Moratuwa, Homagama, Sri Lanka

*Corresponding author: kesharas@itum.mrt.ac.lk

ABSTRACT: Many engineering technology students often struggle with calculus because it requires understanding and remembering strong fundamental mathematical concepts. Traditional forms of teaching methods do not always ensure that students are provided with the right cognitive skills or memory aids to help them learn calculus. The key aim of this study is to examine the effects of writing and performing math-based song lyrics on student understanding and retention in foundational calculus. A sample of 176 Semester I students of the Institute of Technology, University of Moratuwa, was divided into two similar groups. The control group learned through traditional teaching methods, and the experimental group students transformed mathematical steps into song lyrics for active performance. Their academic performance was evaluated through pre-test and post-test. The pre and post scores were analyzed with paired t-test for same group (control or experimental). Then independent sample t-test used to analyze post test scores between control and experimental groups, also similarly pre test scores. Pre-test (independent sample) analysis confirmed group homogeneity, showing no statistically significant difference between the two groups ($t = 0.523$, $p = 0.602$). Post-intervention, the paired t-tests indicated that while the control group showed a significant but average score increase from 4.21 to 4.85 ($t = 4.82$, $p < 0.001$), the experimental group demonstrated a significant increase from 4.28 to 8.24 ($t = 33.41$, $p < 0.001$). Furthermore, a final post-test independent samples t-test revealed that the "Math to Music" intervention drastically outperformed traditional methods ($t = 27.03$, $p < 0.00001$). These empirical findings conclude that integrating music with advanced mathematics significantly boosts conceptual mastery and retention. Ultimately, this study demonstrates the value of the STEAM educational paradigm, proving that blending artistic creativity with technical rigor builds vital interdisciplinary cognitive skills.

Keywords: calculus, STEAM education, musical performance approach

1 INTRODUCTION

The Integration of mathematics with other disciplines has been shown to drive major improvements in student learning. Historically, renowned theorists such as Poincaré et al. (2010) and later Papert (1971) have argued that the most vital feature of the mathematical mind is not pure logic, but aesthetic sensibility that comes naturally. Since musical and mathematical creativity occur in the same four-part stages in conscious and subconscious processing (Poincaré et al., 2010), incorporating music into educational experiences can be considered a powerful example for arts-integrated mathematical pedagogy.

In recent years, the worldwide education system has noted a decline in creative thinking among students. This recognition has led to the evolution from a traditional STEM (Science, Technology, Engineering, Mathematics) framework to an integrated STEAM (Science, Technology, Engineering, Art, Mathematics) paradigm (Gavrilas & Kotsis, 2025). When students use a musical approach to solve mathematical problems, it significantly mitigates mathematics anxi-

ety and stimulates the spatial reasoning pathways, essential to understand abstract mathematic principles. (Holmes & Hallam, 2017).

Furthermore, cognitive research indicates that the structural elements of music provide an intrinsic structure that serves as scaffolding to working memory (Wu, 2024). In early childhood classrooms, steady music beats while learning mathematics increase the attention and engagement of students (Geist et al., 2012). Similarly, tactile actions that involve clapping and tapping to different beats and tempos can considerably help in understanding basic concepts in mathematics, such as fractions and ratios (Asvat, 2024). However, most research conducted so far is focused on primary and secondary students. Empirical utilization as a form of performance by undergraduate students in engineering technology is still not sufficiently covered. Conventional math-music activities tend to overlook advanced calculus, thus leaving out complex concepts in mathematics like hyperbolic functions and complex numbers. This study addresses this literature gap by introducing a novel "Math to Music" framework designed specifically for tertiary-level engineering technology education.

Thus, the objective of this study is to examine the effects of writing and performing math-based song lyrics on student understanding and retention in foundational calculus.

This research aims to offer an evidenced based framework for applying STEAM principles to mathematics at the university level, proving that interdisciplinary creativity can be used to consistently enhance academic performance.

2 METHODOLOGY

The target population for this study comprised all Semester I engineering technology undergraduate 800 students at the Institute of Technology, University of Moratuwa (ITUM), enrolled in foundational calculus. From this population, a sample of 176 students was selected and partitioned into two similar groups: a Control Group ($n_1 = 88$) and an Experimental Group($n_2 = 88$).

2.1 Instructional Procedure & Intervention

To ensure pedagogical consistency, both the control and experimental groups attended the same combined lecture session, where fundamental calculus theories and general examples were taught. The intervention occurred during the subsequent tutorial sessions, where the two groups were exposed to different problem-solving approaches:

- Control Group: Completed traditional, board-based tutorial exercises and standard step-by-step problem-solving methods.
- Experimental Group: Executed the interactive "Math to Music" approach.

2.1.1 Math to Music

The activity began with a short educational YouTube video entitled “e is a magical number” by Tisdell (2019), it was played to create a conceptual base for illustrating how mathematics concepts could be converted to a music rhythm. The experimental group was divided into small teams containing 8-10 students each. Each team was given a mathematical problem from the

area of calculus, which involved complex numbers or hyperbolic functions. The process of the interactive activity "Math to Music" is detailed in Table 1.

Table 1. Steps of Math to Music Activity

Stage	Description
1	Each group worked together to solve the problem from complex numbers and hyperbolic functions, using traditional deductive reasoning under the assistance of a lecturer.(40 minutes)
2	Students converted the rigid steps, formulas, and rules of their solution into a structured rhythmic song lyrics (20 minutes)
3	Students performed their song during Tutorial class. (10 minutes per group performance)

2.2 Assessment Instruments & Testing Timeline

- Pre-Test: Administered prior to the tutorial intervention to establish baseline homogeneity.
- Post-Test: Conducted one week (7 days) after the respective tutorial sessions.

Both the pre-test and post-test were structurally identical in weight and difficulty, consisting of 2 comprehensive problems worth a total of 10 marks per test.

2.3 Paired-sample t-test

The paired sample t-test (Lakens, 2021) compares means from the same group at different times (e.g., pretest and post test). The test statistic is given by equation (1).

$$T = \frac{\underline{d}}{SE} \sim t_{n-1,\ \alpha} \tag{1}$$

$d_i = X_{2,i} - X_{1,i}$, The difference between the post-test score $(X_{2,i})$ and pre-test score $(X_{1,i})$ for student i.
$\underline{d} = \frac{1}{n}\sum_{i-1}^{n} d_i$.
SE : The standard error of the difference between means.
$n-1$: degree of freedom where n is the number of pairs.
α : The significance level of the test, representing the maximum allowable probability of rejecting the null hypothesis (H_0) when it is actually true.
Hypotheses: $H_0 : \mu_d = 0$; $H_1 : \mu_d > 0$, where μ_d is the difference between post and pre-test scores.

2.4 Independent Samples t-test

The independent sample t-test (Ross & Willson, 2017) compares means from the different groups (e.g., control and experimental groups) for same situation. The test statistic is given by equation (2).

$$T = \frac{\underline{X_2} - \underline{X_1}}{SE} \sim t_{n_1+n_2-2,\ \alpha} \tag{2}$$

$\underline{X}_1$: The sample mean of the control group.
$\underline{X}_2$: The sample mean of the experimental group.
SE : The standard error of the difference between means. Assuming equal variances (verified via Levene's test for equality of variances), SE is calculated using pooled variance.
n_1 : Number of observations in the control group (88).
n_2 : Number of observations in the experimental group (88).
$n_1 + n_2 - 2$: degree of freedom($df = 174$). It is sufficiently large ($df > 30$) to apply the standard normal approximation under the Central Limit Theorem.
α : The significance level of the test, representing the maximum allowable probability of rejecting the null hypothesis (H_0) when it is actually true.
Hypotheses: $H_0 : \mu_2 - \mu_1 = 0$; $H_1 : \mu_2 - \mu_1 > 0$, Where μ_1 and μ_2 denote the population mean scores of the control and experimental groups, respectively.

3 RESULTS AND DISCUSSION

This section analyzes and evaluates the pre-test and post-test scores of the students being instructed through the traditional method and the scores of the students who have undergone the interactive "Math to Music" teaching approach. The analysis was done through the use of the R software for performing parametric tests.

3.1 Independent sample t-test for Pre-test scores

The independent sample t-test was performed to test the pre-test scores of two groups. Test statistic T = 0.523 with p-value 0.602, which is higher than 0.05. Thus H_0 cannot be rejected at the 5% significance level. It concludes that the baseline of both student groups was the same.

3.2 Paired sample t-test for the traditional learning group

Academic progress achieved through the use of traditional educational methods was analyzed using the paired samples t-test on the pre-test and post-test scores obtained from the control group. This indicated an increase from the pre-test mean score of 4.21 to the post-test mean score of 4.85. Although the improvement of 0.64 was statistically significant according to the test statistic value
T = 4.82 with p < 0.001, the resultant gain in learning was quite minimal.

3.3 Paired sample t-test for the "Math to Music" activity group

A paired samples t-test was performed on the experimental group to analyze the impact of the interactive "Math to Music" intervention. The data revealed the average score increased from a pre-test of 4.28 to a post-test average of 8.24. Test statistic T = 33.41 with p < 0.001, which is less than 0.05. Thus H_0 is rejected at the 5% significance level. The test results demonstrate a significant improvement in procedural recall and formula retention facilitated by musical mnemonics.

3.4 Independent sample t-test for Post-test scores

Students' academic performance was compared using an independent-samples t-test, directly comparing post-test scores obtained by students in the traditional learning group ($\underline{X}_1 = 4.85, SD =$

0.88) and the "Math to Music" activity group ($\underline{X}_2 = 8.24, SD = 0.81$). The test statistic revealed a highly significant difference ($T = 27.03$ with p< 0.00001 which is less than 0.05). Consequently H_0 is rejected at the 5% significance level and H_1 is accepted. It can be concluded that a musical approach is more helpful than the traditional teaching method in helping students to understand and memorize mathematical concepts.

Figure 1 demonstrates samples of song lyrics from the "Math to Music" intervention, displaying English and Sinhala lyric compositions alongside corresponding algebraic derivations for complex numbers and hyperbolic functions.

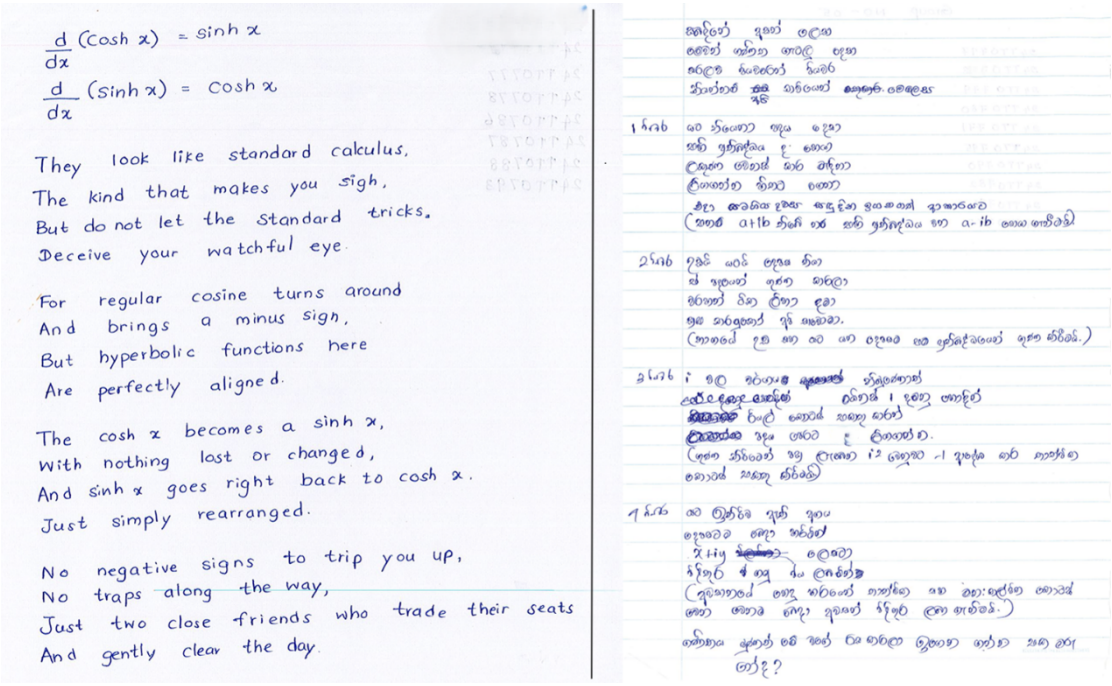


Figure 1. Sample of composed Song Lyrics

4 CONCLUSION

The key finding of this study is that integrating rhythmic lyric composition into calculus tutorials significantly improves short-term retention and procedural performance among diploma-level engineering technology undergraduates compared to traditional instructions. The implementation of the "Math to Music" activity demonstrates the practical utility of the STEAM paradigm, showing how creative arts integration provides an effective memory scaffold for foundational calculus topics like hyperbolic functions and complex numbers. Future work will focus on expanding this methodology across broader university degree programs and utilizing higher-order problem assessments to evaluate long-term conceptual understanding beyond procedural recall.

5 ACKNOWLEDGEMENTS

I gratefully acknowledge the support provided by the academic and non-academic staff of the Division of Interdisciplinary Studies, ITUM. I am also deeply thankful to all participating students for their engagement and valuable contribution to this study.

6 REFERENCES

Asvat, Z.J. (2024). Music and maths: The magical link. *Medihelp* https://www.medihelp.co.za/showcase/blog/music-maths

Gavrilas, L., & Kotsis, K. T. (2025). The evolution of STEM education and the transition to STEAM/STREAM. *Aquademia*, 9(1), ep25002. https://doi.org/10.29333/aquademia/16313

Geist, K., Geist, E., & Kuznik, K. (2012). The Patterns of Music: Young Children Learning Mathematics through Beat, Rhythm, and Melody. Young Children, 67(1), 74–79. https://eric.ed.gov/?id=EJ975497

Holmes, S., & Hallam, S. (2017). The impact of participation in music on learning mathematics. *London Review of Education* (Vol. 15, Issue 3). https://doi.org/10.18546/lre.15.3.07

Lakens, D. (2021). *The Student t-test: An introduction to and comparison of parametric and non-parametric tests for comparing two independent groups.* Collabra: Psychology, 7(1), 18640.
https://doi.org/10.1177/1948550617697177

Papert, S. (1971). *Teaching children thinking* Massachusetts Institute of Technology, Artificial Intelligence Laboratory http://dl.acm.org/citation.cfm?id=1096933

Poincaré, H., Halsted, G. B., & Royce, J. (2010). The Foundations of science : Science and hypothesis, The Value of Science, Science and Method. https://doi.org/10.1017/cbo9781107252950

Ross, A., & Willson, V. L. (2017). Basic and advanced statistical tests. In Basic and Advanced Statistical Tests (pp. 1–19). SensePublishers. https://doi.org/10.1007/978-94-6351-086-8

Tisdell, C. C. (2019). An Arts-Integrated Approach to Learning Mathematics through Music: A Case Study of the Song "e is a Magic Number." *International Journal of Innovation in Science and Mathematics Education*, *27(7).* https://doi.org/10.30722/ijisme.27.07.005

Wu, J. (2024). Research on Techniques in Music Performance: A Comprehensive Analysis of Cognitive, Motor, and Neuroplastic Adaptations. *US-China Education Review A*, 14(6), 410. https://doi.org/10.17265/2161-623x/2024.06.010

ISSN: 2773-7055
Proceedings of the 5th International Research Conference
Institute of Technology, University of Moratuwa
November 5, 2026

Paper ID: 28

FACTORS ASSOCIATED WITH SPORTS INJURY OCCURRENCE AMONG UNIVERSITY ATHLETES: A CASE STUDY FROM UVA WELLASSA UNIVERSITY, SRI LANKA

R P G Amithani[1*], D D G A D S Saparamadu[1]

[1]Division of Interdisciplinary Studies, Institute of Technology, University of Moratuwa, Homagama, Sri Lanka

*Corresponding author: amithanir@itum.mrt.ac.lk

ABSTRACT: Sports injuries represent a significant challenge among university athletes, affecting athletic performance, academic engagement, and overall well-being. This study aimed to identify factors associated with sports injury occurrence among undergraduate athletes at Uva Wellassa University, Sri Lanka. A cross-sectional analytical study was conducted among 200 student athletes actively participating in university sports. Data were collected using a structured self-administered questionnaire that covering demographic characteristics, sports participation, training-related factors, lifestyle behaviors, and injury history. Statistical analyses were performed using Minitab, including descriptive statistics, Chi-square tests, and Mann–Whitney U tests. The mean age of participants was 22.365 (SD=1.985) years, and 60% reported at least one sports-related injury. Sprains and strains were the most common injuries, with the ankle and knee being the most frequently affected anatomical regions. Most injuries were classified as moderate in severity. Chi-square analysis showed significant associations between injury occurrence and gender, main sport, participation type, years of experience, training hours, training intensity, sleep duration, nutrition quality, hydration status, stress level, and previous injury history ($p < 0.001$). Mann–Whitney U tests also revealed significant differences in age and body mass index between injured and non-injured athletes. The findings demonstrate that sports injuries among university athletes are influenced by multiple demographic, training, and lifestyle factors. Injury prevention programme should emphasize training load management, adequate recovery, nutrition, hydration, psychological well-being, and evidenced based rehabilitation to reduce injury risk, improve athletic performance, and support academic participation.

Keywords: Sports injuries, University athletes, Injury risk factors, Training characteristics

1 INTRODUCTION

Participation in sports and physical activities is an important component of university life, contributing to physical fitness, psychological well-being, and social development among students. Regular involvement in sports enhances athletic performance, promotes healthy lifestyles, and supports the development of teamwork and leadership skills. Despite these benefits, sports-related injuries remain a major concern among university athletes, adversely affecting athletic performance, academic engagement, and overall well-being (Kimura et al., 2024). Previous studies have identified demographic, training-related, and lifestyle factors as key determinants of sports injury risk. Higher training loads, increased training intensity, previous injury history, inadequate sleep, poor recovery practices, and elevated stress levels have been identified as important contributors to injury risk among athletes (Jones et al., 2017). Furthermore, lifestyle factors such as nutrition quality and hydration status play a significant role in athlete recovery and injury prevention (Puga et al., 2023). Research has also shown that inadequate sleep duration is associated with an increased likelihood of sports injuries among collegiate athletes (Messman

et al., 2025). The objective of this study was to identify the factors associated with sports injury occurrence among university athletes at Uva Wellassa University, Sri Lanka.

2 METHODOLOGY

A cross-sectional analytical study was conducted among 200 undergraduate athletes at Uva Wellassa University, Sri Lanka. Data were collected using a structured self-administered questionnaire covering demographic characteristics, sports participation, training-related factors, lifestyle behaviors, and injury history. Injury prevalence was calculated as the proportion of athletes reporting at least one sports injury. The overall prevalence of sports injuries was calculated as follows;

$$Injury\ Prevalence\ (\%) = \frac{Number\ of\ injured\ athletes}{Total\ sample\ size} \times 100 \quad (1)$$

(Kimura et al., 2024). Associations between injury occurrence and categorical variables were assessed using Chi-square tests, while continuous variables were compared using Mann–Whitney U tests (Chicco et al., 2025). Statistical analyses were performed using Minitab, with statistical significance set at $p < 0.05$. For hypothesis testing, the null and alternative hypotheses were formulated as follows for the association between demographic, training-related, and lifestyle factors and sports injury occurrence:

H_0: Demographic factors are not significantly associated with sports injury occurrence among university athletes.

H_1: Demographic factors are significantly associated with sports injury occurrence among university athletes.

Similarly, the hypotheses for other factors were considered.

3 RESULTS AND DISCUSSION

Table 1. Descriptive Statistics of Age and Body Mass Index (BMI)

Variable	Gender	N	Mean	StDev
BMI	Female	105	22.558	2.794
	Male	95	24.409	2.657
Age (Years)		200	22.365	1.985

A total of 200 university athletes participated in the study. The mean age was 22.365 (SD = 1.985) years (range: 19–27 years). Male athletes had a higher mean BMI (24.409, SD = 2.657 kg/m^2) than female athletes (22.558, SD = 2.794 kg/m^2). The 60% (n = 120) of participants reported at least one sports-related injury, while 40% (n = 80) reported no injuries. This high injury prevalence indicates that sports injuries are a significant health concern among university athletes and is consistent with previous studies reporting high injury rates among collegiate athletes due to intensive training and competitive sports participation (Lemoyne et al., 2017).

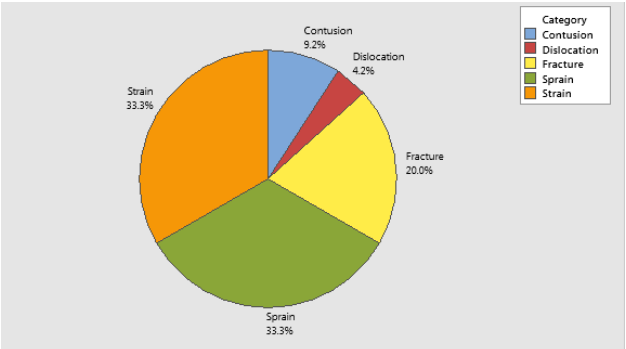


Figure 1. Distribution of injury type among university athletes *The figures include only athletes who reported at least one sports injury (n=120)*

Among injured athletes, sprains (33.3%) and strains (33.3%) were the most common injury types, followed by fractures, contusions, and dislocations.

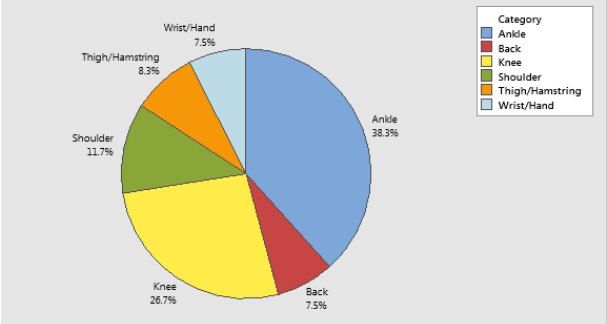


Figure 2. Distribution of body region affected among university athletes[1]

Figure 2 shows that the ankle (38.3%) was the most frequently injured body region, followed by the knee (26.7%), shoulder (11.7%), thigh/hamstring (8.3%), back (7.5%), and wrist/hand (7.5%). The predominance of ankle and knee injuries highlights the vulnerability of the lower extremities during running, jumping, cutting, and landing movements, consistent with previous studies among collegiate athletes (Messman et al., 2025).

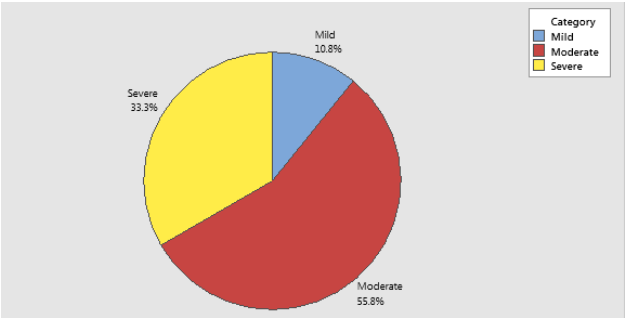


Figure 3. Distribution of severity of injury among university athletes[1]

Figure 3 shows that most injuries were moderate (55.8%), followed by severe (33.3%) and mild (10.8%) injuries. The high proportion of moderate and severe injuries substantial disruption to training and competition, with severe injuries potentially leading to prolonged recovery and reduced athletic performance (Tawfeeq & Malm, 2025).

Table 2. Association Between Risk Factors and Sports Injury Status

Variable	Category	Not Injured n(%)	Injured n(%)	χ^2 (df)	p-value
Gender	Female	56 (28.0)	49 (24.5)	16.374 (1)	<0.001
	Male	24 (12.0)	71 (35.5)		
Main Sport	Athletics	21 (10.5)	13 (6.5)	42.644 (6)	<0.001
	Badminton	13 (6.5)	6 (3.0)		
	Basketball	3 (1.5)	28 (14.0)		
	Cricket	11 (5.5)	10 (5.0)		
	Football	11 (5.5)	34 (17.0)		
	Netball	16 (8.0)	8 (4.0)		
	Volleyball	5 (2.5)	21 (10.5)		
Participation Type	Club/Inter-university	7 (3.5)	39 (19.5)	31.583 (3)	<0.001
	Freshers' games	33 (16.5)	14 (7.0)		
	Leisure Sports	9 (4.5)	23 (11.5)		
	University sports meet	31 (15.5)	44 (22.0)		
Years of Experience	Less than 1 year	32 (16.0)	5 (2.5)	46.657 (3)	<0.001
	1–3 years	22 (11.0)	46 (23.0)		
	4–6 years	20 (10.0)	33 (16.5)		
	More than 6 years	6 (3.0)	36 (18.0)		
Training Hours per Week	<5	28 (14.0)	12 (6.0)	45.035 (3)	<0.001
	5–10	37 (18.5)	35 (17.5)		
	10–15	14 (7.0)	33 (16.5)		
	>15	1 (0.5)	40 (20.0)		
Training Intensity	Low	44 (22.0)	15 (7.5)	62.818 (2)	<0.001
	Moderate	32 (16.0)	41 (20.5)		
	High	4 (2.0)	64 (32.0)		
Sleep Duration	Less than 5 hours	4 (2.0)	25 (12.5)	38.057 (3)	<0.001
	5–6 hours	14 (7.0)	49 (24.5)		
	7–8 hours	34 (17.0)	37 (18.5)		
	More than 8 hours	28 (14.0)	9 (4.5)		
Nutrition Quality	Poor	9 (4.5)	58 (29.0)	49.343 (2)	<0.001
	Fair	31 (15.5)	50 (25.0)		
	Good	40 (20.0)	12 (6.0)		
Hydration Level During Training	Rarely sufficient	3 (1.5)	18 (9.0)	38.887 (3)	<0.001
	Sometimes sufficient	11 (5.5)	53 (26.5)		
	Often sufficient	27 (13.5)	30 (15.0)		
	Always sufficient	39 (19.5)	19 (9.5)		
Stress Level	Low	40 (20.0)	13 (6.5)	52.715 (3)	<0.001
	Moderate	26 (13.0)	31 (15.5)		
	High	11 (5.5)	40 (20.0)		
	Very high	3 (1.5)	36 (18.0)		
Previous Injury History	No	80 (40.0)	0 (0.0)	200.000 (1)	<0.001

Variable	Category	Not Injured n(%)	Injured n(%)	χ^2 (df)	p-value
	Yes	0 (0.0)	120 (60.0)		

The null hypotheses were rejected for the variables that showed statistically significant associations with injury occurrence ($p < 0.05$). Chi-square analysis identified significant associations between injury occurrence and gender, main sport, participation type, years of experience, training hours, training intensity, sleep duration, nutrition quality, hydration level, stress level, and previous injury history ($all\ p < .001$). Higher injury prevalence was observed among male athletes, participants in basketball, football, and volleyball, and those with longer training hours and higher training intensity, supporting evidence that excessive training loads increase injury risk. These findings support the workload–injury relationship described by Rossi & Rodrigues, which suggests that excessive training loads increase injury susceptibility (Rossi & Rodrigues, 2025). Lifestyle-related factors were significantly associated with injury occurrence. Athletes reporting inadequate sleep, poor nutrition, insufficient hydration, and high stress experienced more injuries, consistent with previous evidence linking poor recovery behaviors and psychological stress to increased injury risk (Tawfeeq & Malm, 2025). Previous injury history was the strongest factor associated with injury occurrence, supporting findings that prior injuries increase the risk of subsequent injuries because of residual deficits and incomplete rehabilitation (Kimura et al., 2024). The Mann–Whitney U test also showed significant differences in age (median = 22 years, $p < 0.001$) and BMI (median = 23.2 kg/m^2, $p < 0.001$) between injured and non-injured athletes.

4 CONCLUSION

Sports injuries were highly prevalent among university athletes, with 60% of participants reporting at least one injury. Sprains and strains were the most common injury types, while the ankle and knee were the most frequently affected body regions. Injury occurrence was significantly associated with gender, main sport, participation type, years of experience, training hours, training intensity, sleep duration, nutrition quality, hydration level, stress level, and previous injury history, highlighting the multifactorial nature of sports injuries. The Mann–Whitney U test also identified significant differences in age and BMI between injured and non-injured athletes (both $p < .001$), further indicating the importance of individual characteristics in understanding injury occurrence. These findings emphasize the need for comprehensive injury prevention programmes that promote appropriate training load management, adequate recovery, optimal nutrition and hydration, psychological well-being, and effective rehabilitation. Targeted interventions to prevent lower-limb injuries, particularly those involving the ankle and knee, may further reduce injury risk and improve athlete health, performance, and continued participation in sports.

5 LIMITATION AND FUTURE WORK

This study was limited by its cross-sectional design, relatively small sample size, single-university setting, and reliance on self-reported data, which may limit the generalizability of the findings. Future studies will focus on developing and validating predictive models for

sports injury risk using the significant demographic, sport-related, training-related, and lifestyle factors identified in this study.

6 ACKNOWLEDGEMENTS

The authors would like to express their sincere gratitude to all undergraduate students of Uva Wellassa University who voluntarily participated in this study.

7 REFERENCES

Chicco, D., Sichenze, A., & Jurman, G. (2025). A simple guide to the use of Student's t-test, Mann-Whitney U test, Chi-squared test, and Kruskal-Wallis test in biostatistics. In *BioData Mining* (Vol. 18, Number 1). BioMed Central. https://doi.org/10.1186/s13040-025-00465-6

Jones, C. M., Griffiths, P. C., & Mellalieu, S. D. (2017). Training Load and Fatigue Marker Associations with Injury and Illness: A Systematic Review of Longitudinal Studies. In *Sports Medicine* (Vol. 47, Number 5). Springer International Publishing. https://doi.org/10.1007/s40279-016-0619-5

Kimura, T., Mącznik, A. K., Kinoda, A., Yamada, Y., Muramoto, Y., Katsumata, Y., & Sato, K. (2024). Prevalence of and Factors Associated with Sports Injuries in 11,000 Japanese Collegiate Athletes. *Sports*, *12*(1). https://doi.org/10.3390/sports12010010

Lemoyne, J., Poulin, C., Richer, N., & Bussières, A. (2017). Analyzing injuries among university-level athletes: Prevalence, patterns and risk factors. *Journal of the Canadian Chiropractic Association*, *61*(2), 83–87.

Messman, B. A., Petrie, K. A., Moore, E. W. G., & Petrie, T. A. (2025). Sleep Disturbances and Risk of Sports Injury Among Collegiate Student-Athletes. *Clinical Journal of Sport Medicine*, *35*(5), e54–e60. https://doi.org/10.1097/JSM.0000000000001278

Puga, T. B., Mazumder, R. M., Ruan, T., Scigliano, N., Thiel, G. E., & Treffer, K. (2023). Sleep, nutrition, hydration and rest: The equal importance of external factors outside of training and practice for sports injury prevention. *Scientific Journal of Sport and Performance*, *2*(4), 428–438. https://doi.org/10.55860/LZNO4932.This

Rossi, L., & Rodrigues, B. (2025). *Finding Pre-Injury Patterns in Triathletes from Lifestyle, Recovery and Load Dynamics Features*. http://arxiv.org/abs/2511.17610

Tawfeeq, R., & Malm, C. B. (2025). *The Association Between Sleep Duration and Sports Injury Risk in Athletes: A Structured Litterature Review and Meta-Analysis*.

ISSN: 2773-7055
Proceedings of the 5th International Research Conference
Institute of Technology, University of Moratuwa
November 5, 2026

Paper ID: 32

MACROECONOMIC DETERMINANTS OF THE INDIAN RUPEE TO SRI LANKAN RUPEE EXCHANGE RATE: EVIDENCE FROM AN ARDL ANALYSIS

Nadunika Peiris[1*], Samanthi Mathugama[2], Ravindi Jayasundara[1]
[1]Faculty of Engineering, University of Moratuwa, Sri Lanka,
[2]Division of Interdisciplinary Studies, Institute of Technology, University of Moratuwa, Homagama, Sri Lanka

*Corresponding author: nadu.peiris95@gmail.com

ABSTRACT: This study investigates the macroeconomic drivers of the Indian rupee to Sri Lankan rupee exchange rate from January 2004 to May 2024. With the Indian Rupee gaining increasing prominence in regional trade and financial transactions, the research focuses on how inflation, interest rate movements and money supply growth relate to fluctuations in the bilateral exchange rate. Using monthly data compiled from the Central Bank of Sri Lanka, the analysis follows a structured econometric approach built around the Autoregressive Distributed Lag (ARDL) framework. The descriptive statistics and graphical analysis provide an initial sense of the underlying patterns and volatility in the key variables. Unit root tests indicate a mixture of I(0) and I(1) processes, thereby justifying the use of the ARDL modelling procedure. The chosen ARDL(2,2,2,2) model exhibits strong explanatory capability, and the bounds test confirms the existence of a long-run association among the variables. The subsequent Error Correction Model, however, points to a weak and statistically insignificant adjustment mechanism, suggesting that deviations from long-run equilibrium do not correct rapidly. In contrast, the short-run dynamics are more substantial: movements in money supply growth have an immediate and significant effect on the exchange rate, while the short-run influence of interest rates and inflation becomes comparatively muted once liquidity conditions are taken into account. These results underscore the dominant role of domestic monetary conditions in driving Indian rupee to Sri Lankan rupee fluctuations. Overall, the research adds to the comparatively limited body of Sri Lankan work on Indian rupee to Sri Lankan rupee exchange rate behaviour and offers empirical insights that may help inform more coherent and forward-looking monetary and exchange rate policies.

Keywords: INR/LKR exchange rate, ARDL framework, inflation, interest rates, money supply growth

1 INTRODUCTION

Sri Lanka's exchange rate policy has gradually shifted from a fixed regime to a more flexible system to support trade competitiveness, inflation control, and macroeconomic stability. With increasing economic integration between Sri Lanka and India, movements in the Indian rupee–Sri Lankan rupee (INR/LKR) exchange rate have become increasingly important for trade and financial stability.

1.1 Background of the Study

Exchange rate movements play a crucial role in determining a country's external competitiveness, trade performance, investment flows, and overall macroeconomic stability. In recent years, the Indian Rupee (INR) has gained increasing importance in regional trade and financial transactions, particularly in South Asia, making the INR/LKR exchange rate a subject of growing policy interest (Lanka News Web, 2025). Sri Lanka's recent economic challenges, including high inflation, monetary instability, and balance of payments pressures, have further highlighted the need to understand the macroeconomic factors influencing exchange rate behaviour. An

appreciated exchange rate makes a country's currency expensive, making exports more costly and less competitive, whereas a depreciated exchange rate results in a decline in currency value, making imports more expensive and potentially increasing domestic inflation (Rajakaruna, 2017).

Since the Indo-Sri Lanka Free Trade Agreement went into effect in 2000, bilateral trade has expanded drastically, with India becoming one of Sri Lanka's largest trading partners, accounting for almost 20% of imports and 6% of exports. Furthermore, the formal approval of the INR as a designated foreign currency for trade settlement in Sri Lanka in August 2022 underscores the urgency of modelling this specific currency pair. While a substantial body of literature (Rajakaruna, 2017, Thevakumar and Jayathilaka, 2022, Dissanayake *et al.*, 2025) has examined exchange rate determinants in major economies, empirical evidence focusing specifically on the Indian Rupee to Sri Lankan Rupee exchange rate remains limited. This study therefore investigates the effects of inflation, interest rates, and money supply growth on the INR/LKR exchange rate using monthly data from January 2004 to May 2024.

1.2 Research Objectives

This study seeks to address "What are the macroeconomic determinants that influence the INR/LKR exchange rate in Sri Lanka, and how do these factors interact to explain its short-run and long-run dynamics?"

The answer for the above question was by accomplishing the following objectives in analysing the macroeconomic determinants of the INR/LKR exchange rate over the period from January 2004 to December 2023:

- To summaries the statistical properties of the INR/LKR exchange rate, inflation rates, interest rate, money supply growth.
- To analyses both the short-run and long-run relationships between selected macroeconomic variables and the INR/LKR exchange rate using appropriate time series econometric techniques.

2 METHODOLOGY

2.1 Variable Definition

The dataset consists of 245 monthly observations sourced from the Central Bank of Sri Lanka (CBSL) database. The dependent variable is the Monthly average nominal INR/LKR exchange rate (INRER), which is transformed into its natural logarithmic form (LnINRER) to stabilise variance and allow for elasticity interpretations. The explanatory variables include the Inflation Rate (INF), calculated as the year-on-year change in the Colombo Consumer Price Index (CCPI); the Interest Rate (INT), represented by the monthly average of the Standing Deposit Facility (SDF) and Standing Lending Facility (SLF) rates; and the Money Supply Growth Rate (MG), derived from the monthly growth rate of broad money (M2B). These explanatory variables were retained in levels ensures that estimated coefficients correspond directly to percentage point changes, which is clearer for policy interpretation. Similar approaches were used in prior studies such as Ali *et al.* (2015).

The selection of macroeconomic variables was mainly based on economic theory and previous empirical studies on exchange rate movements, with particular consideration given to the Sri Lankan context. Inflation, interest rate and money supply growth were selected as explanatory variables as they represent important price, monetary policy and liquidity conditions that can influence exchange rate movements. Previous studies on Sri Lanka have identified inflation and interest rates as important factors affecting exchange rate behaviour, while money supply has also been found to have a significant relationship with exchange rate movements. Therefore, these three variables were selected to examine the role of domestic macroeconomic conditions in determining the INR/LKR exchange rate.

2.2 Descriptive Statistics

To understand the baseline statistical properties of the series, key metrics including mean, standard deviation, minimum, and maximum, providing an overview of dispersion and distributional characteristics. Higher order moments, including skewness and kurtosis, offer additional insight into asymmetry and tail behaviour, which is useful in assessing the suitability of the series for time series analysis (Brooks, 2019).

2.3 Testing for Normality

The Jarque-Bera (JB) test is applied to formally evaluate whether the variables follow a normal distribution framework, which underpins the consistency of subsequent standard inferences (Gujarati and Porter, 2009).

2.4 Unit Root Testing

Verifying the stationarity properties of the variables is an essential prerequisite in time-series modelling to avoid spurious regression results. A series is weakly stationary if its mean, variance, and autocovariance remain invariant over time. This study implements the Augmented Dickey-Fuller (ADF) and Phillips-Perron (PP) tests. The ADF test addresses higher-order serial correlation by incorporating lagged difference terms, while the PP test utilises non-parametric methods to adjust for serial correlation and heteroskedasticity in the residuals (Enders, 2014).

2.5 ARDL Model Selection

The Autoregressive Distributed Lag, ARDL modelling strategy, introduced by Pesaran *et al.* (2001), offers a flexible approach for analysing both short-run and long-run dynamics in time series settings. One of its key advantages is that it accommodates regressors that are a mix of I(0) and I(1), so long as none are integrated of order two, I(2). The dynamic ARDL model structure allows for individual optimal lag lengths across variables, selected via the Akaike Information Criterion (AIC). To confirm long-run integration, the Bounds F-test is executed against the null hypothesis of no cointegration. Upon establishing cointegration, the Restricted Error Correction Model (ECM) is estimated to evaluate short-run dynamics and the convergence speed parameter (Enders, 2014).

2.6 Model Diagnostics Tests

To test the model assumptions of residuals with no serial correlation, no heteroscedasticity and normality, Breusch-Godfrey LM test, Breusch-Pagan test and Jarque-Bera test were used (Gujarati and Porter, 2009).

3 RESULTS AND DISCUSSION

3.1 Descriptive Statistical Analysis

Summary statistics reveal that inflation, INF and money supply growth, MG exhibit substantial volatility. INF exhibits a pronounced gap between its mean (9.8245) and median (6.1514), indicating the presence of high inflation episodes that elevate the average level. All series display positive skewness and kurtosis values exceeding 3, signifying leptokurtic and heavy-tailed distributions. The large, highly significant Jarque-Bera statistics reject the null hypothesis of normality for all series, indicating a high degree of macroeconomic turbulence over the sample period.

3.2 Stationarity Analysis

Unit root test results at levels and first differences are summarised in **Table 1**. The nominal log exchange rate (LnINRER), INF, and INT are non-stationary at levels but become stationary at their first differences, establishing that they follow an I(1) process. Conversely, money supply growth (MG) is stationary at level, indicating an I(0) process. This combination of mixed integration orders validates the application of the ARDL bounds testing framework.

Table 1. Unit Root Test Results Summary

Item	Variable	ADF Level (p-value)	PP Level (p-value)	ADF Diff (p-value)	Integration Order
1	LnINRER	-1.8044	-6.7726	-5.7675	I(1)
2	INF	-4.3479	-15.578	-5.5344	I(1)
3	INT	-3.0408	-11.207	-4.9634	I(1)
4	MG	-5.9225	-213.14	-10.274	I(0)

3.3 ARDL Model Estimation

The automated lag selection identifies an ARDL (2,2,2,2) structure as optimal. The framework exhibits high explanatory power with an adjusted R2 of 0.9861 and an F-statistic of 1557 ($p < 0.001$). The Bounds test yields an F-statistic of 5.2084, which comfortably exceeds the upper critical bound of 3.61 at the 5% significance level, providing strong evidence of a valid long-run relationship among the variables.

The restricted Error Correction Model results are detailed in Table 2. Short-run dynamics indicate that money supply growth exerts the most decisive immediate impact on currency depreciation, reflecting the monetary approach framework where excess liquidity drives currency weakening. Inflation presents an alternating pattern, suggesting short-lived cost-push shocks followed by subsequent corrections. Interestingly, short-run interest rate coefficients are positive, which demonstrates that policy rate hikes typically accompany currency depreciation episodes

during periods of severe macroeconomic crisis in Sri Lanka. The Error Correction Term (ECTt-1) is small and positive (0.0133), implying that corrective forces towards long-run equilibrium are practically inactive or heavily delayed due to persistent external structural shocks and capital controls.

Table 2. Restricted Error Correction Model (ECM) Results

Item	Regressor	Coefficient Estimate	Standard Error	t-value	p-value
1	d(L(LnINRER,1))	0.20587	0.07158	2.876	0.0044
2	d(INF)	0.00189	0.00089	2.126	0.0346
3	d(L(INF,1))	-0.00206	0.00084	-2.446	0.0152
4	d(INT)	0.01038	0.00314	3.309	0.0011
5	d(L(INT,1))	0.01003	0.00302	3.126	0.0020
6	d(MG)	0.01100	0.00155	7.072	<0.001
7	d(L(MG,1))	0.00351	0.00172	2.041	0.0424
8	ETC_{t-1}	0.01334	0.00284	4.696	<0.001

Diagnostic checks show that the model residuals are free from serial correlation (Breusch-Godfrey LM test p-value = 0.3611), confirming an adequate dynamic lag structure. However, the Breusch-Pagan test strongly indicates heteroskedasticity ($p < 0.001$) and the Jarque-Bera test confirms non-normal residuals, which is typical for dense macroeconomic series capturing extreme crisis episodes. Model stability tests Recursive Cumulative Sum (CUSUM) and the OLS based CUSUM of squares (CUSUMSQ) tests (Brooks, 2019) validate structural stability across the majority of the sample timeline, although the Bai-Perron multiple breakpoint test (Brooks, 2019) locates an explicit break at observation 206, reflecting the peak of the 2021-2022 balance of payments crisis.

4 CONCLUSION AND POLICY RECOMMENDATIONS

This study establishes that the INR/LKR exchange rate is heavily driven by domestic monetary conditions, with broad money supply growth being the most decisive short-run catalyst for currency depreciation. While inflation and interest rates remain vital indicators, their transmission channels are closely intertwined with broader liquidity cycles and reactive policy environments. The weak and positive error correction mechanism indicates that structural rigidities and policy interventions prevent rapid automatic convergence to equilibrium following macroeconomic shocks.

Based on these empirical findings, several targeted policy recommendations are proposed:

- Disciplined Liquidity Management: The Central Bank of Sri Lanka should strengthen liquidity forecasting and align money supply growth with nominal GDP to reduce exchange rate pressures.

- Proactive Interest Rate Framework: Adopt a forward-looking, flexible inflation-targeting framework with transparent communication to mitigate exchange rate volatility.

- Bilateral Trade Optimisation: Expand the use of the INR/LKR direct settlement system to reduce reliance on intermediary reserve currencies and strengthen regional financial integration.

This study focuses on a limited set of monetary variables and excludes important external sector factors such as the trade balance, foreign reserves, remittances, capital flows, and political risk. Future research should incorporate these variables to better capture exchange rate dynamics. Additionally, advanced econometric approaches, including VECM, time-varying VAR, and GARCH models, could be employed to examine long-run interactions, volatility, and exchange rate behaviour during periods of economic instability.

5 REFERENCES

Ali, I., Hussain, S., Muhammad, R., & Iftikhar, A. (2015). Impact of interest rate, inflation and money supply on exchange rate volatility in Pakistan. *World Applied Sciences Journal*, 33(4), 620–626.

Brooks, C. (2019). *Introductory econometrics for finance* (4th ed.). Cambridge University Press.

Dissanayake, H. R., Hansani, M., Walakumbura, L., & Amarasena, M. (2025). Factors affecting exchange rate variability in Sri Lanka: An ARDL approach. *KDU Journal of Multidisciplinary Studies*, 5(2), 21–33.

Enders, W. (2014). *Applied econometric time series* (4th ed.). John Wiley & Sons.

Gujarati, D. N., & Porter, D. C. (2009). *Basic econometrics* (5th ed.). McGraw-Hill Education.

Lanka News Web. (2025, February 28). India and Sri Lanka explore greater use of local currencies in trade. *Lanka News Web*

Pesaran, M. H., Shin, Y., & Smith, R. J. (2001). Bounds testing approaches to the analysis of level relationships. *Journal of Applied Econometrics*, 16(3), 289–326.

Rajakaruna, H. (2017). An investigation of factors affecting exchange rate fluctuations in Sri Lanka. *Journal of South Asian Studies*, 5(2), 101–115.

Thevakumar, P., & Jayathilaka, R. (2022). Exchange rate sensitivity influencing the economy: The case of Sri Lanka. *PLOS ONE*, 17(6), e0269538.

ISSN: 2773-7055
Proceedings of the 5th International Research Conference
Institute of Technology, University of Moratuwa
November 5, 2026

Paper ID: 36

RELATIONSHIP BETWEEN PARTICIPATION IN UNIVERSITY SPORTS AND FITNESS PROGRAMMES AND RESILIENCE AMONG UNIVERSITY STUDENTS

R G S Kaushalya Weerasinghe*

Division of Interdisciplinary Studies, Institute of Technology, University of Moratuwa, Homagama, Sri Lanka

*Corresponding author: kaushalyas@itum.mrt.ac.lk

ABSTRACT: Resilience is an important psychological characteristic that enables students to cope effectively with academic, personal, and social challenges. Participation in sports and fitness programmes has been identified as a potential factor associated with resilience. This study aimed to examine the relationship between participation in university sports and fitness programmes and resilience among diploma students at the Institute of Technology, University of Moratuwa (ITUM), Sri Lanka. A quantitative cross-sectional survey design was employed. Data were collected from 107 first-year diploma students who participated in sports and fitness activities using an online questionnaire. Resilience was measured using the Connor–Davidson Resilience Scale (CD-RISC-25), while participation was assessed in terms of frequency of participation, duration per session, and length of participation. Data were analysed using descriptive statistics, reliability analysis, and Pearson correlation analysis in SPSS version 27. The resilience scale demonstrated excellent internal consistency (Cronbach's α = .921). The mean resilience score of participants was 70.06 (SD = 14.20). Pearson correlation analysis revealed small, statistically significant positive associations between frequency of participation and resilience (r = .253, p = .009) and between duration per session and resilience (r = .219, p = .023). However, length of participation was not significantly associated with resilience (r = .002, p = .980). The findings indicate that, among the participating students, higher frequency of participation in sports and fitness activities was modestly associated with higher resilience scores. These findings suggest that the regular participation in sports and fitness programmes may be one factor associated with student well-being and resilience.

Keywords: sports participation, physical activity, psychological resilience, university students, CD-RISC

1 INTRODUCTION

Resilience is an important psychological characteristic that enables students to adapt positively and cope with academic, personal, and social challenges. Higher education students, particularly those enrolled in technology-oriented programmes, often experience academic pressure, career uncertainty, and adjustment difficulties that may affect their well-being. Participation in sports and fitness activities has been associated with improved mental health, self-confidence, social connectedness, and coping abilities, suggesting that such activities may contribute to resilience development among university students (Connor & Davidson, 2003; Sarkar & Fletcher, 2014). Similarly, physical activity has been found to positively contribute to resilience among university students (S. Xu et al., 2021). Recent evidence also suggests that higher levels of physical activity are associated with greater psychological resilience among university students, highlighting the potential role of sports and fitness participation in supporting student well-being (Z. Xu et al., 2026).

The Institute of Technology, University of Moratuwa (ITUM), provides various sports and fitness opportunities to support student development. However, limited empirical evidence

is available on the relationship between participation in these activities and resilience among diploma students in Sri Lanka. This knowledge gap highlights the need to examine whether engagement in university sports and fitness programmes is associated with students' resilience levels.

Therefore, this study aimed to investigate the relationship between participation in university sports and fitness programmes and resilience among diploma students at ITUM. The findings may provide useful evidence for educational administrators and student affairs divisions when developing sports and fitness initiatives aimed at supporting student well-being and resilience.

1.1 Objectives

1.1.1 Major Objective

To examine the relationship between the level of participation in university sports and fitness programmes and resilience among diploma students at ITUM.

1.1.2 Specific Objectives

- To describe the resilience levels of diploma students participating in university sports and fitness programmes.
- To examine the relationship between frequency of participation in university sports and fitness programmes and resilience.
- To examine the relationship between duration per session of participation in university sports and fitness programmes and resilience.
- To examine the relationship between length of participation in university sports and fitness programmes and resilience.

2 METHODOLOGY

This study employed a quantitative cross-sectional survey design to examine the relationship between participation in university sports and fitness programmes and resilience among first-year diploma students at the Institute of Technology, University of Moratuwa (ITUM), Sri Lanka. The target population comprised first-year diploma students at ITUM. A convenience sampling method was used, and the online questionnaire was distributed to 400 eligible students. A total of 107 responses were received and therefore, 107 participating students were included in the final study, representing a response rate of 26.75%. Students who were not first-year diploma students, did not participate in sports or fitness activities, or did not provide complete responses were excluded.

Data were collected using a structured online questionnaire comprising demographic information, sports and fitness participation variables, and the Connor–Davidson Resilience Scale (CD-RISC-25). The sports and fitness participation questions were study-specific items developed to obtain information about students' participation characteristics rather than a standardized measurement scale. Participation was assessed using three variables: frequency of participation (1 = less than once per week, 2 = 1–2 times per week, 3 = 3–4 times per week, 4 = five or more

times per week), duration per session (1 = less than 30 minutes, 2 = 30–60 minutes, 3 = more than 60 minutes), and length of participation (1 = less than 6 months, 2 = 6–12 months, 3 = 1–2 years, 4 = more than 2 years). Resilience was measured using the standardized CD-RISC-25, consisting of 25 items rated on a five-point Likert scale ranging from 0 to 4, with total scores ranging from 0 to 100; higher total scores indicate higher level of resilience. The CD-RISC-25 has demonstrated good internal consistency in its original validation study (Connor & Davidson, 2003).

Participation was voluntary, and electronic informed consent was obtained before completing the questionnaire. Confidentiality and anonymity of responses were maintained throughout the study.

Data were analysed using SPSS version 27. Descriptive statistics, including frequencies, percentages, means, and standard deviations, were used to summarize participant characteristics, participation variables, and resilience scores. Frequency, duration per session, and length of participation were coded as ordered categories for statistical analysis. Cronbach's alpha was calculated to assess the internal consistency of the CD-RISC-25. Pearson's correlation coefficient was used to examine the relationships between sport participation variables and resilience scores. Statistical significance was assessed at the 5% significance level ($p < .05$).

3 RESULTS AND DISCUSSION

A total of 107 diploma students who participated in university sports and fitness programmes were included in the study. The mean age of the participants was 22.43 years (SD = 0.93). Participant characteristics are presented in **Table 1** & **Table 2.**

Table 1. Participant Characteristics Gender

Variable	Category	n	%
Gender	Male	71	66.4
	Female	36	33.6

Table 2. Participants Characteristics Age

	N	Minimum	Maximum	Mean	Std. Deviation
Age Years	107	21	25	22.43	.93

Table 3. Descriptive Analysis of Sports and Fitness Participation and Resilience

Variable	Level/Category	Count	Mean	Std. Deviation
Frequency	1 = less than once/week	22	2.18	.845
	2 = 1–2 times/week	52		
	3 = 3–4 times/week	25		
	4 = ≥5 times/week	8		
Duration	1 = <30 min/session	10	2.51	.664
	2 = 30–60 min/session	32		
	3 = >60 min/session	65		
Length	1 = <6 months	82	1.36	.757
	2 = 6–12 months	15		

Variable	Level/Category	Count	Mean	Std. Deviation
	3 = 1–2 years	6		
	4 = >2 years	4		
Resilience score		107	70.06	14.20

The mean resilience score was 70.06 (SD = 14.20), with scores ranging from 37 to 98. Regarding participation characteristics, most students participated 1–2 times per week (n = 52), while 65 students reported sessions longer than 60 minutes. Most participants had been involved in university sports and fitness activities for less than six months (n = 82). The coded mean scores for frequency, duration, and length of participation were 2.18 (SD = 0.85), 2.51 (SD = 0.66), and 1.36 (SD = 0.76), respectively (**Table 3**).

The reliability analysis of the 25-item resilience scale yielded a Cronbach's alpha coefficient of .921, indicating excellent internal consistency (**Table 4**).

Table 4. Reliability Analysis

Cronbach's Alpha	N of Items
.921	25

Pearson correlation analysis was conducted to examine the relationship between participation in university sports and fitness programmes and resilience among diploma students. The results revealed a small, statistically significant positive association between frequency of participation and resilience (r = .253, p = .009). A small, statistically significant positive association was also found between duration per session and resilience (r = .219, p = .023). However, length of participation was not significantly related to resilience (r = .002, p = .980) (**Table 5**).

Table 5. Correlation between Sports Participation Variables and Resilience (N = 107)

Variable	**r**	**p-value**
Frequency of Participation	.253	.009**
Duration per Session	.219	.023*
Length of Participation	.002	.980

Note: *p < .05, **p < .01

The findings of this study indicate that frequency and average duration of participation in university sports and fitness programmes were significantly but weakly associated with resilience among first-year diploma students at the Institute of Technology, University of Moratuwa (ITUM). Frequency of participation demonstrated a weak positive correlation with resilience (r = .253, p = .009), while average duration per session also showed a weak positive correlation (r = .219, p = .023). These findings are consistent with (S. Xu et al., 2021), who reported a positive association between physical activity and resilience among college students. Their findings further indicated that psychological needs related to competence, autonomy, and relatedness helped explain the relationship between physical activity and resilience. The present findings therefore provide similar evidence within a different context, suggesting that more frequent and longer engagement in university sports and fitness activities is associated with higher resilience among diploma students.

The findings are also broadly consistent with Sarkar and Fletcher (2014), who highlighted the importance of psychological characteristics such as motivation, confidence, focus, and perceived social support in helping sport performers cope with stressors and maintain psychological resilience (Sarkar & Fletcher, 2014). Regular participation in university sports and fitness activities may provide students with repeated opportunities to experience challenges, interact with peers, develop confidence, and practice coping with difficulties. These experiences may help explain why students with more frequent participation reported relatively higher resilience. Similarly, longer sessions may provide greater opportunities for physical, social, and psychological engagement. However, the weak correlation coefficients in the present study indicate that these associations are modest and should not be interpreted as evidence that sports participation directly causes higher resilience.

The findings also have relevance to recent evidence from Xu et al. (2026), who examined the relationship between physical activity, psychological resilience, and depressive symptoms among university students. Their study further supports the importance of physical activity and resilience within the university student population (Z. Xu et al., 2026), although its analytical focus differed from the present study. While this study examined participation characteristics frequency, session duration, and length of involvement the 2026 study considered psychological resilience within a broader relationship involving depressive symptoms. Thus, the present findings add context-specific evidence from diploma students in a Sri Lankan technology-oriented institution.

In contrast, the total length of participation was not significantly associated with resilience ($r = .002$, $p = .980$). This finding differs from what might be expected if longer-term involvement alone were sufficient to develop resilience. One possible explanation is that current participation behavior may be more closely related to students' present psychological experiences than the total number of months or years they have participated. The quality, intensity, and nature of students' participation may also vary considerably despite having a similar length of involvement. Therefore, the absence of a significant relationship should not be interpreted as evidence that long-term participation has no psychological value.

4 CONCLUSION

This study examined the relationship between participation in university sports and fitness programmes and resilience among diploma students at the Institute of Technology, University of Moratuwa. Frequency of participation and duration per session were significantly and positively associated with resilience, whereas length of participation was not significantly associated with resilience. The weak correlation coefficients indicate that these relationships were modest and should not be interpreted as evidence of causality. Universities may therefore encourage regular participation in sports and fitness programmes as one potential component of initiatives supporting student well-being and resilience. Future studies could use regression analysis to examine the combined contribution of participation characteristics to resilience and employ a standardized measure such as the IPAQ-SF to assess overall physical activity levels. Longitudinal studies are also recommended to further examine the relationship between physical activity and

resilience over time.

5 REFERENCES

Connor, K. M., & Davidson, J. R. T. (2003). Development of a new Resilience scale: The Connor-Davidson Resilience scale (CD-RISC). *Depression and Anxiety*, *18*(2), 76–82. https://doi.org/10.1002/da.10113

Sarkar, M., & Fletcher, D. (2014). Psychological Resilience in Sport Performers. In *Angewandte Chemie International Edition, 6(11), 951–952.*

Xu, S., Liu, Z., Tian, S., Ma, Z., Jia, C., & Sun, G. (2021). Physical activity and resilience among college students: The mediating effects of basic psychological needs. *International Journal of Environmental Research and Public Health*, *18*(7). https://doi.org/10.3390/ijerph18073722

Xu, Z., Liu, H., Yu, J., Wang, Z., Li, S., & Li, Y. (2026). Path analysis of psychological resilience as a mediator of the relationship between physical activity and depressive symptoms among university students. *BMC Psychology*, *14*(1). https://doi.org/10.1186/s40359-026-04620-4

ISSN: 2773-7055
Proceedings of the 5th International Research Conference
Institute of Technology, University of Moratuwa
November 5, 2026

Paper ID: 40

A NECROPOLITICAL ANALYSIS OF TAMIL TIGRESS BY NIROMI DE SOYZA AND IN THE SHADOW OF A SWORD BY ZAMILINI JEYAKUMARAN

U E Liyanarathna*

Division of Interdisciplinary Studies, Institute of Technology, University of Moratuwa, Homagama, Sri Lanka

*Corresponding author: udarae@itum.mrt.ac.lk

ABSTRACT: This paper offers an in-depth necropolitical reading of the war memoirs, *Tamil Tigress* and *In the Shadow of a Sword,* by former women cadres of the Liberation Tigers of Tamil Eelam (LTTE). Drawing fundamentally on the theory of necropolitics by Achille Mbembe, the study examines how sovereign power was exercised during the Sri Lankan civil war, through the management of death, exposure to violence, and the production of disposable bodies. Employing a qualitative interpretive methodology grounded in close textual analysis and critical theory, narrative representations of bodily vulnerability, militarization, survival, and political agency within the memoirs are analyzed. Through thematic analysis, the study explores how these autobiographical accounts negotiate structures of violence while documenting lived experiences of war, displacement, and post-war trauma. The study argues that these memoirs function as counter-necropolitical archives that simultaneously reveal complicity within militant structures and resist state-centered narratives. By foregrounding embodied violence and post-war survivorship, the texts illuminate how life is lived under conditions where death becomes a primary mode of governance.

Keywords: In the Shadow of a Sword, militarization, necropolitics, Tamil Tigress, violence

1 INTRODUCTION

The Sri Lankan civil war spanned three decades, painting a socio-political landscape in which death was not merely an outcome of conflict but a governing logic. Civilians and militants inhabited zones where the distinction between life and death was constantly blurred. *Tamil Tigress* (2011) by Niromi de Soyza and *In the Shadow of a Sword* (2016)by Thamizhini Jeyakumaran emerge from this context as autobiographical testimonies that narrate life within what Achille Mbembe terms "death-worlds," spaces where populations are subjected to conditions of life conferring upon them the status of the living dead (Mbembe, 2003; Mbembe & Corcoran, 2019).

While much scholarship on Sri Lankan war literature has focused on trauma, memory, and reconciliation, this paper shifts the analysis to necropolitics to foreground how power operates through death in addition to regulating life. These memoirs are narratives produced from within regimes that normalized dying, demanded sacrifice, and valorized martyrdom. Reading them necropolitically allows us to interrogate how the state and the combatants enacted sovereignty, and how bodies became key sites where these competing sovereignties were inscribed.

Scholarship on Sri Lankan war memoirs has extensively examined testimonial and autobiographical writing by women associated with the Liberation Tigers of Tamil Eelam (LTTE). Studies of *Tamil Tigress* read Niromi de Soyza's narrative as a war memoir and a psycho-social account of female child soldiers, emphasizing how the civil war disrupted the subjectivity of young Tamil women and generated disillusionment rather than empowerment (Karmakar, 2022).

These analyses demonstrate that, despite the LTTE's claims of egalitarianism, women remained subjected to gendered hierarchies, surveillance, and moral ambiguity (Karmakar, 2022). Similarly, scholarship on *In the Shadow of a Sword* situates Thamizhini Jeyakumaran's memoir within discourses of militant women's leadership, post-war survival, and rehabilitation, foregrounding how Tamil women remain entangled in militarized structures even post war (Thamizhini, 2020). Studies on Sri Lankan war literature have pondered trauma, memory, reconciliation, violence, and gendered militarization, illustrating how female bodies become sites upon which LTTE discipline and state violence are inscribed (Meegaswatta, 2019; Heidemann, 2019). Some scholars further conceptualize the LTTE female militant as a "living dead" figure, positioned between martyrdom and marginalization within competing patriarchal regimes (Heidemann, 2019). While these studies implicitly gesture toward necropolitical concerns, they stop short of theorizing death itself as a governing logic. This study addresses that gap by employing necropolitics as its primary analytical lens to examine how *Tamil Tigress* and *In the Shadow of a Sword* negotiate sovereignty, death, survival, and post-war subjectivity within militarized contexts, constructing on emerging work that reads testimonial writing from conflict zones through an explicitly necropolitical frame (Malik et al., 2023).

2 METHODOLOGY

The study is situated in the qualitative, interpretive paradigm, and the methodology is grounded in close textual analysis and critical theory. It examines two war memoirs, *Tamil Tigress* by Niromi de Soyza and *In the Shadow of a Sword* by Thamizhini Jeyakumaran, selected for their significance as first-person narratives by women cadres affiliated with the LTTE across militant and post-war contexts. The study primarily employed Achille Mbembe's theory of necropolitics to analyze how sovereignty, death, survival, and agency are politicized within militarized environments. Through thematic analysis, the memoirs were examined as narrative constructions that mediate memory, violence, and political subjectivity. Particular attention was given to narrative voice, embodied violence, and the construction of the militant body as a site where the LTTE and the state inscribed power through the regulation of life and death. Coding proceeded through iterative close readings of both memoirs, with passages depicting bodily exposure, militarized discipline, and post-war regulation flagged and grouped into recurring thematic codes. For instance, passages describing the cyanide capsule, mandatory suicide-mission volunteering, and prohibitions on cadre relationships were grouped under a single code, the internalization and regulation of sovereign power over death, which subsequently structured the analysis in Sections 3.2 and 3.3. This process yielded six thematic categories, corresponding to the necropolitical zone, the internalization of sovereign power, the regulation of legitimate and illegitimate dying, zones of abandonment, necro-sovereignty and agency, and post-war suspended life, each developed as a subsection of the analysis. Rather than seeking empirical generalization, the study aims to provide a theoretically informed interpretation of how these memoirs negotiate ethical ambiguity, post-war subjectivity, and the politics of death in the Sri Lankan civil war context.

3 ANALYSIS

3.1 DEATH-WORLDS AND THE NECROPOLITICAL ZONE

The memoirs bear evidence of how cadres are transformed into necropolitical subjects through prolonged exposure to violence, militarization, and the collapse of civilian life. The Northern and Eastern provinces of the country functioned as necropolitical zones in which civilians and militants alike lived under constant surveillance, aerial bombardment, enforced disappearances, and extrajudicial killings. Even in Colombo, which is the densely populated capital, people lived under perpetual fear of suicide attacks and explosions. Crucially, necropolitical power in these memoirs is not monopolized by the state but circulates between state and non-state actors, as the LTTE itself exercised necro-sovereignty through forced underage recruitment, suicide missions, and internal purges. Both texts thus situate their narratives within Mbembe's conception of "death-worlds," spaces where the distinction between life and death becomes blurred.

3.2 THE INTERNALIZATION OF SOVEREIGN POWER

In *Tamil Tigress*, the writer's transition from schoolgirl to LTTE cadre reflects how conditions of war erase meaningful agency, placing individuals within structures that reorient the body toward expendability. Militant training is depicted as a process of systematic desensitization to death, in which physical hardship, weapons training, and ideological instruction converge to subordinate individual existence to militarized objectives. The compulsory carrying of cyanide capsules epitomizes this necropolitical control; cadres are expected to preemptively choose death over capture, internalizing the sovereign command to die at the appropriate moment. Here, sovereignty is no longer external but implanted within the body itself, positioning death paradoxically as duty and destiny. The cyanide capsule thus functions as a symbol of necropolitical governance, wherein the organization claims ultimate authority over the life and death of its cadres.

3.3 THE REGULATION OF DEATH: LEGITIMATE AND ILLEGITIMATE DYING

Within the military structure of the LTTE, autonomy was strictly regulated by discipline, exposing the selective and hierarchical nature of necropolitical governance. Romantic relationships among lower-rank cadres were prohibited and punished by death, which was not applicable to their leaders. Suicide attacks against the enemy were revered as martyrdom, while individual suicide attempts outside the movement's ideological framework were condemned and fined. Moreover, the killings of the members of fellow military organizations by the LTTE to establish supremacy as the sole liberation movement show the superficiality of the ideology of liberation and how death was politicized. These practices reveal how the LTTE exercised sovereign power by determining which deaths were legitimate and which were punishable. These contradictions expose the hypocrisy embedded within the militant hierarchy, as restrictions imposed on ordinary cadres were often not equally applicable to senior leadership. Through these structures, fighters became expendable bodies whose value was measured solely through their willingness to sacrifice their liberty and lives for the movement.

3.4 ZONES OF ABANDONMENT AND THE LIVING DEAD

This extends previous scholarship that reads the memoir as a psycho-social account of militancy and disillusionment (Karmakar, 2022) by foregrounding how the LTTE constructs and governs expendable bodies within a broader regime of violence. The memoirs portray war as a sustained necropolitical condition in which life unfolds under continuous surveillance, displacement, and the omnipresence of death, reinforcing Heidemann's (2019) notion of the militant as a "living dead." The memoir depicts how cadres inhabit spaces where survival is temporary, individuality is suppressed, and the distinction between life and death becomes indistinct. Militants exist in zones of abandonment where bodily existence is wholly subordinated to militarized objectives, illustrating Mbembe's argument that necropolitics operates through the creation of populations condemned to live in conditions of perpetual violence.

3.5 NECRO-SOVEREIGNTY, AGENCY, AND THE VICTIM-PERPETRATOR BINARY

As per the Necropolitical analysis, individuals within violent systems simultaneously suffer under (knowingly or unknowingly) and reproduce regimes of death, exercising a form of agency that is itself circumscribed and conditioned by the same structures of expendability to which they are subjected. As a leader, Thamizhini occupied a paradoxical position within this necropolitical order: she was both subjected to sovereign power and an agent of it. Her role involved organizing cadres, enforcing discipline, and sustaining morale in the face of mass death, thereby complicating simplistic victim-perpetrator binaries. This paradox is central to understanding how necro-sovereignty is maintained through top-down command and diffusion across the militant hierarchy.

3.6 POST-WAR NECROPOLITICS: SUSPENDED LIFE AND THE BATTLEGROUND OF MEMORY

The memoirs depict post-war survival and memory as extensions, rather than a conclusion, of necropolitical governance. The post-war sections of *In the Shadow of a Sword* reveal how detention camps, rehabilitation programs, and surveillance regimes produce different forms of death-worlds in which former militants exist in states of suspended life. Survival here is marked by guilt and political silencing, as former cadres were denied full reintegration into social and civic life while being subjected to ongoing monitoring and ideological re-inscription. Memory itself becomes a necropolitical battleground, as mainstream narratives seek to erase or criminalize militant histories. Likewise, Niromi's disillusionment and eventual escape from the LTTE constitute an active refusal of a political order that equates meaningful life with sacrificial death.

Both memoirs ultimately resist dominant narratives that reduce militants to terrorist figures by reclaiming lived experience, memory, and survival as sites of counter-testimony, functioning as counter-necropolitical archives that challenge the erasure of minority histories and foreground the ethical ambiguities of life lived under militarized sovereignty.

4 CONCLUSION

This study has examined how necropolitical power operates across *Tamil Tigress* and *In the Shadow of a Sword* to illuminate the political management of life and death within the Sri Lankan civil conflict. Through close readings of the memoirs, it has been brought forth that necropolitical governance circulates between state and non-state actors, with the LTTE exercising its own form of necro-sovereignty over the bodies and deaths of its cadres. In contrast, the post-war state extends control through detention, rehabilitation, and mainstream narratives.

The analysis has demonstrated that death is governed, operating through the mobilization and expendability within militant structures. The LTTE's rhetoric of liberation emerges not as straightforward emancipation but as a conditional inclusion in which bodies are incorporated into the war apparatus while remaining subjected to surveillance, discipline, and sacrificial logic. Crucially, both memoirs resist the erasure that necropolitical systems seek to impose. In narrating their experiences of militarization, survival, and disillusionment, de Soyza and Thamizhini reclaim agency over their own histories, refusing the reduction of lives to either martyrdom or criminality. Their texts thus function as counter-necropolitical archives that challenge silencing and assert the irreducible humanity of those condemned to inhabit death-worlds.

5 REFERENCES

De Soyza, N. (2013). Tamil tigress: My story as a child soldier in Sri Lanka's bloody civil war. Allen & Unwin. https://books.google.lk/books?id=4mwGQuZTqnMC

Heidemann, B. (2019). The symbolic survival of the "living dead": Narrating the LTTE female fighter in post-war Sri Lankan women's writing. The Journal of Commonwealth Literature, 54(3), 384–398. https://doi.org/10.1177/0021989417723414

Karmakar, G. (2022). Women and war: (Dis)illusionment and disclosure in Niromi de Soyza's Tamil Tigress. Journal of International Women's Studies, 24(6), Article 14. https://vc.bridgew.edu/jiws/vol24/iss6/14

Malik, S., Farooq, M., Nawaz, F., Saeed, S., & Anjum, N. (2023). Elegaic literature and the necropolitics: Testimonial poetics in conflict zones. Migration Letters, 20(8), 1347–1359. https://migrationletters.com/index.php/ml/article/view/12070

Mbembe, A. (2003). Necropolitics. Public Culture, 15(1), 11–40. https://doi.org/10.1215/08992363-15-1-11

Mbembe, A. (2019). *Necropolitics* (S. Corcoran, Trans.). Duke University Press.

Meegaswatta, T. N. K. (2019). Violence as a site of women's agency in war: The representation of female militants in Sri Lanka's post-war literature. *Journal of International Women's Studies, 20*(3), Article 4. https://vc.bridgew.edu/jiws/vol20/iss3/4

Tamilini. (2021). *In the shadow of a sword: The memoir of a woman leader in the LTTE* (N. Rodrigo, Trans.). YODA Press; SAGE Select.

ISSN: 2773-7055
Proceedings of the 5th International Research Conference
Institute of Technology, University of Moratuwa
November 5, 2026

Paper ID: 49

SHADOW TRAINING FOR ENHANCING PUBLIC SPEAKING SKILLS: EVIDENCE FROM ENGINEERING TECHNOLOGY UNDERGRADUATES

H G P Maheshika[1*], P B T K Premarathne[1]

[1]Division of Interdisciplinary Studies, Institute of Technology, University of Moratuwa, Homagama, Sri Lanka

*Corresponding author: piyumim@itum.mrt.ac.lk

ABSTRACT: Public speaking, encompassing verbal fluency, accuracy and non-verbal delivery, is a vital yet underdeveloped skill among engineering technology undergraduates. Research highlights weak non-verbal delivery such as flat facial expressions, limited gestures, avoidance of eye contact and nervousness as major obstacles to effective presentations. This study employed a shadow-training intervention designed to enhance students' delivery. Using a single group pre-test/post-test design, twenty first-year students completed shadow-training tasks of 5 to 10 minutes, modelling 10 selected speeches from TED Talks over ten weeks. Pre-test video analysis identified limited purposeful gestures, closed or nervous posture, avoidance of eye contact, flat facial expressions and uneven audience engagement as common weaknesses. Paired-samples t-tests showed statistically significant improvements across all five rubric dimensions ($p < .05$ to $p < .001$), with effect sizes ranging from moderate to very large. The greatest gains were in facial expressions and audience engagement; total scores rose from M = 11.86/25 to M = 16.48/25, a 39% increase. These results align with Cognitive Load Theory and indicate that shadow training is a practical, scalable pedagogical tool for improving public speaking among engineering technology students.

Keywords: shadow training, public speaking, non-verbal delivery, engineering technology undergraduates

1 INTRODUCTION

Public speaking is a critical skill for engineering technology undergraduates to communicate technical knowledge clearly and confidently to diverse audiences. Effective public speaking skills extend beyond verbal fluency to include non-verbal cues such as eye contact, facial expression, posture and gestures. Research consistently highlights that non-verbal elements are among the most influential factors shaping audience perception. For instance, Seli and Santosa (2023) identify nervousness, difficulty in elaborating ideas and weak non-verbal communication as common challenges for EFL students. Similarly, Wahyuni et al. (2025) report body language as a frequent issue in student academic presentations, while Premarathne and Maheshika (2026) find body language to be the strongest predictor of audience engagement even when verbal fluency is adequate. Seminal and recent studies (Lee, 2023; Sopyanti et al., 2025; Mohamed and Asmawi, 2018) similarly attest that non-verbal aspects remain underdeveloped even among students with reasonable verbal competency.

Shadow training, which requires learners to listen to or watch modelled speech while simultaneously vocalizing it, has been shown to enhance fluency and vocal variety through imitation of the pronunciation, intonation, pace and rhythm of competent speakers (Win, 2020; Hamada, 2015). Since shadow training involves repeated, structured practice, it may be particularly beneficial for students with lower self-efficacy, consistent with McNatt's (2019) finding that such students gain the most from structured oral communication experiences. This benefit is often explained through Cognitive Load Theory, which suggests that as verbal skills become automated through

repeated practice, learners are freed to attend to other aspects of performance, such as non-verbal delivery. Despite its benefits for verbal performance, the potential of shadow training to improve non-verbal elements of public speaking skills remains largely underexplored. Therefore, this study contributes new insights by applying shadow training to non-verbal aspects of public speaking in engineering undergraduates, a relatively underexplored area.

Accordingly, this study aims at implementing and evaluating a shadow-training intervention to enhance students' public speaking skills, with a particular interest in non-verbal delivery. The objectives of this study are two-fold: to identify the common non-verbal challenges encountered by first-year engineering technology undergraduates through pre-intervention video-based observation, and to assess the effectiveness of shadow training in improving students' public speaking performance across non-verbal dimensions.

2 METHODOLOGY

The study employed a single group pre-test/post-test design with a sample of 20 first-year engineering technology undergraduates. Participants were selected based on an initial public speaking task, which was video-recorded and evaluated using a rubric adapted from Toastmasters International (2016). The rubric assessed five non-verbal dimensions: eye contact, facial expressions, gestures, audience engagement and stage presence. To ensure reliability and minimize subjectivity, two examiners independently assessed all speeches. A calibration session was conducted prior to assessment to align interpretations of the criteria, and any discrepancies were resolved through discussion, thereby reinforcing the consistency and credibility of the evaluation.

To identify common non-verbal challenges, video recordings were systematically reviewed using a structured observation checklist derived from the five rubric dimensions, employing a behavioural coding approach consistent with Wahyuni et al. (2025). Each student's performance was coded against predefined non-verbal categories to identify recurring challenges across the cohort. Over ten weeks, students engaged in weekly shadow-training tasks lasting 5 to 10 minutes. They were instructed to mimic the intonation, pace, facial expressions, gestures and overall delivery of competent speakers drawn from ten selected TED Talks. Individualized feedback was provided, referencing the specific non-verbal challenges identified during the pre-test observation, since Shi et al. (2024) highlight such feedback as a key driver of meaningful improvement in public speaking performance. This guidance targeted eye contact, gestures, facial expressions, audience engagement and stage presence. At the conclusion of the intervention, students delivered a second individual public speaking task, which was evaluated using the same rubric and by the same examiners. To compare pre- and post-intervention performance across all five dimensions, paired-samples t-tests were conducted, with Cohen's d used to quantify effect sizes.

3 RESULTS AND DISCUSSION

3.1 Common Public Speaking Challenges

Pre-test video analysis revealed patterns consistent with broader findings in the public speaking literature. The most noticeable non-verbal shortcomings observed were limited use of purposeful gestures, resulting in stiff and disengaging delivery (observed in 65% of students), flat or neutral facial expressions conveying little enthusiasm or emotion (60%), weight shifting and closed posture indicating nervousness (55%), avoidance of eye contact with the audience (50%), and uneven audience engagement, with speakers tending to focus on one section of the room (45%). These observations align with Wahyuni et al. (2025), who identified body movement as the most prevalent barrier in student speeches, and with Seli and Santosa (2023), who reported that anxiety-induced nervousness often leads students to forget words and lose composure. Nervousness and lack of confidence, highlighted in both studies, were also evident in the pre-test result of this cohort. These observations were quantitatively confirmed by the pre-test mean scores, where audience engagement (M = 1.86/5) and facial expressions (M = 2.02/5) were the lowest-scoring dimensions, corroborating the observational findings identified in the video analysis.

3.2 Effectiveness of Shadow Training

Following the ten-week shadow-training intervention, paired-samples t-tests revealed statistically significant improvements across all five dimensions, with effect sizes ranging from moderate to very large.

Table 1. Pre- and post-intervention mean scores, t-values and effect sizes (N = 20)

Category (marks)	Pre M	Post M	T	P	Cohen's d
Eye Contact (5)	2.86 (0.45)	3.43 (0.55)	5.43	< .001	1.19
Facial Expressions (5)	2.02 (0.46)	3.24 (0.66)	9.22	< .001	2.01
Gestures (5)	2.24 (0.52)	3.05 (0.71)	3.56	< .01	0.78
Audience Engagement (5)	1.86 (0.42)	3.43 (0.64)	7.36	< .001	1.61
Stage Presence (5)	1.86 (0.48)	3.33 (0.84)	2.74	< .05	0.60
Total (25)	11.86 (0.96)	16.48 (2.40)	8.79	< .001	1.92

The most notable improvements were observed in facial expressions (M = 2.02 to M = 3.24, d = 2.01) and audience engagement (M = 1.86 to M = 3.43, d = 1.61). This suggests that students became noticeably more expressive and engaging following the intervention. Eye contact also showed a large improvement (d = 1.19), followed by gestures (d = 0.78). Stage presence showed the smallest gain (d = 0.60), possibly because it is a more complex and multidimensional skill that requires longer-term development beyond a ten-week period. Total scores increased from M = 11.86/25 to M = 16.48/25 (d = 1.92), representing a 39% gain.

As students repeatedly practiced over ten weeks, shadow training became increasingly automatic, allowing students to focus on non-verbal aspects such as gestures, facial expressions and eye contact. This is consistent with Cognitive Load Theory, as automating basic skills frees mental energy for higher-level performance. It also supports McNatt's (2019) finding that

structured, repeated practice particularly benefits learners with lower initial self-efficacy (Win, 2020; Hamada, 2015).

The non-verbal improvements observed are probably also a result of the tailored feedback provided during the intervention, which specifically addressed the non-verbal challenges identified in the pre-test. Similarly, Shi et al. (2024) discovered that one of the most valued elements of their public speaking intervention was individualized teacher guidance within a project-based learning framework, with students reporting that tailored feedback on particular strengths and weaknesses resulted in significant and meaningful improvement. The present findings indicate that such individualization can be accomplished in a brief, weekly shadowing format.

4 CONCLUSION

This study indicates that engineering technology undergraduates' public speaking performance can be significantly improved across all non-verbal dimensions when a structured shadow-training intervention is integrated. Improvements were observed in eye contact, facial expressions, gestures, audience engagement and stage presence, with the most significant improvements in facial expressions (d = 2.01) and audience engagement (d = 1.61). These findings suggest that shadow training incorporated with targeted feedback on non-verbal delivery provides a practical and scalable strategy for addressing the public speaking challenges frequently observed in this student population. Future research may include a controlled group and larger samples across multiple class sections in order to isolate the specific contribution of the shadow-training technique from general practice effects. The evidence base would be strengthened by extending to other student populations and longitudinal follow-up to evaluate the sustainability of improvements.

5 REFERENCES

Hamada, Y. (2015). Shadowing: Who benefits and how? Uncovering a booming EFL teaching technique for listening comprehension. *Language Teaching Research, 20*(1), 35–52. https://doi.org/10.1177/1362168815597504

Lee, J. C. P. (2023). Gaze and facial expression in engineering student presentations: A comparative case study. *ESP Today, 11*(1), 6–30. https://doi.org/10.18485/esptoday.2023.11.1.1

McNatt, D. B. (2019). Enhancing public speaking confidence, skills, and performance: An experiment of service-learning. *The International Journal of Management Education, 17*(3), 276–285. https://doi.org/10.1016/j.ijme.2019.04.002

Mohamed, A. A., & Asmawi, A. (2018). Understanding Engineering Undergraduates' Technical Oral Presentation: Challenges and Perspectives. *International Journal of Language Education and Applied Linguistics, 8*(1), 41–53. https://doi.org/10.15282/ijleal.v8.529

Premarathne, P. B. T. K., & Maheshika, H. G. P. (2026). Non-verbal communication in academic presentations: Evidence from engineering technology undergraduates. *International Journal of Educational Innovations, 2*(2), 64–73. https://doi.org/10.46451/ijei.260117

Seli, F. Y., & Santosa, I. (2023). University students' difficulties in public speaking skills.

Jurnal Ilmiah Mandala Education, 9(3), 2149–2154. https://doi.org/10.58258/jime.v9i1.5845

Shi, C., Kassim, A., & Radzuan, N. R. M. (2024). Improving EFL Learners' English Public Speaking Performance through Project-based Learning Strategy at Tertiary Level. *Language Teaching Research Quarterly*, *42*, 126–144. https://doi.org/10.32038/ltrq.2024.42.08

Sopyanti, L., Ariyani, A., & Wello, B. (2025). *Exploring nonverbal communication in English presentations at EFL classrooms.* Universitas Negeri Makassar Repository. https://lib.unm.ac.id/layanan/karya-ilmiah/exploring-nonverbal-communication-ineng lish-presentation-at-efl-classsrooms

Toastmasters International. (2016). Evaluation form. https://content.toastmasters.org/image/upload/v1741989017/8104E1-evaluation-resource-ff.pdf

Wahyuni, W., Sudika, I. N., Susanti, P. A., Pratama, J. R., Nazir, Y. N., & Rizkia, S. (2025). Public Speaking in Academic Context: A Study of Student Communication Obstacles and Strategies. *Jurnal Ilmiah Mandala Education*, *11*(4), 926. https://doi.org/10.58258/jime.v11i4.9309

Win, P. Y. (2020). *An investigation of the shadowing technique in teaching speaking to English as a Foreign Language students*. British Council.

ISSN: 2773-7055
Proceedings of the 5th International Research Conference
Institute of Technology, University of Moratuwa
November 5, 2026

Paper ID: 68

THE STUDENTS' PERCEPTION OF AUTONOMY, COMPETENCE AND RELATEDNESS: A STUDY OF STUDENT MOTIVATION IN LEARNING ENGLISH THROUGH SELF-DETERMINATION THEORY

Bhagya Pabasarani*

Division of Interdisciplinary Studies, Institute of Technology, University of Moratuwa, Homagama, Sri Lanka

*Corresponding author: bhagyap@itum.mrt.ac.lk

ABSTRACT: This study serves as a reflection of the students' perception of the Self-Determination Theory proposed by Deci and Ryan (2000), which is also one of the most prominent theories presented under motivation. The three psychological needs of autonomy, competence, and relatedness are the key concerns when determining motivation. The students' perception regarding the aforementioned autonomy, relatedness, and competence is examined in this research, intending to unravel how each psychological need contributes to motivation and what insight can be brought to the classroom when motivating students to achieve academic excellence. The research uses a web-based survey adopting a mixed-method approach, taking thirty-three Engineering undergraduates studying at the Institute of Technology, University of Moratuwa (ITUM) as the sample.

Keywords: Self-Determination Theory, motivation, autonomy, competence, relatedness

1 INTRODUCTION

Motivation plays a key role as a driving force for success in human life. It enhances one's capacity to be resilient and stay focused on achieving goals. Motivation in learning is a widely researched topic in pedagogy. Within this, motivation in learning a Second Language (L2) is an important topic, with an array of theories and concepts that have been extensively researched over decades. The two concepts of 'intrinsic motivation' and 'extrinsic motivation' are two such important concepts. Both intrinsic and extrinsic motivation are equally significant in language learning. Intrinsic motivation is self-centered, while extrinsic motivation is derived from prospects of outside gains. However, intrinsic motivation, which is internally driven, is considered more effective because the concept of 'incentives', which answers "Why should I?", has the ability to motivate learners (Jones, 2007).

Self-determination is a concept that directly links with motivation. Self-determination involves being self-directed and consistently working toward set goals. Therefore, motivation and self-determination are closely linked. Deci and Ryan's (2000) Self-Determination Theory (SDT) is a theory of human motivation that focuses on the three basic psychological needs of autonomy, competence, and relatedness. Autonomy is "the need to experience self-direction and personal endorsement in action", which embodies the independence and freedom of personal choice. Competence is "the need to feel effective in interactions with the environment", which indicates the significance of having confidence and a sense of belongingness. Relatedness is "the need to feel meaningfully connected to others," which conveys the importance of having meaningful connections. It is interesting to explore how these concepts are perceived by students in a formal educational setting.

In a formal setting, knowledge is delivered through instruction, involving two major stakeholders: teachers and learners. The students encounter classroom discourse practices that include interaction patterns, interpersonal relationships, shared experiences, and classroom power relations, forming a holistic learning experience. This is where real learning takes place with motivation, autonomy, competence and relatedness. Learning is viewed as a 'change in behavior resulting from experience or practice' (Schneider, 2024). Learning is defined as a "relatively permanent change in behaviour or knowledge which happens as a result of experience" by Roediger et al. (1984). This research aims to unravel how the three psychological concepts emphasized in SDT; the need for autonomy, competence, and relatedness are perceived by students in learning English.

Exploring the motivation and language learning experiences of ITUM students constitutes a practical concern. Besides, proficiency in English is a critical determinant for success in Engineering education. This research undertakes a mixed-method approach, with a sample of thirty-three engineering undergraduate students studying at ITUM. SDT is a widely used theoretical framework supported by empirical studies. However, applying it within the Sri Lankan tertiary context, specifically with engineering students at ITUM, can reveal deeper insights into student mindsets for a better understanding of student motivation in learning English.

The objectives of this research are:

- To examine the significance of intrinsic motivation and extrinsic motivation in learning English among the selected students
- To examine the students' perception of 'autonomy' as a tool of motivation in learning English
- To examine the students' perception of 'competence' as a tool of motivation in learning English
- To examine the students' perception of 'relatedness' as a tool of motivation in learning English

2 METHODOLOGY

This research adopts a web-based survey using a mixed-method approach. A self-administered questionnaire was circulated. A total of twenty questions were included in the Google questionnaire. A limited sample of thirty-three students studying Engineering Technology at ITUM was selected through convenience sampling. This sample was chosen to capture the adult students' perceptions since they hold their own norms and ideologies on motivation due to their years of experience in learning English and maturity. The Google questionnaire, which included both open-ended and closed-ended questions, was administered to the sample. The questionnaire was designed to derive data aligning with the aforementioned research objectives. The collected quantitative data were analyzed using descriptive statistics. The qualitative data were analyzed using thematic analysis.

3 RESULTS AND DISCUSSION

The first question was directed at motivation, which means exploring the main reason for learning English. 48.5% of students selected the option of *"I need to improve my self-esteem and self-confidence. I care about my personal growth",* while 24.2% selected the option of *"I love learning English and I love the process of learning English because learning English is interesting".* 27.3% selected the option of "*I need to get good grades, and I always think of the future prospects of good job opportunities".* This indicates the fact that intrinsic motivation is the most significant factor behind learning English among the majority. The next question was raised to find out who or what matters in taking decisions related to studies. 45.5% have selected the option of *"I consider only my thoughts and expectations".* While 54.5% have selected the option of *"I consider my thoughts, but also I think what society says if I take this decision".* The interesting point is no one has selected the option, *"I give more importance to what others might say".* The results indicate that the students are aware of the importance of having a self-driven initiative towards learning English. However, even for intrinsically motivated students, the outside perception matters in decision-making. This can be attributed to the cultural norms bound to being "a good child" who does not disappoint society. In the concept of inspiration to study well, 43.8% selected the option of *"I am my own inspiration".* That takes fourteen students in total. Ten students selected the option, *"It is my parents. I cannot disappoint them"* which contributes to being a good child. While eight students have selected *"Both my parents and friends. They believe in me more than I myself do".* This indicates that at points when students feel unmotivated, the guilt and obligation can come as a form of driving force towards learning. The relationships that students have with their parents and friends too can shape how they view themselves, contributing to motivation. Hence, motivation cannot purely derive from internal sources. Intrinsic motivation is strengthened by external factors.

When exploring the mindset of students, this means whether they perceive a positive or negative outlook towards learning and their attitude towards failing; the role of emotions emerges. It is needless to mention that emotions play a key role in motivation. Krashen's (1982) affective filter hypothesis speaks about how emotions affect language learning. This is further elucidated by Grace (2008), stating that 'negative emotions' which affect language learning 'are formed through passive moods, including low motivation, low self-esteem, and debilitating anxiety.'87.9%, which means 29 out of 33 have selected the option of "*I felt sad, but I immediately overcame it. I made sure to think of my next step."* Only three students have said, *"I felt sad and ashamed. I just wanted to release my sadness immediately"*, while one student has given the option, *"I do not care since I have failed many times".* The positive attitude towards failing reflects how easily the students can regain confidence. This mindset can be exploited by teachers to challenge students to reach scholarly achievements. When talking about students' feelings when learning English, seventeen students have chosen the option *"I feel happy, and it is interesting to learn English,"* while fourteen students have chosen the option of *"I do not care about feelings. I learn English because it is important".* Only two students have chosen the option of *"I do not care about feelings. I learn English for the sake of learning."* Nobody has selected the option of *"I feel anxious and stressed."* This indicates the fact that the majority enjoy learning English.

This also indicates that students think rationally and prioritize needs over emotions, as they have prioritized the importance of learning English over their feelings. Overall, the students occupy a growth mindset. Even though the emotional factors were prominent, the importance of learning English has significantly outweighed.

Learner autonomy is directly linked with motivation, as self- initiated actions play an important role in motivation. Only one student chose the option of "*I do not get a chance to choose the learning style, I wish I could. I feel good when I can suggest things."* Such a result can stem from students not knowing their learning styles. However, eleven students have indicated their willingness to openly suggest how they would like to do an activity, but that was particularly concerning for individual or group work. The results indicated that the majority love to do group work. The majority love academic discussions, as the option of *"I like to learn English through discussions. They uplift me as I feel quite independent to say something."* was selected by fifteen students. When asked how students define the independence of learning the students have stated concerns such as *the right to choose subject combinations of his choice, schedules that are not too busy, and relaxing complex rules regarding attendance rates by providing resources such as e-books and recorded lectures, taking responsibility of my own studies, choosing different learning methods and styles, setting goals, and learning at my own pace.* However, the results also indicated that the students' understanding of their individual learning styles was extremely limited, as none of them were able to clearly suggest which study methods work best for them and what strategies they use to plan their study sessions, which can also be utilized for teaching in the classroom. Even though the majority indicated attributes of an intrinsically motivated student, they are incapable of being autonomous in learning as they are not aware of the learning styles which personally suit them best.

In the concept of competence, the students have understood the meaning behind competence in a limited frame only applicable in workplaces or classrooms, as they have viewed it as *'the ability to use the language practically, accurately, and confidently in academic and professional environments, having the actual ability, skill or confidence to do a job or a task successfully and correctly, being able to apply my knowledge and skills to build something valuable and feeling good after completing a task'.* With the response, it was evident that students have identified competence concerning skills that enable them to do academic or professional tasks well.

A question was directed to find out the link between feedback and competence. The students view feedback from the teacher as a positive instrument to become more competent since the classroom is perceived as "positive and welcoming." A total of 48.5% of students have chosen the option of 'strongly agreed,' and an equal percentage of 48.5% have chosen the option of 'agreed' to the fact that the teacher's feedback had helped them to be more competent. When asked about the level of competence in using English, thirteen students agreed with the fact that they feel competent when they get to communicate in English rather than in Sinhala (or Tamil) in an academic setting. Five students strongly agreed with that, while twelve students remained neutral. Thirty students strongly agreed with the fact that what they learn in the English module directly helps in other academic work, which means when learning other Engineering subjects. However, three students have selected the option of 'not sure'. An equal number of

sixteen students have selected the options of ‘strongly agreed’ and ‘agreed’ for the statement of teachers’ feedback, making them feel more competent. Eight students strongly agreed with the fact that they are more competent in English than before, while eighteen students agreed with that. A total of twenty-eight students believe that constantly trying to improve English can make them competent. The results indicate that students view English as a helpful tool to become more competent, the majority do not feel fully confident about the progress they have made so far in learning English.

The concept of relatedness is linked with the idea of having meaningful connections. Out of thirty-three, thirty-two students have said that they feel connected with peers and their teacher while learning English. This is, in fact, a positive trait, as the students do not experience any feeling of intimidation in classrooms, indicating that they feel emotionally and psychologically safe. The majority of the students have mentioned that they believe group work and interactive projects can make them feel more positive and welcomed. Effective use of group work and projects can be exploited in classrooms to enhance learning.

4 CONCLUSION

It is a daunting task to motivate adult learners even though they are mostly aware of the importance of English and how the world of work functions. Motivation is a complex phenomenon, yet nourishing the three psychological needs of autonomy, competence, and relatedness proposed in SDT has the capacity to uplift student motivation. The results indicate that the majority of students view English as a pillar for professional and academic growth and wish to be more independent in learning. However, the students’ own limitations in not identifying the individual learning styles that work best and their over-reliance on group work serve as constraints that limit the learning experience. Since the sample size of this research was limited to only thirty-three students, conducting further research that employs a larger sample can enhance the generalizability of the results.

5 REFERENCES

Deci, E. L., & Ryan, R. M. (2000). The" what" and" why" of goal pursuits: Human needs and the self-determination of behavior. *Psychological inquiry*, *11*(4), 227-268.

Jones, F. H. (2007). Tools for teaching (2nd ed.). Fred Jones & Associates.

Krashen, S. D. (1982). Principles and practice in second language acquisition. Pergamon Press.

Lamb, M. (2017). The motivational dimension of language teaching. Language Teaching, 50(3), 301– 346. https://doi.org/10.1017/S0261444817000088

Legault, L. (2017). Self-determination theory. In V. Zeigler-Hill & T. K. Shackelford (Eds.), Encyclopedia of personality and individual differences. Springer. https://doi.org/10.1007/978-3-319-28099-8_1162-1

Merc, G. (2008). Pedagogies proving Krashen’s theory of affective filter. In Z. Dörnyei (Ed.), Engaging language learners in contemporary classrooms. Cambridge University Press.

Roediger, H. L., III, Rushton, J. P., Capaldi, E. D., & Paris, S. G. (1984). Psychology. Little, Brown and Company.

Schneider, K. (2024). What is learning? Psychology, 15, 779–799. https://doi.org/10.4236/psych.2024.155047

ISSN: 2773-7055
Proceedings of the 5th International Research Conference
Institute of Technology, University of Moratuwa
November 5, 2026

Paper ID: 70

EFFECTIVENESS OF PEER TEACHING ON MATHEMATICS FOR ENGINEERING STUDENTS: A CASE STUDY OF A LEADING UNIVERSITY IN SRI LANKA

Prabathara Erandi[1*], Ravindi Jayasundara[1]

[1]Department of Mathematics, University of Moratuwa, Sri Lanka,

*Corresponding author: prabahewapathiranage@gmail.com

ABSTRACT: Peer teaching is widely recognized as a collaborative learning approach in higher education. This study investigated the effect of time spent in informal peer-teaching sessions on the mathematics performance of first-semester engineering undergraduates. For this study, the time spent in peer teaching sessions, Continuous Assessment (CA) marks, and final written examination (WE) marks were used as variables. An Analysis of Covariance (ANCOVA) was employed to examine the effect of peer teaching duration on WE marks (representing 70% of the final module mark), controlling for CA marks. The findings demonstrated that baseline academic competency, measured through CA marks, is a highly significant predictor of final exam success. After adjusting for this covariate, the time spent in peer teaching sessions showed a weak inverse relationship with final grades, achieving statistical significance only at the 10% level. Although the majority of students reported peer teaching as beneficial and highly prioritized it as a learning activity, the results cautiously suggest that prolonged attendance may indicate underlying academic struggles rather than guaranteeing higher academic achievement. This study contributes to the understanding of collaborative learning in engineering education, offering insights for institutions aiming to optimize the qualitative pedagogical structure of peer support systems.

Keywords: peer teaching, academic performance, continuous assessment

1 INTRODUCTION

The transition to university-level engineering mathematics demands effective teaching and learning practices within the undergraduate curriculum to ensure student success. To meet these academic challenges, peer teaching has increasingly been adopted as a collaborative learning mechanism that shifts students from passive recipients to active participants (Bojos & Plaza, 2026). Recent research highlights that peer-assisted learning significantly improves overall academic achievement across various educational levels and technical disciplines (Babayiğit & Erkuş, 2022; Núñez-Andrés et al., n.d.). By engaging in structured collaborative activities, students not only enhance their conceptual understanding but also develop critical communication, accountability, and self-regulatory skills (Bojos & Plaza, 2026). Furthermore, reciprocal peer learning environments have been shown to boost student confidence, increase intrinsic motivation, and tangibly improve final academic performance in complex coursework (Núñez-Andrés et al., n.d.). Beyond immediate grade improvements, active participation in peer teaching cultivates long-term professional maturity, self-efficacy, and a smoother transition into advanced academic and practical roles (Avonts et al., 2024).

However, the quantitative effectiveness of these informal, student-led networks must be rigorously evaluated against traditional metrics. While students often perceive peer-assisted learning as highly beneficial socially and academically, some comparative studies caution that the sheer duration of peer-led sessions may not always translate to higher examination scores as effectively as formal, faculty-led instruction (AlShareef, 2020). Addressing this gap, this study investigates

the dimensions of undergraduate mathematics education by examining the relative impact of formal continuous assessment performance versus the time spent in informal peer-teaching networks on the final academic achievement of first-year engineering students.

1.1 Peer Teaching and Academic Performance

In the middle of the first-semester students faced multiple continuous assessments comprised of weekly spot tests including a mid-semester examination, accumulatively accounts for continuous assessment (CA) marks. Usually after continuous assessments are conducted but prior to the final exam during the study leave period the peer teaching approaches are organized within student groups. In this analysis, the time spent in peer teaching serves as the primary independent variable, while Continuous Assessment (CA) marks act as a measurable covariate that influences final grades.

2 METHODOLOGY

Data were collected using a structured questionnaire to measure students' participation in peer teaching sessions, along with CA marks and final Mathematics examination grades, achieving a 54.6% response rate. The study aimed to determine whether time spent in peer teaching sessions significantly affects final marks after controlling for prior academic performance. The target population consisted of first-year undergraduate Engineering students. Primary data on peer teaching participation, CA marks and final Mathematics examination grades were collected through a survey. The final Mathematics course mark was calculated by assigning 30% weight to the CA mark and 70% weight to the final written examination mark. The final written examination mark (WE) was calculated using 70% of the midpoint value of each grade's marks interval. Students reported the total number of hours spent participating in peer teaching sessions during the semester through the survey questionnaire.

Although 537 responses were initially collected, 101 cases were excluded from the final analysis due to incomplete questionnaire responses and missing academic data, resulting in a final working sample size of 436. Analysis was conducted using Analysis of Covariance (ANCOVA), where the WE mark was the dependent variable, peer teaching attendance time was the independent variable, and CA marks were used as the covariate. ANCOVA was chosen as it allows comparison of group means while adjusting for a continuous covariate. The key assumptions of ANCOVA were considered, including normality of residuals, homogeneity of variances, linear relationship between the covariate and dependent variable, and homogeneity of regression slopes. The data were analyzed using IBM SPSS Statistics. Descriptive statistics were used to summarize the variables, followed by ANCOVA to test whether differences in final Mathematics grades across peer teaching attendance levels were significant after adjusting for CA marks, using a 0.10 significance level.

3 RESULTS AND DISCUSSION

Table 1 presents the distribution of respondents across different engineering departments along with their response rates. A total of 537 valid responses were collected from the 676 students in the sample. Figure 1 presents the distribution of Continuous Assessments (CA) marks out of

100 for the 537 students. The mean CA final mark is 81.53 (SD = 11.07), indicating generally high student performance, with only a few students obtaining relatively low marks. The final Mathematics grades are categorized as "0 = IWE, 1 = D Pass, 2 = C Pass, 3 = B Pass, and 4 = A Pass". As shown in Figure 2**,** the highest number of students belongs to Category 3 (B Pass), indicating that the majority of students achieved a B grade in the final Mathematics examination. Students were asked to rank the learning activities that contributed most to their learning process. Figure 3 presents the first priority selected by the students. It shows that peer teaching sessions were the second most frequently selected first-priority learning activity. This indicates that many students consider peer teaching sessions to be an important contributor to their learning. Therefore, peer teaching sessions were selected for further analysis in this study.

Table 1. Distribution of respondents by department and response rate among engineering students

Department	Frequency	Total in the field	Response Rate
Biomedical Engineering	11	15	73.3
Civil Engineering	31	114	27.2
Chemical & Process Engineering	29	78	37.2
Computer Science Engineering	158	200	79.0
Electrical Engineering	62	90	68.8
Electronics and Telecommunication Engineering	63	100	63.0
Earth Resource Engineering	41	75	54.6
Mechanical Engineering	43	100	43.0
Material Science Engineering	24	44	54.5
Transport Management & Logistics Engineering	39	87	44.8
Textile & Apparel Engineering	36	80	45.0
Total	537	983	

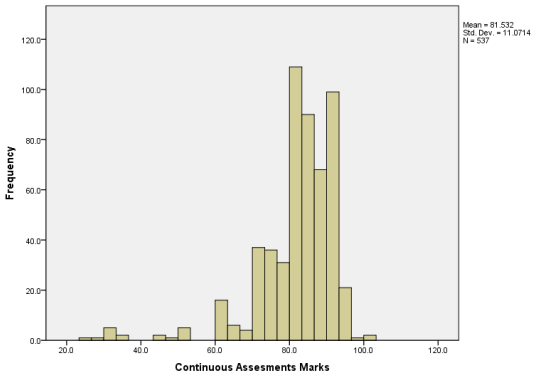


Figure 1. Distribution of Continuous Assessment Marks

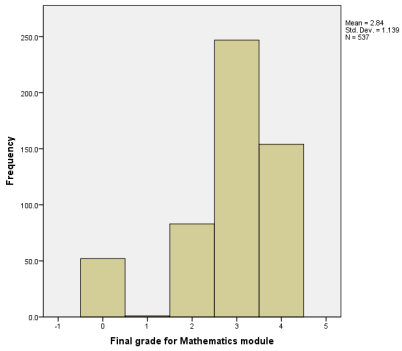


Figure 2. Distribution of the Final Grade for Mathematics

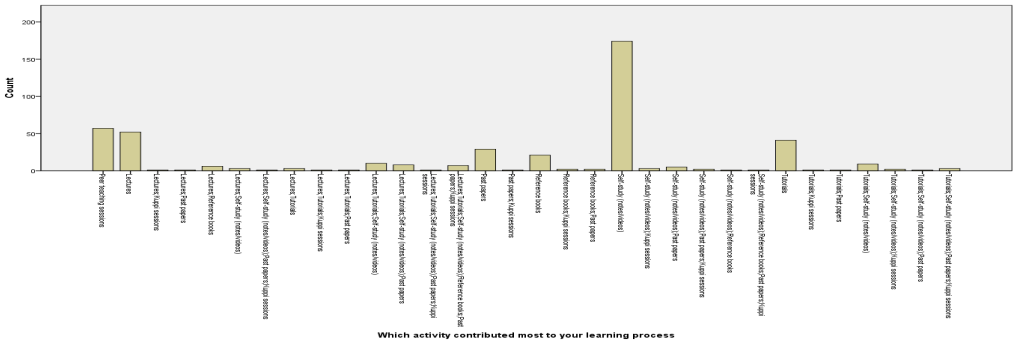


Figure 3. Distribution of which activity contributed most to your learning process

A cross tabulation Table 2 was conducted to examine students' attendance at peer teaching sessions and their perceptions of usefulness. The results show that the majority of students attended peer teaching sessions and reported them as useful. Out of 537 students, 423 students indicated that the sessions were useful, while only 14 students reported them as not useful. This suggests that peer teaching sessions were mostly attended and generally perceived as beneficial by students, which is the reason this variable was selected for further analysis in the study. Figure 4 shows that most students spent between 0 and 10 hours participating in peer teaching sessions, indicating that the majority attended for a relatively shorter duration.

Table 2. Cross tabulation of attending peer teaching sessions vs whether the peer teaching sessions useful

Attending peer teaching sessions	Whether the peer teaching sessions useful		Total
	No	Yes	
No	Not applicable	Not applicable	99
	14	423	438
	14	423	537

Note: One attendee did not provide a response regarding the usefulness of the sessions (n=437)

- Test the Homogeneity

Dependent Variable: WE Mark

Table 3. Test of Between – Subject Effects (Test the Homogeneity)

Source	Type III Sum of Squares	df	Mean Square	F	Sig.	Partial Eta Squared
Corrected Model	8652.600[a]	9	961.400	5.185	.000	.099
Intercept	1645.739	1	1645.739	8.876	.003	.020
Peer teaching time	842.921	4	210.730	1.137	.339	.011
CA marks	5303.508	1	5303.508	28.604	.000	.063
Peer teaching time * CA marks	614.754	4	153.689	.829	.507	.008
Error	78985.620	426	185.412			
Total	919782.430	436				
Corrected Total	87638.221	435				

The assumption of homogeneity of regression slopes is successfully met as shown in **Table 3**. For the interaction term (peer teaching time * CA marks), the output shows a significance value of 0.507. Because 0.507 is strictly greater than the 0.05 threshold, the interaction is not statistically significant. This confirms that the relationship between a student's CA marks and their WE mark remains consistent regardless of how much time they spent in peer teaching sessions.

- Main ANCOVA Test

Table 4. Descriptive Statistics

Dependent Variable: WE Mark

Time spent on peer learning	Mean	Std. Deviation	N
0	45.1547	15.13692	75
1	45.0356	14.30238	101
2	43.6274	12.55427	117
3	43.6538	13.18220	91
4	39.1462	17.08516	52
Total	43.6874	14.19391	436

Table 5. Levene's Test of Equality of Error Variances

F	df1	df2	Sig.
3.264	4	431	.012

Table 6. Tests of Between-Subjects Effects

Source	Type III Sum of Squares	df	Mean Square	F	Sig.	Partial Eta Squared
Corrected Model	8037.846[a]	5	1607.569	8.684	.000	.092
Intercept	1962.266	1	1962.266	10.600	.001	.024
CA marks	6619.871	1	6619.871	35.760	.000	.077
Peer teaching time	1530.600	4	382.650	2.067	.084	.019
Error	79600.374	430	185.117			
Total	919782.430	436				

Source	Type III Sum of Squares	df	Mean Square	F	Sig.	Partial Eta Squared
Corrected Total	87638.221	435				

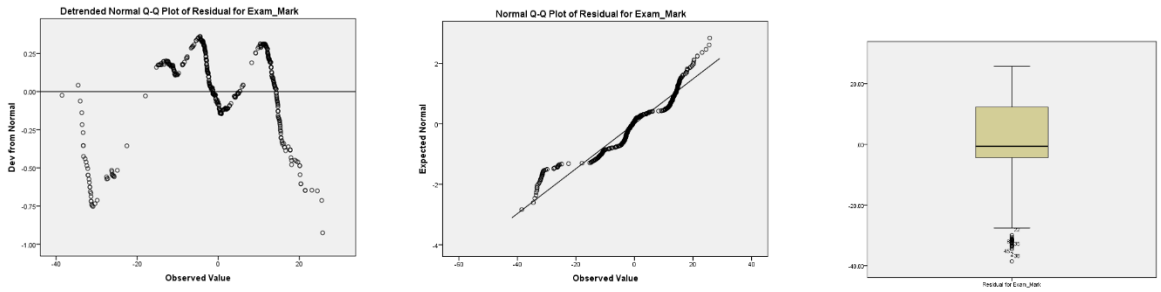


Figure 4. Test of Normality

Residual analysis revealed deviations from absolute normality, which is an expected statistical artifact of deriving the WE marks from 70% of the categorical grade mid-values.

3.1 Methodological Limitations and Assumption Testing

Preliminary checks were conducted to evaluate the underlying assumptions of the Analysis of Covariance (ANCOVA). The assumption of homogeneity of regression slopes was successfully met, as the interaction between time spent in peer teaching and CA marks was not statistically significant. However, Levene's test indicated a violation of the homogeneity of variances, and residual analysis revealed deviations from absolute normality. These violations are expected statistical artifacts of utilizing assigned, scaled grading based on 70% of the mid-values.

3.2 ANCOVA Results

The overall ANCOVA model significantly predicted the estimated final examination marks, $F(5, 430) = 8.684$, $p < .001$, accounting for 9.2% of the variance in exam scores. The covariate, CA marks, emerged as a highly significant positive predictor of the final exam score, $F(1, 430) = 35.760$, $p < .001$, with a medium effect size. This confirms a strong foundational relationship where students demonstrating higher competency in ongoing assessments consistently achieve higher final examination marks in the undergraduate mathematics curriculum. After adjusting for this prior academic performance, the main effect of time spent in peer teaching on the estimated exam grade was statistically significant only at the marginal 10% significance level, $F(4, 430) = 2.067$, $p = 0.084$. Furthermore, the effect size was very small.

4 DISCUSSION

While students highly value peer teaching, quantitative analysis reveals that attendance duration is a weak driver of final success compared to continuous assessment. The marginal significance ($p < .10$) and an observed inverse trend suggest that prolonged reliance on peer sessions indicates underlying academic struggles rather than guaranteed grade improvement. Therefore, the pedagogical quality of these interactions matters far more than total hours spent. Future research should prioritize acquiring raw examination scores to eliminate estimation biases and investigate the qualitative dynamics of student-led support.

5 CONCLUSION

ANCOVA results confirm that continuous assessment is a highly significant predictor of final examination success in undergraduate engineering mathematics. After controlling for this baseline academic competency, the total time spent in informal peer-teaching sessions had only a marginally significant effect (10% level), showing a weak inverse relationship with estimated final grades. This indicates that prolonged reliance on peer support often reflects underlying academic struggles rather than driving actual grade improvement. Consequently, instructional strategies must prioritize strengthening students' early continuous assessment performance. Rather than encouraging more hours of peer learning, future initiatives should focus on the pedagogical quality of these student-led interactions and secure raw exam data to accurately optimize the curriculum.

6 ACKNOWLEDGEMENTS

We are grateful to all voluntary participants who filled the questionnaire for their time and cooperation.

7 REFERENCES

AlShareef, S. M. (2020). Comparing the impacts of reciprocal peer teaching with faculty teaching: A single-centre experience from KSA. Journal of Taibah University Medical Sciences, 15(4), 272-277.

Avonts, M., Michels, N. R., Vanderveken, O. M., De Winter, B. Y., & Bombeke, K. (2024). The perceived long-term impact of peer teaching in the skills lab. A descriptive interview study. Medical Education Online, 29(1), 2412394.

Babayiğit, Ö., & Erkuş, B. (2022). Effect of peer teaching on the academic achievement of fourth grade primary school students. International Journal of Psychology and Educational Studies, 9(3), 782-791.

Bojos, L. M., & Plaza, R. C. O. (2026). The Role of Peer Teaching in Enhancing Students' Achievement: A Collaborative Learning Mechanism. International Journal of Research and Innovation in Social Science (IJRISS), 10(6), 9631-9638.

Núñez-Andrés, M. A., Martinez-Molina, A., Casquero-Modrego, N., & Suk, J. Y. (n.d.). The Impact of Peer Learning on Student Performance in an Architectural Sustainability Course.

ISSN: 2773-7055
Proceedings of the 5th International Research Conference
Institute of Technology, University of Moratuwa
November 5, 2026

Paper ID: 73

EFFECT OF AN 8-WEEK PROGRESSIVE RESISTANCE TRAINING PROGRAM ON FULL-BODY FRONT-TURN MOVEMENT SPEED DURING THE SEOI-NAGE TECHNIQUE IN NOVICE JUDO ATHLETES

R M D L Rajasingha[1*]; S Othalawa[2]

[1]Division of Interdisciplinary Studies, Institute of Technology, University of Moratuwa, Homagama, Sri Lanka

[2]Department of Sport Science and Physical Education, Faculty of Applied Sciences, Sabaragamuwa University of Sri Lanka

*Corresponding author: danushkar@itum.mrt.ac.lk

ABSTRACT: This study evaluated the effectiveness of an 8-week progressive resistance training program on improving full-body front-turn movement speed during the Seoi-Nage technique in novice judo athletes. Analysis of local competitive match play revealed that a major limiting factor preventing novice athletes from scoring via Seoi-Nage was a lack of rotational velocity during execution. To address this gap, a specialized 8-week resistance training regimen focusing on compound foundational movements-including squats, push-ups, sit-ups, chin-ups, and leg presses-was implemented. The training was systematically periodized, starting at 60% of maximum capacity and increasing to 100% by the final two weeks of the macrocycle. To capture functional improvements, the Special Judo Fitness Test (SJFT) was used, with the Total Throws (TT) metric serving as the primary proxy for explosive rotational turning speed. A randomized experimental design divided the cohort into a Treatment Group (TG) and a Control Group (CG). Data were analyzed using a Mixed Design Analysis of Variance (ANOVA). Results demonstrated a highly significant Time*Group interaction effect for Total Throws ($F = 81.880$, $p = 0.000$). The Treatment Group exhibited a 41.44% increase in throwing capacity, with the mean throw count rising from 18.10 ± 1.37 at pre-test to 25.60 ± 1.42 at post-test. Conversely, the Control Group showed negligible changes, moving from 18.80 ± 2.25 to 20.20 ± 2.25. These findings statistically establish that targeted physical conditioning directly enhances the rapid kinetic pivot required for successful throw completion, offering judo coaches a validated framework for athletic development.

Keywords: muscular strength, SJFT, total throws, Seoi-Nage

1 INTRODUCTION

Judo is a highly dynamic combat sport that places extraordinary demands on both the aerobic and anaerobic energy pathways, requiring an optimal blend of technical precision and physiological power. Within the technical repertoire of judo, *Seoi-Nage* (shoulder throw) stands out as one of the most frequently attempted and highly effective throwing techniques in competitive match play. Successful execution of *Seoi-Nage* hinges heavily on the *Kuzushi* (unbalancing) and *Tsukuri* (entry/turning) phases, where the athlete must perform a rapid, full-body front turn to establish back-to-front contact under the opponent's centre of gravity. Retrospective performance analyses of local competitive matches indicate that novice judo athletes consistently struggle to score points with *Seoi-Nage*. While technical positioning is a component, a primary limiting factor is a definitive deficit in full-body front turn movement speed during the entry phase. In modern sport science, this lack of operational speed is frequently traced back to insufficient foundation strength and power in the primary kinetic chains. Executing an explosive pivot under resistance requires substantial force-generation capacity from the lower body to drive rotation,

the core to transfer torque, and the upper body to pull and control the opponent. To bridge this gap, sport scientists emphasize the role of progressive resistance training to enhance athletic power and movement velocity (Casals, et al., 2017). By developing muscular strength through foundational multi-joint movements, athletes can increase their rate of force development (RFD), which directly accelerates functional movement patterns like the *Seoi-Nage* turn (de Almeida, F., et al., 2023). The objective of this study was to evaluate the impact of a structured 8-week progressive resistance training program on the full-body front-turn movement speed of novice judo athletes. It was hypothesized that a systematic conditioning intervention targeting the core, upper, and lower body would manifest as a significant functional improvement in throwing speed, objectively measured by the total throw count achieved during the Special Judo Fitness Test (SJFT).

2 METHODOLOGY

This study utilized a randomized experimental design to investigate the effects of an 8-week progressive resistance training intervention on the execution speed of the *Seoi-Nage* technique in novice judo athletes. Participant Criteria: Participant selection was governed by standardized criteria. The inclusion criteria were: (1) novice male and female judo athletes aged 18–25 years with less than 2 years of formal judo training; (2) regular participation in standard technical practice (>80% attendance rate); and (3) clearance for full physical exertion. The exclusion criteria were: (1) any pre-existing musculoskeletal injury or medical condition limiting maximum strength/speed execution within the preceding six months; (2) simultaneous engagement in any external resistance or conditioning program outside of the study protocol; and (3) failure to attend more than two intervention sessions. The sample population was randomly allocated into two distinct groups: a Treatment Group (TG) that underwent the structured strength and conditioning program, and a Control Group (CG) that maintained their standard judo technical training. The training protocol was executed over an 8-week macrocycle, focusing primarily on foundational compound resistance exercises designed to maximize multi-joint power and core stability. The program integrated five core exercises targeting the primary kinetic chains involved in the *Seoi-Nage* pivot: push-ups, squats, sit-ups, chin-ups, and the leg press. To ensure systematic physiological adaptation, the volume and load intensity were periodized linearly. The training intervention initiated at 60% of the athletes' maximum operational intensity gradually progressed each week, ultimately reaching 100% intensity during the final two weeks (Weeks 7 and 8) of the conditioning cycle. To objectively quantify functional changes in full-body front turn movement speed, the Special Judo Fitness Test (SJFT) was administered as both a pre-test (Week 1) and a post-test (Week 8). The SJFT is a globally validated, judo-specific assessment protocol divided into three distinct work intervals: Series A (15 seconds), Series B (30 seconds), and Series C (30 seconds), with a 10-second passive rest period between series (Sterkowicz et al., 2005). Two partners (*Uke*) of similar height and weight to the performer (*Tori*) were positioned at a distance of 6 meters from one another. The *Tori* started positioned equidistant between the two Uke (3 meters from each).

Upon the auditory signal, the Tori ran to the first Uke, executed a full-body front turn to perform Seoi-Nage, threw the Uke, ran 6 meters to the second Uke, and repeated the process continuously for the duration of the series. While the standard SJFT protocol tracks five physiological and functional variables-including immediate heart rate (HR), HR after 1-minute, total classification, index and total throws-this study strategically isolated Total Throws (TT) as the primary dependent variable. Because the physical boundaries and time constraints of the test are rigidly standardized, an increase in the total throw count from pre-test to post-test serves as a direct functional proxy indicating that the athlete is completing the mechanical Seoi-Nage turn at a significantly higher velocity. All statistical computations were performed using specialized data analysis software (SPSS 26). A Mixed Design Analysis of Variance (ANOVA) was executed to test significant differences within and between the groups across time. The model evaluated the within-subject factor of Time (Pre-test vs. Post-test), the between-subject factor of Group (Treatment vs. Control), and the critical Time*Group interaction effect. Post-hoc comparisons were adjusted using the Bonferroni correction method to isolate distinct mean differences, with the statistical significance threshold established a priori at $p < 0.05$.

3 RESULTS

Mixed Design ANOVA

Table 1. *ANOVA across HR After, HR 1min after, Throws, Index, Classification variables through the SJFT*

Variable	Time*group effect		ANOVA (F, p) Time effect		Group effect			Time effect (Bonferroni)						Group effect (Bonferroni)	
									Pre		Post				
	F	*p*	F	*p*	F	*p*	Group	Mean	SD	Mean	SD	*p*	Δ %	Group	*p*
HR After	4.708	0.004	40.412	0.000	1.546	0.230	CG	171.8	13.011	182.80	8.230	0.080	6.40	CG vs TG	0.230
							TG	162.0	7.272	184.40	8.099	0.000	13.83		
HR 1min After	0.106	0.749	0.4620	0.506	0.330	0.858	CG	141.40	16.160	138.0	7.831	0.487	-2.40	CG vs TG	0.858
							TG	141.00	7.601	139.8	12.090	0.805	-0.85		
TT	**81.880**	**0.000**	**174.301**	**0.000**	**9.373**	**0.007**	**CG**	**18.80**	**2.250**	**20.20**	**2.250**	**0.009**	**-7.45**	**CG vs TG**	**0.007**
							TG	**18.10**	**1.370**	**25.60**	**1.429**	**0.000**	**41.44**		
Index	31.878	0.000	67.574	0.000	5.998	0.025	CG	16.883	2.654	16.073	2.030	0.085	-4.79	CG vs TG	0.025
							TG	16.813	1.387	12.450	0.507	0.000	-25.95		
TC	30.600	0.000	40.694	0.000	2.829	0.110	CG	1.60	1.897	2.00	2.160	0.370	25	CG vs TG	0.110
							TG	1.00	0.000	4.80	1.476	0.000	380		

TT = Total Throws, TC= Total Classification, CG = Control Group, TG = Treatment Group, Δ % = percentage change in mean value.

The functional changes in full-body front turn movement speed were evaluated by isolating the Total Throws (TT) metric from the Special Judo Fitness Test (SJFT). The statistical analysis revealed a highly significant Time*Group interaction effect for Total Throws, $F(1, 18) = 81.880$, $p < 0.000$, indicating that changes in performance over time differed substantially between the experimental groups. Furthermore, a significant main effect for Time was observed, $F(1, 18) = 174.301$, $p < 0.000$, demonstrating an overall change from pre-test to post-test. The between-groups analysis also revealed a significant main group effect for the total throw capacity, F (1,

18) = 9.373, $p < 0.007$.

According to the Bonferroni post-hoc pairwise comparisons, both groups experienced significant internal improvements in throw counts over time. The Control Group exhibited a modest increase ($p = 0.009$). However, the Treatment Group achieved an extensive increase ($p < 0.000$). When comparing the percentage of mean differences, the Treatment Group's throwing capacity increased by a much higher percentage (41.44%) than that of the Control Group (7.45%). Bonferroni post-hoc analysis between the groups confirmed that the Treatment Group achieved a significantly greater mean difference and statistically outpaced the Control Group ($p < 0.05$), demonstrating the superior efficacy of the specialized strength and conditioning protocol.

4 DISCUSSION

The significant escalation in the total throw count achieved by the Treatment Group directly demonstrates an enhancement in full-body front turn movement speed. Because the SJFT protocol requires continuous sprinting and throwing over standardized intervals, an increase in the number of throws explicitly confirms that the athletes completed the repetitive mechanical turn of the Seoi-Nage technique at a faster rate (Franchini & Nakamura, F. Y., 2005). This functional acceleration is directly attributable to the 8-week progressive resistance training intervention. The targeted application of foundational compound exercises—specifically squats and leg presses for lower-body power, push-ups and chin-ups for upper-body pulling force, and sit-ups for core stability—maximized the athletes' rate of force development. In judo, executing a rapid turn requires an explosive initial pivot driven by the lower extremities, accompanied by strong trunk rotation to transfer torque and an aggressive upper-body pull to break the opponent's balance (Kuzushi) (Ishii, Kobayashi, Y., & Suzuki, Y, 2012). By progressively shifting the training intensity from 60% up to 100%, the neuromuscular systems of the novice athletes adapted to generate higher torque during the entry phase (Tsukuri), aligning with prior findings on power transfer in competitive judokas (De Sousa Fernandes Alcobia de Almeida, et al., 2023). The data indicate that regular technical judo training alone (as seen in the Control Group) is insufficient to yield rapid, high-velocity movement adaptations within a short macrocycle. Conversely, integrating structured resistance training provides the physiological foundation necessary to overcome deficiencies in turning speed, enabling novice athletes to complete the full-body front turn swiftly enough to successfully score points in competitive environments adaptations (Ishii, Kobayashi, Y., & Suzuki, Y, 2012).

5 CONCLUSION

This study successfully demonstrates that an 8-week progressive resistance training program significantly enhances the full-body front turn movement speed during the execution of the Seoi-Nage technique in novice judo athletes. Moreover, by systematically progressing foundational compound exercises such as squats, push-ups, sit-ups, chin-ups, and leg presses from 60% to 100% intensity, athletes developed the essential muscular force required to drive rapid rotation. Isolating the functional Total Throws (TT) metric from the standardized Special Judo Fitness Test (SJFT) provided explicit evidence of velocity improvement, with the Treatment Group exhibiting

an outstanding 41.44% increase in throwing execution compared to a minor 7.45% improvement in the technical-only Control Group. These findings confirm that physical conditioning deficiencies underlay the structural turning speed limitations observed in novice competitive match play. Consequently, strength and conditioning macrocycles utilizing multi-joint resistance training protocols should be integrated into standard training schedules to facilitate faster entry phases and maximize technical execution in judo competitions.

6 ACKNOWLEDGEMENTS

The author wishes to express sincere gratitude to the research supervisor, faculty lecturers, and the athletic sample from the Kegalle district judo team whose commitment and dedication made the data collection and evaluation phases of this study possible.

7 REFERENCES

Casals, C., Huertas, J. R., Franchini, E., Sterkowicz-Przybycień, K., Sterkowicz, S., Gutiérrez-García, C., & Escobar-Molina, R. (2017). Special judo fitness test level and anthropometric profile of elite Spanish judo athletes. *The Journal of Strength & Conditioning Research*, *31*(5), 1229-1235.

De Sousa Fernandes Alcobia de Almeida, F., Carratalá, H., Carratalá, V., Feriche Fernández-Castanys, M. B., Padial Puche, P., & Bonitch Góngora, J. G. (2023). Influence of lower-limb muscle power-related variables on the ippon-seoi-nage of elite judokas.

Franchini, E., Nakamura, F. Y., Takito, M. Y., Kiss, M. A., & Sterkowicz, S. (2005). Special judo fitness test in juvenile: Junior and senior Brazilian judo players. *Biol Sport*, *7*(3), 11-8.

Ishii, T., Ae, M., Kobayashi, Y., & Suzuki, Y. (2012). Front-turn movement in seoi-nage of elite judo athletes. In *ISBS-conference proceedings Archive*.

ISSN: 2773-7055
Proceedings of the 5th International Research Conference
Institute of Technology, University of Moratuwa
November 5, 2026

Paper ID: 91

PEDAGOGY OF STEAM EDUCATION IN NEPAL: FOSTERING INNOVATION IN THE CLASSROOM

Chudamani Phayal[1*] and Pooja Gupta[1]

[1]Mewar University, Chittorgarh, Rajasthan, India

*Corresponding author: phayalchudamani@gmail.com

ABSTRACT: STEAM education integrates Science, Technology, Engineering, Arts and Mathematics through interdisciplinary, learner-centred and problem-oriented learning. Although Nepal has introduced curriculum reforms compatible with STEAM principles and developed university, school and extracurricular initiatives, the evidence base remains fragmented and the distinction between policy intent, pilot practice and system-wide implementation is often unclear. This study examines what is known about STEAM pedagogy in Nepal, identifies principal implementation gaps, and develops a Nepal-specific implementation framework. A structured qualitative literature review was undertaken using peer-reviewed studies, Nepalese policy documents, institutional reports and scholarly repositories. The review distinguishes Nepal-specific evidence from international literature and thematically analyses evidence under curriculum, teacher competency, infrastructure, pedagogy, assessment, institutional support and socio-cultural context. The literature indicates that Nepal has a policy foundation for STEAM, particularly through integrated curriculum at the basic level and emerging initiatives, but explicit STEAM integration remains uneven. The most recurrent constraints are teacher preparedness, unequal infrastructure, conventional assessment practices, limited mentoring and disparities between school types. The study contributes a Nepal STEAM Implementation Roadmap linking curriculum design, teacher capacity, resources, pedagogy, assessment, institutional support and contextualisation.

Keywords: STEAM education, Nepal, pedagogy, integrated curriculum, teacher competency, implementation framework

1 INTRODUCTION

STEAM—Science, Technology, Engineering, Arts and Mathematics—has evolved from STEM into an interdisciplinary approach connecting disciplinary knowledge with inquiry, design, creativity and real-world problem solving. International literature associates STEAM with creativity, critical thinking and collaboration, while emphasizing that integration among the five domains varies across contexts. STEAM should not be reduced to adding arts activities to science or mathematics; its distinctive feature is purposeful connection among disciplines, creative processes and authentic problems.

In Nepal, policy provides foundations for such integration without constituting a national STEAM system. Curriculum reforms have moved toward integrated learning, with the National Curriculum Framework providing integrated curriculum at Grades 1–3 and subsequent arrangements emphasizing practical, project-oriented learning. The School Education Sector Plan 2022–2032 emphasizes equitable access, quality learning and teacher capacity. These policies indicate movement toward conditions supporting STEAM, but do not evidence systematic implementation.

The existing Nepal-specific scholarship has examined discrete aspects of this development. Belbase (2019) documented STEAM initiatives and challenges. Koirala and Neupane (2023)

examined headteachers' understanding of integrated curriculum practice. Dahal (2022) approached STEAM from a transformative perspective. Pant et al. (2024) reviewed Nepal's status, opportunities and challenges. However, these studies leave a synthesis gap: they describe initiatives separately, lack analysis of how implementation conditions interact, sometimes transfer international evidence without distinguishing its source, and fail to provide an operational Nepal-specific roadmap.

The present study addresses these gaps by asking: (RQ1) What pedagogical and curricular features of STEAM education are reported in Nepal-specific literature? (RQ2) What implementation barriers and enabling conditions recur? (RQ3) How do curriculum, teacher competency, infrastructure, pedagogy, assessment, institutional support and socio-cultural context interact in shaping STEAM implementation? (RQ4) What Nepal-specific implementation framework can be derived?

2 LITERATURE REVIEW AND METHODOLOGY

2.1 Review Design

The study uses a structured qualitative literature review with thematic synthesis. The review treats Nepalese policy documents, Nepal-focused empirical or conceptual studies, and international STEAM scholarship as distinct evidence streams. Nepal-specific sources were used to make claims about Nepal's curriculum, institutions and school conditions. International sources were used primarily to define STEAM pedagogies and provide comparative conceptual evidence.

2.2 Search Strategy and Eligibility

The publication window was 2014–2026. Inclusion criteria were: (a) peer-reviewed research, scholarly papers or academically credible chapters; (b) official Nepalese curriculum, policy or sector documents; (c) credible institutional reports addressing STEAM or closely related implementation conditions; and (d) substantive relevance to school-level STEAM pedagogy, curriculum, teacher capacity, resources or assessment. Excluded were duplicate records, promotional webpages, sources unrelated to school education, and documents mentioning STEM/STEAM only incidentally.

2.3 Screening and Thematic Analysis

Titles and abstracts were screened first; potentially relevant full texts were assessed for contextual fit and substantive contribution. Sources were coded according to: (1) evidence type and geographical focus; (2) curriculum integration; (3) pedagogical approach; (4) teacher competency; (5) infrastructure and technology; (6) assessment; (7) institutional support; (8) equity; and (9) socio-cultural contextualisation. Thematic analysis followed an iterative process of familiarisation, initial coding, grouping of codes, comparison across sources, development of higher-order themes, and synthesis of relationships.

3 RESULTS

3.1 Nepal-Specific versus International Evidence

The review shows a clear difference between what is known internationally and what is empirically established in Nepal. International literature provides substantial support for project-based, inquiry-based, design-oriented, experiential and collaborative approaches as compatible with STEAM. These findings provide the pedagogical rationale but do not demonstrate effectiveness in Nepal.

Nepal-specific evidence is concentrated on curriculum reform, emerging institutional initiatives, conceptual accounts, and selected studies of school or teacher practice. Statements such as 'STEAM improves creativity' should be understood as supported primarily by international literature unless a Nepalese study directly measures that outcome. Statements such as 'Nepal has an integrated curriculum at the early basic level' are supported by Nepalese policy and literature. This evidential separation is central to interpreting the findings.

3.2 Recurring Pedagogical Approaches

Across the reviewed literature, seven pedagogical approaches recur: Project-Based Learning (PBL), Inquiry-Based Learning (IBL), Design Thinking, Experiential Learning, Collaborative Learning, Argumentation, and approaches associated with multiple intelligences. PBL and inquiry are most consistently connected to interdisciplinary problem solving, while design thinking provides a structured route from problem identification to prototyping. However, recurrence in the literature should not be interpreted as evidence of widespread use in Nepalese schools. The review indicates a substantial implementation gap between pedagogical ideals and classroom conditions.

4 NEPAL STEAM IMPLEMENTATION ROADMAP

The synthesis suggests barriers form a system: curriculum integration creates demand for interdisciplinary teaching; interdisciplinary teaching increases the need for teacher collaboration; project-based pedagogy requires materials and assessment alternatives; and all depend on leadership, mentoring and equitable resource allocation. The study proposes a seven-component roadmap:

1. Curriculum Alignment: Identify interdisciplinary learning outcomes and develop locally relevant STEAM project banks linked to existing curriculum.

2. Teacher Competency: Build staged competency in inquiry, project design, design thinking, technology use and arts integration, supported by coaching and lesson-study cycles.

3. Infrastructure and Technology: Adopt a minimum STEAM resource package using low-cost, locally available materials, shared laboratories and phased makerspaces.

4. Pedagogy: Move from small inquiry tasks to interdisciplinary projects with explicit connections among all five domains.

5. Assessment: Combine curriculum-required assessment with formative rubrics, portfolios, prototypes, presentations and reflection.

6. Institutional Support: Establish STEAM coordinators, teacher learning communities, partnerships and annual monitoring.

7. Socio-cultural Contextualisation and Equity: Use local environmental, agricultural, cultural and community problems as project contexts, with deliberate support for disadvantaged schools and learners.

5 DISCUSSION

The findings extend earlier Nepal-focused work by showing that the central issue has shifted from initial visibility to system integration. The synthesis adds an implementation logic by connecting issues rather than treating them as separate barriers.

Teacher capacity is particularly consequential. A curriculum can be interdisciplinary on paper while classroom practice remains subject-based if teachers are not prepared to plan across disciplinary boundaries. Professional development must move beyond short-term workshops toward sustained mentoring and collaborative planning.

Infrastructure is inseparable from equity. Community/government schools face constraints in laboratories, digital connectivity and specialist staff. Simply importing high-cost models could reproduce rather than reduce educational inequality. Low-cost, place-based STEAM is more compatible with Nepal's diverse resource environments.

Assessment presents another critical issue. STEAM's emphasis on inquiry and creativity sits uneasily with assessment cultures that privilege standardised content knowledge. Curriculum reform without corresponding assessment reform can create a structural incentive for teachers to continue conventional teaching.

The reviewed literature contains an important tension: integrated curriculum is presented as a foundation for transformative learning, yet studies report persistent compartmentalisation of subjects. Rather than treating this as a contradiction, the evidence suggests a policy-practice gap where formal curriculum integration coexists with discipline-based classroom routines.

5.1 Implications for Different School Contexts

Private and well-resourced urban schools may adopt robotics, coding and makerspaces relatively quickly. Community/government schools require a different entry strategy: low-cost materials, shared resource centres, teacher mentoring and projects based on community problems. Rural schools should not be treated as deficient versions of urban schools; their local environments provide rich STEAM contexts through agriculture, water, biodiversity, crafts and disaster preparedness.

6 LIMITATIONS

The study is a literature-based synthesis and does not provide a nationally representative survey of Nepalese schools. The Nepal-focused literature remains relatively small and includes conceptual and institutional documents alongside empirical studies. Consequently, the frequency with which a theme appears should be understood as evidence of research attention, not as a statistical estimate of prevalence. Future work should conduct a mixed-method national study of STEAM readiness.

7 CONCLUSION

STEAM education in Nepal has moved beyond a purely imported concept: curriculum reforms, university programmes, school initiatives and community-focused projects demonstrate an emerging national ecosystem. Yet the evidence does not support the claim that STEAM is already systematically implemented across Nepalese schools. The principal gap is implementation coherence.

The Nepal STEAM Implementation Roadmap provides a practical synthesis. Its central principle is that Nepal should not replicate resource-intensive international models without adaptation. Instead, STEAM implementation should be phased, place-based, equitable and connected to the existing curriculum. Such an approach can convert isolated projects into a more sustainable system of interdisciplinary learning while recognising the substantial diversity of Nepalese schools.

8 REFERENCES

Aldabbus, S. (2018). Project-Based Learning: Implementation and Challenges. *International Journal of Education, Learning and Development*, 6(3), 71-79.

Belbase, S. (2019). STEAM education initiatives in Nepal. *The STEAM Journal*, 4(1), Article 7.

Belbase, S., Mainali, B.R., Kasemsukpipat, W., Tairab, H., Gochoo, M., & Jarrah, A. (2022). At the dawn of STEAM education: prospects, priorities, processes, and problems. *International Journal of Mathematical Education in Science and Technology*, 53(11), 2919-2955.

Bertrand, M.G. & Namukasa, I.K. (2022). A pedagogical model for STEAM education. *Journal of Research in Innovative Teaching & Learning*, 16(2), 169-191.

CDC Nepal. (2018). *Basic Level (Grade 1-8) Curriculum*. CDC, Nepal.

Dahal, N. (2022). Transformative STEAM education as a praxis-driven orientation. *Journal of STEAM Education*, 5(2), 167-180.

Koirala, K.P. & Neupane, N.R. (2023). Headteacher's understanding on STEAM-based integrated curriculum practice in Nepal. *Discover Education*, 2:42.

Pant, B.P., et al. (2024). STEAM education in Nepal: Status, opportunities, challenges and future perspectives.

Sponsors and Well-wishers

Platinum Sponsor	ATG Hand care (Pvt) Ltd
Eng. (Mrs) Namali Siyabalapitiya	RMA (Pvt) Ltd.
Silver Sponsor	Laugfs Gas PLC
Silver Sponsor	Illukumbura Industrial Automation (Pvt) Ltd
Bronze Sponsor	National Paper Company Limited
Bronze Sponsor	The Institution of Incorporated Engineers Sri lanka
Dr. K.M.S.B. Rekogama	NDT 1970 /71 Batch
Eng. S.D.G.C.P. Sampath Bandara	NDT 1985/86 batch.
Sponsor	Silvermill Natural Beverages (Pvt) Ltd.

Platinum Sponsor

Silver Sponsors

Bronze Sponsors

Sponsor



Volume: 12 | ISSN: 2773-7055
Published by :
The Research Unit of ITUM
November 2026

© ITUM-IRC 2026, Institute of Technology, University of Moratuwa
https://irc.itum.mrt.ac.lk